

# **Signalling of E3 ubiquitin-protein ligases in the regulation of priming and tolerance of T cells**

**Luis Manuel Fernandes Bicheiro**

A thesis submitted to the Faculty of Medicine, University of Glasgow for the degree of  
Doctor of Philosophy

Division of Immunology, Infection and Inflammation  
Glasgow Biomedical Research Centre  
University of Glasgow  
120 University Place  
Glasgow  
G12 8TA

© Luis M. F. Bicheiro  
September 2010

## Summary

An effective immune system is essential for constant surveillance of potential threats to the organism, its' primary role being to provide resistance to infection. Thus, the immune system must be able to discriminate between pathogenic and self or harmless foreign antigens in order to not only achieve a productive immune response but also to avert unwarranted hyperreactivity and the potential development of autoimmunity. A delicate balance between these two fundamental requirements of the immune system must therefore exist.

T cells take central roles in the orchestration of the immune response. They are responsible for adaptive cell-mediated immunity and as such they can eliminate infected cells, produce cytokines that help in the resolution of the infection, stimulate other cells of the immune system to participate in the immune response and turn into long-lived memory cells. It is not surprising then that a wealth of mechanisms exist in order to ensure that T cells mediate immunity against pathogenic antigens but not to self or harmless ones. Indeed, various checkpoints in T cell development exist in the thymus to enable, on the one hand a large pool of diverse and functional T cells capable of recognising virtually all antigens while, on the other hand, eliminating self-reactive T cells. As some self-reactive T cells manage to leave the thymus, additional mechanisms have evolved to continually protect against auto-reactive and allergic inflammatory responses in the periphery. These mechanisms of peripheral tolerance include cell-mediated suppression of T cell responses, T cell apoptosis and T cell anergy. Anergy is a long-lived, cell-intrinsic mechanism that is characterised by cell cycle progression arrest and reduced IL-2 production. While T cell priming requires recognition of the cognate antigen in the context of MHC and co-stimulation via the interaction of its CD28 receptor with CD80/86 on an APC, recognition of the cognate antigen in the context of MHC without co-stimulation, such as when antigen is presented by immature APCs in the absence of inflammation, leads to anergy. These anergic T cells will also be hyporesponsive to re-challenge, even under immunogenic conditions.

The acquisition of the anergic phenotype is an active process, with negative regulators of T cell signalling being induced. Among these are some E3 ubiquitin-protein ligases which recognize target proteins for ubiquitination and catalyse the transfer of ubiquitin to them, directing them to the proteasome or to the endosomes. While a protein targeted to the proteasome is degraded by it, proteins in the endosomes can either be recycled for further signalling or directed to the lysosomes, where they are

also degraded; in any case, ubiquitination leads to downregulation of the activity of signalling elements, whether permanently (degradation) or temporarily (recycling). Therefore a stable difference in the gene expression profile between anergic and primed T cells could be achieved through ubiquitin modification translating into an increase in turnover of signalling mediators involved in the T cell response, thereby establishing a persistent unresponsive state. In fact, some key signalling mediators involved in T cell activation, such as PLC $\gamma$ -1 and PKC $\theta$ , have been shown to be downregulated by the ubiquitin pathway in the context of anergy induction. Conversely, the E3 ubiquitin-protein ligases Cbl-b, Itch and Grail have been shown to be upregulated during anergy. These and other E3-ubiquitin-protein ligases have also been shown to ubiquitinate and downregulate TCR signalling elements.

However, many of the studies leading to these findings have relied upon biochemical assessment of signalling in T cell lines or clones, at the population level following pharmacological stimulation *in vitro*. The data generated in this way is sometimes conflicting with that of studies which focused on the knockout of a single gene, followed by analysis of the phenotype. Moreover, as *in vitro* pharmacological stimulation data represents the responses of all cell types in the sample population at any one time, it does not necessarily reflect the responses of individual antigen-specific T cells within their environmental niche within lymphoid tissue. Information relating to differential kinetics or subcellular localisation of signals generated by functionally distinct subgroups within a population could help assess the full picture regarding the role of E3 ubiquitin-protein ligases during the induction and maintenance phases of T cell anergy.

The main objectives of this thesis were therefore to determine the expression of Cbl-b, Itch and Grail in individual antigen-specific CD4<sup>+</sup> T cells in both the induction and maintenance phases of anergy, *in vitro* and *in vivo*, and to investigate their functional signalling role(s) in the maintenance of the tolerance phenotype. In order to accomplish these objectives, induction of priming or tolerance in ovalbumin (OVA<sub>323-339</sub> peptide)-specific T cells from DO11.10 TCR transgenic mice *in vitro* or, following adoptive transfer of near physiologically relevant numbers of such cells into recipients, *in vivo*, was carried out. Functional outcome, measured in terms of cell cycle progression, proliferation, cytokine readout assays, antibody production and T cell migration was correlated with E3 ubiquitin-protein ligases expression and the ubiquitination status of the TCR signalling machinery. Cbl-b, Itch and Grail protein expression in LN tissue, antigen-specific CD4<sup>+</sup> T cells and subcellular compartments

was assessed. Moreover, quantitative analysis at the single cell level was carried out by tracking the antigen-specific CD4<sup>+</sup> T cells *in vitro* and *in vivo* by using Laser Scanning Cytometry. This relatively new technology combines the quantitative capabilities of flow cytometric analysis of cells with the ability to analyse them within a tissue *in situ* within their microenvironmental niche, thus more within physiological parameters.

This study shows Cbl-b expression to be upregulated in CD4<sup>+</sup> T cells undergoing induction of both anergy and priming, when compared to naïve cells. This is a departure from the view that states Cbl-b is a differential factor promoting anergy. In the maintenance phase, Cbl-b levels also appear upregulated in both anergic and primed antigen-specific T cells. Interestingly, Cbl-b concentrates in the periphery of anergic cells immediately after re-stimulation and this concentration of Cbl-b in the periphery of the cells was also observed for primed T cells after re-stimulation but at later time points. These data may therefore implicate Cbl-b in the modulation of T cell activation in the context of CD28 co-stimulation, rather than acting solely as a selective agent in the promotion of anergy.

Itch was similarly found to be upregulated in anergising and priming CD4<sup>+</sup> T cells, when compared to naïve cells. In fact, cells undergoing priming were found to express more Itch than those undergoing anergy. Likewise, in the maintenance phase, re-stimulation of primed cells resulted in higher Itch expression than re-stimulation of anergic antigen-specific T cells. Itch appears therefore to not play an exclusive role in anergy but instead acting in the general context of TCR signalling. Moreover, Grail expression was found to be upregulated in priming CD4<sup>+</sup> T cells while there is also evidence it was transiently expressed at high levels during the anergy induction phase. Intriguingly, in the maintenance phase, Grail is associated with the migration of antigen-specific T cells into the follicles.

In summary, the data presented here indicate that upregulation of Cbl-b, Itch and Grail is not exclusive to T cells undergoing or maintaining anergy, as priming and primed T cells also exhibit expression and upregulation of these signals. While these data therefore show that these molecules cannot be used as markers for T cell anergy, and while the search for a *bona fide* T cell anergy marker continues, it also opens up new possibilities for their role(s) in modulation of T cell activation. By advancing knowledge of the key signalling events that take place during antigen recognition, more targeted approaches for enhancing or inhibiting immunity or tolerance can be devised.

## **Declaration**

The work presented in this thesis represents original work carried out by the author.  
This thesis has not been submitted in any form to any other University.

Luis Manuel Fernandes Bicheiro  
University of Glasgow  
September 2010

## Funding

Luis Manuel Fernandes Bicheiro was awarded a research scholarship, reference SFRH / BD / 15851 / 2005, by the Fundacao para a Ciencia e a Tecnologia, Lisboa, Portugal and financed by POPH – QREN.



## Acknowledgments

I would first like to thank my supervisor, Professor Maggie Harnett. For all the encouragement, advice and support throughout these years, for the thorough discussions, keen interest and guidance for the writing of this thesis.

I would also like to thank all the members of the MMH lab, past and present. Special thanks to Angela, with whom I learned many of the things I would need for the completion of my thesis. Thanks to Natalie, Christina, Theresa, Mairi, Miguel and Rusty for help and technical assistance with experiments.

Thanks also to Professor Paul Garside and Professor Allan Mowat for all their advice and helpful discussions regarding the project at hand and general topics of immunology. I would also like to thank Barbara, Ivan, Andy, Elinor, Yvonne and Paola for helpful assistance in many situations.

Very big thanks to everyone in the Division of Immunology, Infection and Inflammation. For being there when necessary; for fostering an environment which promotes critical thinking and is prone to the development of innovative research.

Thanks to all my Glasgow friends, for making my stay in this city a memorable experience extending far beyond the scope of research life. From a night out to a café around the corner, you made it so much more worthwhile: Sérgio, Adriana, Joana, Jane, Francis, Cíntia, Catarina, Monika, Fujimi, Miguel, André, Raquel, Bárbara, Anna, Elsa.

A warm thanks to all my long-time friends, who have seen very little of me in this period, but will always remain close. And a special mention to Natacha and Márcia.

A special thanks to everyone involved in the Gulbenkian PhD Programme in Biomedicine for taking me in and giving me the opportunity to choose where and what my PhD project would be. A warm thanks to all my colleagues of the 5<sup>th</sup> PGDB, for all the comradeship in that eventful year.

Finally, I would like to thank my parents and family for all the support throughout these years and for their interest in all things related to my adventures in the lab.

# Table of contents

<b>Summary</b>	<b>ii</b>
<b>Declaration</b>	<b>v</b>
<b>Funding</b>	<b>vi</b>
<b>Acknowledgements</b>	<b>vii</b>
<b>Table of contents</b>	<b>viii</b>
<b>List of figures and tables</b>	<b>xi</b>
<b>List of abbreviations</b>	<b>xiii</b>
1 INTRODUCTION	2
1.1 The immune system	2
1.1.1 Innate immunity	2
1.1.2 Adaptive immunity	3
1.1.2.1 B cells	4
1.1.2.2 T cells	4
1.1.2.2.1 The TCR	5
1.1.2.2.2 T cell development	6
1.1.2.2.3 T cell activation	7
1.1.2.2.4 T cell differentiation	8
1.2 The lymphoid organs	9
1.2.1 The lymph nodes	10
1.3 Immune tolerance	10
1.3.1 Peripheral tolerance	11
1.3.1.1 Antigen ignorance	11
1.3.1.2 Cytokine deviation	11
1.3.1.3 Active suppression	11
1.3.1.3.1 Tr1	12
1.3.1.3.2 T <sub>H</sub> 3	12
1.3.1.3.3 CD8 <sup>+</sup> suppressor T cells	12
1.3.1.4 Clonal deletion	12
1.3.1.5 Anergy induction	13
1.4 T cell signalling	14
1.4.1 TCR-mediated signalling	14
1.4.2 CD28-mediated signalling	16
1.4.3 The role of inhibitory co-stimulatory molecules	17
1.4.4 Signalling in anergy	19
1.4.5 The immunological synapse	22
1.5 Apoptosis and cell cycle	23
1.5.1 Apoptosis	23
1.5.2 Cell cycle	24
1.6 Ubiquitination	25
1.6.1 Ubiquitination in T cell tolerance	27
1.6.1.1 E3 ubiquitin-protein ligases	27
1.6.1.1.1 Cbl-b	27
1.6.1.1.2 Itch	32
1.6.1.1.3 Grail	34
1.6.1.1.4 Smurfs	38
1.7 Aims	39
2 MATERIALS AND METHODS	52
2.1 Animals	52
2.2 Reagents and cell culture	52
2.3 Preparation of primary murine T cells for <i>in vitro</i> analysis	52
2.3.1 Extraction of lymph node cells	52

2.3.2	Isolation of CD4 <sup>+</sup> T cells	52
2.3.3	Stimulation of murine T cells	53
2.3.4	Analysis of the maintenance phase of anergy and priming of T cells	54
2.3.4.1	Production of GM-CSF-conditioned media	54
2.3.4.2	Generation of DCs	54
2.3.4.3	Maturation and stimulation of DCs	54
2.3.4.4	Re-stimulation of DO11-10 TCR transgenic T cells	54
2.3.4.5	Isolation of DO11.10 TCR transgenic T cells	55
2.4	<i>In vivo</i> tolerance assay	55
2.4.1	Preparation and purification of T cell suspensions	55
2.4.2	Adoptive transfer of antigen-specific T cells	56
2.4.3	Administration of antigen	56
2.5	Flow cytometry	56
2.5.1	Staining for surface markers	56
2.5.1.1	Identification of DO11.10 TCR transgenic T cells	57
2.5.2	Detection of intracellular signalling molecules	57
2.5.3	Biotinylation of KJ1-26 antibody	57
2.6	Western Blotting	58
2.6.1	Preparation of whole cell lysates	58
2.6.2	Protein quantification	58
2.6.3	SDS Page	58
2.6.4	Western blotting	59
2.6.5	Immunoprecipitation	60
2.7	Immunofluorescence of cells	60
2.7.1	Preparation of cells	60
2.7.2	Immunocytochemistry	60
2.8	Immunofluorescence of tissue sections	61
2.8.1	Preparation of tissue sections	61
2.8.2	Immunohistochemistry	62
2.9	Laser scanning cytometry	63
2.9.1	LSC data collection on individual cells	63
2.9.1.1	Identification of antigen-specific T cells	65
2.9.1.2	Cell cycle analysis	65
2.9.2	LSC data collection on lymph node tissue	66
2.9.3	Immunofluorescence microscopy	67
2.10	Other functional assays	67
2.10.1	[ <sup>3</sup> H]thymidine uptake DNA synthesis/ proliferation assay	67
2.10.2	Assessment of antigen-specific cytokine production	67
2.11	Statistical analysis	68
3	RESULTS	84
3.1	The induction phase of anergy and priming in CD4 <sup>+</sup> T cells	84
3.1.1	Functional assessment of the induction of anergy and priming in CD4 <sup>+</sup> T cells, <i>in vitro</i>	84
3.1.2	Analysis of the expression of E3 ubiquitin-protein ligases in the induction phase of anergy and priming	85
3.1.3	Analysis of the expression of E3 ubiquitin-protein ligases in the induction phase of anergy and priming at the single-cell level	92
3.1.3.1	Cbl-b	92
3.1.3.2	Itch	94
3.1.3.3	Grail	96
3.1.4	Distribution of the E3 ubiquitin-protein ligase-expressing cells according to the cell cycle stage	97

3.1.4.1	Cbl-b	98
3.1.4.2	Itch	99
3.1.4.3	Grail	101
3.1.5	Analysis of the expression of E3 ubiquitin-protein ligases in the induction phase of anergy and priming, in vivo	102
3.1.5.1	Cbl-b	103
3.1.5.2	Itch	104
3.1.5.3	Smurf1	104
3.1.5.4	Smurf2	105
3.2	The maintenance phase of anergy and priming in CD4 <sup>+</sup> T cells	105
3.2.1	Functional analysis of DO11.10 T cells in the maintenance phase of anergy and priming	106
3.2.2	Analysis of the expression of E3 ubiquitin-protein ligases in the maintenance phase of anergy and priming	107
3.2.3	Analysis of the expression of E3 ubiquitin-protein ligases in the maintenance phase of anergy and priming at the single-cell level	110
3.2.3.1	Arf6	110
3.2.3.2	Ubiquitination	111
3.2.3.3	Cbl-b	112
3.2.3.4	Itch	113
3.2.4	Distribution of the E3 ubiquitin-protein ligase-expressing cells according to the cell cycle stage	114
3.2.4.1	Cbl-b	115
3.2.4.2	Itch	116
3.2.5	Analysis of the expression of E3 ubiquitin-protein ligases in the maintenance phase of anergy and priming, in vivo	117
3.2.5.1	Cbl-b	118
3.2.5.2	Itch	119
3.2.5.3	Grail	120
4	DISCUSSION	183
4.1	Methods and results	183
4.2	Cbl-b	184
4.2.1	Induction	184
4.2.2	Maintenance	186
4.3	Itch	189
4.3.1	Induction	189
4.3.2	Maintenance	191
4.4	Grail	194
4.4.1	Induction	194
4.4.2	Maintenance	197
4.5	Smurfs	199
4.6	Other potential anergy markers	200
4.6.1	Traf6	201
4.6.2	Ikaros	202
4.7	Ubiquitination	203
4.8	E3 ubiquitin-protein ligases in the context of T cell anergy	206
4.9	Dissecting the mechanisms underlying differential signalling in anergy and priming	207
4.10	Summary	212
5	References	215

# List of figures and tables

Figure 1.1: The TCR:CD3 complex structure.	40
Figure 1.2 T cell development takes place in the thymus.	41
Figure 1.3: Optimum activation of naïve T cells requires two signals.	42
Figure 1.4: T cell differentiation.	43
Figure 1.5: Lymph node structure.	44
Figure 1.6: TCR-mediated signalling.	45
Figure 1.7: CD28-mediated signalling.	46
Figure 1.8: Signalling in anergy induction.	47
Figure 1.9: Signalling in the maintenance phase of anergy.	48
Figure 1.10: The immunological synapse.	49
Figure 1.11: Ubiquitination.	50
Figure 2.1: Identification of DO11.10 TCR transgenic T cells by flow cytometry.	69
Table 2.1: List of antibodies used in flow cytometry.	70
Table 2.2: List of fluorochromes used in flow cytometry (A) and laser scanning cytometry (B).	71
Table 2.3: List of primary antibodies used in Western blotting.	72
Table 2.4: List of primary anti-ubiquitin moieties antibodies (A) and secondary antibodies (B) used in Western blotting.	73
Figure 2.2: Assessment of antibody specificity by Western blotting.	74
Table 2.5: List of antibodies used in immunocytochemistry.	75
Figure 2.3: Tyramide indirect signal amplification.	76
Figure 2.4: Tyramide direct signal amplification.	77
Table 2.6: List of antibodies used in immunohistochemistry.	78
Figure 2.5: Cell detection by the LSC.	79
Figure 2.6: Identification of CD4 <sup>+</sup> T cells with the LSC.	80
Figure 2.7: Analysis of cell cycle progression with the LSC.	81
Figure 2.8: Analysis of lymph node tissue sections with the LSC.	82
Figure 3.1: Induction of anergy and priming in T cells.	121
Figure 3.2: Expression of E3 ubiquitin-protein ligases in T cells.	122
Figure 3.3: Ubiquitination of proteins in T cells.	123
Figure 3.4: Immunoprecipitation of ubiquitin in T cells.	124
Figure 3.5: Induction of anergy and priming in CD4 <sup>+</sup> T cells.	125
Figure 3.6: Expression of E3 ubiquitin-protein ligases in CD4 <sup>+</sup> T cells.	126
Figure 3.7: Expression of E3 ubiquitin-protein ligases in CD4 <sup>+</sup> T cells after proteasome inhibition.	127
Figure 3.8: Inducing anergy and priming in CD4 <sup>+</sup> T cells.	128
Figure 3.9: Expression of E3 ubiquitin-protein ligases in anergising and priming CD4 <sup>+</sup> T cells.	129
Figure 3.10: Expression of ubiquitinated proteins in anergising and priming CD4 <sup>+</sup> T cells.	130
Figure 3.11: Quantification of Cbl-b expression in CD4 <sup>+</sup> T cells after 20 h of in vitro stimulation.	131
Figure 3.12: Visualisation of Cbl-b expression in CD4 <sup>+</sup> T cells after 20 h of in vitro stimulation.	132
Figure 3.13: Quantification of Cbl-b expression in CD4 <sup>+</sup> T cells after 40 h of in vitro stimulation.	133
Figure 3.14: Visualisation of Cbl-b expression in CD4 <sup>+</sup> T cells after 40 h of in vitro stimulation.	134
Figure 3.15: Quantification of Itch expression in CD4 <sup>+</sup> T cells after 20 h of in vitro stimulation.	135
Figure 3.16: Visualisation of Itch expression in CD4 <sup>+</sup> T cells after 20 h of in vitro stimulation.	136
Figure 3.17: Quantification of Itch expression in CD4 <sup>+</sup> T cells after 40 h of in vitro stimulation.	137
Figure 3.18: Visualisation of Itch expression in CD4 <sup>+</sup> T cells after 40 h of in vitro stimulation.	138
Figure 3.19: Quantification of Grail expression in CD4 <sup>+</sup> T cells after 20 h of in vitro stimulation.	139
Figure 3.20: Visualisation of Grail expression in CD4 <sup>+</sup> T cells after 20 h of in vitro stimulation.	140
Figure 3.21: Quantification of Grail expression in CD4 <sup>+</sup> T cells after 40 h of in vitro stimulation.	141
Figure 3.22: Analysis of cell cycle stage distribution in CD4 <sup>+</sup> T cells.	142
Figure 3.23: Analysis of Cbl-b expression according to cell cycle stage in CD4 <sup>+</sup> T cells after 20 h of in vitro stimulation.	143
Figure 3.24: Analysis of Cbl-b expression according to cell cycle stage in CD4 <sup>+</sup> T cells after 40 h of in vitro stimulation.	144
Figure 3.25: Analysis of Itch expression according to cell cycle stage in CD4 <sup>+</sup> T cells after 20 h of in vitro stimulation.	145
Figure 3.26: Analysis of Itch expression according to cell cycle stage in CD4 <sup>+</sup> T cells after 40 h of in vitro stimulation.	146
Figure 3.27: Analysis of Grail expression according to cell cycle stage in CD4 <sup>+</sup> T cells after 20 h of in vitro stimulation.	147

Figure 3.28: Analysis of Grail expression according to cell cycle stage in CD4 <sup>+</sup> T cells after 40 h of in vitro stimulation.	148
Figure 3.29: Functional analysis of T cells from naïve, tolerised and primed mice.	149
Figure 3.30: Cbl-b expression in DO11.10 TCR transgenic T cells within the lymph node of tolerised and primed mice.	150
Figure 3.31: Itch expression in DO11.10 TCR transgenic T cells within the lymph node of tolerised and primed mice.	151
Figure 3.32: Smurf1 expression in DO11.10 TCR transgenic T cells within the lymph node of tolerised and primed mice.	152
Figure 3.33: Smurf2 expression in DO11.10 TCR transgenic T cells within the lymph node of tolerised and primed mice.	153
Figure 3.34: Setting up antigen-specific T cells for anergy and priming analysis in the maintenance phase.	154
Figure 3.35: Functional analysis of DO11.10 T cells in the maintenance phase of anergy and priming.	155
Figure 3.36: Setting up DO11.10 TCR transgenic, antigen-specific T cells in the maintenance phases of anergy and priming for Western blotting analysis.	156
Figure 3.37: Expression of E3 ubiquitin-protein ligases in the maintenance phase of anergic and primed T cells.	157
Figure 3.38: Ubiquitination of proteins in the maintenance phase of anergic and primed T cells.	158
Figure 3.39: Setting up DO11.10 TCR transgenic, antigen-specific T cells in the maintenance phases of anergy and priming for Western blotting analysis.	159
Figure 3.40: Expression of E3 ubiquitin-protein ligases in the maintenance phase of anergic and primed DO11.10 TCR transgenic, antigen-specific T cells.	160
Figure 3.41: Quantification of Arf6 expression in KJ1-26 <sup>+</sup> T cells after 20 h of in vitro re-stimulation.	161
Figure 3.42: Quantification of the ubiquitination of proteins in KJ1-26 <sup>+</sup> T cells after in vitro re-stimulation.	162
Figure 3.43: Visualisation of ubiquitinated proteins in KJ1-26 <sup>+</sup> T cells after 20 h of in vitro re-stimulation.	163
Figure 3.44: Quantification of Cbl-b expression in KJ1-26 <sup>+</sup> T cells after 1 h of in vitro re-stimulation.	164
Figure 3.45: Quantification of Cbl-b expression in KJ1-26 <sup>+</sup> T cells after 20 h of in vitro re-stimulation.	165
Figure 3.46 Quantification of Itch expression in KJ1-26 <sup>+</sup> T cells after 1 h of in vitro re-stimulation.	166
Figure 3.47: Visualisation of Itch expression in KJ1-26 <sup>+</sup> T cells after 1 h of in vitro re-stimulation.	167
Figure 3.48: Quantification of Itch expression in KJ1-26 <sup>+</sup> T cells after 20 h of in vitro re-stimulation.	168
Figure 3.49: Visualisation of Itch expression in KJ1-26 <sup>+</sup> T cells after 20 h of in vitro re-stimulation.	169
Figure 3.50: Analysis of cell cycle stage distribution in KJ1-26 <sup>+</sup> T cells after in vitro re-stimulation.	170
Figure 3.51: Analysis of Cbl-b expression according to cell cycle stage in KJ1-26 <sup>+</sup> T cells after 1 h of in vitro re-stimulation.	171
Figure 3.52: Analysis of Cbl-b expression according to cell cycle stage in KJ1-26 <sup>+</sup> T cells after 20 h of in vitro re-stimulation.	172
Figure 3.53: Analysis of Itch expression according to cell cycle stage in KJ1-26 <sup>+</sup> T cells after 1 h of in vitro re-stimulation.	173
Figure 3.54: Analysis of Itch expression according to cell cycle stage in KJ1-26 <sup>+</sup> T cells after 20 h of in vitro re-stimulation.	174
Figure 3.55: The maintenance phase in tolerised and primed mice.	175
Figure 3.56: Cbl-b expression in DO11.10 TCR transgenic T cells within the lymph node of tolerised and primed mice after re-stimulation.	176
Figure 3.57: Analysis of the effect of Cbl-b expression in DO11.10 T cells' migration into B cell follicles in tolerised and primed mice after re-stimulation.	177
Figure 3.58: Itch expression in DO11.10 TCR transgenic T cells within the lymph node of tolerised and primed mice after re-stimulation.	178
Figure 3.59: Analysis of the effect of Itch expression in DO11.10 T cells' migration into B cell follicles in tolerised and primed mice after re-stimulation.	179
Figure 3.60: Grail expression in DO11.10 TCR transgenic T cells within the lymph node of tolerised and primed mice after re-stimulation.	180
Figure 3.61: Analysis of the effect of Grail expression in DO11.10 T cells' migration into B cell follicles in tolerised and primed mice after re-stimulation.	181
Table 4.1: Summary of the results yielded by the main experimental approaches regarding the expression of Cbl-b, Itch and Grail.	213
Figure 4.1: Expression of Cbl-b, Itch and Grail after 20 h of stimulation and potential targets for their action in the downmodulation of T cell activity.	214

## List of abbreviations

AICD - Activation-induced cell death  
AP-1 - Activator protein-1  
APC - Antigen presenting cell  
Arf6 - ADP-ribosylation factor-6  
BCA - Bicinchonnic acid  
Bcl10 - B cell lymphoma 10  
BCR - B-cell receptor  
BSA - Bovine serum albumin  
BTLA - B- and T-lymphocyte attenuator  
CARD - Caspase-recruitment domain  
Carma1 - Caspase-recruitment domain-containing membrane associated guanylate kinase protein 1  
Cbl - Casitas B lineage lymphoma  
CCL4 - CC chemokine ligand 4  
CD - Cluster of differentiation  
CDK - Cyclin-dependent kinase  
Cn - Calcineurin  
Csk - C-terminal Src kinase  
CTLs - Cytotoxic T lymphocytes  
CTLA-4 - Cytotoxic T-lymphocyte-associated antigen 4  
DAG - Diacylglycerol  
DCs - Dendritic cells  
DGK - Diacylglycerol kinase  
DNA - Deoxyribonucleic acid  
DUBs - Deubiquitylation enzymes  
E1 - Ubiquitin-activating enzyme  
E2 - Ubiquitin-conjugating enzyme  
E3 - Ubiquitin-protein ligase  
ECL - Enhanced chemiluminescence  
EDTA - Ethylenediaminetetraacetic acid  
Egr - Early growth response  
ELISA - Enzyme-linked immunosorbent assay  
ER - Endoplasmic reticulum

Erk - Extracellular signal-regulated kinase  
FACS - Fluorescence-associated cell sorter  
FBS - Fetal bovine serum  
FCS - Fetal calf serum  
FcR - Fc receptor  
FSC - Forward scatter  
GADS - Grb2-related adapter downstream of Shc  
GDP - Guanosine diphosphate  
GEF - Guanine nucleotide exchange factor  
GM-CSF - Granulocyte-macrophage colony-stimulating factor  
Grail - Gene related to anergy in lymphocytes  
GTP - Guanosine triphosphate  
HECT - Homologous to the E6-associated protein C terminus  
HEVs - High endothelial venules  
HRP - Horseradish peroxidase  
ICOS - Inducible co-stimulator  
IFN $\gamma$  - Interferon $\gamma$   
I $\kappa$ B - Inhibitor of NF- $\kappa$ B  
IKK - I $\kappa$ B kinase  
IL - Interleukin  
IP<sub>3</sub> - Inositol 1, 4, 5-trisphosphate  
IS - Immunological synapse  
ITAM - Immunoreceptor tyrosine-based activation motifs  
Itk - IL-2 tyrosine kinase  
i.v. - intravenously  
Jnk - c-Jun N-terminal kinase  
LAT - Linker for activation of T cells  
LFA-1 - Leukocyte function-associated antigen-1  
LNs - Lymph nodes  
LPS - Lipopolysaccharide  
MACS - Magnetic-associated cell separation  
Malt1 - Mucosa-associated-lymphoid-tissue lymphoma translocation gene 1  
MAPK - Mitogen-activated protein kinase  
MAPKK - Mitogen-activated protein kinase kinase  
MEK - MAPK Erk kinase

MFI - Mean fluorescence intensity  
MLNs - Mesenteric lymph nodes  
mRNA - Messenger ribonucleic acid  
NFAT - Nuclear factor of activated T cells  
NFDC - Newly-formed daughter cell  
NF- $\kappa$ B - Nuclear factor  $\kappa$ B  
NK - Natural Killer  
NKT - Natural Killer T cells  
OCT - Optimal cutting temperature  
p56<sup>lck</sup> - Lck  
p59<sup>fyn</sup> - Fyn  
PA - Phosphatidic acid  
PAMPs - Pathogen-associated molecular patterns  
PBS - Phosphate buffered saline  
PD-1 - Program death-1  
PDK1 - Phosphoinositide-dependent kinase 1  
PH - Pleckstrin homology  
PI3K - Phosphatidylinositol 3-kinase  
PIP<sub>2</sub> - Phosphatidylinositol 4, 5-bisphosphate  
PIP<sub>3</sub> - Phosphatidylinositol 3, 4, 5-trisphosphate  
PKC - Protein kinase C  
PLC $\gamma$ -1 - Phospholipase C $\gamma$ 1  
PLNs - Peripheral lymph nodes  
PMA - Phorbol 12-myristate 13-acetate  
PMT - Photomultiplier tube  
PRRs - Pattern recognition receptors  
PTK - Protein tyrosine kinase  
RasGRP1 - Ras guanyl-releasing protein 1  
RING - Really interesting new gene  
RT - Room temperature  
SA - Streptavidin  
SHP-1 - SH2 domain-containing phosphatases 1  
SLP-76 - SH2 domain-containing leukocyte protein of 76 kDa  
SMAC - Supramolecular activation cluster  
Smurf - Smad ubiquitination regulatory factor

SOS - Son of Sevenless  
Src - Rous sarcoma oncogene  
SSC - Side scatter  
T<sub>C</sub> - Cytotoxic T cells  
T<sub>H</sub> - T helper cells  
TCR - T cell receptor  
TGF- $\beta$  - Transforming growth factor- $\beta$   
TLRs - Toll-like receptors  
Traf6 - Tumour-necrosis-factor-receptor-associated factor 6  
UBL - Ubiquitin-like protein  
WASP - Wiskott-Aldrich syndrome protein  
wt - Wild type  
ZAP-70 -  $\zeta$ -associated protein of 70 kDa

h - Hour  
min - Minutes  
s - Seconds  
cpm - Counts per minute  
 $\mu$ Ci - Microcurie  
g - Gram  
g - Times gravity  
mg - Milligram  
 $\mu$ g - Microgram  
ng - Nanogram  
ml - Millilitres  
 $\mu$ l - Microlitres  
LC - Loading control  
M - Molar  
mM - Millimolar  
 $\mu$ M - Micromolar  
mW - Milliwat

CHAPTER 1  
INTRODUCTION

# 1 INTRODUCTION

## 1.1 The immune system

An effective immune system is essential for constant surveillance of potential threats to the organism, its' primary role being to provide resistance to infection. The immune system is made up of two arms: innate immunity and adaptive immunity, which together provide the immune system with the ability not only to recognize the difference between “danger” (e.g., a pathogen) and a harmless situation but also to mount protective responses that are increasingly effective on re-encounter with the particular pathogen [1].

### *1.1.1 Innate immunity*

The innate immune system is involved in resisting infection by way of barrier mechanisms, by ingesting and killing the pathogen and by mediating inflammation. Anatomical barriers like the skin and the mucous membranes, physiological barriers such as body temperature and pH are the first defences a potential pathogen must face. Inflammation has three major functions: deliver additional effector molecules and cells to the site of infection (which contribute to the killing of pathogens), to induce local blood clotting (which provides another barrier to the spread of the infection) and to promote the repair of injured tissue. Innate immunity can be mediated by cells, circulating proteins such as the complement system, and anti-microbial peptides such as defensins and cathelicidins [2].

The cells of the innate branch of the immune system are the macrophages, dendritic cells (DCs), neutrophils, eosinophils, basophils, mast cells and natural killer cells (NKs). Macrophages and neutrophils are phagocytic cells that engulf pathogens and destroy them in intracellular vesicles. DCs are also phagocytic cells, but they are involved in presenting antigen to cells of the adaptive immune system, thus allowing its activation. Eosinophils, basophils and mast cells are secretory cells, releasing the contents of their granules after antibody activation. Unlike all the other cells of the innate immune system, which differentiate from the common myeloid progenitor together with platelets and erythrocytes, NK cells differentiate from the common lymphoid progenitor (together with B and T cells); they are involved in recognition and elimination of tumour and virus-infected cells [2].

DCs are a specialised population of professional antigen presenting cells (APCs) that appear to be the cells primarily responsible for initiating naïve T cells responses. Immature DCs are highly phagocytic and act to capture microbial antigens in the periphery. DCs are induced to migrate from the site of infection to the T cell-rich areas of the lymph nodes (LNs) after antigen uptake and, once exposed to microbial products or proinflammatory cytokines, they become mature DCs. Mature, LN-located DCs express high levels of MHC-associated peptides derived from the pathogen and cell surface molecules such as B7.1/CD80, B7.2/CD86 and CD40 (ligands for CD28 (CD80/86) and CD154 (CD40), which are expressed on most naïve T cells, especially those in the CD4 subset). Once activated, APCs also produce cytokines that contribute to the stimulation and modulation of T cells and their responses [1].

Recognition in the innate immune system is based on non-clonally distributed receptors called pattern recognition receptors (PRRs), which recognize certain molecular patterns (pathogen-associated molecular patterns, PAMPs), that are conserved across a range of pathogens [3]. Triggering of certain receptors by some pathogen products is also important in the induction of adaptive immunity, because, as described above, DCs and macrophages are led to display co-stimulatory molecules that contribute to their priming of T cells. The most characterised class of PRRs that lead to such a response is the Toll-like receptor family (TLRs). Each of the members of the TLR family recognise a different set of PAMPs; for instance, TLR-3 recognises dsRNA, TLR-4 dimer (with MD-2 and CD14) recognises lipopolysaccharide (LPS) and lipoteichoic acids, and TLR-5 recognises flagellin [2].

### ***1.1.2 Adaptive immunity***

Unlike innate immune responses, adaptive immune responses are reactions to specific antigenic challenges. The adaptive immune system is constituted by B and T cells which function as the mediators of humoral (antibody-mediated) and cell-mediated immunity, respectively. It is essentially a self-regulated system, since both the mature, naïve T cell receptor repertoire and the mature, naïve B cell receptor repertoire are generated by interaction with self-ligands rather than non-self ligands to ensure self-tolerance. Another important characteristic is the development of immunological memory which allows the immune system to respond more rapidly and more effectively to a second encounter with an antigen [1].

### 1.1.2.1 B cells

B cells are responsible for humoral immunity. They produce and secrete antibodies upon activation and differentiation into plasma cells. In the majority of cases, binding of antigen to the B-cell receptor (BCR) on a naïve mature B cell will lead to its activation only when T cell help is provided. The BCR comprises antigen-binding and signal transducing units. Every B cell clone produces an antibody with unique specificity that can carry out various functions depending on its isotype. After receiving T cell help in the form of cytokines and CD40 ligation, B cells proliferate and differentiate into populations of antibody-secreting plasma cells or memory B cells; isotype class switching also occurs during this process. Antibodies, depending on their isotype, can act via neutralisation, opsonisation or complement activation, but the ultimate common goal is dealing with extracellular forms of pathogens and their toxic products. Antibodies are immunoglobulin proteins which consist of re-arranged heavy (H) and light (L) chains which contain variable (V) regions that bind to specific antigens [2].

As B cells constitutively express MHC class II molecules and are efficient at acquiring antigen, they can also act as APCs for T cells, although they are not the most efficient ones. Evidence for B cells having cytokine effector (Be1 and Be2) and regulatory functions (B<sub>regs</sub>) also exists [2, 4].

### 1.1.2.2 T cells

T cells are responsible for cell-mediated immunity and can be broadly subdivided into several classes according to their expression of certain cell surface proteins (“markers”).

Two distinct lineages arise early in T cell development: the  $\alpha\beta$  and the  $\gamma\delta$  T cells, which have different types of T cell receptor (TCR). The  $\gamma\delta$  T cells are the minor population of T cells; when mature, they will express CD3 but not CD4 or CD8; they can be found in the gut mucosa and the epidermis.  $\gamma\delta$  T cells are non-peptide-MHC-restricted; and they are thought to be involved in immune regulation, tumour surveillance and specific primary immune responses [5].

$\alpha\beta$  T cells also express CD3 when mature and can be split into two main types, according to their co-receptor: CD8<sup>+</sup> and CD4<sup>+</sup> T cells. However, Natural Killer T cells (NKT), which are a minor population of  $\alpha\beta$  T cells, can also be CD4<sup>+</sup> or CD8<sup>+</sup>, or neither, but their expression of a variety of molecular markers that are typically associated with NK cells warrants them this different designation. Another point of their

distinction from conventional  $\alpha\beta$  T cells is that the TCRs of NKT cells are far more limited in diversity; also, they recognise lipids and glycolipids presented by CD1d, not classical peptide:MHC complexes [6].

CD8<sup>+</sup> T cells, also known as cytotoxic T cells (T<sub>C</sub>), exhibit MHC class I restriction and upon recognising their specific antigen in association with MHC class I in the presence of interleukin-2 (IL-2) proliferate and differentiate into effector cells known as cytotoxic T lymphocytes (CTLs). CTLs are responsible for eliminating tumour cells, grafted cells or virally infected cells from the body [2].

CD4<sup>+</sup> T cells are MHC class II restricted and are also known as T helper (T<sub>H</sub>) cells as they act to stimulate other cells of the immune system to participate in the immune response, namely T<sub>C</sub> and B cells [2].

MHC class I presents peptides derived from proteins synthesised in the cytosol. For example, in virus-infected cells, viral proteins expressed in the cytosol are subject to proteasomal proteolysis and the resulting peptides are translocated into the endoplasmic reticulum (ER) lumen for loading onto waiting MHC class I molecules. In contrast, extracellular antigens are presented by MHC class II molecules. Such antigens can be taken up by immature DCs and targeted to lysosomes, where MHC class II molecules are located in the MHC Class II compartment for loading with processed peptide. After maturation, the DCs undergo cytoplasmic reorganization and a redistribution of peptide-MHC class II molecules occurs with their migration to the plasma membrane where they can present the antigen to T cells. Another mechanism, termed cross-presentation, allows some forms of extracellular antigen to also stimulate CD8<sup>+</sup> T cells via the MHC I pathway. This is helpful for immunity against viruses that do not infect DCs directly or against tumour antigens that are not endogenously expressed by DCs [7].

#### ***1.1.2.2.1 The TCR***

The TCR recognises peptide antigens; however this recognition only takes place if the peptide antigen is combined with the MHC – the TCR is specific for peptide antigen combined with the MHC rather than antigen alone. The process of T cell maturation includes random rearrangements of a series of gene segments that encode the antigen-binding receptor chains. This random rearrangement of genes (combinatorial V-J and V-D-J joining and alternative joining of D gene segments), coupled with other mechanisms for generating diversity (like junctional flexibility and P- and N-region nucleotide addition) is capable of generating over 10<sup>9</sup> unique antigenic specificities, though this vast potential is in practise restricted/reduced due to selection processes in

the thymus. These selection processes eliminate T cells with self-reactive receptors, allowing only those which have receptors capable of weakly recognizing antigen associated with MHC molecules to mature [8]. The end result of these processes is the production of a vast, diverse and functional self-tolerant repertoire of TCRs, capable of recognising virtually all antigens.

The TCR has two chains ( $\alpha$  and  $\beta$  or  $\gamma$  and  $\delta$ , the  $\alpha\beta$  heterodimer being the most common), each comprising an amino-terminal domain which exhibits marked sequence variation due to the aforementioned gene rearrangement and a constant domain. Each TCR chain also contains a short connecting sequence (connecting to the other chain of the heterodimer) and a transmembrane region which anchors each chain in the plasma membrane and allows the TCR to interact with the chains of the CD3 complex that allows transport of the TCR to the cell surface and acts to transduce TCR signals [8]. The CD3 complex comprises two heterodimers, made of  $\gamma\epsilon$  and  $\delta\epsilon$  chains, which associate with the TCR (**Figure 1.1**), and a homodimer of  $\zeta\zeta$  chains (some T cells (~10%) will express a heterodimer of  $\eta\zeta$  chains instead). The cytoplasmic tails of the CD3 complex and of the  $\zeta$  chains contain a motif called the immunoreceptor tyrosine-based activation motif (ITAM) which forms the basis of TCR signalling [8].

#### ***1.1.2.2.2 T cell development***

T cells develop from progenitors that are derived from the pluripotent haematopoietic stem cells in the bone marrow and migrate through the blood to the thymus, where T cell development takes place (**Figure 1.2**). Developing T cells (thymocytes) are initially double-negative (ie, not expressing CD4 or CD8), turn double-positive and exit the thymus as single-positive. There are at least four different double-negative stages, which are identified based on the expression of CD44 and CD25. Double-positive thymocytes are selected by self-peptide:self-MHC molecules and if nothing at all is recognized, the cell will most likely suffer death by neglect [8]. However, if the TCR weakly recognizes such antigen, T cell development continues, this process being termed positive selection [9]. However, if the recognition is too strong, cell death by apoptosis usually occurs, in a process known as negative selection [10]. It is interesting to point out that in peripheral lymphoid organs (like the lymph nodes) ligation of the TCR by a peptide:MHC complex would lead to activation and subsequent proliferation and cytokine production; elimination of these T cells in the thymus thus prevents their potentially harmful activation later on. Tissue-specific and developmental-specific proteins would not be expected to be expressed in the thymus

but they are so by stromal cells, namely medullary epithelial cells, under control of the AIRE gene in order to optimise the processes of self-tolerance. Moreover, although negative selection may not remove all T cells reactive to self antigens, there are other mechanisms that prevent their activation once they leave the thymus [2]. Interestingly, natural regulatory T cells are hypothesized to come from the group of cells whose avidities for self-antigens are between the lower end of the negative selection spectrum and the higher end of the remaining positively selected cells [11].

The thymocyte's fate is determined during positive selection. Double-positive cells ( $CD4^+/CD8^+$ ) that are positively selected on MHC class II molecules will eventually become  $CD4^+$  cells, by downregulating CD8; this occurs through signalling via the ITAM pathway. On the other hand, cells positively selected on MHC class I molecules become  $CD8^+$  cells [2]. Unless they recognise antigen, such T cells that emigrate from the thymus and join the recirculating pool in the periphery divide and die off slowly, maintaining T cell homeostasis [2]. Such mature recirculating T cells play a pivotal role in defending the organism against invading pathogens.

#### ***1.1.2.2.3 T cell activation***

Naïve T cells are found concentrated in the lymphoid organs such as the lymph nodes and spleen, but they constantly re-circulate, thus providing an effective immune surveillance system. The naïve T cells enter the LNs from the blood via the high endothelial venules (HEVs) and pass through to the paracortex, a specialized T cell compartment. The high surface expression of CD62L and the chemokine receptor CCR7 on naïve T cells are associated with their migration into the LN. Once there, T cells scan avidly for recognisable antigen; this is presented to them by APCs [12].

Optimum activation of naïve  $CD4^+$  T cells in the LNs requires signals through the TCR via peptide bound to class II MHC as well as secondary signals from costimulatory ligands such as CD80, CD86 and CD40 provided by activated DCs [13]. This two signal requirement also ensures immune responses develop only when they are needed (**Figure 1.3**). Coordinated action between these signals leads to proliferation of naïve cells and begins the process of their differentiation to fully functional effectors capable of secreting high levels of cytokines and participating in helper and inflammatory reactions.

#### ***1.1.2.2.4 T cell differentiation***

CD4<sup>+</sup> T<sub>H</sub> cells activation leads to the generation of a clone of effector T<sub>H</sub> cells. Effector CD4<sup>+</sup> T<sub>H</sub> cells are characterized phenotypically by a decrease in the expression of CD62L and a concomitant increase in CD44 expression. Effector cells of different types can be generated, depending on the cytokine milieu in which the antigenic stimulus is received (**Figure 1.4**). For example, T<sub>H1</sub> cells express the signature transcription factor T-bet and produce IL-2, IFN $\gamma$  and TNF- $\alpha$ . IFN $\gamma$  upregulates IL-12 production by DCs and macrophages and this IL-12, in turn, causes an increase in IFN $\gamma$  production in T<sub>H</sub> cells and so promotes T<sub>H1</sub> cell differentiation in a positive feedback loop. Moreover, IFN $\gamma$  downregulates IL-4 production thus, further promoting a T<sub>H1</sub> phenotype. T<sub>H1</sub> cells contribute to the cellular immune response by improving the bactericidal activities of macrophages, by stimulating proliferation of CTLs and by inducing B cells to produce opsonising antibodies [14].

T<sub>H2</sub> cells promote humoral immunity. They express the transcription factor GATA-3 and can produce IL-4, IL-5, IL-6, IL-10 and IL-13 [15]. IL-4 stimulates T<sub>H</sub> cells to differentiate into T<sub>H2</sub> cells and induces B cell production of neutralising antibodies [14]. IL-10 inhibits IL-2 and IFN $\gamma$  production; it also abrogates IL-12 production by DCs and macrophages.

T<sub>H17</sub> cells are thought to have evolved to cope with a range of extracellular bacterial pathogens although they have been reported to play critical roles in the induction and propagation of autoimmune and allergic inflammation [16]. T<sub>H17</sub> cells can produce IL-17A, IL-17F, IL-6 and IL-21. Transforming growth factor- $\beta$  (TGF- $\beta$ ) and IL-6 act co-operatively and non-redundantly to promote T<sub>H17</sub> commitment although it has been proposed that IL-21 can replace IL-6 and act alongside TGF- $\beta$  [17, 18]. Retinoic acid-related orphan receptors (ROR) are the key transcription factors underlying T<sub>H17</sub> differentiation; both ROR $\alpha$  and ROR $\gamma$ t are critical and somewhat redundant in promoting its differentiation [19, 20].

There is yet another functional type of T cells: regulatory T cells (T<sub>reg</sub>). As well as acting to homeostatically control immune responses, T<sub>reg</sub> cells suppress pathological immune responses to self antigens in autoimmune disorders or foreign antigens in transplantation and graft versus host disease [11]. Naturally occurring T<sub>reg</sub> cells (CD4<sup>+</sup>CD25<sup>+</sup>Foxp3<sup>+</sup> T<sub>reg</sub> cells) arise in the thymus whereas the adaptive T<sub>reg</sub> cells may originate during an immune response; it is thought these differentiate from naïve T cells in the presence of TGF- $\beta$ , following TCR stimulation. Adaptive T<sub>reg</sub> cells can be further

subdivided in Tr1 and T<sub>H</sub>3 cells. The general mechanism by which they act involves the inhibition of the proliferation of other T cell populations [20].

Once effector cells are generated, their functional role requires that they relocate so they can interact with responding B cells and provide help and/or to migrate to the sites of infection. Evidence indicates that these relocations are regulated by the acquisition or increase in expression of multiple adhesion molecules (such as the integrin VLA-4 for T<sub>H</sub>1 cells migrating into the periphery) and a switch in the pattern of chemokine receptor expression [2].

Following pathogen clearance, contraction of the population(s) of effector T cells takes place, as well as the development of long-lived memory cells. Both CD4<sup>+</sup> and CD8<sup>+</sup> T cells can differentiate into two different types of memory cells: effector memory cells and central memory cells. Effector memory T cells can rapidly mature into effector T cells and secrete large amounts of IFN- $\gamma$ , IL-4 and IL-5 after re-stimulation; their integrin profile also suggests that they are specialized for rapidly entering inflamed tissues. On the other hand, central memory T cells take longer to mature into effector T cells after re-stimulation and they seem more programmed to help B cells in the LNs than migrating to inflamed tissues [2].

## 1.2 The lymphoid organs

Lymphocytes circulate in the blood and lymph but can also be found concentrated in some specific locations, called lymphoid organs. These are actually more than just a concentration of lymphocytes: they are organized aggregates of lymphocytes in a framework of non-lymphoid cells [2].

Lymphoid organs can be divided into three groups: central or primary lymphoid organs, peripheral or secondary lymphoid organs, and tertiary lymphoid organs. Primary lymphoid organs are the ones in which production of lymphocytes occurs: the bone marrow (B cells) and the thymus (T cells). The secondary lymphoid organs are those in which adaptive immune responses are initiated, where mature naïve lymphocytes are maintained and where effector cells of the B and T cell lineages are differentiated. The peripheral lymphoid organs comprise the lymph nodes, the spleen and the mucosal lymphoid tissues of the gut, the nasal and respiratory tract, the urogenital tract and other mucosa. They are widely distributed in order to detect and respond to offending antigens wherever they enter the body [21]. Tertiary lymphoid organs are ectopic

accumulations of lymphoid cells that arise in chronic inflammation through a process called lymphoid neogenesis. They arise in non-lymphoid locations [22].

### ***1.2.1 The lymph nodes***

Lymph nodes are situated at the interface of the blood and lymphatic systems, where they contribute to efficient initiation of adaptive immune responses by bringing cell-associated and soluble antigens draining from peripheral tissues together with circulating lymphocytes entering from the blood. LNs have a highly organized and complex architecture composed of distinct cellular compartments and structures, at the heart of which is a non-haematopoietic cell backbone (**Figure 1.5**). Among the cells that are critical for generating this backbone are the fibroblastic reticular cells (FRCs) and the follicular dendritic cells (FDCs) [23].

Lymph nodes are interconnected by a system of lymphatic vessels which drain extracellular fluid from tissues, from the lymph nodes, and back into the blood. They are enveloped by a fibrous capsule and an underlying subcapsular sinus. The lymph node has three distinct regions: cortex, paracortex and medulla. The cortex, located closer to the periphery of the LNs, contains B cells and FDCs. In the centre of the LN lies the paracortex, which is composed of T cells and DCs. The medulla consists of lymphatic tissue. T and B cells circulate constantly through the LN by entering via the HEVs and exiting via efferent lymphatic vessels. Antigen and DCs enter via afferent lymphatic vessels at multiple sites along the capsule [22].

These structural features of the LNs promote interactions between the APCs and the few lymphocytes specific for any given antigen.

## **1.3 Immune tolerance**

Tolerance in the immune system is required in order to prevent immune responses to self components, harmless environmental antigens and necessary foreign materials, like food. T-cell tolerance to self-antigens is generated through both central and peripheral mechanisms. Central tolerance takes place during T cell development in the thymus and includes both negative selection and the generation of natural regulatory T cells as outlined above (section 1.1.2.2.2). By contrast, peripheral tolerance refers to the processes that lead to tolerance if a T cell recognizes self-antigen or harmless foreign antigens outside of the thymus [24, 25].

### ***1.3.1 Peripheral tolerance***

Since central tolerance is not sufficient to prevent autoimmunity or allergy, additional mechanisms have evolved to continually protect against auto-reactive and allergic inflammatory responses in the periphery. These processes include antigen ignorance, cytokine deviation, active suppression, clonal deletion and anergy induction [26].

#### **1.3.1.1 Antigen ignorance**

Antigen ignorance is elicited when the antigen is not presented to the T cells or when their TCR has low avidity to it. In the first case, a physical barrier is involved in preventing the antigen's access to the lymphoid system or, alternatively, in excluding T cells from the site of antigen expression [27].

#### **1.3.1.2 Cytokine deviation**

Cytokine deviation consists of a shift in the differentiation process of naïve T cells to T<sub>H2</sub> cells, which translates into limiting inflammatory cytokine secretion, thus hampering potential autoimmune responses; it is thought to occur after partial signalling via the TCR [28].

#### **1.3.1.3 Active suppression**

Active suppression or dominant tolerance is carried out by regulatory T cells. These may act on effector T cells, suppressing their production of IL-2 and inhibiting their proliferation by means of cell-cell contact but they may also mediate bystander suppression by exerting non-specific suppressive effects on other antigen-reactive cells in the vicinity [26, 29].

Most regulatory T cells express CD25; these CD4<sup>+</sup>CD25<sup>+</sup> T<sub>regs</sub> have the capacity to suppress bystander populations of naïve T cells specific for an unrelated antigen [30, 31]. Moreover, CD4<sup>+</sup>CD25<sup>+</sup> T<sub>regs</sub> can suppress the cytokine production and proliferation of both CD4<sup>+</sup> and CD8<sup>+</sup> T cells *in vitro* [32, 33]. It is thought the immunosuppressive cytokine transforming growth factor- $\beta$  (TGF- $\beta$ ) can lead to the generation of T<sub>regs</sub> in the periphery as mice with a disruption in the TGF- $\beta$  signalling have decreased numbers of CD4<sup>+</sup>CD25<sup>+</sup> T<sub>regs</sub> [34]. At the same time, T cells which are unable to respond to TGF- $\beta$  are not suppressed by T<sub>reg</sub> cells [35].

Natural regulatory T cells (CD4<sup>+</sup>CD25<sup>+</sup>Foxp3<sup>+</sup> T<sub>regs</sub>, section 1.1.2.2.2) arise in the thymus and are considered part of the central tolerance mechanisms, though they too

will emigrate from the thymus and exert their functions elsewhere. The transcription factor Foxp3 drives their differentiation but TCR/MHC class II interactions, IL-2 signalling, B7:CD28 signalling are also required [26].

Also, as discussed above, adaptive regulatory cells can arise after contact with antigen. These cells have been grouped in a number of classes that will be described in the following sections.

#### ***1.3.1.3.1 Tr1***

CD4<sup>+</sup> T regulatory 1 (Tr1) cells were first identified, following multiple stimulations of naïve T cells with antigen, in the presence of high concentrations of IL-10 *in vitro* [36]. Such Tr1 cells produce TGF- $\beta$  but not IL-4, being able to suppress T<sub>H2</sub> responses in an antigen-specific manner [36] and OVA-specific Tr1 cells have been shown to prevent inflammatory bowel disease when they are adoptively transferred into recipient mice subsequently fed OVA [37].

#### ***1.3.1.3.2 T<sub>H3</sub>***

Another subset of CD4<sup>+</sup> T<sub>regs</sub> has been described, which produce varying amounts of the T<sub>H2</sub> cytokines IL-4 and IL-10, but have been shown to be a population distinct from T<sub>H2</sub> cells since they also produce TGF- $\beta$  [37]. The produced IL-10 suppresses T<sub>H1</sub> activity via downregulation of the expression of costimulatory molecules and IL-12 production by APCs [38].

#### ***1.3.1.3.3 CD8<sup>+</sup> suppressor T cells***

Early studies pointed towards the involvement of CD8<sup>+</sup> T cells in active suppression although their mechanisms of action were not fully elucidated [39, 40]. While systemic tolerance was unaffected, CD8<sup>-/-</sup> mice exhibited deficient local suppression of IgA responses in the gut after feeding antigen, indicating that CD8<sup>+</sup> T<sub>regs</sub> may be important for the regulation of mucosal immune responses [41]. Subsequently, a population of CD8<sup>+</sup> T<sub>regs</sub> which expresses Foxp3 was found in human; these CD8<sup>+</sup> T<sub>regs</sub> act by secretion of the CC chemokine ligand 4 (CCL4) which can inhibit T cell activation by interfering with TCR signalling [42].

#### **1.3.1.4 Clonal deletion**

Clonal deletion or activation-induced cell death (AICD) in T lymphocytes provides a mechanism of tolerance in both a central (when it is happening in the context

of negative selection) and a peripheral context. Clonal deletion leads to the elimination of reactive T cell clones upon encountering antigen [43] via a process in which activation through the TCR results in apoptosis. AICD can occur in a cell-autonomous manner (for example, during negative selection) and is influenced by the nature of the initial T-cell activation events [44]. In peripheral T cells it is often caused by interaction of the death ligand, Fas ligand (CD95 ligand, FasL) with Fas (which is expressed in T cells); FasL expression can be induced in T cells – leading to T cell suicide – or in nonlymphoid tissues in response to activated T lymphocytes – leading to T cell fratricide - [44].

### **1.3.1.5 Anergy induction**

Anergy is the functional inactivation of T cells. Anergy induction occurs upon encountering antigen presented by immature DCs, after which naïve T cells fail to mount a productive immune response and most importantly, will also be hyporesponsive to re-challenge. Anergy is therefore a long-lived, cell-intrinsic mechanism that contributes to the prevention of autoimmune and allergic diseases [43]. Hyporesponsiveness, or unresponsiveness, translates as a lack of interleukin-2 production by these T cells, as well as non-proliferation in response to antigen [45].

Anergy induction occurs when T cells are stimulated through the TCR in the absence of co-stimulation [46, 47]. Several methods have been used to mimic induction of such anergy *in vitro* [48-50], including exposure to immobilised anti-CD3 antibodies in the absence of co-stimulatory signals [49, 51]. Under such conditions, relative to priming conditions (TCR ligation + co-stimulation, mimicked by anti-CD3+anti-CD28), re-stimulation with antigen leads to downregulated IL-2 production and decreased proliferation of the T cells. This state of anergy can be (partially) reversed by the addition of exogenous IL-2 to the T cells [52].

While some experimental protocols of tolerance induce both anergic and regulatory T cells, the primary factors that differentially promote the appearance of one group of these cells over the other have not been identified [26]. Moreover, to date, the identification of a marker specific for anergic T cells has remained elusive.

## 1.4 T cell signalling

### 1.4.1 TCR-mediated signalling

TCR binding by the MHC-peptide complex results in the activation of the Src kinases, Fyn and Lck, the latter being associated with the co-receptors CD4 and CD8 (**Figure 1.6**). Activated Lck and/or Fyn then phosphorylate the ITAMs in the  $\zeta$  chains associated with the TCR-CD3 complex [53] with the result that the phosphorylated ITAMs recruit the tyrosine kinase  $\zeta$ -associated protein of 70 kDa (ZAP-70) [14]. ZAP-70 is then phosphorylated and activated by Lck/Fyn leading to the phosphorylation of the transmembrane adapter protein, linker for activation of T cells (LAT) [54]. Phosphorylated LAT delivers the activation signals through recruitment and assembly of a signalosome containing Grb2, Grb2-related adapter downstream of Shc (GADS), SH2 domain-containing leukocyte protein of 76 kDa (SLP-76), and phospholipase C $\gamma$ 1 (PLC $\gamma$ -1) [55].

To counter-regulate these tyrosine kinase and lipid signals, TCR signalling can be negatively regulated by several kinases and phosphatases, including C-terminal Src kinase (Csk), SH2 domain-containing phosphatases 1 and 2 (SHP-1/2), SH2 domain-containing inositol phosphatase (SHIP) and Phosphatase and Tensin homolog deleted on chromosome 10 (PTEN) [56]. These actions occur in a highly organized membrane structure, the immunological synapse (IS).

PLC $\gamma$ -1, after activation by phosphorylation, hydrolyses phosphatidylinositol 4, 5-bisphosphate (PIP<sub>2</sub>) to yield inositol 1, 4, 5-trisphosphate (IP<sub>3</sub>) and diacylglycerol (DAG) [14]. IP<sub>3</sub> binds to its receptor on the membrane of the ER triggering Ca<sup>2+</sup> release and subsequent Ca<sup>2+</sup> influx through plasma membrane channels [26]. This leads to an increased intracellular Ca<sup>2+</sup> concentration which is required for the activation of calmodulin, which in turn activates calcineurin (Cn). Cn is a calcium-dependent phosphatase consisting of a catalytic and calmodulin-binding subunit A (CnA) and a Ca<sup>2+</sup>-binding regulatory subunit B (CnB); in resting T cells, enzymatic activity of CnA is kept inactive by binding to CnB. Calmodulin binding to CnA after the binding of Ca<sup>2+</sup> to CnB results in the activation of enzymatic activity of CnA [57]. Activated Cn dephosphorylates the transcription factor nuclear factor of activated T cells (NFAT), revealing its nuclear localisation sequence, allowing its translocation to the nucleus where it associates with activator protein-1 (AP-1) to direct the synthesis of genes like IL-2 [58]. AP-1 activation is discussed below.

DAG promotes membrane association and activation of signalling proteins with C1 domains like Ras guanyl-releasing protein 1 (RasGRP1) and various members of the protein kinase C (PKC) family [45, 59] to propagate intermediate downstream signalling events including serine/threonine phosphorylation,  $\text{Ca}^{2+}$  mobilisation, G-protein activation and membrane lipid phosphorylation [14]. For example, the GADS-mediated recruitment of the guanine nucleotide exchange factor (GEF) RasGRP1 promotes the conversion of Ras-GDP (inactive form) to Ras-GTP (active form) in a DAG-dependent manner [60-62]. In addition, Grb2 forms a complex with Son of Sevenless (SOS), a GEF also capable of promoting exchange of guanosine triphosphate (GTP) for guanosine diphosphate (GDP) on Ras [63]. Thus GADS-mediated recruitment of the Ras GEFs, SOS and RasGRP1 to the signalosome couples the TCR to Ras activation. Consequently, active Ras-GTP recruits the serine/threonine kinase Raf1 to the plasma membrane [64], where it is fully activated by phosphorylation involving p21-activated kinase-1 (Pak1) and Pak3 [65]. Pak1 and Pak3 are activated by Cdc42 and Rac, and this will be discussed further below. Activated Raf1 then phosphorylates the mitogen-activated protein kinase kinase (MAPKK), MEK (MAPK extracellular signal-regulated kinase (Erk) kinase) which, in turn, phosphorylates Erk [67, 68]. Erk activates Elk-1 [66], a transcription factor required for transactivation of c-Fos [67].

A major role of the PKC family of serine/threonine kinases in T cell activation lies in the activation of the transcription factor nuclear factor  $\kappa\text{B}$  (NF- $\kappa\text{B}$ ). Of the isoforms present in T cells, PKC $\theta$  is probably the only one that localizes to the IS during antigen-specific interactions [68]. Here, it mediates the phosphorylation of caspase-recruitment domain (CARD)-containing membrane associated guanylate kinase protein 1 (Carma1) (also known as CARD11), an event that induces binding of Carma1 to B cell lymphoma 10 (Bcl10) and mucosa-associated-lymphoid-tissue lymphoma translocation gene 1 (Malt1), thus forming the Carma1-Bcl10-Malt1 (CBM) complex [69]. Malt1, acting from the CBM complex, recruits the E3 ubiquitin-protein ligase tumour-necrosis-factor-receptor-associated factor 6 (Traf6) which promotes the activation of the inhibitor of NF- $\kappa\text{B}$  (I $\kappa\text{B}$ ) kinase (IKK) complex [70, 71]. The IKK complex is formed by IKK $\alpha$ , IKK $\beta$  and IKK $\gamma$  (also known as NEMO); the ubiquitination of the catalytically inactive subunit IKK $\gamma$  allows the phosphorylation of IKK $\alpha$  and IKK $\beta$  subunits, fully activating IKK; it is thought Traf6 is also involved in the recruitment of Tak1, the serine/threonine thought to phosphorylate IKK $\alpha$  and IKK $\beta$  [72].

Once activated, the IKK complex phosphorylates I $\kappa$ B, which in resting T cells associates with NF- $\kappa$ B, retaining it in the cytoplasm. However, following IKK-mediated phosphorylation and consequent degradation of I $\kappa$ B, NF- $\kappa$ B translocates to the nucleus [73]. The NF- $\kappa$ B transcription factor family comprises the Rel proteins p65 (RelA), RelB, c-Rel, NF- $\kappa$ B1 (p105/p50) and NF- $\kappa$ B2 (p100/p52), which can form various combinations of homo- and heterodimers [73]. NF- $\kappa$ B has many and diverse roles in adaptive as well as innate immunity; in T cell activation it is involved in mediating antiapoptotic effects as well as promoting cytokine production like IL-2, IL-12, IFN $\gamma$  [74].

### ***1.4.2 CD28-mediated signalling***

The signalling events described so far report only to those emanating from the TCR alone. However, as stated before, these signals are not sufficient for effective T cell priming; for this to occur, co-stimulation is required (**Figure 1.7**) [8]. Indeed, in the absence of co-stimulation, TCR-signalling results in a state of hypo-responsiveness characterised by a lack of IL-2 production, which is required for autocrine and paracrine stimulation of T cell proliferation associated with priming [45].

T cell co-stimulation via CD28 engagement enhances TCR proximal signals through Lck and phosphatidylinositol 3-kinase (PI3K) activation. PI3K activation is necessary for optimal lymphocyte proliferation; it consists of a p85 regulatory subunit, which is recruited to CD28 and a p110 catalytic subunit, which is activated by the regulatory subunit when recruited by CD28 [75]. PI3K is then in position to convert PIP<sub>2</sub> into the second messenger phosphatidylinositol 3, 4, 5-trisphosphate (PIP<sub>3</sub>) which recruits cytoplasmic proteins containing pleckstrin homology (PH) domains to the plasma membrane [75]. Phosphoinositide-dependent kinase 1 (PDK1) and Akt (also known as PKB) are two of these proteins and their presence at the same site leads to Akt phosphorylation and subsequent activation by PDK1 [76]. Activated Akt will contribute to the activation of NF- $\kappa$ B by what is thought to be indirect activation of the IKK complex [80]. By contrast, PTEN negatively regulates Akt activation by dephosphorylating PIP<sub>3</sub>, resulting in PIP<sub>2</sub> production [77].

PDK1 may also phosphorylate PKC (although its membrane localisation is not PH domain-mediated), thus contributing to its full activation and hence, leading to more NF- $\kappa$ B nuclear translocation [78].

Co-stimulation via CD28 also allows for the activation of two more classes of MAPKs: Jnk (c-Jun N-terminal kinase) and p38 MAPK. To understand how this happens it is important to describe the mechanism of action of Vav1, a GEF with a PH domain. Vav1 activation occurs in two waves, the first being mediated by Fyn immediately after TCR ligation and the second by ZAP-70 after its recruitment to the IS. Binding to PIP<sub>3</sub> (mediated by the PH domain) enhances its GEF activity and such Vav activation leads to further cytoskeletal rearrangements, IS stabilisation and signal transduction [79]. Thus, Vav1 associates with phosphorylated SLP-76 via its SH2 domain and also binds the Tec family protein tyrosine kinase (PTK) and IL-2 tyrosine kinase (Itk), which are required for optimal PLC $\gamma$ -1 activation [80]. Vav1 then activates the plasma membrane-localised Cdc42 and Rac, members of the Rho family of GTPases, which in turn activate Pak1 and Pak3 [65, 81]. Cdc42 can also activate Wiskott-Aldrich syndrome protein (WASP) which leads to actin polymerisation and cytoskeletal rearrangement [82]. The Paks will activate MKK4 (also known as SEK1) which in turn phosphorylates Jnk, thus activating it [83, 84] resulting in phosphorylation of c-Jun [85]. These Paks are also thought to activate MKK3/6 which in turn phosphorylates p38 MAPK [86]. Similarly to Erk, p38 MAPK contributes to the activation of c-Fos [87], and the activation of c-Fos and Jun resulting from Erk, p38 and Jnk MAPkinase recruitment allows formation of the heterodimeric transcription factor AP-1, which is necessary but not sufficient for IL-2 transcription and production [58].

Thus integration of the signalling events emanating from TCR and CD28 results in the activation of the full complement of transcription factors required for cell survival, proliferation and cytokine production, all necessary components of any effective immune response. These transcription factors are most prominently NFAT and NF- $\kappa$ B, and similarly IL-2 is the most important immediate product of these signalling transduction pathways leading to T cell priming.

### ***1.4.3 The role of inhibitory co-stimulatory molecules***

The CD28 family of receptors (CD28, cytotoxic T-lymphocyte-associated antigen 4 [CTLA-4, also known as CD152], inducible co-stimulator [ICOS], program death-1 [PD-1, also known as CD279], and B- and T-lymphocyte attenuator [BTLA, also known as CD272]) plays a critical role in controlling the adaptive arm of the immune response [88]. CD28 is constitutively expressed on T cells but in contrast CTLA-4, ICOS, PD-1 and BTLA are sequentially induced following T-cell activation [89]. T cell co-stimulators and co-inhibitors belong to two structural families of surface proteins, either

the immunoglobulin superfamily (to which the B7 family of ligands belongs) or the tumour necrosis factor receptor (TNFR) superfamily. Costimulatory members of the TNFR superfamily include OX40, CD40, HVEM and others [90].

CTLA-4 shows high homology with CD28 and is capable of binding CD80 and CD86 at an even higher affinity [91, 92]. However, unlike CD28, it is responsible for inhibiting the activation of T cells [93]. This effect is illustrated by the phenotype of CTLA-4 deficient mice, which develop a fatal lymphoproliferative disease with massive organ infiltration by immune cells [94]. This disease is mainly mediated by CD4<sup>+</sup> T cells; these were characterized as being highly activated, showing enhanced proliferation and increased production of T<sub>H</sub>2 associated cytokines [95]. Normally, upon T cell activation CTLA-4 surface expression increases and out-competes CD28 for ligand (CD80/86) binding [96]. Such crosslinking of CTLA-4 leads to cell cycle arrest at the G1 phase and reduced production of IL-2, which is accompanied by reduced activation of the transcription factors NF- $\kappa$ B, NFAT and AP-1 [97-99]. Precisely how CTLA-4 is able to mediate consequent inhibitory signals remains elusive, although upregulation of Cbl-b levels appears to be involved [100].

By contrast, ICOS has a unique ligand, ICOS-L (also known as CD275, B7RP-1 and B7-H2) and induction of ICOS expression is influenced by both TCR and CD28 signalling. To date, the p85 $\alpha$  subunit of PI3K is the only signalling molecule shown to interact with ICOS and ICOS stimulation results in greater recruitment, phosphorylation and activation of Akt. Like CD28, ICOS delivers positive signals and has been shown to play roles in T-cell differentiation, cytokine secretion (increased production of IL-4, IL-6 and IL-10), and survival (namely by inhibiting AICD) [89].

PD-1 is an inhibitory receptor which binds to PD-ligand1 (PD-L1, also known as B7-H1 and CD273) and PD-L2 (also known as B7-DC and CD274) [14]. PD-L1 is constitutively expressed by lymphoid cells (T and B cells), myeloid cells (DCs, macrophages and mast cells) and non-haematopoietic cells ( $\beta$  cells of the pancreas and endothelial cells of the heart) [101, 102] whereas PD-L2 is inducibly expressed on DCs, macrophages and mast cells [103]. Before their exit to the periphery, T cells in lymphoid organs rapidly up-regulate PD-1 upon tolerogen recognition [104]; this upregulation is thought to be mediated by the common gamma-chain cytokines IL-2, IL-7, IL-15, and IL-21 [105]. The role of PD-1 in peripheral tolerance was first indicated by PD-1 knockout mice, which spontaneously develop autoimmune diseases [106]. Moreover, both PD-1 and its ligands are required for the inhibitory signal to occur as the loss of the PD-1:PD-L1 interaction (by antibody blockade) was shown to

break CD8<sup>+</sup> T cell tolerance to intestinal self-antigen, leading to severe enteric autoimmunity [107]. Further work revealed PD-L1 expression in non-haematopoietic tissue (pancreatic islets) protected against immunopathology after transplantation of syngeneic islets into diabetic recipients as such PD-L1 signalling inhibited pathogenic self-reactive CD4<sup>+</sup> T cell-mediated tissue destruction and effector cytokine production [108]. Indeed, when T cells are still in the lymphoid organs, ablation of the PD-1:PD-L1 interaction prevents anergy and, most interestingly, blockade of this interaction can in fact render anergic T cells responsive to antigen [104].

Finally, BTLA is an inhibitory receptor preferentially expressed in T<sub>H</sub>1 cells. BTLA engagement of HVEM (its only ligand) produces pro-inflammatory signals via activation of NF- $\kappa$ B whereas HVEM engagement of BTLA produces inhibitory signals through SHP-1/2. HVEM is highly expressed in naïve T cells but its expression decreases during T cell activation and is restored to high levels as cells become quiescent [90].

#### ***1.4.4 Signalling in anergy***

It is curious to note that the induction of anergy leads initially to the clonal expansion of T cells. In fact, anergy induction requires T cell activation and new protein synthesis [109]. Nevertheless, relating to proximal TCR signalling, while still capable of being recruited to the TCR-CD3 complex under conditions of anergy, the levels of tyrosine phosphorylation of ZAP-70 were significantly reduced compared to primed cells [110]. Moreover, the recruitment and localisation of LAT to the IS also appears to be defective in anergic T cells as a result of impaired palmitoylation of LAT [111]. The mechanisms thought to be involved in anergy induction and maintenance include transcriptional regulation of cytokines, inhibition of cell cycle progression and blockade of intracellular signalling [112, 113]. An overview of the modulation of signalling pathways involved in the induction and the maintenance of anergy can be found in **Figure 1.8** and **Figure 1.9**, respectively.

In anergy induction, Ca<sup>2+</sup> flux and the subsequent mobilisation of NFAT occurs as in priming [114]. However, in the absence of co-stimulatory signalling, IL-2 production does not occur; this is due to a block at the transcriptional level caused by reduced binding of the AP-1 heterodimer complex to the IL-2 promoter. The AP-1 complex is no longer being formed in the nucleus due to incomplete activation of the Jnk and p38 MAPK pathways as CD28 signalling is required for their full activation [45]. Incomplete activation of Jnk and p38 MAPK also reflects in reduced NF- $\kappa$ B activity

[112]. In anergic T cells  $\text{Ca}^{2+}$ -mediated translocation of NFAT to the nucleus is unaffected but induction of c-Fos and Jun is severely impaired as a result of downregulated activity of Erk and Jnk [115].

Although at first sight perhaps rather surprising, NFAT is in fact critical for anergy induction, as inhibiting Cn with cyclosporin A to prevent NFAT translocation into the nucleus also blocks anergy induction [49]. Clearly, the acquisition of an anergic phenotype is not simply a passive default process due to lack of costimulatory signalling but rather a very active process as seen by the induction of negative regulators of T cell signalling [116]. Induction of these negative regulators at the transcriptional level is in part mediated by NFAT.

An immediate target of NFAT-mediated transcription following  $\text{Ca}^{2+}$  mobilisation in T cells is the early growth response (Egr) family of transcription factors. Microarray analysis of  $\text{CD4}^+$   $\text{T}_{\text{H}1}$ , clone A.E7 cells either anergised with anti-CD3 antibody alone or fully stimulated with both anti-CD3 and anti-CD28 antibodies indicated that high levels of expression of Egr2 (but not Egr1), persisted for 2 or 5 days in anergised T cells [117]. Moreover, treatment of T cells with Egr2-targeted small interfering RNA (siRNA) before antibody stimulation prevented the induction of anergy. Egr2 and Egr3 were both found upregulated in anergised  $\text{CD4}^+$   $\text{T}_{\text{H}1}$ , clone A.E7 cells and their transduction with Egr2 or Egr3 decreased *Il2* transcription while increasing Cbl-b expression [118]. By contrast, *in vivo* peptide administration revealed Egr3-deficient T cells to be resistant to anergy induction [118]. Egr2 and Egr3 expression is dependent on the activity of calcineurin and PKC [118]. Together these results indicate Egr2 and Egr3 have a role in conferring the anergic state; although their mechanism of action is yet to be fully determined; it is possible that in the absence of CD28 co-stimulatory signals, transcriptional complexes of NFAT and Egr proteins (or Egr proteins alone) drive the induction of the anergic programme.

Another target of NFAT-mediated transcription is the transcriptional repressor of the *Il2* gene Ikaros. Ikaros is required for the induction of anergy but is also expressed in naïve cells, where it blocks *Il2* transcription in the absence of co-stimulatory signals [119]. During anergy induction its mRNA expression is upregulated [116] and it binds to the *Il2* promoter where it induces histone deacetylation, an epigenetic change enabling stable repression of *Il2* transcription [120]. In antigen-experienced  $\text{T}_{\text{H}1}$  cells activation through the TCR and CD28 downregulates Ikaros activity while treatment with ionomycin upregulates it [112, 120]. Curiously, therefore, Ikaros has also been

identified as a positive regulator for T<sub>H</sub>2 cell differentiation by promoting chromatin accessibility for T<sub>H</sub>2-related transcription factors [121].

NFAT is also responsible for proximal TCR signalling defects in anergic cells. For instance, it induces diacylglycerol kinase (DGK) which inhibits RasGRP activation by converting the secondary messenger DAG into phosphatidic acid (PA), thus depleting DAG levels [116]. Both DGK $\alpha$  and DGK $\zeta$  contribute to such blockage of the Erk MAPK pathway and as such, they are both required for the induction of anergy [122, 123]. There are also a number of additional signals that have been reported to block the Erk MAPK pathway, without affecting DGK expression and leading to the establishment of anergy [124]. For example, Fyn-mediated activation (by means of phosphorylation) of phosphoprotein associated with glycosphingolipid-enriched microdomains (PAG) leads to the recruitment of Csk to the membrane, where Csk will phosphorylate and inhibit Lck [125]. In fact, a decrease in the level of Lck with a concomitant increase in the level of Fyn in anergic T<sub>H</sub>1 cell clones had long been observed [126-128].

Indeed, lack of full Erk MAPK pathway activation has long been associated with anergy [129]. For example, another way that this pathway can be inhibited in anergy is via the GTPase, Rap1 as Rap1 accumulation has been shown to suppress Erk activation in anergic T cells [48]. Moreover, while anergic antigen-specific T cells have less phospho-Erk than primed cells following re-stimulation with antigen [130], Rap1 was shown to be expressed by more anergic than primed T cells. Also, whereas phospho-Erk localises to the TCR and lipid rafts in such primed cells, it exhibits a diffuse cellular distribution in anergic cells. By contrast, Rap1 localises with the TCR and lipid raft structures in anergic cells, but not in primed cells [131]. The precise mechanisms involved are not clear but the Fyn-Cbl-CrkL-C3G-Rap1 signalling complex, which cannot be found in primed T cells, allows inhibition of the Erk MAPK pathway to occur by Rap1 competing with, and sequestering Raf1 from Ras [48]. C3G is a GEF which activates Rap1 [132] whilst CrkL, a SH2-containing adaptor protein is involved in the recruitment of C3G [133]. It is hypothesised Cbl could enable CrkL's recruitment, though the exact mechanism is still open to debate [134]. The Cbl proteins, as well as Itch and Grail are E3 ubiquitin protein ligases; these have been reported to have diverse roles in anergy, which will be addressed further below.

IL-2R-mediated signalling is required for T cells to escape anergy induction. The *Ii2* gene is transcribed via CD28 co-stimulation, thus contributing to anergy avoidance. IL-2 binding to the IL-2R induces activation of the MAPK and Jak3-Stat5 pathways

although avoidance of anergy appears to be as a result of the PI3K-Akt pathway [112] possibly because Akt targets p27<sup>kip1</sup>, a cyclin-dependent kinase (CDK) inhibitor (CKI) for proteolytic degradation, leading to de-repression of CDK1/2 and cell cycle progression [112]. p27<sup>kip1</sup> can also bind RhoA, inhibiting actin polymerisation and co-operation with Rap1 [135]; it can also bind Jab1, which is a co-activator of Jun, thus inhibiting gene transactivation by AP-1 [136].

#### ***1.4.5 The immunological synapse***

In lymphocytes, many of the molecules involved in cell signalling are associated with detergent-insoluble, sphingolipid and cholesterol-rich domains in the plasma cell membrane, known as lipid rafts [14]. These structures play a role in T cell signalling as they function as specialised signalling compartments in the cell membrane, wherein molecules are recruited, phosphorylated and activated [137]. For example, in resting T cells the TCR-CD3 complex is thought to reside outside lipid rafts translocating to it after  $\zeta$  chain phosphorylation by Lck [138]. It is believed lipid raft macrodomains assemble to form the IS as the composition of lipid rafts is indistinguishable from that of the IS [14].

The IS is composed of several molecules which are found together and spatially segregated from others at the contact interface between a T cell and an APC [14]. The IS is thought to be the fundamental level of cellular organization that must be achieved to obtain full T-cell activation [139, 140]. It works by allowing relatively small molecules to come into contact with their ligands on the APC, which would be difficult to occur as they would be blocked by large, abundant glycoproteins on an unpolarised T cell. High-resolution immunofluorescence imaging of T cell-APC conjugates reveals that a mature IS has a specific doughnut shaped arrangement in which molecules are arranged in distinct spatial domains: smaller molecules such as the TCR, CD4 and CD28, which originate from small clusters of lipid rafts, coalesce to form a single, large molecular platform called the central supramolecular activation complex (cSMAC) at the T cell-APC contact site; larger molecules such as leukocyte function-associated antigen-1 (LFA-1) and talin form the peripheral SMAC (pSMAC) (**Figure 1.10**) [140]. As mentioned earlier, the localisation of LAT to the IS is defective in anergic T cells and moreover, upon re-stimulation with antigen, anergic T cells fail to translocate CD3 into the cSMAC and hence, assembly of the IS in human anergic T cells is arrested [141].

## 1.5 Apoptosis and cell cycle

The numbers of a population of cells can be controlled via programmed cell death, proliferation and differentiation. Programmed cell death, also called apoptosis, is a tightly regulated and multi-step process which requires the cleavage of intracellular proteins, DNA degradation and loss of cell shape and volume. Proliferation is dependent on cell cycle progression, which usually also involves cell growth. Differentiation implies functional differences between cells which usually reflect on the expression of different surface proteins and other immune mediators, in the case of T cells.

### 1.5.1 Apoptosis

Apoptosis provides a mechanism for the disposal of unwanted cells in a coordinated manner and without the generation of inflammation (unlike necrosis, which also leads to cell death, but arising from injury, the organelles swell and the cell bursts, releasing its intracellular contents which can trigger an inflammatory response and potentially, autoimmunity). This mechanism also protects the organism by enabling the destruction of damaged or potentially harmful cells [142].

Most of the observed changes associated with apoptosis (such as DNA degradation, protein cleavage, etc) are implemented by a set of cysteine proteases called caspases. Caspases are localised in the cytosol in an inactive pro-caspase form and upon apoptotic stimuli are converted into active caspases. Caspases can be divided into two main groups: the initiator caspases which are processed first, and the effector caspases which can be activated by initiator caspases to drive the ordered disassembly of the apoptotic cell [143].

There are two major pathways known to activate caspase-dependent apoptosis: the classical caspase pathway and the mitochondrial pathway. The classical caspase, or extrinsic, pathway is initiated upon ligation of death receptors such as Fas/CD95 which in turn recruit Fas associated protein with a death domain (FADD). FADD can convert pro-caspase 8 into caspase 8 (active form), which can then activate the effector caspase, caspase 3 [144].

On the other hand, the mitochondrial, or intrinsic, pathway involves the loss of mitochondrial membrane potential. The B cell lymphoma-2 (Bcl-2) family proteins are important regulators of the mitochondrial pathway [145]. Bcl-2 family members are regulated predominantly at the level of transcription and the balance of expression of

pro-survival and pro-apoptotic Bcl-2 family proteins determines the fate of the cell [146]. In activated T cells, PKC $\theta$ -mediated NF- $\kappa$ B transcriptional activity leads to upregulation of Bcl-2 and Bcl-x<sub>L</sub>, two pro-survival members of the Bcl-2 family [147].

### ***1.5.2 Cell cycle***

Proliferation requires cell cycle progression while cell cycle arrest prevents the expansion of a population of cells. The eukaryotic cell cycle comprises four distinct phases. G1 is characterised by the cell undergoing induction of gene expression and protein synthesis, resulting in an increase in cell size and production of all the proteins required for DNA synthesis. DNA duplication occurs in S phase (synthesis) and after chromosome replication, a second growth period, G2, allows the cell to monitor DNA integrity and cell growth prior to M phase (mitosis) when the cell finally divides. The resulting daughter cells either immediately enter G1, potentially to go through the full cycle again or alternatively, enter the G0 phase (quiescence) [148].

To make sure cell division yields functional and DNA-healthy daughter cells, checkpoints exist throughout the cell cycle, namely in G1, G2 and M phases [149]. Cell cycle checkpoints and cell cycle progression are mediated by a variety of signalling molecules. Progression through the cell cycle, which is crucial for optimal activation of T cells, is driven by complexes formed by cyclins and CDKs. CDK activation requires cyclins; depending of the phase of cell cycle, different cyclins associate with the CDKs [150]. Activity of the cyclin/CDK complexes is inhibited by direct binding of CKIs, such as p27<sup>kip1</sup>, whose expression is downregulated by transcriptional and post-transcriptional mechanisms [151].

The commitment of cells to DNA synthesis occurs at the G1 checkpoint; upon receiving an activation signal, Ras-mediated Erk activation and subsequent AP-1 transcription are induced, with the latter causing the upregulation of cyclin D [152]. Cyclin D can then bind to CDKs 4 or 6 and the resulting complexes promote G1/S transition by initiating the sequential phosphorylation of the retinoblastoma protein (Rb). Hypophosphorylated Rb binds the transcription factor E2F, which is required for transcription of S phase genes such as cyclins E and A. Cyclin E-CDK2 and cyclin A-CDK1/2 complexes will further phosphorylate and inactivate Rb, leading to cell cycle progression [153].

p27<sup>kip1</sup>, which can inhibit CDK4/6 as well as CDK1/2 is most highly expressed in quiescent cells [151]. It exerts its inhibitory effects on CDK activity when it is localised in the nucleus [154] and consistent with this, Erk activation has been associated with the

nuclear export of p27<sup>kip1</sup> [155]. Once in the cytoplasm p27<sup>kip1</sup> binds to SCF<sup>Skp2</sup>, a protein complex that targets it for ubiquitination and degradation [156].

## 1.6 Ubiquitination

Ubiquitination, also sometimes referred to as ubiquitylation or ubiquitynylation, is a posttranslational modification of proteins that involves the conjugation of ubiquitin to a target protein. It has a broad impact on many cellular processes, including transport, DNA replication, modification of protein function, facilitation of cell-surface-receptor turnover and control of gene transcription.

The steps involved in ubiquitination are as follows (**Figure 1.11**): an ubiquitin-activating enzyme, enzyme 1 (E1) binds ubiquitin, a 76-amino-acid peptide, by forming a thioester bond via its active site cysteine with the carboxyl group of glycine 76 of ubiquitin. The activated ubiquitin molecule is then transferred to the cysteine residue of the active site of an ubiquitin-conjugating enzyme, enzyme 2 (E2). The ubiquitin-E2 complex is then recruited by a third enzyme, a ubiquitin-protein ligase, enzyme 3 (E3), which specifically binds a protein substrate and facilitates the transfer of ubiquitin from the E2 to the target protein by promoting the formation of an isopeptide bond between a lysine residue in the substrate and the active carboxy terminus of ubiquitin [157].

Upon the addition of the first ubiquitin to the substrate, several other ubiquitins may be added (polyubiquitination) essentially by repetition of the same biochemical reaction, but with the modification that the isopeptide bond is formed between glycine 76 of the activated ubiquitin and the  $\epsilon$  group of one of seven lysines (K6, K11, K27, K29, K33, K48 and K63) of the ubiquitin moiety already attached to the substrate to form an elongated ubiquitin chain [158]. Alternatively, a substrate can be tagged with a single ubiquitin molecule (monoubiquitination) and such monoubiquitination can occur on a single lysine residue or on several lysine residues, leading to multiubiquitinated substrates. The same E2-E3 complex can have the dual role of adding either a monomer of ubiquitin or elongating the chain. Thus, the decision to add one or more ubiquitin moieties does not appear to be regulated by fundamental differences between E3s [159].

Whilst monoubiquitination, multiubiquitination and polyubiquitination via K63 are usually associated with non-degradative processes, including cellular trafficking, subcellular location, function, stability, protein-protein recognition, and activity, in general, substrates with a polyubiquitin chain of four or more ubiquitins linked through K48 are destined to be degraded by the 26S proteasome [160-163]. The 26S proteasome

catalyses the unfolding and proteolysis of its substrates and is formed by two complexes: the 20S core complex and the 19S regulatory complex. The 19S complex, located at either end of the 20S complex, recognizes polyubiquitinated substrates and unfolds them for degradation by proteases to simple aminoacids by the proteolytic active sites within the interior chamber of the proteasome formed by the cylindrical stack of four heptameric rings of the 20S complex [157]. Polyubiquitination via K11, K29 and K33 is also associated with non-degradative processes, but there are less examples of this type of cellular regulation [164]. Polyubiquitination via K6 and K27 is not yet very well understood [165]. Despite not promoting proteasomal-mediated degradation of proteins, K63-linked ubiquitination appears to have an important role in targeting proteins to the lysosome, where they are processed [160].

It is important to appreciate that ubiquitination is a reversible process, an essential feature for regulating subcellular location, protein-protein interaction and, generally speaking, protein function [166]. Regulatory roles of ubiquitin arise partially due to the fact that ubiquitin and polyubiquitin chains serve as three-dimensional signals that are recognised by many different types of ubiquitin-binding domain-containing proteins [167]. The removal of ubiquitin from proteins is carried out by deubiquitylation enzymes (DUBs), which are proteases that cleave ubiquitin chains from protein substrates or their degraded fragments [166].

Target substrates, despite being quite diverse, are recognized with high selectivity due to the existence of many E3s (there are more E3s than E2s and more E2s than E1s) with different substrate specificities recognizing only a few proteins that share a particular ubiquitination signal, usually a small primary sequence motif [164]. The recognition of this primary signal allows the substrate to be marked with the secondary signal, ubiquitin, which can be extended; all the proteasome needs for substrate recognition is a K48-linked polyubiquitin chain of four or more ubiquitins, allowing it to successfully interact with and degrade many unrelated proteins [158].

The concept that cellular proteins can be targeted for modification by small proteins is now expanding beyond ubiquitin. A growing list of ubiquitin-like (UBL) proteins, which also bind substrate proteins, thus altering their fate or function is being identified and characterized [168]. UBLs include at least five distinct proteins that are related in sequence to ubiquitin - such as SUMO-1 and ISG15, which has been reported as involved in immune system regulation - as well as two that are not [157, 164].

### **1.6.1 Ubiquitination in T cell tolerance**

Ubiquitination of selected target proteins has been shown to contribute to both central tolerance and peripheral tolerance mechanisms [157]. As ubiquitination can affect signalling pathways in multiple ways, from reversible protein inactivation to protein degradation, it is a plastic and, as such, useful process to rapidly modulate signals [169]. In T cell tolerance both E3 ubiquitin-protein ligases and DUBs have been reported to be specifically induced and/or exert specific activity towards or against the acquisition of a certain functional outcome [157, 166].

#### **1.6.1.1 E3 ubiquitin-protein ligases**

E3 ligases play a pivotal role in ubiquitination, because they recognize the target acceptor protein and so dictate the specificity of the reaction. Interestingly, they often catalyse the transfer of ubiquitin from E2 not only to target proteins but also to themselves (self-ubiquitination) [170]. They exist both as multisubunit enzyme complexes and as single chain polypeptides and can be classified into three major families: RING- (Really interesting new gene), HECT- (homologous to the E6-associated protein C terminus) and U-box-type E3 proteins [171]. No information exists so far regarding involvement of U-box E3s in vertebrate immunity. However, the single polypeptide RING- and HECT-type E3 ligases have been implicated in regulating immunity, as they have been found to antagonise immune function through the counter-regulation of the TCR signalling machinery [170] and the RING E3 proteins have also been found to regulate cell cycle and apoptotic mechanisms [172]. The mechanisms they employ are distinct: thus, the zinc RING finger domain recruits the ubiquitinated E2 and facilitates the transfer of the ubiquitin monomer to the target protein [164] whilst the HECT domain of the HECT E3 ligases itself binds ubiquitin from the E2-ubiquitin complex and transfers it to the target protein [164]. The HECT E3 proteins may also contain a WW domain, which is involved in targeting the substrates for ubiquitination by mediating interactions with proline-rich regions in other proteins, and a C2 domain that mediates translocation to the plasma membrane/endosome in response to increase in intracellular  $Ca^{2+}$  [164].

##### **1.6.1.1.1 Cbl-b**

The Casitas B lineage lymphoma (Cbl) family has three mammalian homologues: c-Cbl, Cbl-b and Cbl3 (also known as Cbl-c) [173]. Cbl-b is expressed throughout a great number of different cell types and tissues; on a cell-to-cell basis, the protein levels

of Cbl-b are highest in bone marrow-derived mast cells and lowest in the thymus, while spleen and LN cells express equivalent levels [174]. In macrophages, Cbl-b is a negative regulator of TLR-mediated inflammatory responses by binding to, and promoting the degradation of, MyD88 and TRIF [175]. Also in macrophages, Cbl-b-deficiency leads to LFA-1 activation and increased endothelial adhesion [176]. Similarly, in neutrophils, Cbl-b promotes the downregulation of TLR4 expression from the cell surface. It also prevents unchecked inflammatory responses [177]: for example, in human neutrophils, Cbl is a negative regulator of IL-8-mediated chemotaxis by a mechanism potentially involving p85 regulatory subunit of PI3K [178]. Likewise, in mast cells, Cbl-b works as a negative regulator of IgE-mediated production of inflammatory cytokines such as TNF- $\alpha$ , IL-6 and MCP-1 via a mechanism which might include modulation of Syk and I $\kappa$ B activity [174]. In B cells, Cbl-b is a regulator of BCR-mediated signalling via PLC $\gamma$ -2 and Syk [179, 180] and Cbl and Cbl-b both take part in mediating B cell anergy to protein antigen [181].

Cbl-b, a 120 kDa RING-type single polypeptide E3 ligase, is the main Cbl family member found in mature T cells [173, 182]. Initial experiments with a T cell line revealed Cbl-b mRNA and protein levels to be upregulated during ionomycin-induced anergy; this upregulation required calcineurin [183]. Other studies have reported Cbl-b downregulation as an early event that seems to be required for optimal T cell activation and which is potentiated by CD28 co-stimulation; Cbl-b levels recover at later time points, however, and appear to contribute to the triggering of TCR trafficking to the lysosome associated with homeostatic control of T cell activation [182, 184-187]. Further support for a role for Cbl family members in preventing T cell activation was provided by a study in which a T<sub>H</sub>1 cell line, adenovirally transduced with dominant-negative Cbl (inhibits both c-Cbl and Cbl-b) and stimulated by TCR ligation and CD28 co-stimulation, revealed increased production of IL-2 and increased phosphorylation of Vav, Akt, Erk and p38 when compared to cells transduced with an empty vector [188]. Vav, which can be synergistically activated by CD28 co-stimulation, appears to be required for the infiltration and retention of primed T cells in antigenic tissue [80], and has been further confirmed to be regulated by Cbl-b [189].

Globally, therefore, it is thought Cbl-b activity contributes to the downregulation of TCR signalling, allowing the onset and maintenance of anergy. Consistent with this idea, Cbl-b deficiency allows activation of NF- $\kappa$ B immediately upon TCR ligation in the absence of CD28 co-stimulation of primary CD3<sup>+</sup> splenic T cells, *in vitro* [190]. This effect is thought to be achieved by the loss of Cbl-b releasing the need for CD28-

mediated activation of PI3K-Akt, which is required for the formation of the CBM complex, and PKC $\theta$ , which is responsible for coupling the IKKs to the CBM complex, thus enabling NF- $\kappa$ B activation [190]. This is because Cbl-b-mediated ubiquitination of the p85 $\alpha$  regulatory subunit of PI3K reduces its binding to CD28 and TCR $\zeta$ , resulting in reduced downstream Akt activation [191]. Loss of Cbl-b however was not shown to affect the activation of Erk, Jnk, p38, AP-1, PLC $\gamma$ -1, calcium flux and NFAT [190]. By contrast, a study involving the generation of a double knockout mouse reported that Cbl-b<sup>-/-</sup>c-Cbl<sup>-/-</sup> CD4<sup>+</sup> T cells showed reduced downmodulation of the TCR upon TCR engagement which did translate into prolonged activation of Erk [182] suggesting that c-Cbl may play a differential role such as in the regulation of Erk activation. Nevertheless, to some extent, closely related members of the Cbl family appear to display functional redundancy.

Cbl-b is a promoter of peripheral tolerance as seen *in vivo* by its prevention of clinical onset of autoimmunity resulting from AIRE deficiency [192]; also, Cbl-b<sup>-/-</sup> mice develop spontaneous autoimmunity evidenced by lymphoid infiltration in various organs and the formation anti-dsDNA antibodies [193-195]. *In vitro*, Cbl-b<sup>-/-</sup> T cells show enhanced proliferation and IL-2 production in response to TCR stimulation, displaying CD28-independent cell activation [194, 195]. These are characteristics of deficient anergy induction; defects in the development of anergy *in vitro* and *in vivo* have been described in some, but not all, studies relating to autoimmunity resulting from Cbl-b deficiency [183, 193, 196]. However, an alternative mechanism potentially involved in the autoimmunity of Cbl-b<sup>-/-</sup> mice has been proposed, involving resistance to T<sub>reg</sub> suppression; Cbl-b<sup>-/-</sup> effector T cells were shown to be resistant to suppression by wild-type and Cbl-b<sup>-/-</sup> T<sub>reg</sub> cells, *in vitro* [197, 198]. *In vivo*, such Cbl-b<sup>-/-</sup> effector T cells are resistant to suppression by Cbl-b<sup>-/-</sup> natural T<sub>reg</sub> cells, which are fully functional [199]. However, generation of adaptive T<sub>reg</sub> cells seems affected by Cbl-b deficiency as CD4<sup>+</sup> T cells from Cbl-b RING finger mutant knockin or Cbl-b deficient mice showed impaired TGF- $\beta$ -induced Foxp3 expression [200]. Cbl-b<sup>-/-</sup> CD8<sup>+</sup> T cells were also shown to be resistant to T<sub>reg</sub>-mediated suppression, and to exhibit enhanced activation and rapid tumour infiltration and rejection [201]. Consistent with this, in wild-type CD8<sup>+</sup> T cells, Cbl-b was shown to regulate antigen-induced TCR downregulation and IFN- $\gamma$  production [186]. However, in anergic NKT cells, Cbl-b primarily induces the ubiquitination of Carma1, while also affecting NF- $\kappa$ B-mediated IFN- $\gamma$  production, which can lead to failed tumour rejection [202].

Cbl-b and c-Cbl are recruited to the IS of both naïve and anergic T cells, but at the naïve synapse, after TCR ligation and CD28 co-stimulation, CD28 signalling leads to the ubiquitination and degradation of Cbl and this does not occur in anergic cells [100]. Interestingly, in unstimulated naïve cells, polyubiquitination of Cbl-b also takes place but does not lead to its degradation [203] and with the lack of a CD28 signal during anergy induction, Cbl molecules are not degraded, leading to significantly higher expression of Cbl-b and c-Cbl in the anergic relative to naïve cells [100]. CD28 co-stimulation induces greater ubiquitination and proteasomal degradation of Cbl-b than CD3 stimulation alone although in both cases ubiquitination starts as soon as 1 h after stimulation [185]. CD28 co-stimulation has been shown to downregulate Cbl-b at both posttranslational and transcriptional levels whilst CTLA-4-B7 interaction prevents Cbl-b downregulation primarily at the transcriptional level [100]. The p85 $\beta$  regulatory subunit of PI3K - which, like p85 $\alpha$  that Cbl-b downregulates, also binds to CD28 and also promotes Akt activation - is associated with and promotes CD28-mediated downregulation of Cbl-b [184]. PKC $\theta$  has also been found to be required for the downregulation of Cbl-b in pre-activated CD3<sup>+</sup> T cells responding to TCR ligation and CD28 co-stimulation [204]; PKC $\theta$  associates with Cbl-b and phosphorylates it on Ser282, allowing it to be ubiquitinated [204]. The E3 ligases, Nedd4 and Itch then bind Cbl proteins and target them for proteasomal degradation [205]; at least Nedd4 is required for the polyubiquitination of Cbl-b induced by CD28 co-stimulation [203].

Cbl-b protein expression was also found up-regulated in antigen-induced anergic transgenic T cells (by means of OVA peptide presentation by irradiated splenic cells) after ionomycin re-stimulation [193]. Consistent with this, Cbl-b<sup>-/-</sup> CD4<sup>+</sup> T cells displayed higher proliferation and IL-2 production when compared to wild type (wt) cells after both populations were anergised with ionomycin and re-stimulated; similarly, Cbl-b<sup>-/-</sup> cells from OVA-tolerised mice proliferated after antigen re-stimulation while wt cells did not [193]. Reflecting these functional responses, following ionomycin-induced anergy, Cbl-b<sup>-/-</sup> CD4<sup>+</sup> T cells showed increased expression of total and phosphorylated PLC $\gamma$ -1 after anti-CD3 re-stimulation when compared to wt cells and consistent with this, PLC $\gamma$ -1 ubiquitination is reduced in Cbl-b<sup>-/-</sup> cells compared to wt cells [193]. However, the finding that re-stimulation of primed (anti-CD3+anti-CD28-stimulated) Cbl-b<sup>-/-</sup> cells with anti-CD3+anti-CD28 also resulted in increased p-PLC $\gamma$ -1 when compared to wt cells [193], suggests that Cbl-b also plays a dynamic role in regulating priming responses, perhaps in a homeostatic manner.

Decreased PKC $\theta$  protein expression in T cells subjected to ionomycin-mediated anergy has been reported after anti-CD3-re-stimulation of the cells, while Cbl<sup>-/-</sup> T cells did not show this effect [183]. It is therefore thought that Cbl-b downregulates PKC $\theta$  by promoting its ubiquitination; as Cbl-b also promotes the ubiquitination of PLC $\gamma$ -1 in anergic T cells, both these mechanisms are thought to contribute to the block in T cell activation in response to priming T cell stimulation subsequent to induction to anergy [183, 193].

Cbl family members have also been proposed to be involved in regulating IS activity. For example, the microclusters of MHC:peptide-engaged TCRs at the IS are the site of TCR signalling [206], and their persistence is controlled, in part, by c-Cbl-mediated ubiquitination [207]. Anergic cells, which form a mature IS albeit with reduced p-Erk levels, display enhanced accumulation of c-Cbl and Cbl-b in the pSMAC and Cbl-b in the cSMAC, compared to naïve cells, after (re-)stimulation [208]. Nevertheless, in this model of *in vitro* peptide-mediated anergy induction, anergic CD4<sup>+</sup> T cells formed stable T cell-APC conjugates but with less frequency than naïve cells, after (re-)stimulation [208]. These results would therefore appear to be inconsistent with the findings of a previous study which showed, in a planar lipid bilayer system, that mature IS formed by ionomycin-energised CD4<sup>+</sup> T cells were not stable and were disintegrating at 1 h [183]. However, at earlier time points, such anergic T cells did form mature synapses with an ICAM-1 ring surrounding the accumulated MHC:peptide molecules [183]. Cbl-b-deficient T cells also display increased Rap1 activity and enhanced LFA-1 mediated adhesion of T cells to ICAM-1, *in vitro* [209].

However the role of Cbl-b in T cell anergy is still under scrutiny. For instance, although Cbl<sup>-/-</sup> T cells are resistant to anergy induction at low doses of ionomycin, this effect can be partially overcome at higher doses [183]. Moreover, one study has shown that Cbl-b is not necessary for the maintenance phase of anergy, as T cells energised with anti-CD3 antibody, adenovirally transduced with dominant-negative Cbl (inhibits both c-Cbl and Cbl-b) and later re-stimulated revealed no production of IL-2 [123]. Consistent with this, in an *in vivo* system in which anergy is induced by constitutively expressed peripheral self-antigen, Cbl-b expression was found to be increased in anergic wt CD4<sup>+</sup> T cells and Cbl-b<sup>-/-</sup> CD4<sup>+</sup> T cells proliferated more upon encountering the cognate self-antigen, compared to wt counterparts [196]; however, both wt and Cbl-b-deficient T cells developed the same impaired ability to respond to antigenic re-stimulation, as measured by IL-2, TNF- $\alpha$  and IFN- $\gamma$  production [196].

### **1.6.1.1.2 Itch**

Itch is a HECT-type single polypeptide E3 ligase [157] for which a role in the immune system was first brought to light when nonagouti-lethal or itchy mice were analysed; these mice, which have a disruption of Itch, develop severe immune and inflammatory disorders, leading to a fatal autoimmune disease characterised by itching of the skin, hyperplasia of the LNs, splenomegaly and lymphocytic infiltration of lungs, liver, kidneys and heart [210-212]. The severe chronic inflammation and associated premature death that characterizes the Itchy phenotype is dependent on lymphocytes as Itch-deficient mice lacking mature T and B lymphocytes (*Itch*<sup>-/-</sup>*Rag1*<sup>-/-</sup> mice) did not have the severely deleterious immune phenotype, whilst still showing mild inflammation [213]. The fact that the inflammatory phenotype partially persists in *Itch*<sup>-/-</sup>*Rag1*<sup>-/-</sup> mice [213] suggests Itch is also playing a role in regulating the innate immune response, perhaps by controlling signalling downstream of the NOD2:RIP2 complex, preventing NF-κB activation [214]. Moreover, in human leukocyte cell lines, phosphorylation of the G protein coupled chemokine receptor CXCR4, involved in leukocyte chemotaxis and other biological processes [215], allows the recruitment of Itch to the plasma membrane, where it ubiquitinates CXCR4 [216]. Activated CXCR4 also promotes the formation of a complex between arrestin-2 and Itch; while Itch is involved in targeting CXCR4 to the endocytic pathway, the arrestin-2-Itch complex mediates CXCR4 sorting into the lysosome [217]. *Itch*<sup>-/-</sup> cells were also shown to be resistant to T<sub>reg</sub> cell-mediated inhibition and to TGF-β treatment [218] reflecting the finding that Itch ubiquitinates the transcription factor TIEG1, which is induced after TGF-β stimulation, promoting its activation and leading to Foxp3 expression [218], an interesting role for Itch and ubiquitination as positive regulators of the activity of a transcription factor. In mouse embryonic fibroblasts, Itch binds and ubiquitinates MKK4, promoting its proteasomal degradation [219]. MKK4 degradation is stress-induced and dependent on activation of the MKK4 substrate Jnk, which phosphorylates and activates Itch; MKK4 is therefore regulated by a negative feedback loop [219]. Also in mouse embryonic fibroblasts, Nedd4-binding partner-1 (N4BP1) has been shown to behave as a negative regulator of Itch by binding to it and inhibiting its ubiquitination activity, resulting in increased transcriptional activity of c-Jun [220].

Itch's role in anergy induction was first described following ionomycin-mediated anergy of a T cell line, in which Itch protein and mRNA levels were upregulated in a calcineurin-dependent way, when compared to unstimulated cells [183]. Moreover, under these conditions, Itch was shown to ubiquitinate PLCγ-1, in this case

downregulating it mostly by a non-proteasomal pathway [183]. Generally, Itch's role in peripheral tolerance is thought to be helping in implementing the anergic status of T cells by downregulating TCR signal in the absence of CD28 co-stimulation, and modulating transcription factors.

It is thought both Cbl-b and Itch cooperate to regulate T cell activation and autoimmunity by polyubiquitinating TCR $\zeta$  via a K33 linkage, which reduces its association with Zap-70 [221]. As already mentioned, Itch can also ubiquitinate PLC $\gamma$ -1 in ionomycin-induced anergic cells [183] but it does not seem to regulate Erk, Jnk or p38 signalling in either anergic (anti-CD3-) or primed (anti-CD3+anti-CD28-stimulated) cells [222]. Regulation of NF- $\kappa$ B activation has been reported to occur through Itch-mediated ubiquitination and lysosomal degradation of Bcl-10 [223]; TCR ligation in the context of CD28 co-stimulation was found to activate Bcl-10 but later promote its Itch-mediated degradation [223]. However, another study reported that T cells from Itch<sup>-/-</sup> mice stimulated with anti-CD3+anti-CD28 antibodies have normal NF- $\kappa$ B activation [222], whilst TNF-mediated NF- $\kappa$ B activation is down-regulated [213].

Itch has also been reported to play a role in T cell differentiation. Upon activation, Itch<sup>-/-</sup>  $\alpha\beta$  T cells showed preferential differentiation towards the T<sub>H</sub>2 lineage, as seen by increased production of IL-4 and IL-5 by T cells, although IL-2 production (but not IFN- $\gamma$ ) was also increased compared to wt cells [222]. Itch<sup>-/-</sup>  $\alpha\beta$  T cells were also shown to drive the expansion of B1b cells and elevated IgM levels; elevated IgE levels were also observed in Itchy mice and these were induced by IL-4 production by Itch<sup>-/-</sup>  $\gamma\delta$  T cells [224]. Unlike conventional B cells (B2 cells), B1 cells undergo self renewal in the periphery and have no memory; B1b cells, unlike B1a cells do not express CD5 [225].

Itch's effects on T cell differentiation appear to be mediated by JunB [226], a transcription factor whose degradation diminishes the transcription of *Il4*, a critical gene for T<sub>H</sub>2 differentiation [227]. Itch can polyubiquitinate JunB via K48 linkage, targeting it to the proteasome, after being activated by Jnk [222, 226, 228]. Itch can also ubiquitinate c-Jun, but in this case, this action is antagonised by c-Abl, which following localisation to the nucleus after T cell activation phosphorylates c-Jun, preventing its ubiquitination and targeting for degradation by Itch [229].

Itch can itself be phosphorylated in its proline-rich region (Ser199, Ser232 and Thr222) by activated Jnk following TCR stimulation [222] and this phosphorylation is necessary to disrupt an inhibitory interaction between the WW domain of Itch and its catalytic HECT domain, inducing the catalytic activity of Itch [226, 228]. By contrast, Fyn-mediated phosphorylation of Tyr371 leads to reduced activity of Itch [230] while

CTLA-4-mediated signal transduction leads to de-phosphorylation of Itch, activating it and leading to increased overall ubiquitination of proteins; knocking down Itch prevented CTLA-4-mediated inhibition of IFN- $\gamma$  and IL-4 but not IL-2 mRNA upregulation [231]. Nedd4 family interacting protein 1 (Ndfip1), which is upregulated after T cell activation, binds to and can also lead to Itch activation, contributing to the degradation of JunB [232].

Studies of the maintenance phase of anergy revealed PKC $\theta$  as another potential target of Itch as, while ionomycin-induced anergic wt T cells showed a decrease in PKC $\theta$  protein expression after anti-CD3-stimulation of T cells, Itch<sup>-/-</sup> ionomycin-energised T cells did not show this effect [183]. Also, Itch was shown to be relocated from the cytoplasm to the detergent-insoluble fraction of the cell, probably the endosomes or endocytic vesicles, when anergic cells are re-stimulated with antigen [183].

#### **1.6.1.1.3 Grail**

Grail is a transmembrane RING-type single polypeptide E3 ligase of 62-66 kDa that has been reported to localise to endosomal compartments [233]; an intact RING finger domain is required for its function as an E3 ligase [233]. Grail mRNA was found in the brain, kidney, heart, liver, ovary, testes and thymus [233] and has been reported to be upregulated in a T cell line, after re-stimulation of such energised T cells with peptide antigen [233]. In addition, following ionomycin-mediated anergy of a clonal T cell line, Grail protein expression was also found to be upregulated when compared to the naïve T cells and this upregulation depended on calcineurin signalling [233]. Consistent with this, expression of Grail in retrovirally-transduced T cell hybridomas limited anti-CD3+anti-CD28-induced IL-2 and IL-4 production [233]; this was found to be dependent on the ubiquitination activity of Grail and its actin-driven endocytic trafficking [233].

Further work explored the correlation between expression of Grail and functional outcome. For instance, in CD4<sup>+</sup>KJ1-26<sup>+</sup> T cells, Grail mRNA levels were found to be upregulated 3 d after immunisation with peptide in a tolerising regime when compared to those from untreated mice or mice immunised with peptide plus LPS (priming protocol) [234]. Also, constitutive expression of Grail in naïve CD4<sup>+</sup> T cells was found to result in reduced proliferation and IL-2 production levels, while a dominant-negative form of Grail prevented the reduced proliferation and IL-2 production levels associated with tolerising stimuli [234]. Another study showed that Grail mRNA expression was

found to be high in resting and stimulated T<sub>H</sub>1 cells; however, while T<sub>H</sub>1 Grail<sup>-/-</sup> T cells produced more IFN- $\gamma$  than Grail<sup>+/+</sup> cells, neither T<sub>H</sub>2 nor T<sub>H</sub>17 Grail<sup>-/-</sup> T cells produced more IL-4 or IL-17, respectively, than their wt counterparts [235].

Regarding the maintenance phase of anergy, initial experiments in a T cell line showed Grail mRNA expression to be upregulated after re-stimulation of anergised cells with peptide-antigen, when compared to unstimulated cells [233]. Moreover, Grail<sup>-/-</sup> mice stimulated under tolerising conditions show no reduction of proliferation and IL-2, IL-4 and IFN- $\gamma$  production after re-stimulation when compared to unstimulated mice and wt mice stimulated under tolerising conditions [236]. Consistent with Grail-deficiency preventing the onset of tolerance, aged Grail<sup>-/-</sup> mice also showed splenomegaly, increased size of mesenteric lymph nodes, lymphocyte infiltration of the lungs and high titers of anti-dsDNA antibodies [236]. Moreover, a putative role in the development of autoimmune diseases was implicated by the findings that Grail<sup>-/-</sup> mice displayed exacerbated experimental autoimmune encephalomyelitis [236]. Suppression of Grail expression was also found to prevent the immune hyporesponsiveness that develops as a result of chronic schistosomiasis [237].

There is a strong association between Grail expression and some of the functional hallmarks of anergy, such as reduced cytokine production. However, Grail function in peripheral tolerance is certainly not restricted to T cell anergy. For instance, forced expression of Grail in a T cell line was sufficient for conversion to a suppressor phenotype in a contact-dependent manner [238]. In fact, it was found Grail mRNA and protein are more highly expressed in naturally occurring T<sub>reg</sub> cells than in effector T cells [238]. Also, in a systemic model of peptide-specific tolerance induction via intravenous peptide administration, adaptive T<sub>reg</sub> cells were induced which expressed higher levels of Grail mRNA than either tolerised or primed effector cells [238]. Moreover, in T<sub>reg</sub> cells from Grail<sup>-/-</sup> mice, expression of T<sub>H</sub>17 cell-specific genes IL-17, IL-21, ROR $\alpha$  and ROR $\gamma$  were found to be upregulated when compared to wt T<sub>reg</sub> cells [236]. Unlike the previous forced expression studies, here Grail was not found to be required for the generation of naturally occurring or adaptive T<sub>reg</sub> cells but was instead found to be required for their suppressive functions [236]. Another group showed Grail-deficient T cells had increased proliferation and IL-2 production *in vitro* when re-stimulated after ionomycin- or TGF- $\beta$ -induced anergy, or when stimulated while co-cultured with T<sub>reg</sub> cells from either Grail<sup>-/-</sup> or Grail<sup>+/+</sup> mice. In addition, Grail<sup>-/-</sup> T<sub>reg</sub> cells were less effective in suppressing Grail<sup>+/+</sup> effector T cells further implicating Grail in the suppressive functions of T<sub>reg</sub> cells [235]. Grail is thought to be required for these by

means of mediating the suppression of the T<sub>H</sub>17 cell-specific genes [236]. For instance, IL-21 production is promoted by NFATc1; in Grail-deficient, anti-CD3 stimulated, naïve T and T<sub>reg</sub> cells, NFATc1 mRNA expression is upregulated [236] whereas, in wt cells, it is proposed that NFATc1 mRNA expression decreases due to Grail-mediated proteasomal degradation of the TCR-CD3 complex [236]. However, unlike the situation in murine cells, Grail expression in human CD4<sup>+</sup>CD25<sup>+</sup> T cells is no higher than in CD4<sup>+</sup>CD25<sup>-</sup> T cells [239]. Nevertheless, in humans, it was found that the level of Grail mRNA expression in CD4<sup>+</sup> T cells is higher in ulcerative colitis patients in remission than in those from healthy humans or active ulcerative colitis patients [239]. By contrast, *in vitro* ionomycin-induced anergic CD4<sup>+</sup> T cells from human peripheral blood express more Grail, Itch and c-Cbl mRNA than unstimulated cells [239]. Moreover, another study in human CD4<sup>+</sup> T cells in which Jagged-1-induced Notch signalling during stimulation inhibits T cell proliferation and T<sub>H</sub>1- and T<sub>H</sub>2-associated cytokine production, whilst re-stimulation induces normal proliferation but inhibits cytokine production [240], revealed that this T cell hyporesponsiveness was found to be associated with up-regulation of Grail, while c-Cbl and Itch did not vary much [240].

The mechanisms associated with the above Grail-mediated mechanisms of anergy are not clear but it was found that anergic DO11.10 T cells (induced by ionomycin), re-stimulated with peptide pulsed A20 B cells, exhibited severe disruption of actin polarisation, unlike (re-)stimulated naïve DO11.10 T cells [241], suggesting that Grail may be involved in the formation of unstable IS in anergic T cells. This impaired actin polarisation in re-stimulated anergic T cells was indeed found to require Grail, as shown by siRNA knockdown experiments [241] and, corroborating this, increased Grail expression results in reduced T cell:APC conjugation efficiency [241].

Therefore, Grail may promote decreased proliferation and cytokine production via regulation of mediators of actin reorganization that is triggered by CD28 co-stimulation and is required for productive IS formation and endocytic traffic. As to which intermediaries might be affected, in Grail-overexpressing cells Vav1 phosphorylation levels were no different than those of control cells in the initial minutes after TCR ligation, just as there were no differences in calcium flux and LFA-1 function [241]. Also, consistent with this model, no differences in the activation status of p38 or Erk in Grail-overexpressing cells was observed [233, 241]; however the effect of Grail on Jnk activation is disputed as Grail-overexpressing cells were reported to exhibit reduced Jnk phosphorylation in the initial minutes after TCR ligation [241] while other work reported the Jnk pathway as not being affected [233, 242]; these latter two studies both

involved ionomycin+PMA activation, in which Jnk phosphorylation proceeds as usual [115] and this may explain why the other group did find modulation of Jnk activation by Grail, using a non-ionomycin+PMA approach.

Grail has also been found to bind and ubiquitinate Rho guanine dissociation inhibitor (RhoGDI), favouring its binding to and sequestration of RhoA from the membrane (where RhoA needs to be for activation [243]) [242]. Consistent with this, Grail expression in the Jurkat T cell line inhibited RhoA activation but not Rac1, cdc42 or Ras while expression of constitutively active RhoA overcame Grail-mediated inhibition of IL-2 production [242].

Another potential direct target of Grail is CD154, also known as CD40L. CD154 expression is low and intracellular on naïve CD4<sup>+</sup> T cells, but following TCR stimulation cell surface CD154 increases rapidly within 6–8 h [244]. Consequent CD154-mediated trimerisation of CD40 on mature APCs results in elevation of cell surface expression of CD80 and CD86, which in turn bind CD28 on T cells and provide reciprocal bidirectional costimulatory signals for full T cell activation [244]. Grail upregulation in ionomycin-energised CD4<sup>+</sup> T cells, compared to unstimulated and ionomycin+PMA-stimulated cells, was correlated with CD154 downregulation [245]. Indeed, Grail was found to bind to the extracellular portion of CD154 and facilitate transfer of ubiquitin molecules from the intracellular RING domain to the small cytosolic portion of CD154, leading to its proteasomal degradation [246]. Grail also targets CD154 trafficking to the cell surface through the Grail-positive endosomal compartments [245]. However, a recent study did not find CD154 expression changed in Grail-deficient mice [235], perhaps hinting at another, redundant regulatory mechanism to keep CD154 expression in check.

Interestingly, Grail has also been implicated in the direct downregulation of the TCR:CD3 complex as Grail<sup>-/-</sup> CD4<sup>+</sup> T cells energised via stimulation with anti-CD3 antibody were showed to express more TCR $\beta$  and CD3 $\zeta$  than wt cells [236]. In fact, Grail was demonstrated to downmodulate the TCR-CD3 complex through ubiquitin-dependent proteasomal degradation [236].

Grail is associated with and regulated by two isoforms of the ubiquitin-specific protease otubain 1 [247]. Retrovirally transduced otubain 1-expressing T cells contained negligible amounts of endogenous Grail, proliferated well and produced large amounts of IL-2 after ionomycin+PMA stimulation [247]. Otubain 1, whose expression is positively regulated by the Akt-mTOR pathway [248], thus controls Grail instability by promoting its autoubiquitination and degradation [247]. In contrast, cells expressing the

alternatively spliced isoform, otubain 1 alternative reading frame 1, contained large amounts of endogenous Grail and were functionally anergic, proliferating poorly and producing little or no IL-2 after ionomycin+PMA stimulation [247]. Stabilisation of Grail is thus controlled by otubain 1 alternative reading frame 1, which in association with USP8 (a DUB), promotes deubiquitination and hence, prevents degradation of Grail [247].

#### ***1.6.1.1.4 Smurfs***

It has recently been shown that Rap1 is ubiquitinated by Smad ubiquitination regulatory factor-2 (Smurf2), in developing neurons [249]. The ubiquitination of Rap1 by this HECT domain E3 ubiquitin-protein ligase targets it for proteasomal degradation and, by doing so, restricts its expression to a single neurite in developing neurons, which is necessary to ensure neurons extend only one axon [249]. Although only inactive Rap1 is a substrate for Smurf2, increased Smurf2 expression allows the complete degradation of Rap1 [249]. Similarly, the closely related Smurf1 has been shown to regulate cell polarity and motility in tumour cells by the ubiquitination of another GTPase, RhoA [250]. Smurf1 is recruited to the leading edge of the cell by PKC $\zeta$  where it regulates the local level of active RhoA [250].

Both Smurf1 and Smurf2 form complexes with Smad proteins, which allows both proteins to be exported from the nucleus to the cytoplasm [251, 252]. For example, the active Smurf2-Smad7 complex will promote the ubiquitination of TGF- $\beta$  receptors, thus terminating TGF- $\beta$  signalling [252]; in the end Smurf2 ubiquitinates itself and Smad7, promoting the degradation of the complex [253]. In human breast cancer MDA-MB-231 cells, Smurf2 also interacts with Smurf1, ubiquitinating it and promoting its degradation and inhibiting the migration of the cancer cells. By contrast, Smurf1 failed to induce degradation of Smurf2 [254].

These data illustrate the direct role of the Smurf proteins in regulating some signalling proteins also involved in T cell activation. As this regulatory role involves the selected, localised targeting of signalling intermediaries for ubiquitination and proteasomal degradation it is possible Smurf1 and/or Smurf2 are active and playing a similar role in events that lead to T cell anergy.

## 1.7 Aims

The core aim of this work is to identify key differential signalling events in antigen-specific T cells that direct priming or tolerance, at the single cell level both *in vitro* and *in vivo*. In particular, the investigation of the role of the E3 ubiquitin-protein ligases, such as Cbl-b, Itch and Grail in the induction and maintenance phases of anergy will take centre stage. The working hypothesis is that Cbl-b, Itch and Grail are differentially upregulated during the induction of anergy and contribute to its onset by promoting ubiquitin-mediated downregulation of specific key signalling elements that transduce TCR-mediated priming, thus preventing T cell proliferation and cytokine production; it is also hypothesised that after re-stimulation of anergic T cells these E3 ligases would remain highly expressed and further contribute to the maintenance phase of the anergic state. In order to address the role of Cbl-b, Itch and Grail in the induction and maintenance phases of anergy, their expression and localisation in tolerised and primed antigen-specific CD4<sup>+</sup> T cells *in vitro* and *in vivo* will be determined and following assessment of the expression and ubiquitination levels of the TCR signalling machinery these parameters will be correlated with the functional responses of priming or tolerance. Functional parameters for priming or tolerance such as cytokine production, proliferation and migration into B cell follicles (priming) versus cell cycle arrest and apoptosis (tolerance) will be analysed.

**Figure 1.1: The TCR:CD3 complex structure.**

The TCR consists of two chains, each comprising an amino-terminal domain which exhibits marked sequence variation and a constant domain; the most common form of association of the two chains in T cells is the  $\alpha\beta$  heterodimer. Each TCR chain also contains a short connecting sequence which connects to the other chain of the heterodimer - not depicted - and a transmembrane region which anchors each chain in the plasma membrane, allowing the TCR to interact with the chains of the CD3 complex. While the TCR recognises and binds its peptide, the CD3 complex signals to the cell that antigen has bound. The CD3 complex comprises two heterodimers, made of  $\gamma\epsilon$  and  $\delta\epsilon$  chains, and a homodimer of  $\zeta\zeta$ ; the cytoplasmic tails of the  $\gamma$ ,  $\delta$ ,  $\epsilon$ , and  $\zeta$  chains contain the ITAM signalling motif which forms the basis of TCR signalling.

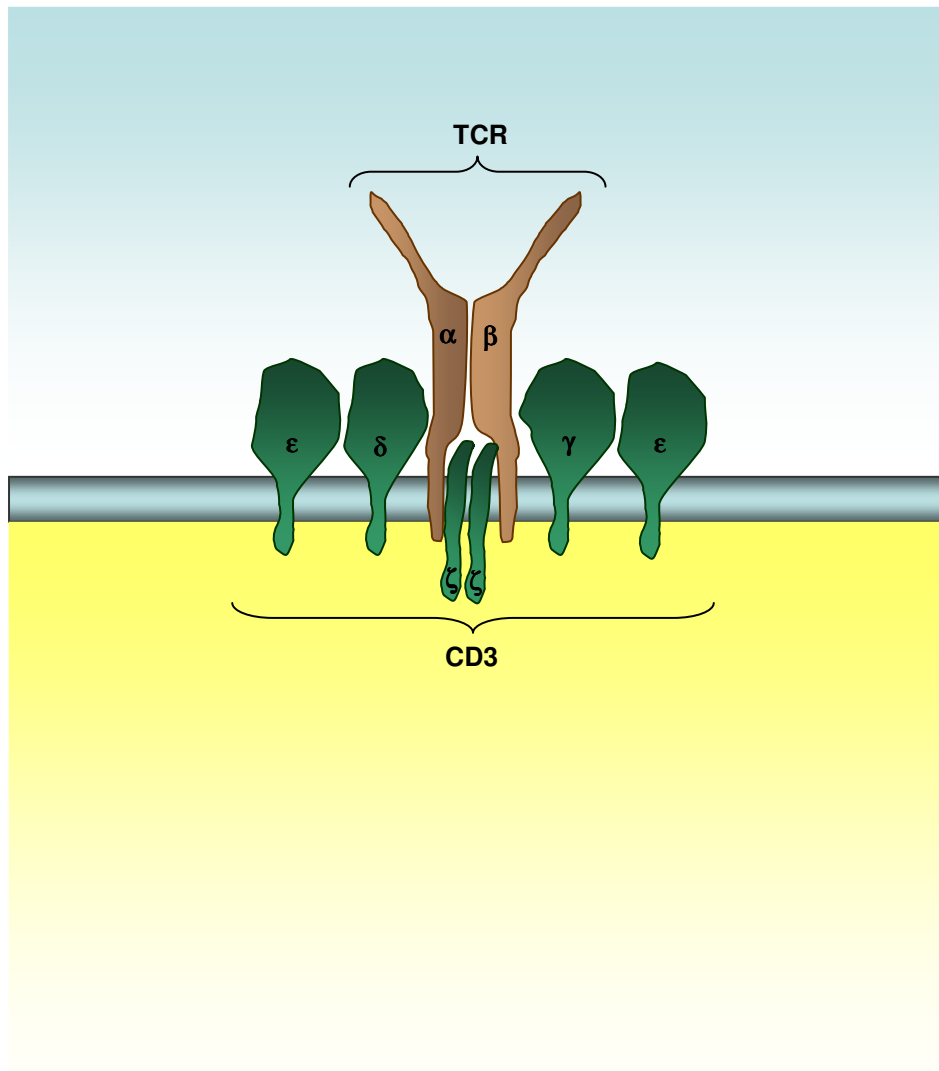


## **Figure 1.2 T cell development takes place in the thymus.**

The earliest precursor T cells, the haematopoietic stem cells (HSC) enter the thymus via venules near the cortico-medullary junction. The developing T cells (thymocytes) are initially double-negative (DN; ie, not expressing CD4 or CD8) and CD44<sup>+</sup>CD25<sup>-</sup> (DN1), and go through a controlled program of gene expression that leads them to DN2 (CD44<sup>+</sup>CD25<sup>+</sup>), DN3 (CD44<sup>low</sup>CD25<sup>+</sup>, with expression of pre-TCR) and DN4 (CD44<sup>-</sup>CD25<sup>-</sup>, still expressing pre-TCR). As thymocytes turn double-positive (DP; CD4<sup>+</sup>CD8<sup>+</sup>), they re-arrange the  $\alpha$ -chain locus and form the TCR  $\alpha\beta$  heterodimer in association with CD3, being ready to recognise peptide:self-MHC molecules; however, most double-positive thymocytes die by failing to be positively selected or as a consequence of negative selection. Eventually, some DPs cease to express one of the two co-receptor molecules, becoming either CD4 or CD8 single-positive cells (SPs), which will exit the thymus to form the peripheral T cell repertoire. The cortical stroma is composed of epithelial cells which contribute to thymocyte's proliferation and cell survival; they also express both MHC class I and MHC class II, which determine the thymocyte's fate during positive selection. After positive selection thymocytes migrate from the cortex to the medulla, which plays a role in negative selection. DCs, which express co-stimulatory molecules absent from the cortex, and medullary epithelial cells, which express tissue-specific and developmental-specific peptides, can be found in this environment.

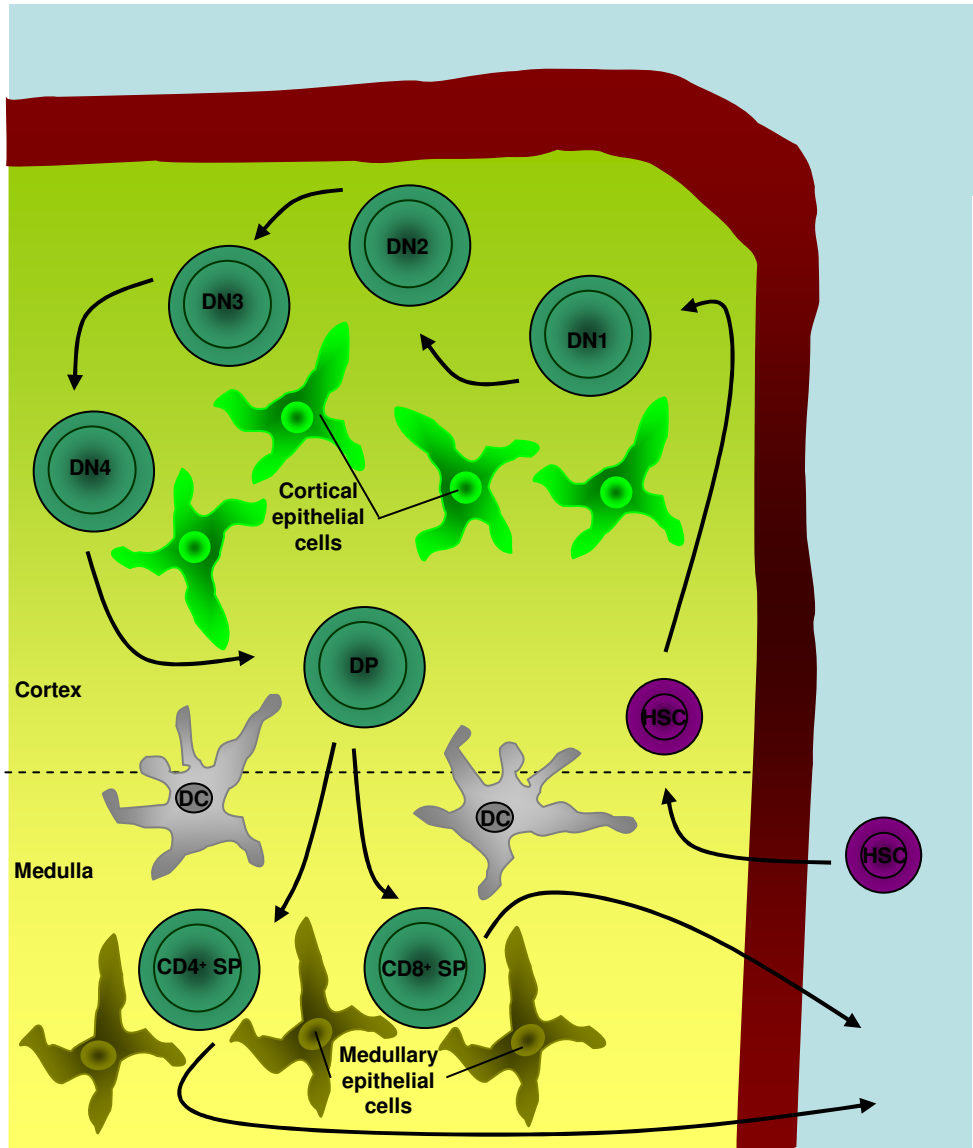


**Figure 1.3: Optimum activation of naïve T cells requires two signals.**

Engagement of the TCR by peptide:MHC complex (signal 1) in the absence of co-stimulation can lead to T cell anergy and/or apoptosis. In order for T cells to proliferate and begin the process of differentiation and production of effector cytokines, CD80/CD86 engagement of CD28 (signal 2) must take place alongside TCR engagement by peptide:MHC complex. APCs, namely DCs, upregulate CD80/CD86 expression after maturation, which occurs after activation by the pathogen's products, ensuring immune responses develop only when needed.

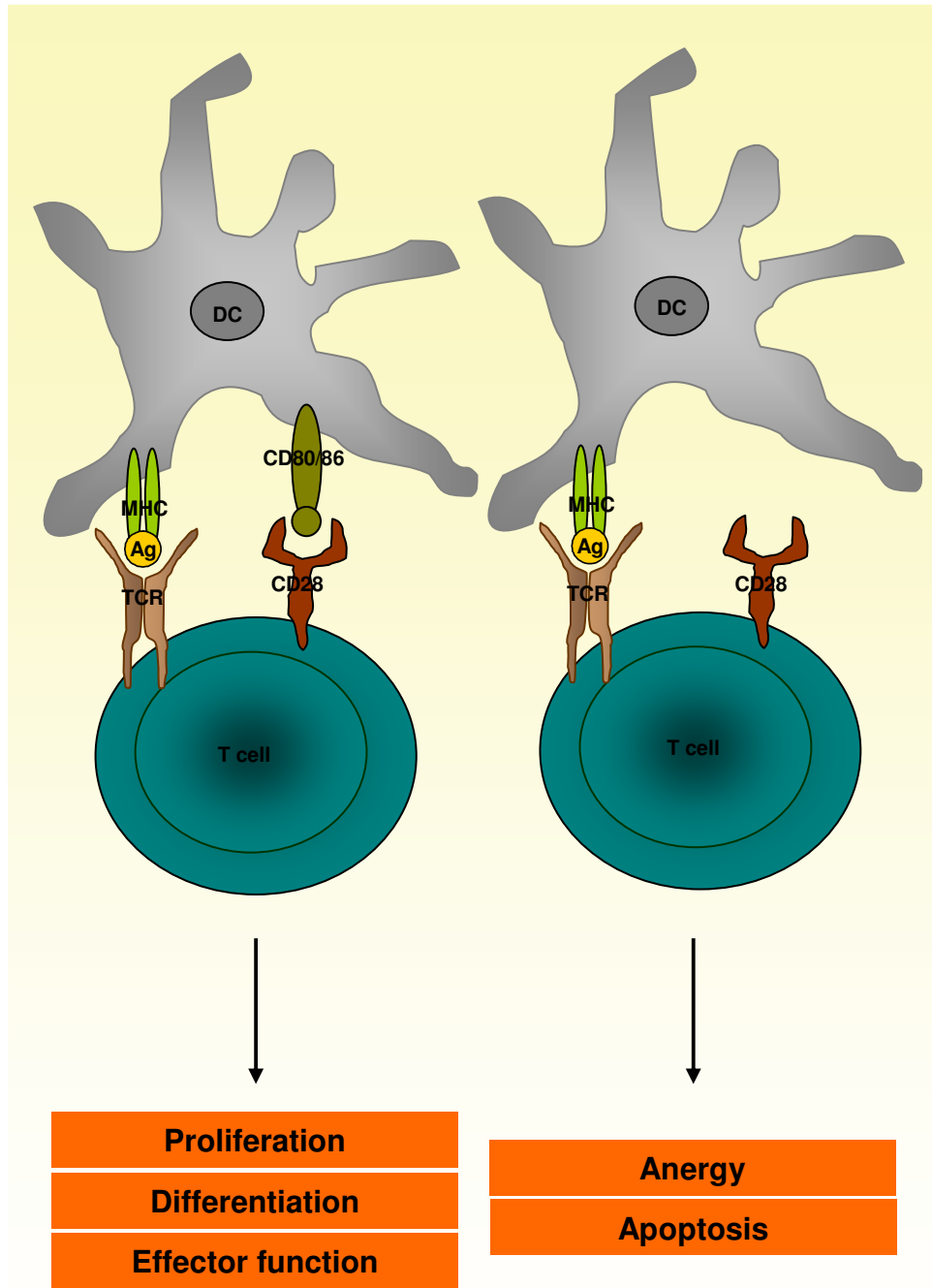


**Figure 1.4: T cell differentiation.**

Activation of naïve CD4<sup>+</sup> T<sub>H</sub> cells leads to the generation of a clone of effector T<sub>H</sub> cells. Effector cells of different types can be generated, depending on the cytokine milieu in which the antigenic stimulus is received. This milieu is strongly influenced by mature DCs, which produce different cytokines depending on the environmental conditions along with upregulation of CD80/CD86. These cytokines are the basis for the third signal, which is required for T cell differentiation. Differentiation of T<sub>H</sub>1 cells requires IFN $\gamma$  and IL-12; this clone expresses the signature transcription factor T-bet and produces IL-2, IFN $\gamma$  and TNF- $\alpha$ . Differentiation of T<sub>H</sub>2 cells requires IL-4 and they can produce IL-4, IL-5, IL-6, IL-10 and IL-13; the transcription factor GATA-3 is required for their differentiation. Differentiation of T<sub>H</sub>17 cells requires TGF- $\beta$  and IL-6; this clone expresses the signature transcription factor ROR $\gamma$ t and produces IL-17A, IL-17F, IL-6 and IL-21.

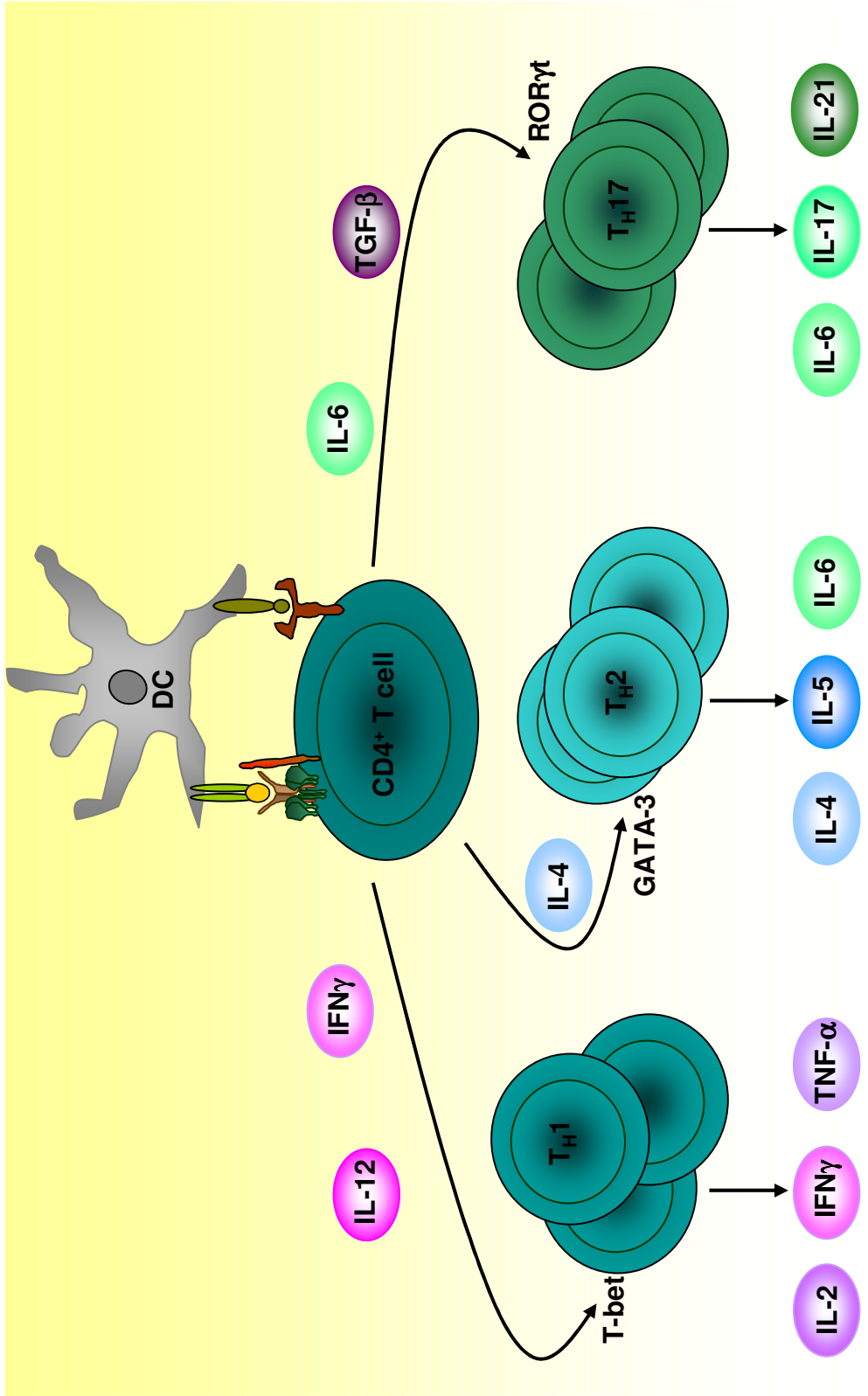


**Figure 1.5: Lymph node structure.**

Lymph nodes are enveloped by a fibrous capsule and have three distinct regions: cortex, paracortex and medulla. The cortex, located closer to the periphery of the LNs, contains B cells and FDCs. In the centre of the LN lies the paracortex, which is composed of T cells and DCs. The medulla consists of lymphatic tissue. T and B cells circulate constantly through the LN by entering via the high endothelial venules (HEVs) and exiting via efferent lymphatic vessels, together with lymph. Lymph draining from the extracellular spaces of the body carries antigens and DCs from the tissues to the LNs via the afferent lymphatics vessels. T cells migrate to the paracortex where they encounter DCs; T cells that do not encounter their specific antigen leave the LN to return to the circulation while T cells that encounter their specific antigen on the surface of mature DCs proliferate, differentiate and migrate to the follicular areas where they provide B cell help. Some follicles may contain areas of intense B cell proliferation called germinal centers; FDCs attract naïve and activated B cells to the follicles. Primed T cells will themselves exit the LN after a few rounds of proliferation.

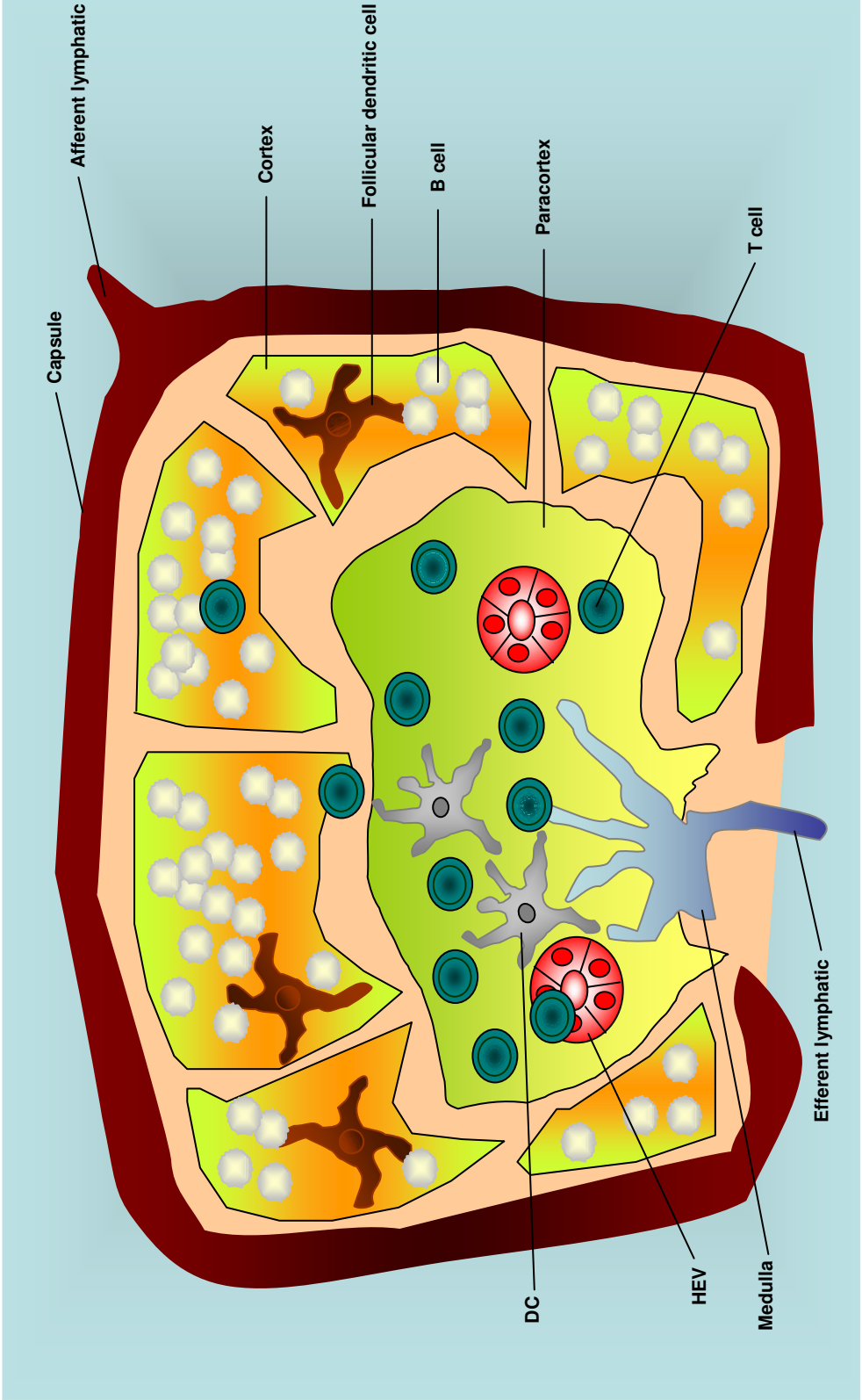


**Figure 1.6: TCR-mediated signalling.**

TCR binding by the MHC-peptide complex results in the activation of Fyn, associated with CD3, and Lck, associated with CD4. Activated Lck and Fyn then phosphorylate the ITAMs of CD3, allowing the recruitment and activation of ZAP-70. ZAP-70 phosphorylates LAT, which delivers the activation signals through recruitment and assembly of a signalosome containing Grb2, GADS, SLP-76 and PLC $\gamma$ -1. PLC $\gamma$ -1, hydrolyses PIP<sub>2</sub> to yield IP<sub>3</sub> and DAG. IP<sub>3</sub> binds to its receptor on the membrane of the ER triggering Ca<sup>2+</sup> release and subsequent Ca<sup>2+</sup> influx through plasma membrane channels; this leads to an increased intracellular Ca<sup>2+</sup> concentration which will lead to the activation of calcineurin. Activated calcineurin de-phosphorylates NFAT, allowing its translocation to the nucleus where it associates with other transcription factors, promoting transcription of many genes. DAG promotes membrane association and activation of PKC $\theta$  and RasGRP1. PKC $\theta$  mediates the phosphorylation of Carma1, an event that induces binding of Carma1 to Bcl10 and Malt1, thus forming the Carma1-Bcl10-Malt1 (CBM) complex. Malt1, acting from the CBM complex promotes the activation of the IKK complex (by recruiting Traf6). Once activated, the IKK complex phosphorylates I $\kappa$ B, releasing it from NF- $\kappa$ B, and thus allowing NF- $\kappa$ B to translocate to the nucleus, where it will promote gene transcription. RasGRP1 promotes the conversion of Ras to its activated form and active Ras recruits Raf to the plasma membrane, allowing its activation. Raf phosphorylates MEK, which, in turn, phosphorylates Erk. Erk activation leads to the activation of c-Fos, allowing the formation of the heterodimeric transcription factor AP-1.

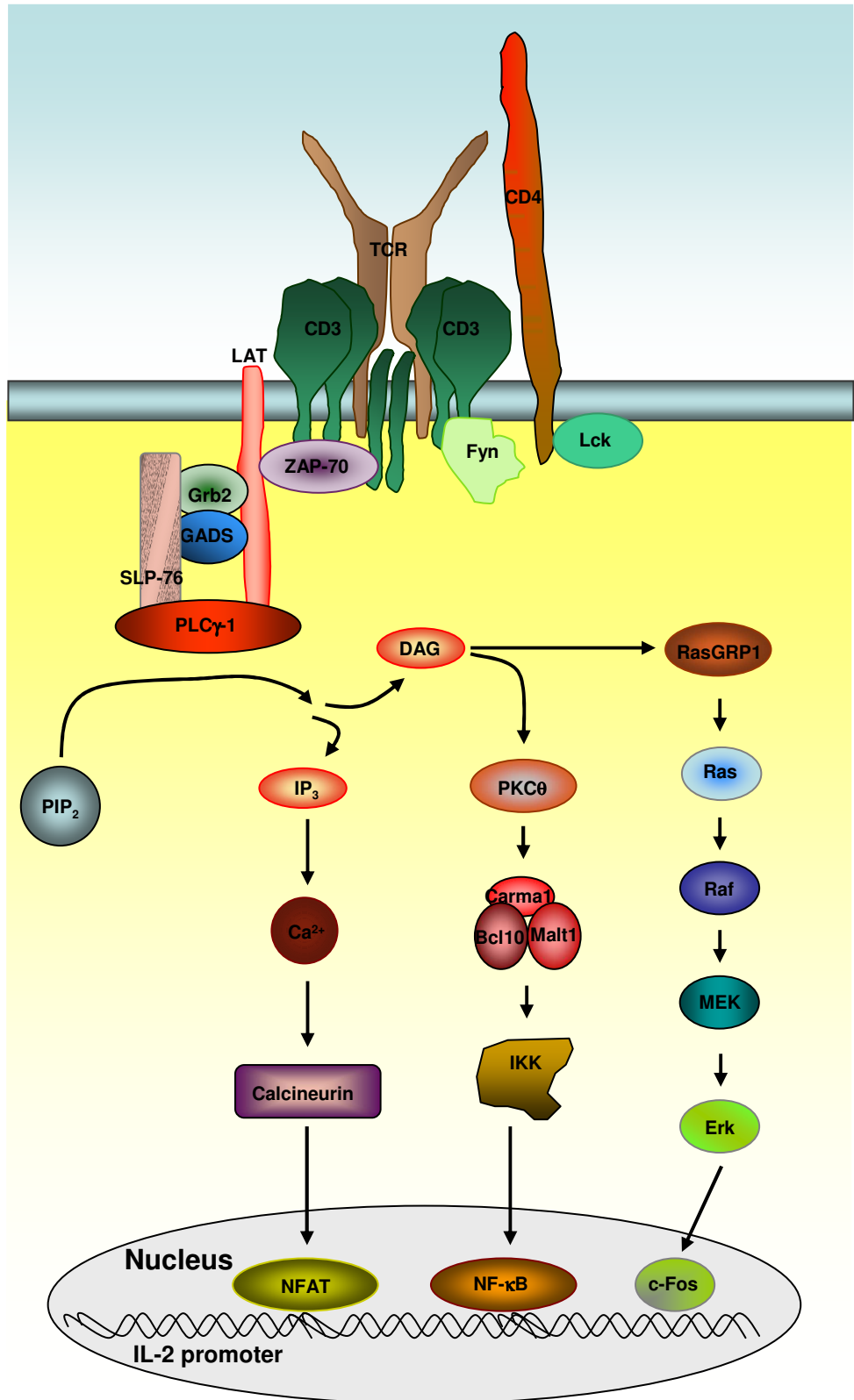


### **Figure 1.7: CD28-mediated signalling.**

TCR binding by the MHC-peptide complex in the presence of CD28 co-stimulation allows the full activation of the signalling events which lead to T cell priming. In this figure, signalling events induced by the TCR-mediated signalling are also depicted, but not described; see text and **Figure 1.6** for explanation on them. CD28 engagement enhances TCR proximal signals through Lck and PI3K. Activated PI3K converts PIP<sub>2</sub> into PIP<sub>3</sub> which allows the recruitment of cytoplasmic proteins containing pleckstrin homology domains to the plasma membrane, such as PDK1, Akt and Vav1. Akt is activated by PDK1 and will contribute to the activation of NF-κB by what is thought to be indirect activation of the IKK complex. PDK1 may also phosphorylate PKCθ thus contributing to its full activation and hence, leading to more NF-κB nuclear translocation. Vav1 requires Fyn, ZAP-70 and PIP<sub>3</sub> to become fully activated. Activated Vav1 associates with phosphorylated SLP-76 and then activates the plasma membrane-localised Cdc42 and Rac, which in turn activate Pak1 and Pak3. The Paks will activate MKK4, which in turn phosphorylates Jnk, thus activating it resulting in phosphorylation of Jun. The Paks also activate MKK3/6, which in turn phosphorylates p38 MAPK. Similarly to Erk, p38 MAPK contributes to the activation of c-Fos, and the activation of c-Fos and Jun resulting from Erk, p38 and Jnk MAPkinase recruitment allows formation of the heterodimeric transcription factor AP-1, which is necessary for IL-2 transcription.

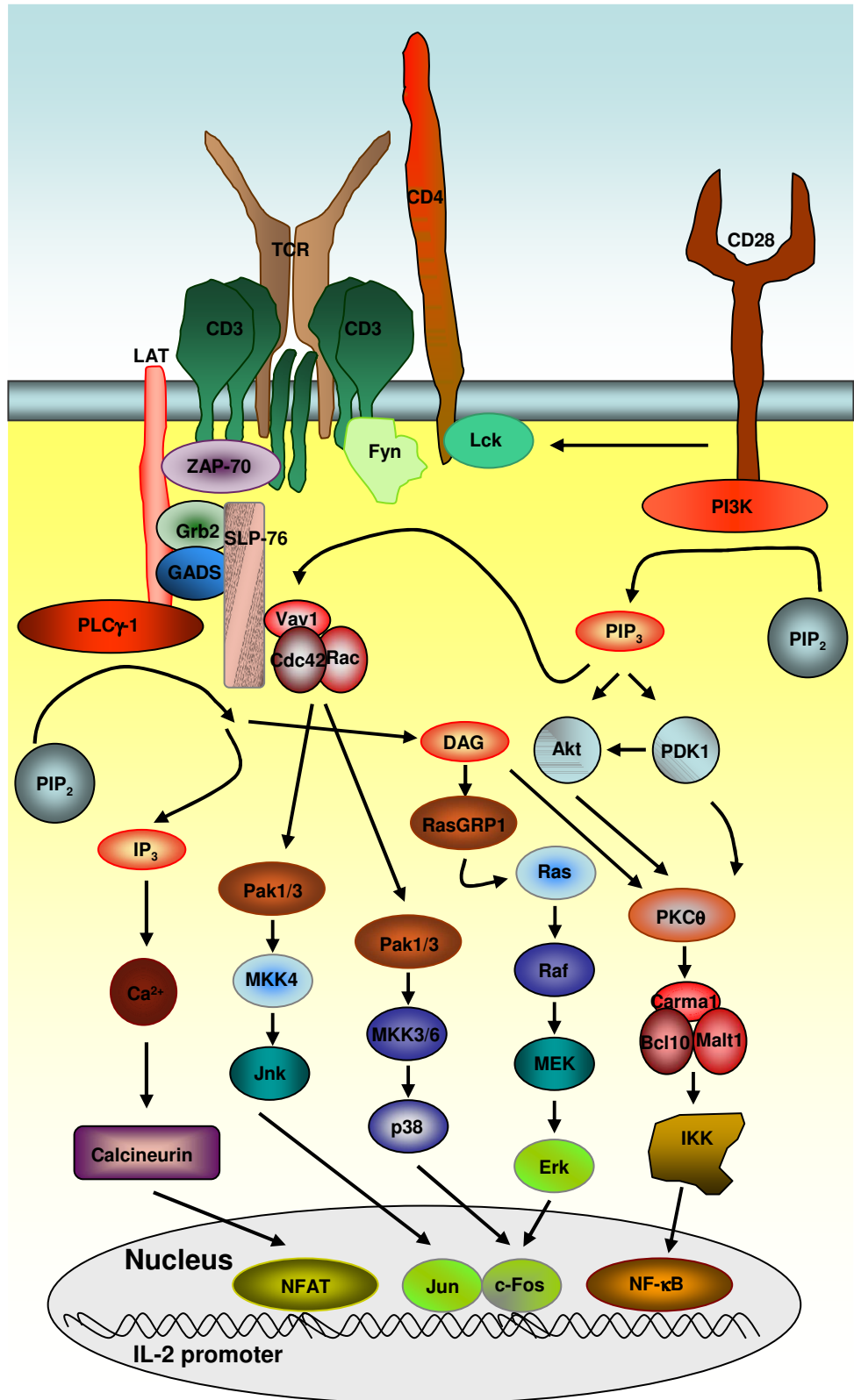


### **Figure 1.8: Signalling in anergy induction.**

In this figure, some of the signalling events induced by TCR ligation are also depicted, but not described in full; see text and **Figure 1.6** for explanation on them. In anergy induction,  $\text{Ca}^{2+}$  flux and the subsequent mobilisation of NFAT occurs as in priming. However, in the absence of co-stimulatory signalling, AP-1 and NF- $\kappa$ B are not activated, and hence the priming program can not be completed; without these two transcriptional factors, NFAT promotes the transcription of anergy-inducing genes, such as *Egr2*, *Egr3*, *Ikaros*, *DGK*, *Cbl-b*, *Itch* and *Grail*. The Egr proteins will further drive the induction of the anergic transcriptional programme, while Ikaros acts as a repressor of *Il2* transcription by binding to the *Il2* promoter. DGK converts DAG into PA, thus depleting its levels and preventing full activation of PKC $\theta$  and RasGRP1. Fyn activation leads to a decrease in the levels of Lck, in the absence of CD28-co-stimulation. Fyn is also involved in the Fyn-Cbl-CrkL-C3G-Rap1 signalling complex which allows Rap1 to sequester Raf1 from Ras, thus preventing Erk phosphorylation. In the absence of CD28 co-stimulation, p27<sup>kip1</sup> is found inhibiting CDK1/2, thus preventing cell cycle progression. Also in the absence of CD28 co-stimulation, Cbl-b ubiquitinates the p85 $\alpha$  regulatory subunit of PI3K, inhibiting PI3K signalling. Grail ubiquitinates RhoGDI, allowing its sequestration of RhoA, and preventing cytoskeletal polarisation. Itch and Cbl-b can also promote the downregulation of PLC $\gamma$ -1.

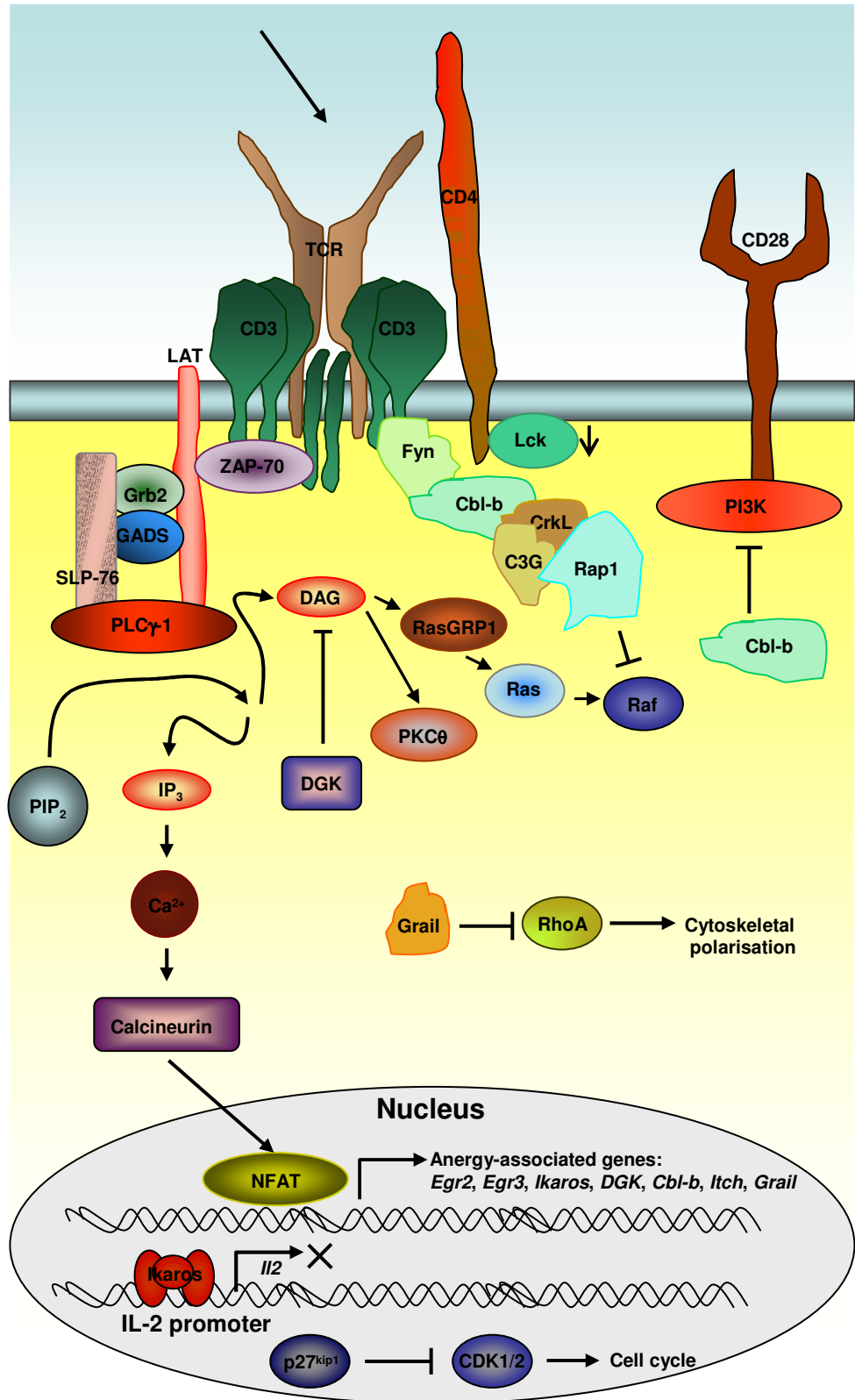


**Figure 1.9: Signalling in the maintenance phase of anergy.**

When anergic T cells re-encounter antigen in the context of CD28 co-stimulation, the genes that were induced or upregulated during the induction phase will come into play to maintain the hyporesponsive state of the cell. Some of the mechanisms are the same as those in effect during anergy induction. For instance, Ikaros acts as a repressor of *Il2* transcription by binding to the *Il2* promoter, possibly with the help of the Egr proteins. DGK converts DAG into PA, thus depleting its levels and preventing full activation of PKC $\theta$  and RasGRP1. The Fyn-Cbl-CrkL-C3G-Rap1 signalling complex allows Rap1 to sequester Raf1 from Ras, thus preventing Erk phosphorylation. In the absence of CD28-dependent Akt signalling, p27<sup>kip1</sup> inhibits CDK1/2, thus preventing cell cycle progression. Itch and Cbl-b promote the downmodulation of PLC $\gamma$ -1 and PKC $\theta$ . Itch can also ubiquitinate Jun, targeting it to degradation in the proteasome; the activity of Jun can also be prevented by p27<sup>kip1</sup>, which also inhibits cytoskeletal polarisation via inhibition of RhoA, which is also inhibited by Grail.

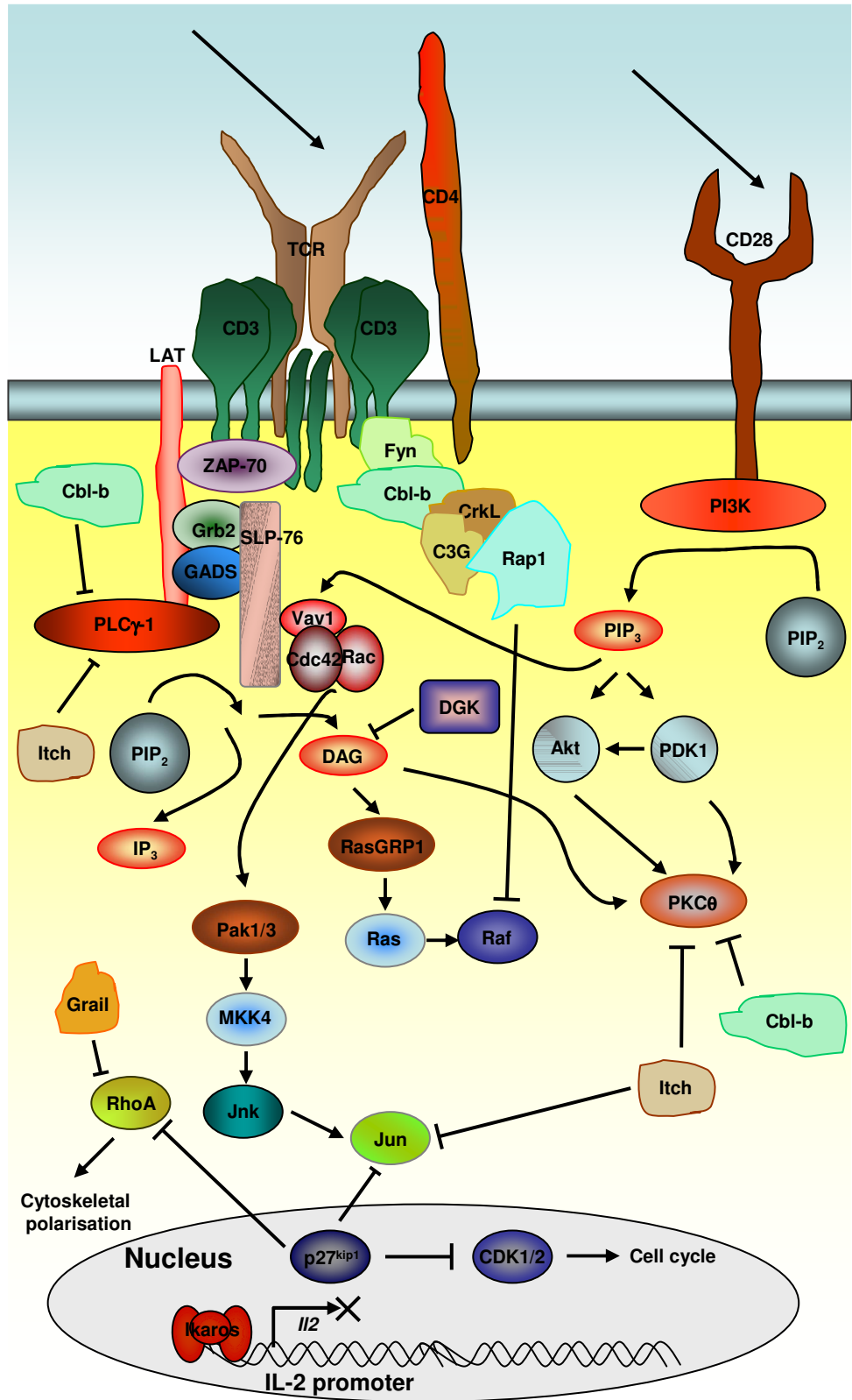
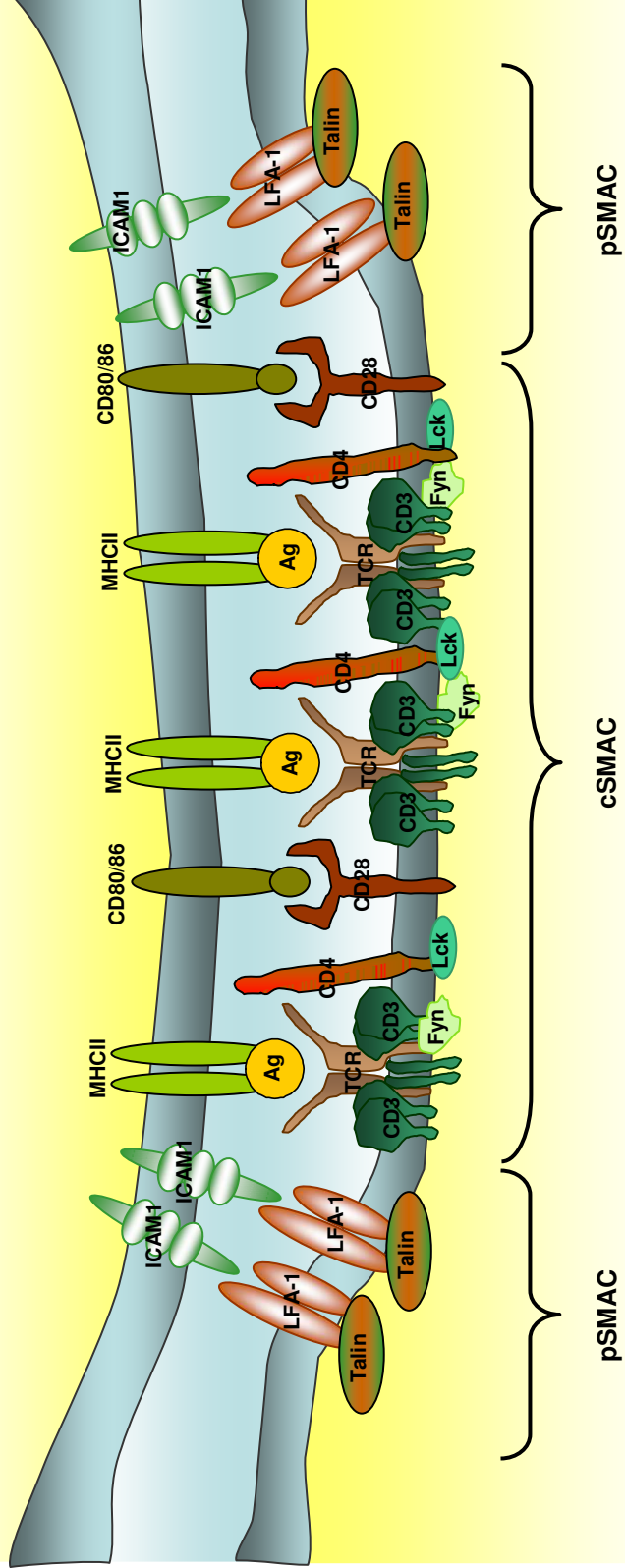


**Figure 1.10: The immunological synapse.**

A mature IS has a specific arrangement in which molecules are arranged in distinct spatial domains: smaller molecules such as the TCR, CD4 and CD28 form a large molecular platform called the central supramolecular activation complex (cSMAC) at the T cell-APC contact site; larger molecules such as LFA-1 and talin form the peripheral SMAC (pSMAC).

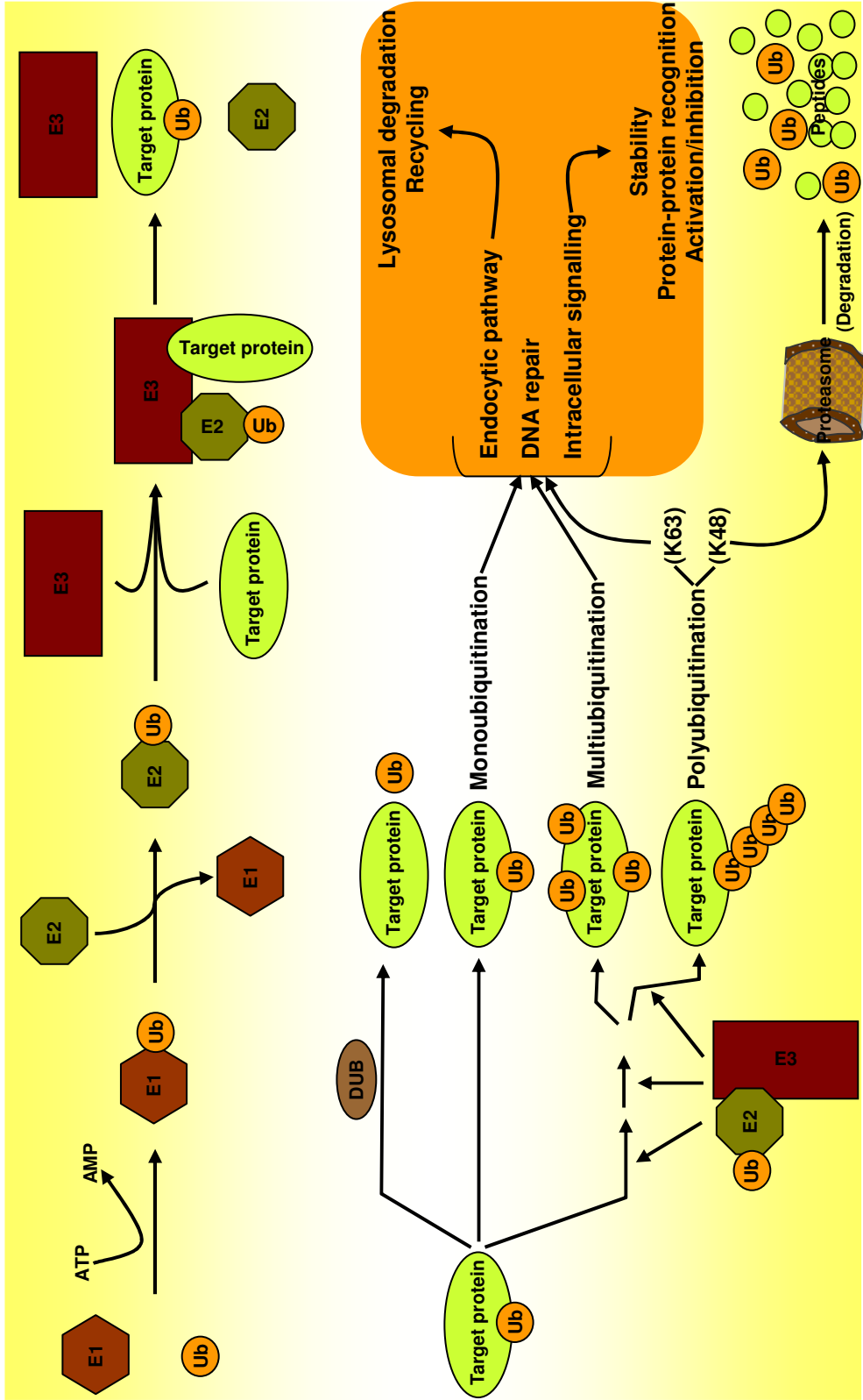
APC



T cell

**Figure 1.11: Ubiquitination.**

The steps involved in ubiquitination are as follows: an ubiquitin-activating enzyme (E1) binds ubiquitin. The activated ubiquitin molecule is then transferred to an ubiquitin-conjugating enzyme (E2). The ubiquitin-E2 complex is then recruited by a third enzyme, an ubiquitin-protein ligase (E3), which specifically binds a protein substrate and facilitates the transfer of ubiquitin from the E2 to the target protein. Upon the addition of the first ubiquitin to the substrate, several other ubiquitins may be added (polyubiquitination) essentially by repetition of the same biochemical reaction. Polyubiquitination can develop through isopeptide bonds between glycine 76 of the activated ubiquitin and the  $\epsilon$  group of one of seven lysines of the ubiquitin moiety already attached to the substrate; the most commonly found polyubiquitin chains are those composed of ubiquitins linked through lysine 48 (K48) and lysine 63 (K63). Alternatively, a substrate can be tagged with a single ubiquitin molecule (monoubiquitination) and such monoubiquitination can occur on a single lysine residue or on several lysine residues, leading to multiubiquitinated substrates. It is important to appreciate that ubiquitination is a reversible process, the removal of ubiquitin from proteins being carried out by deubiquitylation enzymes (DUBs). Substrates with a polyubiquitin chain of four or more ubiquitins linked through K48 are targeted to the 26S proteasome, where they are degraded. Monoubiquitination, multiubiquitination and polyubiquitination via K63 of a substrate protein usually result in different regulatory outcomes other than proteasomal degradation of the protein.



CHAPTER 2  
MATERIALS AND METHODS

## 2 MATERIALS AND METHODS

### 2.1 Animals

DO11.10 TCR transgenic mice on a BALB/c background were used as donors of defined antigen-specific T cells [255]. These transgenic T cells recognize OVA<sub>323-339</sub>/I-A<sup>d</sup> and are detectable using the KJ1-26 clonotypic antibody, allowing studies in a defined, clonal T cell population [256].

BALB/c (H-2<sup>d</sup>, IgM<sup>a</sup>) mice, as well as DO11.10 TCR transgenic mice on a BALB/c background, were used as donors of DCs. The BALB/c is an inbred mouse strain originated in 1923 by McDowell. All animals were maintained under standard animal house conditions and in accordance with Home Office regulations.

### 2.2 Reagents and cell culture

All cell culture reagents were purchased from Invitrogen (UK) whilst other experimental reagents were from Sigma-Aldrich (UK) unless otherwise stated. Cell culture was carried out under aseptic conditions in an incubation chamber at 37°C with 5% CO<sub>2</sub>.

### 2.3 Preparation of primary murine T cells for *in vitro* analysis

#### 2.3.1 *Extraction of lymph node cells*

Peripheral (axillary, brachial, inguinal, cervical and popliteal) (PLNs) and mesenteric lymph nodes (MLNs) were removed from DO11.10 TCR transgenic mice, pooled and forced through Nitex (Cadisch Precision Meshes, UK) to generate single cell suspensions. The cells were washed in sterile RPMI-1640 medium, counted by trypan blue exclusion and the percentage of CD4<sup>+</sup>KJ1-26<sup>+</sup> T cells was determined by flow cytometry (as described in section 2.5.1.1 and **Figure 2.1**).

#### 2.3.2 *Isolation of CD4<sup>+</sup> T cells*

Where indicated, CD4<sup>+</sup> T cells were isolated by negative selection via indirect magnetic labelling of non-CD4<sup>+</sup> T cells. The method, as supplied and described by Miltenyi Biotec (UK), consists of labelling non-CD4<sup>+</sup> T cells (cytotoxic T cells, B cells,

NK cells, DCs, macrophages, granulocytes and erythroid cells) with a cocktail of biotin-conjugated monoclonal antibodies (against CD8a (Ly-2), CD45R (B220), DX5, CD11b (Mac-1) and Ter-119) and, later, binding these with anti-biotin monoclonal antibodies coupled to MicroBeads. The magnetically labelled non-CD4<sup>+</sup> T cells are depleted by retaining them on a MACS column in the magnetic field of a MACS separator, while the unlabelled CD4<sup>+</sup> T cells pass through the column.

The steps involved in the process were as follows: cells were centrifuged (300 g, 10 min) and the pellet re-suspended in 40 µl of MACS buffer (PBS, 0.5% bovine serum albumin (BSA), 2 mM EDTA) per 10<sup>7</sup> total cells, and incubated with the biotin-conjugated antibodies (10 µl per 10<sup>7</sup> total cells, for 10 min). Anti-biotin MicroBeads (20 µl per 10<sup>7</sup> total cells) in 30 µl of MACS buffer (per 10<sup>7</sup> total cells) were added and incubated for 15 min. Cells were washed in MACS buffer and centrifuged (300 g, 10 min). After assembling the LS column in the SuperMACS separator and washing it, the cell pellet was re-suspended in 500 µl of MACS buffer (per 10<sup>8</sup> total cells) and added to the column. The effluent (unlabelled cells) was collected. All procedures were carried out at 4°C.

### ***2.3.3 Stimulation of murine T cells***

DO11.10 TCR transgenic T cells were cultured at a concentration of 10<sup>6</sup> cells/ml well in complete medium (RPMI-1640, 10% FCS, 2 mM L-glutamine, 100 U/ml penicillin, 100 U/ml streptomycin, 0.05 mM β-mercaptoethanol) with 1 µg/ml immobilised anti-CD3 antibody (clone 145-2C11, BD Pharmingen) for the time indicated in the absence or in the presence of 1 µg/ml anti-CD28 antibody (clone 37.51, BD Pharmingen) to induce anergy or priming, respectively [49, 51, 130, 257, 258]. Anti-CD3 antibody was immobilised by incubation for 3 h at 37°C in the plastic plate; immobilised anti-CD3 antibody will be referred throughout the thesis as anti-CD3 or α-CD3. Alternatively, T cells were cultured in complete medium and stimulated with 200 ng/ml ionomycin or 200 ng/ml ionomycin plus 20 ng/ml phorbol 12-myristate 13-acetate (PMA) in order to induce anergy or priming, respectively [222, 235, 259-261]. There was also a population of T cells cultured *in vitro* that received no stimulus; this control group was termed naïve T cells.

Where indicated, the proteasome inhibitor lactacystin (Biomol/Enzo Life Sciences, UK) was added to the T cell culture at a concentration of 25 µM [262, 263].

### ***2.3.4 Analysis of the maintenance phase of anergy and priming of T cells***

#### **2.3.4.1 Production of GM-CSF-conditioned media**

The supernatant from GM-CSF-secreting X63 myeloma cell line was used as the source of GM-CSF for the generation of DCs. X63 cells were quickly thawed at 37°C from liquid nitrogen, washed and plated in 5 ml complete medium supplemented with 0.5 mg/ml G418. After one week cells were re-suspended in fresh complete media without G418 and split. A week later cells were centrifuged, the supernatant stored at -20°C and the cells re-plated. Further rounds of cell culture and supernatant recovery ensued. The supernatant contains highly concentrated granulocyte-macrophage colony-stimulating factor (GM-CSF) secreted by the X63 cells and was filter-sterilised before freezing.

#### **2.3.4.2 Generation of DCs**

Single cell suspensions were generated from harvested bone marrow from BALB/c mice. Cells were counted by trypan blue exclusion and DC progenitors were plated at  $2 \times 10^5$  cells/ml in DC media (RPMI-1640, 10% GM-CSF-conditioned media, 10% FBS, 2 mM L-glutamine, 100 U/ml penicillin, 100 U/ml streptomycin, 0.05 mM  $\beta$ -mercaptoethanol). DC cultures were subsequently fed at day three after plating with further 10 ml of DC media per plate. At day 6 after plating, 10 ml of media from each plate was removed and the DCs were fed with 10 ml of DC “reduced” media (RPMI-1640, 5% GM-CSF-conditioned media, 10% FBS, 2 mM L-glutamine, 100 U/ml penicillin, 100 U/ml streptomycin, 0.05 mM  $\beta$ -mercaptoethanol).

#### **2.3.4.3 Maturation and stimulation of DCs**

Day 8 DCs were matured with 1  $\mu$ g/ml of LPS (*Salmonella abortus*, Sigma-Aldrich) for 24 h before being loaded with 1  $\mu$ g/ml of OVA<sub>323-339</sub> peptide for 2-3 h and then washed.

#### **2.3.4.4 Re-stimulation of DO11-10 TCR transgenic T cells**

DO11.10 TCR transgenic T cells were extracted from mice and incubated with anti-CD3 or anti-CD3 plus anti-CD28 for 48 h, as described before. After that time, cells were washed twice with RPMI-1640, re-plated and rested in complete medium for an additional 48 h. Following the induction of anergy or priming, the viable

transgenic T cells were counted by trypan blue exclusion and re-stimulated by co-culture with LPS-matured, OVA<sub>323-339</sub>-loaded DCs at a ratio of 1:1 ( $5 \times 10^5$  DO11.10 TCR transgenic T cells +  $5 \times 10^5$  DCs in 2 ml medium/ well) for 1 and 20 h in 6-well plates (Corning, Netherlands). Freshly extracted (naïve) DO11.10 TCR transgenic T cells were also co-cultured with LPS-matured, antigen-pulsed DCs for the same periods of time. After that, all cells were scraped off the bottom of the plates and, where indicated, DO11.10 TCR transgenic T cells and non-DO11.10 cells were separated and isolated.

#### **2.3.4.5 Isolation of DO11.10 TCR transgenic T cells**

DO11-10 TCR transgenic T cells were isolated by MACS. For this, a positive selection protocol was used. Here, magnetically-labelled cells are first retained in the column and, after the unlabelled cells run through and after the column is removed away from the magnetic field, later recovered. Cells extracted from lymph nodes were incubated with biotin-conjugated KJ1-26 antibody and later anti-biotin MicroBeads, in an analogous manner to that for CD4<sup>+</sup> T cells isolation by negative selection. The unlabelled cells (non-DO11.10 cells) were collected, after which the LS column was removed from the separator and placed on a new collection tube. MACS buffer was added to the column and the magnetically labelled cells (DO11.10 TCR transgenic T cells) were flushed out and collected.

## **2.4 *In vivo* tolerance assay**

### **2.4.1 *Preparation and purification of T cell suspensions***

Lymph nodes and spleen were removed from DO11.10 TCR transgenic mice, pooled and forced through Nitex to generate single cell suspensions. CD4<sup>+</sup> T cells were purified from freshly harvested tissue using T cell enrichment immunocolumns (VH Bio Ltd, UK) according to the manufacturer's instructions. Briefly, single cell suspensions were layered over Lympholyte-M media and centrifuged at 1000 g for 20 min at room temperature (RT). The lymphocyte layer was then carefully removed from the interface, diluted to a final volume of 10 ml in PBS, centrifuged at 1000 g for 5 min and re-suspended in 2 ml PBS. Cell Reagent (1.5 ml, supplied with kit) was added and the total volume was made up to 5 ml with PBS before incubation for 20 min at 4°C. PBS (4 ml) was then added and the cells were centrifuged at 1000 g for 5 min and re-suspended in 1

ml PBS. Next, the solution was transferred to CD4 negative selection immunocolumns (supplied with kit) and PBS was added until 10 ml of eluate was collected. The eluate was centrifuged at 1000 g for 5 min and re-suspended in RPMI 1640 medium. The cells were washed, counted and the percentage of purified T cells was calculated using flow cytometry (by staining an aliquot for CD4<sup>+</sup>KJ1-26<sup>+</sup> T cells) [264].

#### ***2.4.2 Adoptive transfer of antigen-specific T cells***

Enriched (75-85% CD4<sup>+</sup>KJ1-26<sup>+</sup> T cells) T cell suspensions were generated from lymph nodes and spleens from DO11.10 mice as described above. After calculating the number of KJ1-26<sup>+</sup> T cells in the suspension, 3 x 10<sup>6</sup> DO11.10 TCR transgenic T cells in 200 µl sterile RPMI 1640 medium were injected intravenously (i.v.) into age-matched, female BALB/c recipients [264, 265].

#### ***2.4.3 Administration of antigen***

Recipient mice were injected with OVA<sub>323-339</sub> (100 µg i.v.) in the absence or presence of 1 µg LPS in 200 µl PBS, to induce systemic tolerance or priming, respectively, 24 h after adoptive transfer. Naïve mice received the same amounts of PBS i.v.. To elicit a secondary response, mice were challenged with OVA<sub>323-339</sub> (100 µg i.v. in 200 µl PBS) and LPS (1 µg), 7 days later [266-268].

## **2.5 Flow cytometry**

#### ***2.5.1 Staining for surface markers***

Aliquots of cells (10<sup>5</sup>-10<sup>6</sup> per sample) in 5 ml polystyrene tubes (Falcon, BD Pharmingen) were washed with 200 µl cold FACS buffer (0.05% sodium azide, 2% FCS in PBS) at 450 g for 5 min at 4°C. Cells were re-suspended in 200 µl Fc receptor (FcR) blocking buffer (anti-CD16/32, clone 2.4G2, hybridoma supernatant, 10% mouse serum, 0.1% sodium azide) containing the appropriate fluorochrome-conjugated or biotinylated primary antibodies, or the respective isotype controls for 15-30 min in the dark, at 4°C. The FcR blocking buffer blocks non-specific binding of antibody to such FcR-bearing cells because anti-CD16/32 binds to FcγRII/III and the immunoglobulin in mouse serum binds to FcγRI. Details of the antibody clones, their specificities and isotype controls used are provided in **Table 2.1**. **Table 2.2** contains details regarding the

different fluorochromes used. Cells were then washed with 1 ml FACS buffer as before and, where appropriate, biotinylated antibodies were detected following incubation with fluorochrome-conjugated streptavidin for 15-30 min in the dark, at 4°C. Finally, cells were washed again in FACS buffer and re-suspended in 100-300 µl FACSFlow (BD Pharmingen) immediately before analysis using a FACSCalibur (BD Pharmingen) fluorescence-associated cell sorter (FACS) and CellQuest software (BD Pharmingen). When immediate acquisition of events was not possible, cells were fixed while in suspension in FACSFlow by adding 1% formaldehyde. Two, three or four-colour analysis was performed on a minimum of 10,000 events.

#### **2.5.1.1 Identification of DO11.10 TCR transgenic T cells**

Cells were incubated with PE-conjugated anti-CD4 antibody and biotinylated anti-DO11.10 TCR antibody, or their respective isotype controls, for 20 min at 4°C. Cells were then washed in FACS buffer and incubated with FITC-conjugated Streptavidin for 10 min at 4°C. Two-colour flow cytometry acquisition with a FACSCalibur machine was performed on 20,000 events and these analysed with CellQuest software (**Figure 2.1**).

#### **2.5.2 Detection of intracellular signalling molecules**

Cells were firstly stained for surface markers, prior to permeabilisation as described above. For staining intracellular proteins, cells were washed with 1 ml PBS before addition of 200 µl Cytofix/Cytoperm solution (BD Pharmingen) for 20 min at 4°C and further washing twice with 500 µl Perm/Wash solution (BD Pharmingen) (450 g, 5 min). The relevant anti-intracellular protein antibodies or their respective isotype controls were added in 50 µl Perm/Wash solution/tube and incubated with the cells in the dark at RT for 30 min. After washing, cells were incubated with fluorochrome-conjugated secondary antibody, in the dark at RT for 30 min. Finally, cells were washed again, re-suspended in 250 µl FACS flow and analysed using FACSCalibur and CellQuest software.

#### **2.5.3 Biotinylation of KJ1-26 antibody**

The clonotypic monoclonal antibody KJ1-26 detects the transgenic  $\alpha/\beta$  TCR expressed by DO11.10 mice and was purified from the original hybridoma as described previously [256]. Solutions containing 1 mg/ml purified antibody were dialysed

overnight in Slide-A-Lyzer dialysis cassettes (Pierce) against 50 mM Sodium Bicarbonate buffer (pH 8.5) at 4°C and 1 ml aliquots were then mixed with 75 ng Sulfo-NHS-Biotin (Pierce) for 30 min at RT. Free biotin was then removed by dialysing overnight with PBS/0.05% NaN<sub>3</sub> at 4°C and the biotinylated antibody stored at 4°C [269].

## **2.6 Western Blotting**

### ***2.6.1 Preparation of whole cell lysates***

After stimulation, the reactions were terminated by washing the cells in ice-cold PBS. The cell pellets were then re-suspended in 100 µl of ice-cold modified RIPA lysis buffer (50 mM Tris buffer, pH 7.4 containing 150 mM sodium chloride, 2% (v/v) NP 40, 0.25% (w/v) sodium deoxycholate, 1 mM EGTA, 10 mM sodium orthovanadate, 0.5 mM phenylmethylsulfonylfluoride, 10 µg/ml chymostatin, 10 µg/ml leupeptin, 10 µg/ml antipain, 10 µg/ml pepstatin A and 10 µg/ml aprotinin). After re-suspending the pellet, the cells were solubilised for 30 min on ice before centrifugation of lysates at 16,000 g for 15 min. The resulting supernatants (whole cell lysates) were stored at -20°C.

### ***2.6.2 Protein quantification***

The protein concentration of the whole cell lysates was assessed by the BCA protein assay. This method, supplied and described by Pierce, utilizes bicinchonic acid (BCA) as the detection reagent for Cu<sup>1+</sup>, which is formed when Cu<sup>2+</sup> is reduced by protein under alkaline conditions; when two molecules of BCA chelate one Cu<sup>1+</sup> ion, a purple-coloured product is formed; this exhibits a strong absorbance at 562 nm, which is linear with increasing protein concentrations. Briefly, 5 µl of sample, or 5 µl of differently diluted albumin standards, or 5 µl of water were added to 95 µl of the Micro BCA working solution in triplicate in a 96-well plate, incubated for 30 min at RT and absorbance values determined by spectrometry (Dyner Technologies, UK). Absorbance data was converted into protein concentration with Revelation (Dyner Technologies) software.

### ***2.6.3 SDS Page***

Equal protein amounts of whole cell lysates were resolved using the XCell SureLock Mini-Cell kit with NuPAGE Novex high-performance pre-cast Bis-Tris gels

and NuPAGE buffers and reagents (all supplied by Invitrogen). The appropriate volume of 4 x NuPAGE LDS (Lithium Dodecyl Sulfate) sample buffer and 10 x NuPAGE reducing agent were added to the whole cell lysates (sample) prior to heating (70°C for 10 min). Sample solutions (40 µl) containing 30 µg of protein was added to each well (Seeblue Plus2 marker in buffer was added to one well) and samples were resolved using NuPAGE Bis-Tris gels (10%, 12% or 4-12%) with NuPAGE MOPS or MES running buffer (supplemented with NuPAGE antioxidant) at 180 V for 1 h following the manufacturers instructions. Gels were then transferred onto nitrocellulose membranes (Amersham, UK) using NuPAGE transfer buffer with 20% (v/v) methanol at 30 V for 1 h.

#### **2.6.4 Western blotting**

Following transfer, nitrocellulose membranes were washed once in TBS/Tween (0.5 M NaCl and 20 mM Tris pH 7.5 with 0.1% (v/v) Tween-20) and blocked for 1 h in TBS/Tween containing 5% non-fat milk protein. Membranes were washed with TBS/Tween (3 x 5 min) and incubated with the appropriate primary detection antibody (**Tables 2.3 and 2.4**) overnight at 4°C. All antibodies were diluted in TBS/Tween with 5% BSA. Following incubation with primary antibody, nitrocellulose membranes were washed with TBS/Tween (3 x 5 min) and incubated in the appropriate HRP-conjugated secondary antibody (**Table 2.4**) containing 5% non-fat milk protein for 1 h. Nitrocellulose membranes were then washed with TBS/Tween (3 x 5 min) and protein bands were visualised using the enhanced chemiluminescence (ECL) detection system. Nitrocellulose membranes were incubated in a mixture of equal volumes of ECL solution A (2.5 mM luminol, 0.4 mM p-coumaric acid and 100 mM Tris pH 8.5) and ECL solution B (0.002% hydrogen peroxide and 100 mM Tris pH8.5) for 1 min before exposing membranes to Kodak X-Ray film in a dark chamber. Nitrocellulose membranes were sometimes stripped and re-probed with an alternative primary antibody. Membranes were stripped for 1 h at RT in stripping buffer (100 mM 2-mercaptoethanol, 2% SDS and 62.5 mM Tris pH 7) after which they were washed in TBS/Tween (4 x 10 min) and blocked, washed and re-probed again.

All the antibodies showed themselves specific (**Figure 2.2**) and thus of use in immunocytochemistry. The anti-Itch and anti-Grail antibodies detect not only the full length Itch and Grail proteins but also their degradation products, which appear as a band of lower molecular weight.

### **2.6.5 Immunoprecipitation**

Samples (50 µg of protein from each condition) were normalized to 1 µg/µl with modified RIPA lysis buffer, incubated with 10 µl protein G bead slurry (Pierce) for 1 h at 4°C on orbital rotator and centrifuged (16,100 g, 2 min, 4°C) to clear non-specific binding of proteins to the subsequently discarded protein G-containing pellet. Antibody was pre-loaded with protein G beads (5 µg antibody per 50 µg protein, 25 µl protein G slurry per sample) for 1 h at 4°C, centrifuged (16,100 g, 2 min, 4°C) and the pellet re-suspended in lysis buffer (25 µl per sample). The samples were incubated with the pre-loaded protein G beads (overnight, 4°C, on orbital rotator) and washed 3 times with ice-cold lysis buffer (16,100 g, 2 min, 4°C). Sample buffer and reducing agent were added to the pellet which was boiled (5 min, 100°C) and then centrifuged (16,100 g, 2 min, 4°C). The supernatant was resolved using NuPAGE Bis-Tris gels and analysed via Western blotting as described above.

## **2.7 Immunofluorescence of cells**

### **2.7.1 Preparation of cells**

*In vitro* cultured T cells or T cells co-cultured *in vitro* with DCs were cytocentrifuged (75 µL of cells for 4 min at 40 g) onto a slide using a Cytospin3 centrifuge (Thermo Shandon, UK). The area to be stained was marked with wax pen and the cells were fixed in 4% formaldehyde in PBS for 15 min. The cells were washed with PBS for 5 min and incubated in 1% blocking reagent (Perkin Elmer, UK) in PBS for 10 min.

### **2.7.2 Immunocytochemistry**

Staining for a plasma membrane protein was carried out in most of the experiments. The DO11.10 transgenic TCR or the CD4 co-receptor were the membrane proteins chosen for staining. To identify DO11.10 TCR T cells, biotinylated KJ1-26 antibody was added for 30 min at RT (100 µL of a 1:250 dilution in 1% blocking reagent in PBS from a 1.6 mg/ml stock was used). To identify CD4<sup>+</sup> T cells, biotinylated anti-CD4 antibody was added for 30 min at RT (in 100 µL of a 1:250 dilution in 1% blocking reagent in PBS). At the same time, isotype controls were added to another set of cytopins (**Table 2.5**). In either case, the cells were then washed in

PBS for 3 min for three times and incubated with 50  $\mu$ L of a 1:100 dilution from stock in 1% blocking reagent in PBS of SA-HRP for 25 min at RT. After three more 3 min PBS washes, 50  $\mu$ L of a 1:50 dilution from stock of biotinylated tyramide was added and incubated for 10 min at RT, the tissue washed again three times in PBS and 50  $\mu$ L of a 1:500 dilution from 1 mg/ml stock in 1% blocking reagent in PBS of SA-Alexa Fluor 647 added to the samples; incubation lasted 30 min at RT (**Figure 2.3**). The cells were incubated three times in PBS containing 0.1% azide/ 3% H<sub>2</sub>O<sub>2</sub> for 5 min for quenching excess SA-HRP.

After three washes in PBS for 3 min, the cells were permeabilised in 50  $\mu$ L permeabilisation buffer (2% FCS, 2 mM EDTA, pH 8.0, 0.1% w/v saponin in PBS) for 5 min. After three 10 s washes in PBS, the cells were incubated in 50  $\mu$ L 1% blocking reagent, 0.1% w/ v saponin in PBS for 15 min. The cells were then incubated with 50  $\mu$ L of an appropriate dilution from stock of the antibody of choice or relevant isotype control. Cells were washed again (3 x 3 min) in PBS before incubation with the corresponding HRP-linked secondary antibody (in 1% blocking reagent, 0.1% w/ v saponin in PBS, for 25 min). After three more 3 min PBS washes, 50  $\mu$ L of a 1:150 dilution from stock in 0.0015% H<sub>2</sub>O<sub>2</sub> in amplification buffer of Alexa Fluor 488-labelled tyramide was added for 10 min at RT (**Figure 2.4**), the cells were washed in PBS a further 3 min for three times, allowed to dry and mounted in one drop of Vectashield with DAPI (Vector Laboratories). A coverglass was mounted and sealed onto the slide with nail varnish and the slide stored in aluminium foil at 4°C. The resulting cytopins were analysed in the Laser Scanning Cytometer (LSC) (CompuCyte). LSC data analysis was performed using WinCyte software (CompuCyte). Fluorescence images were also taken using the attached fluorescence microscope, as described further below.

## **2.8 Immunofluorescence of tissue sections**

### ***2.8.1 Preparation of tissue sections***

Inguinal lymph nodes were removed from DO11.10 TCR transgenic mice and fixed in 1% paraformaldehyde in PBS at 4°C for 24 h. They were then transferred into 30% sucrose in PBS for a further 48 h before being frozen in liquid nitrogen in optimal cutting temperature (OCT) embedding medium (Sakura) and stored at -70°C. Sections

(6  $\mu\text{m}$ ) were cut and subsequently stored at  $-20^{\circ}\text{C}$  for up to 72 h before staining. Sections were stained as described below.

### **2.8.2 Immunohistochemistry**

Slides were fixed in acetone, areas to be stained were marked with wax pen and allowed to dry; samples were re-hydrated with PBS for 5 min and incubated with 100  $\mu\text{L}$  PBS containing 0.1% azide/ 3%  $\text{H}_2\text{O}_2$  for 15 min, three times. Tissue was then washed with PBS for 3 min, two times, incubated with 100  $\mu\text{L}$  of a solution of four drops of stock avidin (Vector Laboratories) in 1 ml 3% BSA for 12 min to block endogenous biotin-binding proteins, and washed again with PBS for 5 min. Next, tissue was incubated with 100  $\mu\text{L}$  of a solution of four drops of stock biotin (Vector Laboratories) in 1 ml 3% BSA for 12 min to block the remaining biotin binding sites on the avidin, and washed again with PBS for 5 min.

The sections were incubated with biotinylated KJ1-26 antibody (100  $\mu\text{L}$  of a 1:250 dilution in 3% BSA from a 1.6 mg/ml stock was used), or matching isotype, for 30 min at RT. The tissue was then washed in PBS for 3 min three times and incubated with 100  $\mu\text{L}$  of a 1:100 dilution from stock in 3% BSA of Streptavidin-HRP (Perkin Elmer) for 25 min at RT. After three more 3 min PBS washes, 100  $\mu\text{L}$  of a 1:50 dilution from stock in amplification buffer (Perkin Elmer) of biotinylated-tyramide (Perkin Elmer) was added and incubated for 10 min at RT. The tissue was washed again three times in PBS and 50  $\mu\text{L}$  of a 1:500 dilution from 1 mg/ml stock in 3% BSA of Streptavidin-Alexa Fluor 647 (Perkin Elmer) was added for 30 min at RT (**Figure 2.3**). The tissue was washed in PBS for 3 min (for three times), followed by incubation in PBS containing 0.1% azide/ 3%  $\text{H}_2\text{O}_2$  for 10 min. After one 10 s wash in PBS, the tissue was permeabilised in PBS containing 3% BSA, 0.1% Triton X-100 for 1 h.

The tissue was then washed with PBS for (3 x 10 s) and incubated with PBS containing 0.1% azide/ 3%  $\text{H}_2\text{O}_2$  (2 x 10 min). After another step of washing (3 x 3 min) with PBS, the tissue was incubated with 100  $\mu\text{L}$  of an appropriate dilution of antibody raised against the target signal transducer of choice, or the matching isotype, in 3% BSA, 0.1% Triton X-100 (**Table 2.6**) for 16 h at  $37^{\circ}\text{C}$ . The tissue was then washed in PBS (3 x 3 min) before addition of 50  $\mu\text{L}$  of a 1:100 dilution of stock of the desired anti-IgG-HRP conjugate antibody, with or without anti-B220-FITC antibody, or matching isotype, in 3% BSA, 0.1% Triton X-100 (30 min, at RT). After three more 3 min PBS washes, 50  $\mu\text{L}$  of a 1:100 dilution from stock in 0.0015%  $\text{H}_2\text{O}_2$  in

amplification buffer (Molecular Probes) of Pacific Blue-labelled tyramide (Molecular Probes) was added for 10 min, at RT (**Figure 2.4**), the tissue was washed in PBS a further 3 min for three times, allowed to dry and mounted in one drop of Vectashield (Vector Laboratories) mounting media. A coverglass was mounted and sealed onto the slide with nail varnish and the slide stored in aluminium foil at 4°C. The resulting tissue sections were analysed in the LSC. Fluorescence levels were quantified and photographs taken, as described in the next section.

## **2.9 Laser scanning cytometry**

Laser scanning cytometry is a very useful tool for analysing signal transduction events at the single-cell level [270]. It allows the quantification of fluorescent signals while also allowing imaging of each and every cell in the slide. It possesses a xy re-location feature that allows locating in the slide a cell that has been acquired previously and is represented in a scattergram plot. It combines both scanning, automated quantification with more fine-tuned, manually-taken photography. Unlike the FACS, in which cells have to be in suspension and dissociated from their native surrounding tissue, the LSC can be used to analyse scattered cells and cells within a tissue - *in situ* - in the midst of their niche, thus more within physiological parameters. Also unlike the FACS, which only allows detection of positive cells and their fluorescence intensity, the LSC enables analysis of subcellular localisation of the molecules, which is very important since the activity of many molecules is determined by their localisation. The use of the LSC for assessment of signalling pathways in immune cells and tissue has been established in this laboratory [271].

Alexa Fluor 488 and FITC (green) were excited using the argon ion laser and measured using filter cube D 530/ 30 nm. Alexa Fluor 647 (long red) was excited using the Helium-Neon laser and measured using filter cube H1 650/ LP. Alexa Fluor 350, DAPI and Pacific Blue (blue) were excited using the UV laser [272, 273].

### ***2.9.1 LSC data collection on individual cells***

Analysis of any sample by LSC involves setting up adequate data collection display (.DPR) and protocol (.PRO) files and parameters in WinCyte. In the *Parameters* sub-menu of the *Instrument settings* menu, the blue, green and long red sensor boxes were checked to ensure fluorescence detected by these sensors was included in the data file. To detect cytocentrifuged cells (cytospins) it is necessary to establish “contours”

first (**Figure 2.5A**). The primary contour, or threshold contour, is usually set on the cell's nucleus [130, 271]. This is identified by staining with dyes that bind to the DNA, like DAPI [274]. In the *Computation* sub-menu, the threshold contour was set on blue, as this is the colour of the DAPI stain. The minimum area was then set to  $5 \mu\text{m}^2$ , enabling detection of DAPI stained nuclei that are sized  $5 \mu\text{m}^2$  and above. This is the optimal minimum area for the T lymphocytes described hereafter. Using the LSC scan data display, the integration contour was then situated 11 pixels (1 pixel =  $0.5 \mu\text{m}$  (x-axis) and  $0.5 \mu\text{m}$  (y-axis) for 40x objective) outside the threshold contour, so as to define the outer edge of the cells already identified on the basis of their nuclear staining. The integration contour allowed calculation of the total fluorescence within each cell (fluorescence integral value) and this integration contour setting was optimal for collecting data on T lymphocytes. *Peripheral contouring* was enabled to define the peripheral area of the cell. Peripheral contours were set between the threshold contour (defined by the nucleus when contouring on DAPI) and the integration contour (defined by the edge of the cell) and so the fluorescence emitted peripheral to the nucleus could be measured (fluorescence peripheral integral value). Finally, two background contours measure the background fluorescence outside the cells and this value is automatically subtracted from the measured fluorescence values.

The area of the slide to be scanned (the area of the slide where the cells were) was delimited in the *Scan Area* section. Next the photomultiplier tube (PMT)-Voltage, Offset, and Gain settings were set to 15-35%, 1800-2200, and 255, respectively, for blue, green, and long red. The optimal settings for these parameters would change slightly depending on different reagents and other cell types used. A setting is considered optimal when there is little or no saturation. Saturation occurs when the detector no longer responds to increased levels of signal and is indicated by the presence of dark blue lines in the upper third of the PMT scale. Settings would be changed to achieve no more than 75 saturated pixels. The power of the Argon laser was set to 5 mW.

Next, the threshold value was set to 3000 thus, ensuring all cells emitting blue fluorescence at a level  $\geq 3000$  fluorescence units were detected as events. This setting was verified for each batch of staining and varied from 2000 to 4000 depending on the intensity of the nuclear staining. Setting the optimal threshold value for detection of cells is crucial so as to allow maximal cellular resolution and collection. For example, if the threshold value is set too low then multiple cells may be detected as one cell and conversely, if a high threshold value is set, cells with low or medium intensity staining

will not be detected at all (**Figure 2.5B**). Therefore, a compromise must be made when setting the threshold value so as to detect the maximum number of true single cells in a sample. The area was then scanned and the data file saved.

### **2.9.1.1 Identification of antigen-specific T cells**

When analysing cytopins, the primary contouring parameter was set on the nuclear localization of the DNA dye, DAPI, to detect all of the cellular events as described above. Antigen-specific T cells were identified via their DO11.10 transgenic TCR receptor after staining with the KJ1-26 antibody. As the TCR is expressed on the plasma membrane of the cell, the data derived from the integration contour was used to distinguish the antigen-specific T cells. In addition, the expression level of intracellular molecules in antigen-specific T cells was quantified by gating on the KJ1-26<sup>+</sup> cells and measuring the integral fluorescence value for the intracellular molecule in question. The expression level of intracellular molecules was also measured in the peripheral-to-the-nucleus area of the cell, using the peripheral contours. For analysis purposes the positive gate was positioned according to the fluorescence obtained using the appropriate isotype controls. CD4<sup>+</sup> T cells can also be identified in the same way as KJ1-26<sup>+</sup> cells, also allowing for further analysis of the intracellular molecule of choice in CD4<sup>+</sup> T cells (**Figure 2.6**).

### **2.9.1.2 Cell cycle analysis**

The LSC can be used for determining the stage of the cell cycle a cell is in since it allows the measurement of content and concentration of DNA at the same time via DAPI nuclear staining [273]. The content of DNA can be assessed via DAPI Integral (sum of all fluorescence in the cell) while the concentration of DNA (condensation) can be assessed via DAPI Max Pixel (the most highly fluorescent pixel value in the cell). Therefore, by plotting Max Pixel against Integral values of DAPI nuclear staining the different cell cycle stages can easily be identified (**Figure 2.7**). For example, cells in S phase can be identified by their increased DNA content. However, cells in the other mitotic stages (G2/M phase) which also contain high amounts of DNA can be differentiated due to the higher level of chromatin condensation. By contrast, cells arrested at the G1/G0 stage (red gate) of the cell cycle contain half the amount of DNA (2n DNA) compared to cells in G2/M (4n DNA) and can therefore be identified by the lower DNA content, as detected by lower DAPI Integral values. Cells undergoing apoptosis contain subdiploid DNA content due to their fragmented DNA placing them

below cells in G1/G0 on the scattergram. Newly-formed daughter cells (NFDCs) represent cells which have recently undergone mitosis and can be identified due to their small nuclei which still conserve highly condensed DNA.

### ***2.9.2 LSC data collection on lymph node tissue***

The LSC can also be used to assess fluorescence signals in sections of tissue. As with analysis of single cells, adequate data collection display and protocol files and parameters must be set up in WinCyte. The blue, green and long red sensor boxes were checked. Contours must also be created; here, the primary contouring parameter was set using the long red sensor which detects the Alexa Fluor 647-stained transgenic TCR on the cell surface, thus identifying all the antigen-specific T cells in the section and allowing measurement of any signal expressed by these T cells *in situ*. An advantage of using the adoptive transfer system for this analysis is that it generates a relatively low, near physiological, frequency of antigen-specific transgenic T cells. This approach overcomes the usual problem encountered with cells in tissue, where they can be so densely packed to prevent setting an accurate threshold based on a cell surface marker. The optimal settings for such sporadically distributed T cells are as follows: threshold value: 3500; minimum area: 5  $\mu\text{m}^2$ ; power of Argon laser: 5 mW; PMT, offset, and gain settings: 22-32%, 2048, and 255, respectively, for blue; 30-40%, 2048, and 255, for green; and 22-32%, 2048, and 255, for long red. PMT settings varied depending on the intensity of staining in different batches of tissue.

By contrast, in order to detect the densely packed B cell follicles, phantom contours are required (**Figure 2.8**). Phantom contours differ from the contours described thus far in that they comprise a lattice of contours, which is placed over the tissue section, consequently generating fluorescence values which represent the relevant area of the tissue section as a whole, rather than individual cells [271]. For example, when phantom contours are set to detect fluorescence emitted from the B cell stain, B220-FITC, this allows the identification of B cell rich areas, not individual B cells, and permits the generation of tissue maps on which the x- and y-position of the B cell rich areas can be plotted. Phantom contours were generated as follows. On the *Phantoms* tab, phantom contouring was enabled, and the *lattice* pattern and *allow overlap of events* options were selected; the radius was set to 6  $\mu\text{m}$  and the minimal distance between phantoms centres was set to 20  $\mu\text{m}$ .

It is possible to combine the tissue maps showing B cell distribution with the ones showing DO11.10 TCR transgenic T cells, thus allowing assessment of the position of

the antigen-specific T cells regarding the different areas of the lymph node (follicular versus paracortical areas).

As before, the expression level of intracellular molecules in antigen-specific T cells was quantified by gating on the KJ1-26<sup>+</sup> cells and measuring the integral fluorescence value for the intracellular molecule in question. For analysis purposes the positive gate was positioned according to the fluorescence obtained using appropriate negative/isotype controls

### ***2.9.3 Immunofluorescence microscopy***

Fluorescence images were taken using a connected 3CCD colour vision camera (regulated by a Hamamatsu and Orbit controller) and the OpenLab version 3.0.9 digital imaging program (Improvision, Warwick, UK).

## **2.10 Other functional assays**

### ***2.10.1 [<sup>3</sup>H]thymidine uptake DNA synthesis/ proliferation assay***

Cells were cultured at a concentration of  $4 \times 10^5$  cells per well ( $2 \times 10^5$  T cells +  $2 \times 10^5$  DCs per well, for re-stimulation), in complete RPMI 1640 medium, in triplicate, for 48 or 72 h, in 96-well flat-bottomed plates (Corning) at 37°C in a 5% CO<sub>2</sub> incubator. DNA synthesis was assessed in all samples by addition of 1 µCi per well of [<sup>3</sup>H] thymidine (Western Infirmary, Glasgow). Cells were then harvested onto glass fibre filter mats (Wallac, Warrington, UK) using a Betaplate 96-well harvester (Amersham) after an additional 16 h. [<sup>3</sup>H]thymidine incorporation was assessed using a 1205 Betaplate liquid scintillation counter (Amersham). Where indicated, 10 ng/ml rIL-2 (gift from Dr D. Xu, University of Glasgow, Glasgow, UK) was added at the beginning of the proliferation assay.

### ***2.10.2 Assessment of antigen-specific cytokine production***

Production of relevant cytokines by T cells was quantified by enzyme-linked immunosorbent assay (ELISA). To detect IL-2 and IFN $\gamma$  in culture supernatants, Immulon-4 plates (Costar) were coated with rat anti-mouse IL-2 or IFN $\gamma$  capture antibodies (1 or 1.5 µg/ml, respectively; 50 µl/well; BD Pharmingen) for 16 h at 4°C before being blocked with 10% FCS in PBS for 1 h at 37°C. Sample supernatants were added for 3 h at 37°C and following washing with 0.05% Tween20 in PBS, were

subsequently incubated with biotinylated rat anti-mouse IL-2 or IFN $\gamma$  detection antibodies (0.5 or 1  $\mu$ g/ml, respectively; 50  $\mu$ l/well; BD Pharmingen) for 1 h at 37°C. Plates were then incubated with 50  $\mu$ l extravidin peroxidase per well (diluted 1:1000 in PBS/0.2% FCS/0.05% Tween20) for 1 h at 37°C before being treated with TMB Microwell Peroxidase Substrate. Recombinant murine IL-2 or IFN $\gamma$  preparations (BD Pharmingen) were used to produce standard curves from which cytokine levels in samples were calculated.

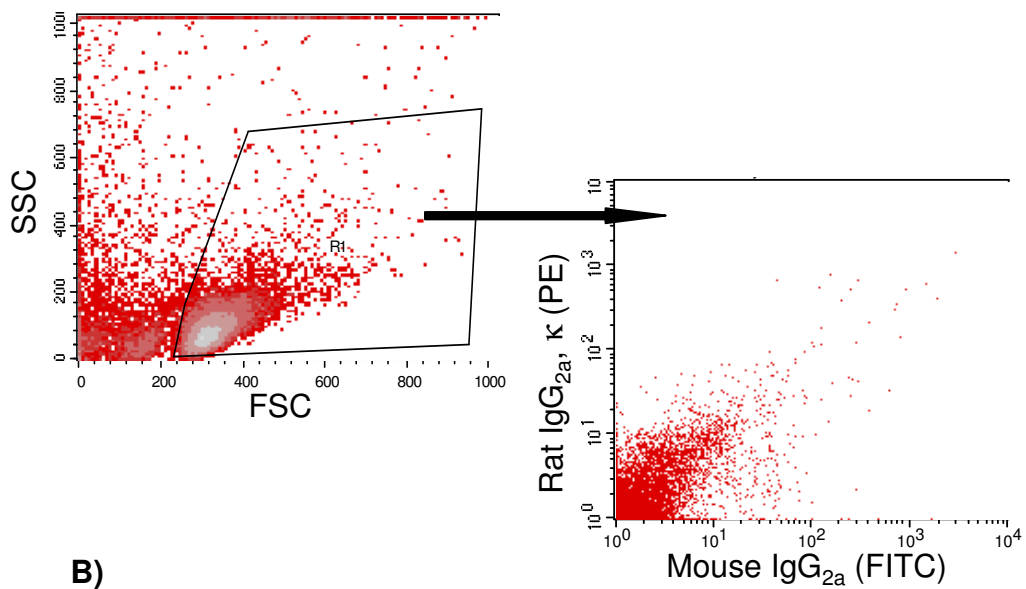
## **2.11 Statistical analysis**

Results are expressed as mean  $\pm$  SEM, unless otherwise stated. To test significance, different types of statistical tests were performed, the type of test varying according to the experimental setup; it was considered  $p \leq 0.05$  to be significant and there is further discrimination of  $p$  values of \* $\leq 0.05$ , \*\* $< 0.01$ , \*\*\* $< 0.001$ . All statistical tests were performed using GraphPad Prism version 5.00 for Windows, GraphPad Software, USA, [www.graphpad.com](http://www.graphpad.com).

**Figure 2.1: Identification of DO11.10 TCR transgenic T cells by flow cytometry.**

Lymphocytes are first distinguished via their forward scatter (FSC), which correlates with their size, and side scatter (SSC), which correlates with their granularity; events gated within region 1 (R1) are lymphocytes. These events are then analysed for the expression of CD4 co-receptor (CD4<sup>+</sup> T cells) and DO11.10 TCR (**B**). Usually, 30-40% of lymphocytes were found to be CD4<sup>+</sup>DO11.10<sup>+</sup> T cells (gated within R2). Isotype controls for the CD4 and KJ1-26 antibodies are also shown (**A**).

**A)**



**B)**

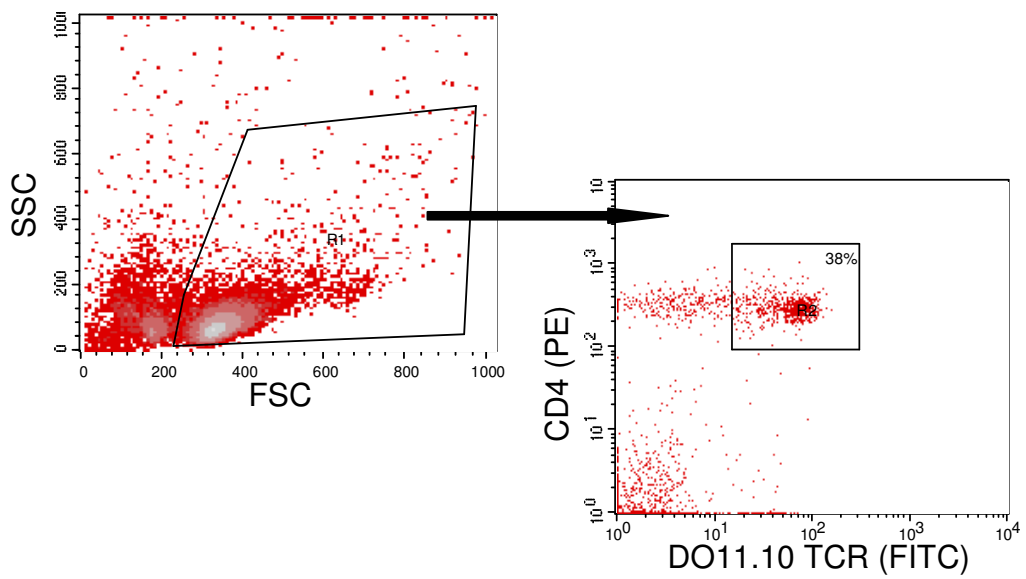


**Table 2.1: List of antibodies used in flow cytometry.**

Specificity of Antibody	Clone	Isotype	Conjugate	Manufacturer	Catalogue number
Surface antibodies					
CD4	RM4-5	Rat IgG <sub>2a</sub> , κ	PE, PerCP	BD Pharmingen	553049, 553052
CD69	H1.2F3	Armenian Hamster IgG <sub>1</sub> , λ3	FITC	BD Pharmingen	553236
DO11.10 TCR	KJ1-26	Mouse IgG <sub>2a</sub>	APC	Caltag	MM7505
DO11.10 TCR	KJ1-26	Mouse IgG <sub>2a</sub>	Biotin	(In house)	
Intracellular antibodies					
IL2	JES6-5H4	Rat IgG <sub>2b</sub>	PE	Caltag	RM9024
Itch	32/Itch	Mouse IgG <sub>1</sub>	Pure	BD Pharmingen	611198
<b>Isotype controls</b>	<b>Clone</b>		<b>Conjugate</b>	<b>Manufacturer</b>	<b>Catalogue number</b>
Armenian Hamster IgG <sub>1</sub> , λ3	G235-2356		FITC	BD Pharmingen	553953
Mouse IgG <sub>1</sub>	MOPC-31C		Pure	BD Pharmingen	557273
Mouse IgG <sub>2a</sub>	5.205		APC	Caltag	MG2a05
Mouse IgG <sub>2a</sub>	G155-178		Biotin	BD Pharmingen	553455
Rat IgG <sub>2a</sub> , κ	R35-95		FITC, PE, PerCP	BD Pharmingen	553929, 553930, 553933
Rat IgG <sub>2b</sub>	LO-DNP-57		PE	Caltag	R2b04
<b>Secondary reagents</b>	<b>Clone</b>	<b>Isotype</b>	<b>Conjugate</b>	<b>Manufacturer</b>	<b>Catalogue number</b>
Anti-mouse IgG <sub>1</sub>	A85-1	Rat IgG <sub>2a</sub> , κ	FITC	BD Pharmingen	553443
Streptavidin			FITC, PE	BD Pharmingen	554060, 554061

**Table 2.2: List of fluorochromes used in flow cytometry (A) and laser scanning cytometry (B).**

**A)**

Label	Excitation (nm)	Emission (nm)	Laser used to excite fluorochrome	Filter used to detect emission
FITC	488	525	Argon	530/30 (FL1)
PE	488	575	Argon	585/42 (FL2)
PerCP	488	675	Argon	670LP (FL3)
APC	635	660	Red Diode	661/16 (FL4)

**B)**

Label	Excitation (nm)	Emission (nm)	Laser used to excite fluorochrome	Filter used to detect emission
Alexa Fluor 350	346	442	UV	UV
DAPI	358	461	UV	UV
Pacific Blue	410	455	UV	UV
FITC	494	525	Argon	D 530/30 nm
Alexa Fluor 488	495	519	Argon	D 530/30 nm
Alexa Fluor 647	650	668	Helium-Neon	H1 650/LP

**Table 2.3: List of primary antibodies used in Western blotting.**

Specificity of antibody	Clone	Isotype	Dilution	Conjugate	Manufacturer	Catalogue number
DO11.10 TCR	KJ1-26	Mouse IgG <sub>2a</sub>	1:500	Biotin	(In house)	
Cbl-b	(polyclonal)	Rabbit IgG	1:1000	Purified	Santa Cruz	sc-1705
Erk 1/2	(polyclonal)	Rabbit IgG	1:500	Purified	Cell Signaling	9102
Grail	H11-744	Rat IgG <sub>2a</sub> , κ	1:1000	Purified	BD Pharmingen	557799
Ikaros	(polyclonal)	Rabbit IgG	1:400	Purified	Abcam	ab26083
Itch	32/Itch	Mouse IgG <sub>1</sub>	1:500	Purified	BD Pharmingen	611198
Lck	(polyclonal)	Rabbit IgG	1:1000	Purified	Cell Signaling	2752
Plcy1	(polyclonal)	Rabbit IgG	1:500	Purified	Millipore	06-159
Smurf1	(polyclonal)	Rabbit Ig	1:500	Purified	Abgent	AP2104a
Smurf2	(polyclonal)	Rabbit Ig	1:500	Purified	Abgent	AP2105a
Traf6	EP591Y	Rabbit IgG	1:2000	Purified	Abcam	ab33915

**Table 2.4: List of primary anti-ubiquitin moieties antibodies (A) and secondary antibodies (B) used in Western blotting.**

**A)**

Specificity of antibody	Clone	Isotype	Dilution	Conjugate	Manufacturer	Catalogue number
Ubiquitin	P4D1	Mouse IgG <sub>1</sub>	1:1000	Purified	Cell Signaling	3936
Mono- and polyubiquitinylyated conjugates	FK2	Mouse IgG <sub>1</sub>	1:1000	Purified	Biomol	PW8810
Polyubiquitinylyated conjugates	FK1	Mouse IgM	1:1000	Purified	Biomol	PW8805
K63-linked polyubiquitinylyated conjugates	HWA4C4	Mouse IgG <sub>2a</sub>	1:500	Purified	Biomol	PW0600

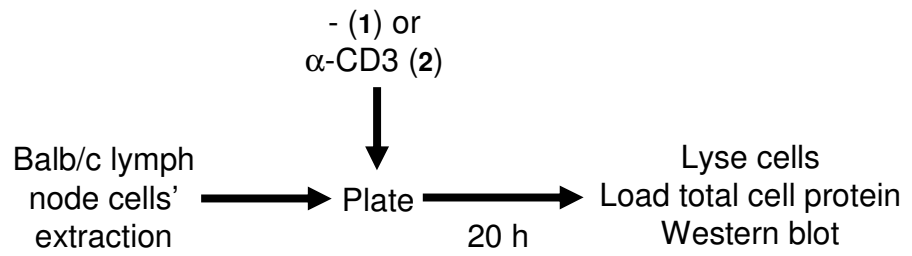
**B)**

Secondary antibodies	Clone	Isotype	Dilution	Conjugate	Manufacturer	Catalogue number
Anti-biotin	(polyclonal)	Goat	1:2000	HRP	Cell Signaling	7075
Anti-mouse IgG	(polyclonal)	Horse	1:2000	HRP	Cell Signaling	7076
Anti-mouse IgM	(polyclonal)	Goat	1:2000	HRP	Santa Cruz	sc-2973
Anti-rabbit IgG	(polyclonal)	Goat	1:2000	HRP	Cell Signaling	7074
Anti-rat Igs	(polyclonal)	Goat	1:2000	HRP	BD Pharmingen	554017

**Figure 2.2: Assessment of antibody specificity by Western blotting.**

Lymph nodes were extracted from BALB/c mice and mashed up. Viable T cells were cultured *in vitro* without stimuli (1) or in the presence of anti-CD3 antibody (2); cells were cultured for a total of 20 h, after which they were harvested and lysed (A). Total protein extracts were separated by SDS-PAGE and transferred onto a nitrocellulose membrane. The membrane was analysed by Western blotting for proteins of interest: it was blocked in 5% milk/ TBS-T for 1 h, washed 3 x 10 min with TBS-T, probed with primary antibody overnight in the cold room, washed 3 x 5 min with TBS-T, incubated with HRP-linked secondary antibody for 1 h, washed 3 x 5 min with TBS-T, incubated with ECL solution for 1 m, and developed. The membrane was then stripped and subsequently re-probed again; antibodies for Itch, Cbl-b and Grail were used (B).

**A)**



**B)**

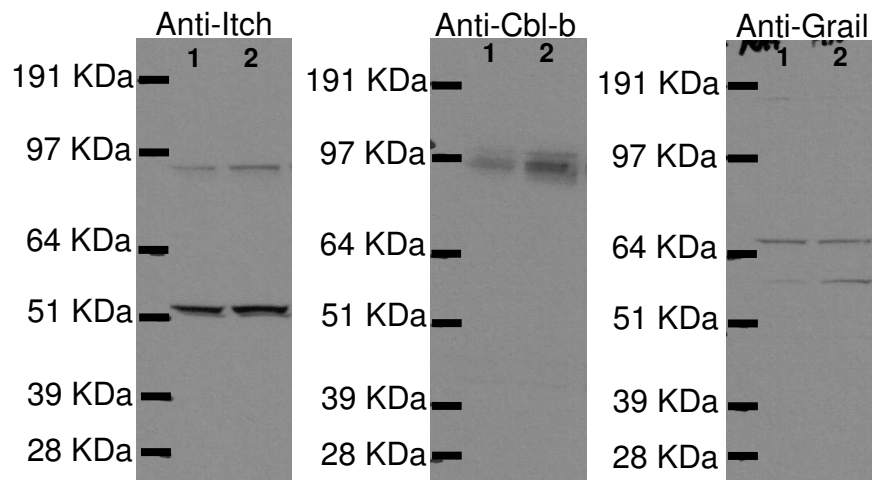


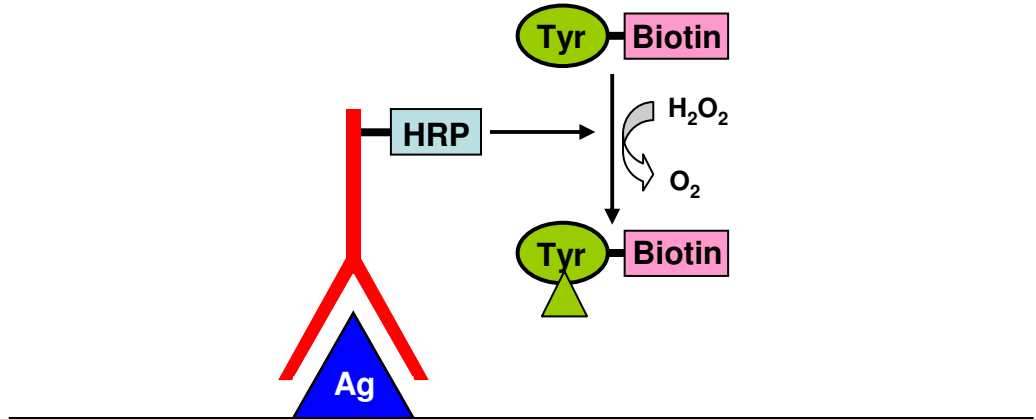
**Table 2.5: List of antibodies used in immunocytochemistry.**

Specificity of antibody	Clone	Isotype	Dilution	Conjugate	Manufacturer	Catalogue number
DO11.10 TCR	KJ1-26	Mouse IgG <sub>2a</sub>	1:250	Biotin	(In house)	
CD4	RM4-5	Rat IgG <sub>2a</sub> , κ	1:250	Biotin	BD Pharmingen	553045
Arf6	3A-1	Mouse IgG <sub>2b</sub>	1:250	Pure	Santa Cruz	sc-7971
Cbl-b	(polyclonal)	Rabbit IgG	1:50	Pure	Santa Cruz	sc-1705
Grail	H11-744	Rat IgG <sub>2a</sub> , κ	1:50	Pure	BD Pharmingen	557799
Itch	32/Itch	Mouse IgG <sub>1</sub>	1:50	Pure	BD Pharmingen	611198
Ubiquitin	P4D1	Mouse IgG <sub>1</sub>	1:250	Pure	Cell Signaling	3936
<b>Isotype controls</b>	<b>Clone</b>			<b>Conjugate</b>	<b>Manufacturer</b>	<b>Catalogue number</b>
Mouse IgG <sub>1</sub>	MOPC-31C		Adequate	Pure	BD Pharmingen	550878
Mouse IgG <sub>2a</sub>	G155-178		Adequate	Biotin	BD Pharmingen	553455
Mouse IgG <sub>2b</sub>	MPC-11		Adequate	Pure	BD Pharmingen	557351
Rabbit IgG			Adequate	Pure	Sigma	I5006
Rat IgG <sub>2a</sub> , κ	R35-95		Adequate	Pure, Biotin	BD Pharmingen	559073, 553928
<b>Secondary antibodies</b>	<b>Clone</b>	<b>Isotype</b>		<b>Conjugate</b>	<b>Manufacturer</b>	<b>Catalogue number</b>
Anti-mouse IgG	(polyclonal)	Horse	1:100	HRP	Cell Signaling	7076
Anti-rabbit IgG	(polyclonal)	Goat	1:100	HRP	Cell Signaling	7074
Anti-rat Igs	(polyclonal)	Goat	1:100	HRP	BD Pharmingen	554017

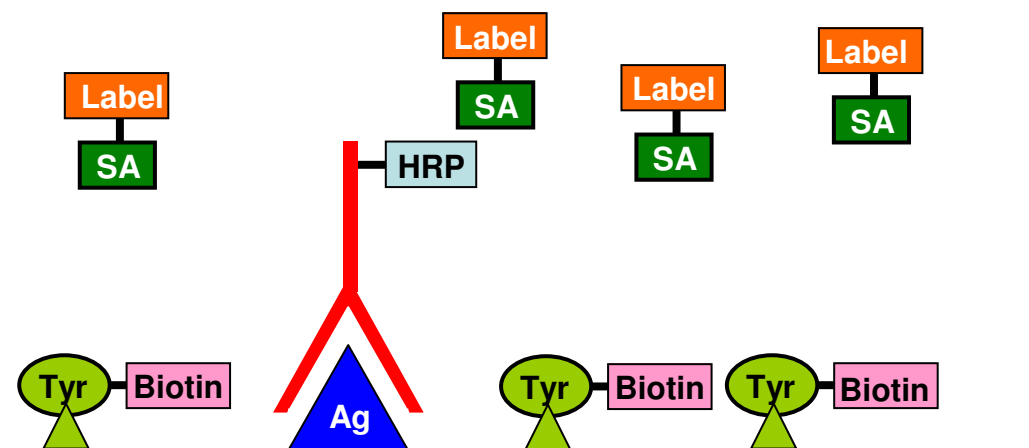
**Figure 2.3: Tyramide indirect signal amplification.**

Tyramide signal amplification is an enzyme-based system for high density labelling of target proteins. HRP-coupled primary antibody was first used to detect the protein. Next, biotin-labelled tyramide was added and the HRP catalysed the deposition of multiple biotin moieties close to the target protein. Finally, streptavidin-coupled fluorochrome was added, binding to the biotin, allowing the fluorochrome to localise nearby the target protein, thus generating a stronger signal, and allowing the target protein's detection.

A)



B)



C)

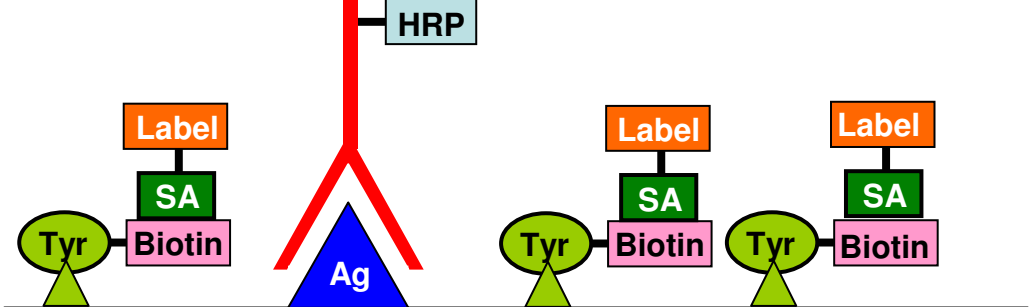
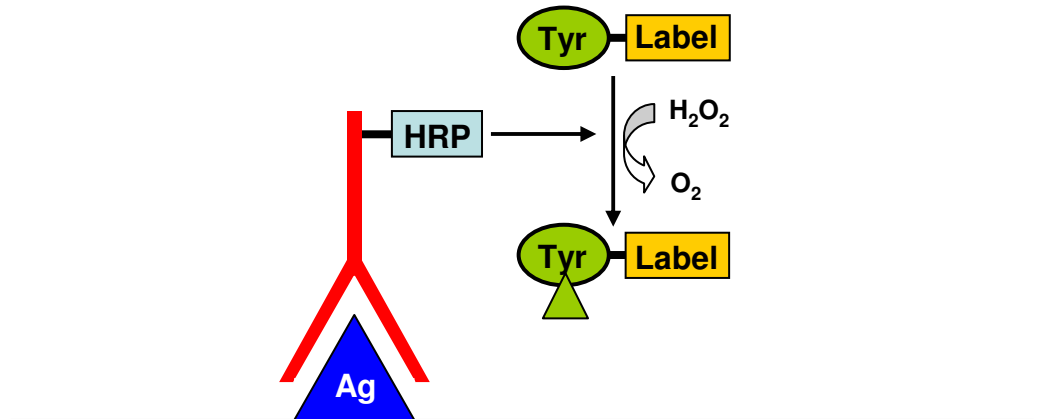


**Figure 2.4: Tyramide direct signal amplification.**

Tyramide signal amplification is an enzyme-based system for high density labelling of target proteins. HRP-coupled primary antibody was first used to detect the protein. Next, fluorochrome-labelled tyramide was added and the HRP catalysed the deposition of multiple fluorochromes close to the target protein, thus generating a stronger signal, and allowing its detection.

A)



B)

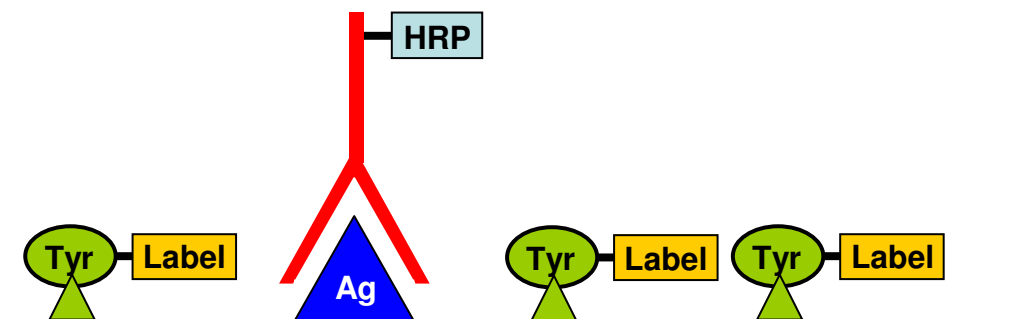


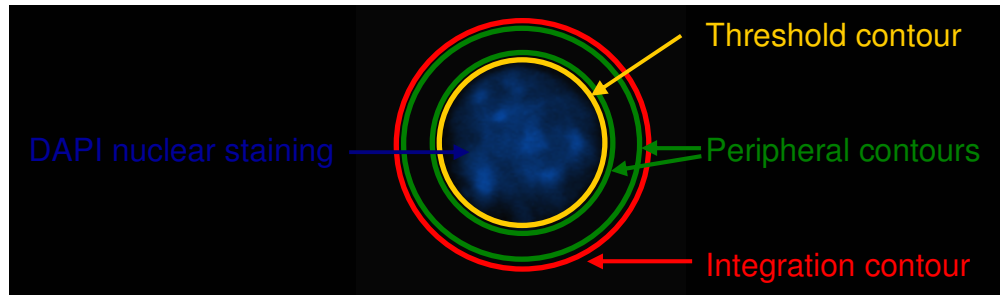
**Table 2.6: List of antibodies used in immunohistochemistry.**

Specificity of antibody	Clone	Isotype	Dilution	Conjugate	Manufacturer	Catalogue number
CD45R/ B220	RA3-6B2	Rat IgG <sub>2a</sub> , κ	1:250	FITC	BD Pharmingen	553088
DO11.10 TCR	KJ1-26	Mouse IgG <sub>2a</sub>	1:250	Biotin	(In house)	
Cbl-b	(polyclonal)	Rabbit IgG	1:50	Pure	Santa Cruz	sc-1705
Grail	H11-744	Rat IgG <sub>2a</sub> , κ	1:50	Pure	BD Pharmingen	557799
Itch	32/Itch	Mouse IgG <sub>1</sub>	1:50	Pure	BD Pharmingen	611198
Smurf1	(polyclonal)	Rabbit Ig	1:50	Pure	Abgent	AP2104a
Smurf2	(polyclonal)	Rabbit Ig	1:50	Pure	Abgent	AP2105a
Isotype controls	Clone	Isotype	Dilution	Conjugate	Manufacturer	Catalogue number
Mouse IgG <sub>1</sub>	MOPC-31C		Adequate	Pure	BD Pharmingen	550878
Mouse IgG <sub>2a</sub>	G155-178		Adequate	Biotin	BD Pharmingen	553455
Rabbit IgG			Adequate	Pure	Sigma	I5006
Rat IgG <sub>2a</sub> , κ	R35-95		Adequate	Pure, FITC	BD Pharmingen	559073, 553929
Secondary antibodies	Clone	Isotype	Dilution	Conjugate	Manufacturer	Catalogue number
Anti-mouse IgG	(polyclonal)	Horse	1:100	HRP	Cell Signaling	7076
Anti-rabbit IgG	(polyclonal)	Goat	1:100	HRP	Cell Signaling	7074
Anti-rat Igs	(polyclonal)	Goat	1:100	HRP	BD Pharmingen	554017

### **Figure 2.5: Cell detection by the LSC.**

Cells are identified in the LSC by means of contours (**A**). Here, the threshold contour was set on the nucleus (which is identified by means of DAPI DNA staining). The integration contour is set on an optimal number of pixels out from the threshold contour, a value which is based on the average size of the cell type, to allow definition of the edge of the cell. The inner peripheral contour is set one pixel out from the threshold contour and the outer peripheral contour is set one pixel in from the integration contour, allowing definition of the periphery of the cell. Two background contours (not shown here, but always used in LSC analysis) measured the background fluorescence outside the cells and allowed for the automatic subtraction of this value from the measured fluorescence values within the other contours. A cell is discriminated if it emits nuclear fluorescence above a threshold value set by the user (**B**). A high threshold detects mainly individual events, whilst an intermediate threshold may detect two or more cells as one event and a low threshold will detect multiple cells as one event.

A)



B)

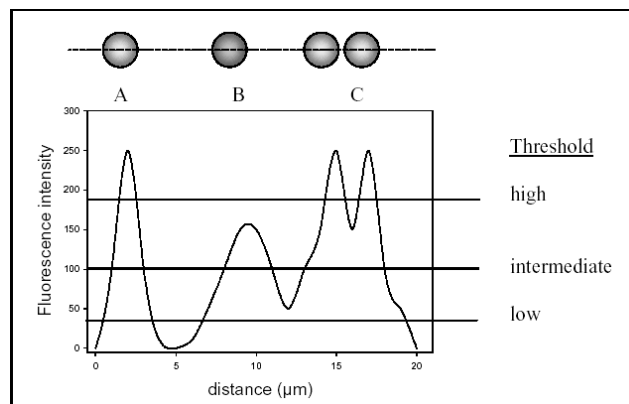
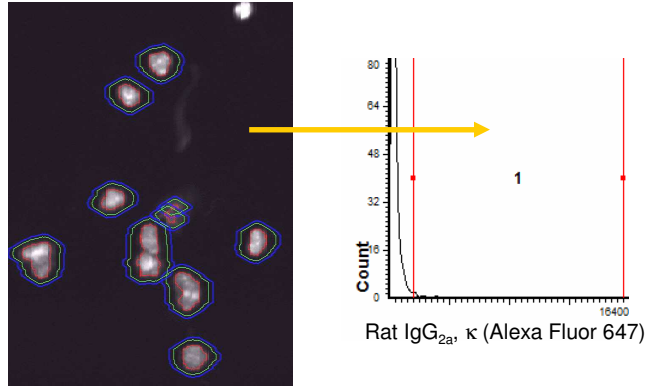


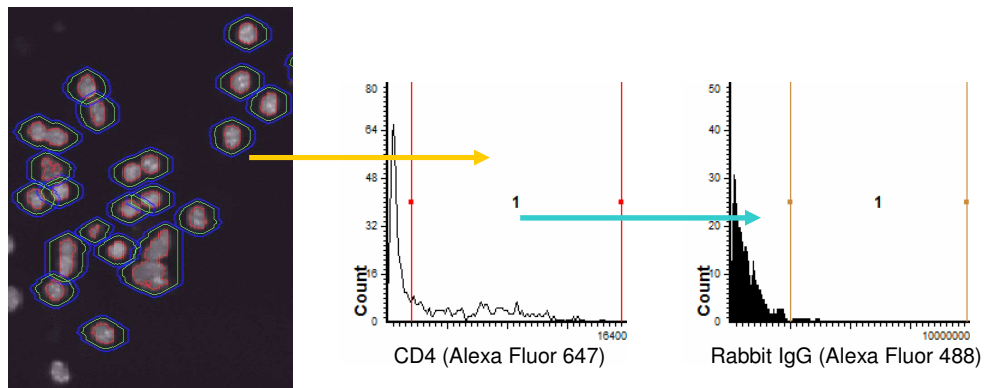
**Figure 2.6: Identification of CD4<sup>+</sup> T cells with the LSC.**

Firstly (leftmost panels) cells are identified by means of contouring on their nucleus, as described in **Figure 2.4** (here, the contours' colour scheme is different). The threshold contour was therefore used to select all nucleated cells by their staining with DAPI (showing in light grey). Next, using the integration contour, fluorescence coming from CD4 co-receptor-bound fluorochrome was measured (fluorescence coming from within the integration contour), thus allowing the identification of CD4<sup>+</sup> T cells. Positive staining for CD4 (cells within area "1" in middle panels) was gated relative to the isotype control (**A**). Finally, gating on those nucleated and CD4<sup>+</sup> events (also using the integration contour), the fluorescence from the fluorochrome bound to the intracellular protein of choice was measured (**C**). Positive staining (cells within area "1" in rightmost panels) for the intracellular protein of choice (here, Cbl-b) was gated relative to the isotype control (**B**).

A)



B)



C)

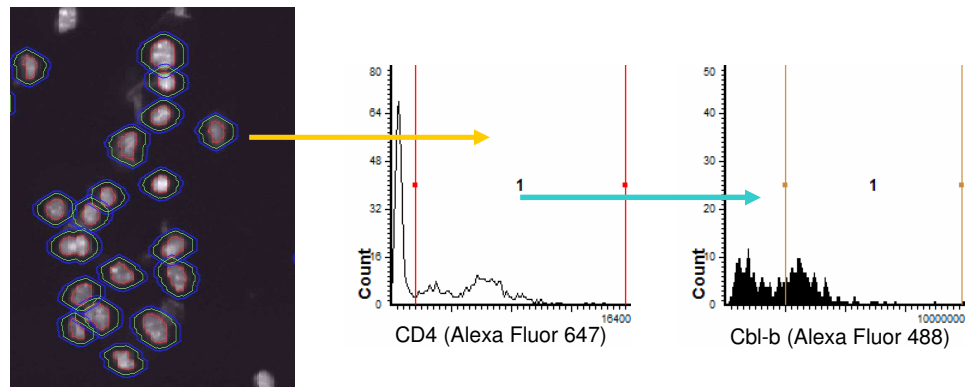


**Figure 2.7: Analysis of cell cycle progression with the LSC.**

Nuclei of cytocentrifuged cells were stained with DAPI and analysis carried out by LSC by plotting the Max Pixel value (depicting chromatin condensation) along the x-axis and the Integral value (representing DNA content) along the y-axis of the scattergram. The plotted cells were then gated according to their xy-position on the scattergram. Apoptotic cells (light green gate) have the least DNA content: they contain subdiploid DNA due to its fragmentation, placing them leftmost and bottommost of all the cells on the scattergram. Cells arrested at the G1/G0 phase (red gate) of the cell cycle are diploid (2n DNA) and can therefore be identified on the scattergram above the apoptotic cells. Cells in the S phase (blue gate) can be identified by their increased DNA content above the G1/G0 phase cells. Moreover, cells in the other mitotic stages (G2/M phase) which also contain high amounts of DNA (4n DNA) can be differentiated due to a higher level of chromatin condensation (dark green gate), being placed rightmost and topmost of all the cells in the scattergram. Newly-formed daughter cells (NFDCs; yellow gate), while still exhibiting a high level of chromatin condensation do not have 4n DNA and as such can be spotted below the G2/M phase cells on the scattergram. Representative images of cells validating for each stage of the cell cycle are shown.

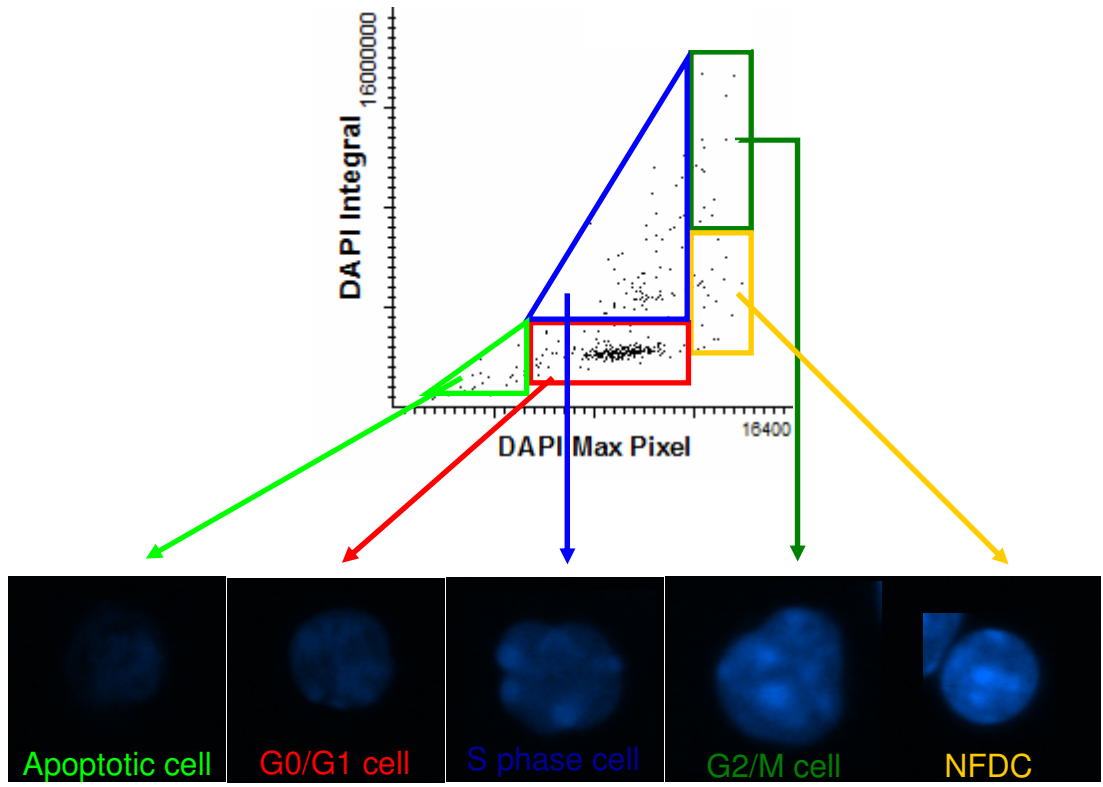
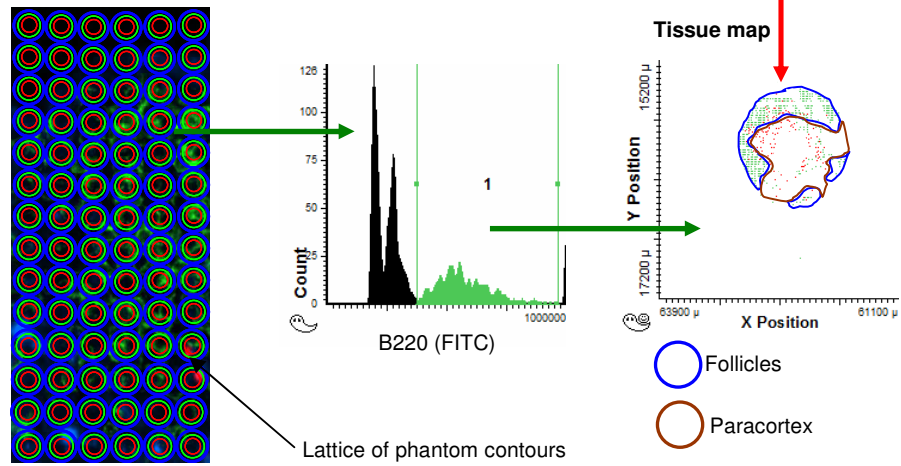
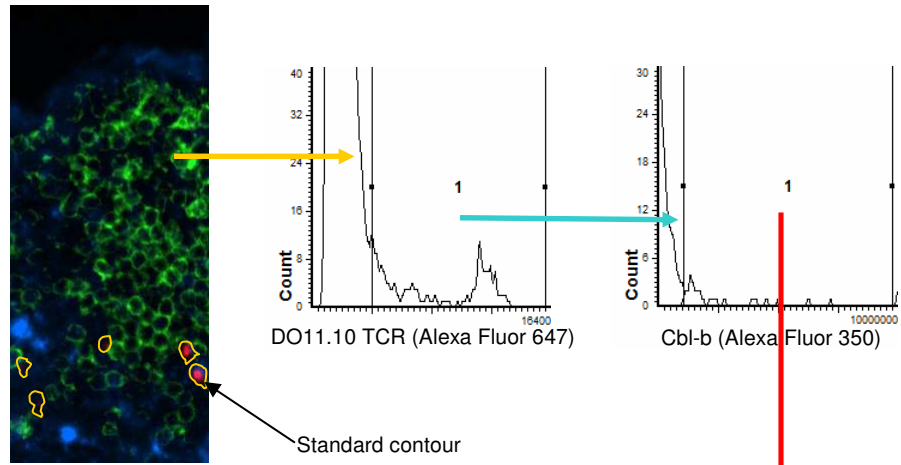


**Figure 2.8: Analysis of lymph node tissue sections with the LSC.**

Tissue sections were stained for B220 (B cells, in green), DO11.10 TCR (antigen-specific transgenic T cells, in red) and Cbl-b (in blue) as shown in the leftmost panels. LSC detected antigen-specific T cells using standard contours (yellow contours; top leftmost panel) and measured the levels of Cbl-b inside these cells (cells gated in region “1” in the top middle panel). B cell rich areas were identified (similarly to antigen-specific T cells, these were considered to be the ones in region “1” in the bottom middle panel) using phantom contours (these look like a lattice that overlaps the section, as exemplified in bottom leftmost panel). A tissue map depicting the location of Cbl-b-expressing antigen-specific T cells within the lymph node was generated (bottom, rightmost panel). This also incorporated the B cell areas (follicles) and allowed the identification of the paracortex (B cell-free area, in the centre of the lymph node). Adequate isotype controls were used to set the gates of positive staining for B cells, antigen-specific transgenic T cells and Cbl-b. Numbers and statistics on these cells in both types of area within the lymph node can be quantified.



CHAPTER 3  
RESULTS

## 3 RESULTS

### 3.1 The induction phase of anergy and priming in CD4<sup>+</sup> T cells

#### 3.1.1 Functional assessment of the induction of anergy and priming in CD4<sup>+</sup> T cells, *in vitro*

CD4<sup>+</sup> T cells were extracted and purified from mice as described in the Materials and Methods chapter. These cells were then stimulated *in vitro* in order to render them anergic or primed. CD4<sup>+</sup> T cells were cultured with immobilised anti-CD3 antibody to induce anergy while culture with immobilised anti-CD3 antibody and anti-CD28 antibody induced priming [130]. This is because the CD28 receptor acts as the co-stimulator necessary to fully activate the pathways that lead to T cell activation and proliferation, while CD3 stimulation is the necessary first step that if not followed, however, leads to quiescence [275]. Addition of anti-CD3 and anti-CD28 antibodies to the cell culture allows for the stimulation of these receptors in the T cells. An alternative method to induce anergy or priming was also used: this involves the *in vitro* stimulation of the CD4<sup>+</sup> T cells with ionomycin for the induction of anergy and ionomycin and PMA for the induction of priming [276]. A schematic of the stimulation procedure can be found in **Figure 3.1A**.

Ionomycin is a calcium ionophore which permits the increase of the intracellular Ca<sup>2+</sup> levels. Increased intracellular Ca<sup>2+</sup> concentration (which occurs under normal situations following TCR stimulation) together with calmodulin leads to activation of Cn, a calcium-dependent phosphatase, which de-phosphorylates the transcription factor NFAT [57, 116]. The phorbol ester PMA activates PKC directly [277].

While ionomycin is sufficient to induce anergy in T cells, IL-2 production, CD69 expression, growth and proliferation can be induced by the addition of ionomycin and PMA to *in vitro* cultured T cells; however, both pharmacological agents bypass TCR ligation and, hence, the initial steps in TCR signalling [122].

To confirm induction of priming and tolerance, CD4<sup>+</sup> T cells were analysed for their functional responses. The functional outcome of the different conditions was first assessed via an early activation assay measuring CD69 upregulation (**Figure 3.1B**). Here, expression of the early activation marker CD69 was determined by flow

cytometric analysis, with values represented as mean fluorescence intensity (MFI) plotted as fold increase of the MFI of naïve (unstimulated) CD4<sup>+</sup> T cells where the MFI value of these cells was taken as basal and assigned the “1” value. Anergising conditions (anti-CD3 antibody or ionomycin) were found to yield a slight increase in CD69 expression (roughly 2-fold) indicating that there is some degree of activation in CD4<sup>+</sup> T cells under these conditions. However, priming conditions (anti-CD3+anti-CD28 antibodies and ionomycin+PMA) yield a much higher increase in CD69 expression (4- and 8-fold, respectively) indicating not only that CD4<sup>+</sup> T cells are being activated but showing that their activation is considerably higher than that exhibited under anergy-inducing conditions. This is what would be expected of priming stimuli. The percentage of CD4<sup>+</sup> T cells positive for CD69 was also analysed, showing similar results to the MFI (not shown).

The functional outcome of the different conditions was also assessed via a proliferation assay (**Figure 3.1C**). Here, [<sup>3</sup>H]thymidine was added to the *in vitro* CD4<sup>+</sup> T cell culture and its incorporation in the cells' DNA was measured to demonstrate how much newly-synthesised DNA was produced and hence provide an indication of cell cycle progression resulting in proliferation. As expected, unstimulated CD4<sup>+</sup> T cells exhibit near-zero proliferation and the anergising stimuli induced above no-stimulus-level proliferation. However, priming stimuli induced strong proliferation of the CD4<sup>+</sup> T cells with well over 10-times the [<sup>3</sup>H]thymidine levels than their anergising counterparts.

Collectively therefore, it is possible to say that the stimuli intended to induce priming (anti-CD3+anti-CD28 antibodies and ionomycin+PMA) are doing so, and that the functional outcome they are inducing in CD4<sup>+</sup> T cells is qualitatively different than the outcome generated by the intended anergising stimuli. Also, it is important to stress that this is happening in the intended time-frame scheduled for the induction phase experiments.

### ***3.1.2 Analysis of the expression of E3 ubiquitin-protein ligases in the induction phase of anergy and priming***

A number of E3 ubiquitin-protein ligases have been reported to be involved in signalling processes in T cells with some of these being described as playing key roles in the anergy versus priming decision these cells undergo [183, 193, 233]. The role(s) of Itch, Cbl-b and Grail warranted further clarification in regard to these processes. Initially, antibodies were acquired and tested for the detection of these proteins via

Western blotting. Cells were extracted and stimulated *in vitro* as described before in the Materials and Methods chapter and following termination of reactions, total cell protein was extracted and analysed for the expression of relevant proteins (**Figure 3.2A**). For example, the intensity of expression of PLC $\gamma$ -1 is highest in the anti-CD3+anti-CD28-stimulated cells and lowest in the ionomycin-stimulated cells (**Figure 3.2B**). This correlates nicely with the need for PLC $\gamma$ -1 involvement in the signalling transduction pathways leading to priming in T cells, while during induction of anergy PLC $\gamma$ -1 is downregulated [111, 183].

With respect to the E3 ubiquitin-protein ligases, Itch is induced in all stimulated cells (comparing to unstimulated, naïve ones, which nonetheless do express some degree of Itch) and as expected, it is highly expressed in ionomycin-stimulated cells (**Figure 3.2B**). Rather unexpectedly, it is also highly expressed in anti-CD3+anti-CD28-treated cells whilst the anti-CD3-stimulated population expresses Itch with less intensity than the other two stimulated populations. Cbl-b is expressed most intensely in both the anti-CD3- and anti-CD3+anti-CD28-stimulated cells. However, ionomycin-stimulated cells also express it, indicating that it is upregulated in all stimulated cells relative to the unstimulated ones. The blot shows a ladder of Cbl-b bands around the 109 KDa mark, though there is one band more intense than all the others. This ladder of bands is possibly the result of differential ubiquitination of Cbl-b as mono- or poly-ubiquitination of a protein (progressive addition of the 8-KDa ubiquitin monomer) yields it an increasingly higher molecular weight [278] with the corresponding slower migration in a bis-tris gel, just as observed here. Smurf1 also exhibits a similar ladder pattern. This E3 ubiquitin-protein ligase is expressed in the cells under all tested conditions although it seems to be upregulated when cells are stimulated with any of the stimuli. Unstimulated cells not only have less Smurf1 but they also exhibit less ubiquitinated Smurf1 as indicated by a reduced ladder effect. By contrast, Smurf2 did not exhibit this ladder effect nor upregulation as its expression does not appear to change with the different stimuli. As with Itch, Grail is expressed more intensely in both the ionomycin- and anti-CD3+anti-CD28-stimulated cells, while in anti-CD3-stimulated and naïve cells there is roughly the same amount of protein.

The expression of the adaptor protein Traf6, which can act as an E3 ubiquitin-protein ligase as well, was also assessed (**Figure 3.2B**). Traf6 promotes the activation of NF- $\kappa$ B [70, 71], a transcription factor required for full T cell activation [74]. As such, Traf6 is potentially a positive mediator of T cell priming whilst its contribution to the regulation of the priming Vs anergy decision is yet to be ascertained. Its expression

levels in unstimulated, anergising and priming T cells were firstly analysed, looking for differential expression. Traf6 is expressed in all unstimulated and stimulated populations. There is clearly more Traf6 protein in anti-CD3+anti-CD28-stimulated cells than in anti-CD3- stimulated ones, which in turn express more than unstimulated ones. However, it is the ionomycin-stimulated cells that express the least Traf6. It would appear Traf6 is being differentially expressed and that its highest expression correlates to its requirement for T cell activation.

As this analysis did not give any indication of the activity of E3 ubiquitin-protein ligases, the total protein lysates were also tested for the presence of ubiquitinated proteins (**Figure 3.3**). Globally, the ubiquitination of proteins (**Figure 3.3A**) is most intense in the anti-CD3+anti-CD28-stimulated cells, with the anti-CD3-stimulated cells almost comparable. Ionomycin-stimulated cells also express ubiquitinated proteins intensely while naïve cells exhibit only basal levels of ubiquitination indicating that these processes are stimulated under all conditions. Next, to address the mechanisms involved more closely, assessment of the prevalence of mono- and poly-ubiquitinated proteins under the different conditions was carried out (**Figure 3.3B**). It was expected that this should yield a pattern of ubiquitinated proteins very similar to the one previously described, however this does not happen and the band pattern is very distinct. Nevertheless, anti-CD3+anti-CD28-stimulated cells do seem to express mono- and poly-ubiquitinated proteins most intensely, with the anti-CD3-stimulated cells coming in a close second and the naïve cells expressing least. Blotting the membrane for the presence of only polyubiquitinated proteins (**Figure 3.3C**) reveals some of the “missing” bands encountered in **Figure 3.3A**, with again the highest expression being in anti-CD3+anti-CD28- and anti-CD3-stimulated cells although there were not many differences between any of the stimuli. In **Figure 3.3D** only K63-linked polyubiquitinated proteins are shown and here, this blot most closely mirrors the global ubiquitination profile as many of the bands encountered in **Figures 3.3A and B**, come up again. There are some proteins more intensely K63-linked polyubiquitinated in some of the stimuli than others, predominantly in the anti-CD3+anti-CD28- and anti-CD3-stimulated cells.

The fact cells undergoing both priming and anergy exhibit such increased ubiquitination is an indication this process might be involved in the general regulation of T cell signalling. Possibly this might occur by the targeting of TCR signal transducers by E3 ubiquitin-protein ligases, and to address this, protein from naïve, anergising and priming T cells was immunoprecipitated with an antibody against all

ubiquitinated conjugates and then blotted for proteins of interest (**Figure 3.4A**). Moreover, pull-down of E3-ligases in ubiquitin-containing complexes could begin to identify those selectively recruited and activated under differential functional outcomes. Indeed, PLC $\gamma$ -1, Itch, Cbl-b, Smurf1, Smurf2 and Grail were all found to co-precipitate with ubiquitin as early as following 1 h of stimulation with anti-CD3 antibody but not in unstimulated or anti-CD3+anti-CD28-stimulated cells (**Figure 3.4B**). However, at 20 h, PLC $\gamma$ -1 and Itch co-precipitate with ubiquitin in unstimulated, anti-CD3- and anti-CD3+anti-CD28-stimulated T cells whilst Smurf1 and Smurf2 co-precipitate with ubiquitin in the unstimulated and anti-CD3-stimulated T cells; on the contrary, Cbl-b appears to co-precipitate with ubiquitin only in the anti-CD3+anti-CD28-stimulated population of T cells.

That PLC $\gamma$ -1 is found in ubiquitin-containing complexes suggests ubiquitination as a possible modulation factor for its expression levels. The complexing of Itch, Cbl-b, Smurf1, Smurf2 and Grail suggests something else, though; since these are E3 ubiquitin-protein ligases, their recruitment and/or ubiquitination points for them playing an active role in the modulation of proteins involved in signal transduction in the anergising and priming T cells.

The Western blotting data so far relates to cells extracted from lymph nodes and hence may be complicated by bidirectional signalling in accessory cells, particularly as the strong preferential induction of E3 ligases under conditions of anergy (but not priming) predicted by the ionomycin system [183, 233] were not replicated when cells were stimulated with anti-CD3 $\pm$ anti-CD28 antibodies. In order to have a clear picture of what happens in a homogenous T cell population, CD4<sup>+</sup> T cells were purified from the whole lymph node cell population before *in vitro* cell culture and stimulation, and subsequently analysed by Western blotting (**Figure 3.5**). Nevertheless, PLC $\gamma$ -1 is again most intensely expressed in the anti-CD3+anti-CD28-stimulated T cells and least in the anti-CD3-stimulated T cells (**Figure 3.6A and B**), as expected and a good indication that both these stimuli are inducing the predicted differential functional outcome for the populations. However, as with the LN populations, all E3 ligases were more highly expressed in anti-CD3+anti-CD28 than in anti-CD3-stimulated cells (**Figure 3.6A**). Indeed, Grail was barely upregulated in anti-CD3-treated cells showing comparable levels to those of unstimulated CD4<sup>+</sup> T cells.

Although anti-CD3+anti-CD28 antibodies induce the highest expression of Smurf1 in CD4<sup>+</sup> T cells, its expression does not change much with the different stimuli (**Figure 3.6B**). There is a ladder of Smurf1 bands around the 86 KDa mark, just as

observed for the unpurified T cells (**Figure 3.2B**). This might be an indication that Smurf1 is active in CD4<sup>+</sup> T cells. Lck was also blotted for; this protein is involved in TCR signalling and it has been reported that, like PLC $\gamma$ -1, anergised T cells (stimulated with anti-CD3 in the absence of co-stimulation) express less of it than primed T cells (stimulated with anti-CD3+anti-CD28) [183]; here, anti-CD3-stimulated T cells are expressing Lck the least, as expected (**Figure 3.6B**).

Smurf2 expression was also analysed in CD4<sup>+</sup> T cells (**Figure 3.6B and C**) and, unlike the LN cells, it seems to be upregulated in the anti-CD3+anti-CD28-stimulated population. Also unlike the LN cells, here (**Figure 3.6C**), there is not much difference in expression of Traf6 between the two conditions; however, anti-CD3-stimulated CD4<sup>+</sup> T cells seem to express a little bit more than anti-CD3+anti-CD28-stimulated CD4<sup>+</sup> T cells. Ikaros, the transcriptional repressor involved in *Ii2* transcription repression by promoting histone deacetylation [120], also seems to be a little bit more expressed in anti-CD3-stimulated CD4<sup>+</sup> T cells than anti-CD3+anti-CD28-stimulated CD4<sup>+</sup> T cells, agreeing with previous reports of mRNA upregulation during anergy induction [116].

Proteins involved in the signalling transduction pathways conveying the signal from the TCR leading to differential outcomes (ie, anergy Vs priming) are under tight regulation by a number of mechanisms [111, 126, 128]. Proteins can be downmodulated upon receiving a specific signal and this can be a functional downmodulation by means of inactivation, re-location or downmodulation by degradation of the protein [111, 130, 183]. Ubiquitination is involved in all of these processes as it can lead to conformational changes resulting in inactivation, re-location and signalling for degradation via the proteasome or lysosomes [183, 242, 279, 280]. At the same time, E3 ubiquitin-protein ligases can auto-inhibit themselves [253] and be modulated by means of ubiquitination, including self-ubiquitination [247]. The data above show that anergising and priming T cells exhibit many ubiquitinated proteins. Some of these are K63-linked polyubiquitinated proteins, which should be targeted for downmodulation by proteasome-independent processes [159, 164]. It is important to assess if ubiquitination is taking an active role in the downmodulation of proteins in the TCR signalling transduction pathway. And, at the same time assess if the E3 ubiquitin-protein ligases involved in the modulation of these signal transducers are themselves being modulated by ubiquitination. The most common form of regulation by ubiquitination is thought to be protein degradation in the proteasome. By using proteasome inhibitors it is possible to block proteasome function, preventing protein degradation from occurring and as a consequence, resulting in an accumulation of the ubiquitinated proteins in the cell.

Lactacystin is one such potent, cell permeable and selective proteasome inhibitor affecting all three ATP-independent activities of the 20S complex of the proteasome [281] and as such was used to block proteasome-mediated degradation of ubiquitinated proteins. Cells treated with lactacystin showed generally less protein than un-treated cells (**Figure 3.6E**).

PLC $\gamma$ -1 has been reported to be degraded following ubiquitination during ionomycin-induced anergy [183]. This degradation however requires a second signal (high cell density re-plating) and the use of another proteasome inhibitor (MG132) did not block its degradation [183]. Here, in anti-CD3-stimulated CD4<sup>+</sup> T cells grown with lactacystin we observe higher expression of PLC $\gamma$ -1 than in unstimulated cells also treated with lactacystin (**Figure 3.7A**). This would suggest PLC $\gamma$ -1 is being downmodulated in the anti-CD3-stimulated CD4<sup>+</sup> T cells by means of proteasome-mediated degradation since in lactacystin-free grown cells (**Figure 3.6A and B**) PLC $\gamma$ -1 was more expressed in unstimulated than anti-CD3-stimulated CD4<sup>+</sup> T cells. Also, using another anergy-inducing stimulus (ionomycin) and comparing cells thus stimulated with anti-CD3+anti-CD28-stimulated CD4<sup>+</sup> T cells (**Figure 3.7D**) shows once again higher expression of PLC $\gamma$ -1 in the anergising cells. Since in lactacystin-free grown cells the priming population expressed the highest levels of PLC $\gamma$ -1 (**Figure 3.6A and B**), this would suggest lactacystin promotes the accumulation of PLC $\gamma$ -1 in anergising cells and this is being accomplished via inhibition of proteasome-mediated degradation of PLC $\gamma$ -1. These data suggest PLC $\gamma$ -1 can be degraded, at least in part, via the ubiquitin-proteasome pathway, although its degradation via the lysosomal pathway has been previously reported [183].

In a non-anergy model, TCR plus CD4 co-ligation induces Cbl-mediated Lck ubiquitination in the human CD4<sup>+</sup> T cell line SPF1, and that ubiquitination targets Lck to the proteasome [282] whilst in CTLs TCR triggering results in rapid degradation of Lck through a mechanism that is proteasome- and lysosome-independent, but sensitive to cysteine protease inhibitors [283]. Here (**Figure 3.7A**), there is not much difference between the two conditions, which points to Lck downregulation, as observed in anti-CD3-stimulated CD4<sup>+</sup> T cells in the absence of lactacystin (**Figure 3.6B**), not involving proteasomal degradation. By contrast, expression of Itch, Cbl-b, Smurf1 and Smurf2 is slightly enhanced in anti-CD3 stimulated, proteasome-inhibited CD4<sup>+</sup> T cells (**Figure 3.7A and B**). For Itch and Cbl-b this merely reflects the trend observed in lactacystin-free grown cells and might indicate proteasomal degradation is not involved in regulating the expression of these proteins or, if it is involved it does not play the

decisive role under these stimuli. The intensity of Smurf1 and Smurf2 expression did not change from unstimulated to anti-CD3-stimulated, lactacystin-free grown cells (**Figure 3.6B**) but here, when the proteasome was inhibited, both Smurf1 and Smurf2 are slightly more expressed in anti-CD3-stimulated CD4<sup>+</sup> T cells than in unstimulated ones indicating a dynamic turnover of these E3 ligases during induction of anergy. This, as also happens for PLC $\gamma$ -1, is an indication that both Smurfs are being downmodulated in anti-CD3-stimulated CD4<sup>+</sup> T cells by means of proteasome-mediated degradation. Comparing anti-CD3- with anti-CD3+anti-CD28-stimulated CD4<sup>+</sup> T cells grown with lactacystin (**Figure 3.7C**) suggests Smurf2 is in fact being regulated in anergising T cells by means of proteasomal degradation as it is more intensely expressed in these cells rather than the T cells undergoing priming, while in lactacystin-free grown cells the opposite was observed (**Figure 3.6B**).

Like Smurf2, Itch, Cbl-b and Grail are also more intensely expressed in anti-CD3-stimulated CD4<sup>+</sup> T cells than anti-CD3+anti-CD28-stimulated CD4<sup>+</sup> T cells, when grown with lactacystin (**Figure 3.7C**). Because the opposite was true in lactacystin-free conditions (**Figure 3.6A**), addition of anti-CD3 antibody seems likely to induce proteasomal degradation of these proteins more extensively than addition of anti-CD3+anti-CD28 antibodies. This effect is specific of the anti-CD3 antibody-way of inducing anergy as stimulating the cells with ionomycin in the presence of lactacystin does not lead to accumulation of Itch, Cbl-b or Grail in greater extent than that observed in anti-CD3+anti-CD28-stimulated CD4<sup>+</sup> T cells (**Figure 3.7D**).

Considering induction of anergy and priming involves dynamic processes that most likely involve upregulation and downregulation of multiple signal transducers in different time-frames, time-course experiments were run for 3, 6, 20 and 48 h, covering the induction period (**Figure 3.8**). Reflecting this, whilst at 3 h there are roughly comparable levels of Itch, Cbl-b and Grail in anti-CD3+anti-CD28- and anti-CD3-stimulated CD4<sup>+</sup> T cells, at 48 h Itch and Cbl-b are expressed more highly in anti-CD3+anti-CD28- relative to anti-CD3-stimulated CD4<sup>+</sup> T cells (**Figure 3.9**). Also at 48 h, Grail is more highly expressed in anti-CD3- than anti-CD3+anti-CD28-stimulated CD4<sup>+</sup> T cells. By contrast, ionomycin+PMA-stimulated cells express Grail more intensely than cells stimulated with ionomycin alone, at 3 and 6 h of *in vitro* culture, but at 20 h the opposite happens. Cbl-b is also more intensely expressed at 6 h in ionomycin+PMA-stimulated cells than cells stimulated with ionomycin alone whilst the opposite happens at 20 h.

These total protein lysates were also tested for the presence of ubiquitinated proteins (**Figures 3.10**). Globally, the ubiquitination of proteins is more intense in the ionomycin+PMA-stimulated cells than ionomycin-stimulated cells at 3 and 6 h and perhaps consistent with this, ubiquitination of proteins also looks more intense in anti-CD3+anti-CD28-stimulated CD4<sup>+</sup> T cells than in anti-CD3-stimulated CD4<sup>+</sup> T cells but predominantly at later time-points such as 48 h. Next, assessment of the prevalence of mono- and poly-ubiquitinated proteins in the different conditions was carried out and this showed a similar but less pronounced pattern. Analysis of only K63-linked polyubiquitinated proteins showed that, at 3 h, anti-CD3-stimulated cells are expressing K63-linked polyubiquitinated proteins more intensely than anti-CD3+anti-CD28-stimulated CD4<sup>+</sup> T cells but at later time-points this difference is lost and reversed at 48 h mirroring the global ubiquitination pattern. Likewise, reflecting the global ubiquitination profile, ionomycin+PMA-stimulated cells are expressing K63-linked polyubiquitinated proteins more intensely than ionomycin-stimulated CD4<sup>+</sup> T cells.

Taken together, unlike previous reports [183, 233], these results indicate that upregulation of E3 ligase expression and ubiquitin-mediated proteasomal degradation is not necessarily a key signal regulating commitment to anergy versus priming. As there is increasing evidence [242, 279, 280] for a role(s) for E3 ligases in regulation of signal transduction by proteasome-independent ways, namely by modulating the activity (via stability and protein-protein recognition interference), by promoting changes in subcellular localisation and by targeting proteins to the endocytic pathway (which can lead either to recycling or to degradation in the lysosome) [159], it was decided to analyse the role of E3 ligases in the induction of anergy and priming of T cells at the single cell level.

### ***3.1.3 Analysis of the expression of E3 ubiquitin-protein ligases in the induction phase of anergy and priming at the single-cell level***

#### **3.1.3.1 Cbl-b**

After having demonstrated that the different stimuli are inducing different functional outcomes (anergy and priming), the expression of some of the E3 ubiquitin-protein ligases described above and postulated to be involved in enforcing induction of anergy was assessed by analysis of immunofluorescence staining of cytospin preparations of primed and tolerised CD4<sup>+</sup> T cells. First, Cbl-b expression in CD4<sup>+</sup> T cells undergoing induction of anergy or priming *in vitro* was imaged and quantified

(**Figure 3.11**). This was done by staining the cells for the CD4 co-receptor and Cbl-b after 20 h of *in vitro* culture stimulation and then quantifying the resultant fluorescence by LSC. Surprisingly, Cbl-b was found to be expressed in a higher percentage of CD4<sup>+</sup> T cells undergoing induction of priming (anti-CD3+anti-CD28 antibodies and ionomycin+PMA stimuli) than that of CD4<sup>+</sup> T cells undergoing anergy induction (anti-CD3 antibody and ionomycin). In fact, all populations express Cbl-b but those undergoing anergy induction showed the lowest proportion that expressed it, with even a lower percentage positive population than that of the naïve CD4<sup>+</sup> T cell group (**Figure 3.11A**). Moreover, analysis of the mean fluorescence intensity of Cbl-b expression of CD4<sup>+</sup>Cbl-b<sup>+</sup> cells showed little or no difference between the different stimuli (**Figure 3.11B**), meaning cells which are expressing Cbl-b express it at the same intensity regardless of whether they are undergoing anergy or priming.

LSC also allows for the determination of the location of Cbl-b expression within a cell and therefore it was investigated whether Cbl-b showed a differential subcellular location in cells undergoing induction of priming and tolerance. For example, in **Figure 3.11C** the proportion of CD4<sup>+</sup> cells expressing Cbl-b at the cell periphery is shown. Interestingly, the CD4<sup>+</sup> T cells treated with anti-CD3+anti-CD28 antibodies exhibited by far the highest percentage of cells expressing Cbl-b at the cell periphery, suggesting that there may be differential location of Cbl-b in this CD4<sup>+</sup> T cell population versus any of the other populations of cells as, whilst the other CD4<sup>+</sup> T cell populations also express Cbl-b at the periphery, they do not do it to the extent of the primed CD4<sup>+</sup> T cell population (taking in account **Figure 3.11A**). With respect to the levels of expression of Cbl-b in CD4<sup>+</sup>Cbl-b<sup>+</sup> T cells at the periphery, Cbl-b is expressed most highly at the periphery of naïve T cells and at lower, but comparable levels in the primed and anergic populations (**Figure 3.11D**).

In order to visualise the expression of Cbl-b during the induction and priming of CD4<sup>+</sup> T cells, images of the different populations were captured using a fluorescent microscope (**Figure 3.12**). As microscopy can often be subjective, the LSC was used blind to quantitate and then corroborated by relocating to selected cells, of which photographs were taken. All nucleated cells were imaged initially based on DAPI staining (blue) and T cells were identified by their expression of CD4 (red), while the expression of Cbl-b was also detected (green). In the end the three images were merged, allowing visual assessment of Cbl-b expression in CD4<sup>+</sup> T cells. In these images we can gather a better understanding of Cbl-b expression and location: for example, rather unexpectedly given the current proposals regarding the role of E3-ligases in tolerance

induction, anti-CD3- and anti-CD3+anti-CD28-stimulated cells appear to exhibit a similar intensity of expression of Cbl-b, as seen in **Figure 3.11B**). More interestingly perhaps, anti-CD3+anti-CD28-stimulated cells appear to exhibit a more peripheral Cbl-b expression, suggesting co-localisation with the TCR. Although the anti-CD3-stimulated cells express Cbl-b more diffusely, they also have it at the periphery, and here it seems to concentrate in one of the poles.

In another experiment, the expression of Cbl-b in CD4<sup>+</sup> T cells was also analysed at 40 h post-commencement of the stimuli (**Figure 3.13**). Again at this time-point there is a higher percentage of cells expressing Cbl-b in the primed relative to the anergic populations (**Figure 3.13A**) though this effect is no longer as marked as at 20 h post-stimulation (**Figure 3.11A**). Cbl-b seems to be more expressed in cells cultured with ionomycin+PMA than any other stimulus (**Figure 3.13B**) and, similarly, it seems it is more intensely expressed within the periphery of these cells than within the periphery of cells stimulated with any of the other stimuli (**Figure 3.13D**). These results should take in account that only 3% of CD4<sup>+</sup> T cells stimulated with ionomycin+PMA are expressing Cbl-b at the cell periphery (**Figure 3.13C**) and that even lower proportions of cells cultured *in vitro* under the other conditions expressed Cbl-b at the cell periphery. For instance, ionomycin-stimulated cells showed no Cbl-b within its periphery; this may be more of a secondary effect of culturing T cells with such a high concentration of ionomycin for so long than a reliable trend; visual inspection of the field of large portions of the slide revealed few normal-topology cells at this time-point (not shown).

In order to visualise these data, colour images of the different populations were captured using a fluorescent microscope (**Figure 3.14**). In the cells chosen for photography, anti-CD3- and anti-CD3+anti-CD28-stimulated cells appear to have a higher intensity of expression of Cbl-b, with peripheral focal points of distribution.

### 3.1.3.2 Itch

Itch is another E3 ubiquitin-protein ligase reported to be involved in the induction of anergy and thus its expression in CD4<sup>+</sup> T cells was quantified in the same fashion as for Cbl-b: cells were stained for the CD4 and Itch after 20 h of *in vitro* induction of anergy and priming and then analysed by LSC (**Figure 3.15**). Itch was found to be expressed in 34% of naïve CD4<sup>+</sup> T cells (**Figure 3.15A**) and following stimulation with anti-CD3 and anti-CD3+anti-CD28 stimuli this was found to be increased, with the percentage of CD4<sup>+</sup> T cells expressing it being 70% and 65%, respectively. By contrast,

under conditions of stimulation via direct calcium release (ionomycin and ionomycin+PMA) a lower percentage of CD4<sup>+</sup> T cells were found to express Itch (19% and 15%, respectively). These results suggest that Itch expression during induction of anergy or priming is not so much related to the final outcome of the stimulus (quiescence versus activation/proliferation) but more to how the stimulus acts upon the cell. Interestingly though, in CD4<sup>+</sup>Itch<sup>+</sup> T cells, Itch is more highly expressed in cells stimulated via the calcium pathway alone than by any other means (**Figure 3.15B**). As for the peripheral expression of Itch (**Figure 3.15C**), anti-CD3- and anti-CD3+anti-CD28-stimulated populations are again the ones with the highest percentage of Itch-positive CD4<sup>+</sup> T cells but it is noteworthy to stress that ionomycin and ionomycin+PMA-stimulated populations, considering their relatively low percentage of CD4<sup>+</sup> T cells expressing Itch, appear to predominantly express Itch at their periphery, while this is not the case for naïve, anti-CD3 and anti-CD3+anti-CD28-stimulated populations of CD4<sup>+</sup> T cells. Again at the periphery, Itch is more intensely expressed in cells stimulated via the calcium pathway alone than via any of the other stimuli (**Figure 3.15D**), though here the trend is not so pronounced as for total cell expression (**Figure 3.15B**).

Representative images of these populations (**Figure 3.16**) suggested that cells from all groups appeared to predominantly express Itch at the periphery relative to the rest of the cell. Furthermore, apart from anti-CD3-stimulated cells, all of the groups appear to exhibit to some extent foci of Itch expression. For example, ionomycin+PMA-stimulated cells exhibit a polarised pattern of Itch expression, with little expression around the cell, rather the majority focused in one major locus.

Itch expression was also analysed in CD4<sup>+</sup> T cells after 40 h of *in vitro* culture stimulation (**Figure 3.17**). At this time-point, populations of CD4<sup>+</sup> T cells stimulated with anergising stimuli have slightly higher percentage of cells expressing Itch than populations of CD4<sup>+</sup> T cells stimulated with priming stimuli, although this effect is not very pronounced (**Figure 3.17A**). However, cells stimulated under all conditions exhibit roughly the same expression levels of Itch, whether in the whole of the cell (**Figure 3.17B**), or its periphery (**Figure 3.17D**). The percentage of CD4<sup>+</sup> T cells expressing Itch within their periphery also appears not to change according to the different conditions of *in vitro* culture (**Figure 3.17C**). Consistent with this, visualisation of these 40 h cells reveals a more peripheral distribution of Itch with focal points present in the ionomycin+PMA-representative cell. Cells representative from the other populations do

not display these intense foci but rather display a more uniform peripheral staining (**Figure 3.18**).

### 3.1.3.3 Grail

It is hypothesised Grail is also involved in anergy as its expression was reported to be upregulated during T cell anergy induction. Thus, expression of Grail at the single cell level during the induction of anergy and priming was quantified via LSC. This analysis showed Grail to be expressed in CD4<sup>+</sup> T cells under all conditions tested but the ionomycin+PMA-stimulated population contained the lowest proportion of Grail<sup>+</sup> cells (**Figure 3.19A**). In fact, not only is this the population least expressing Grail but there is also a striking difference when compared with the ionomycin-stimulated population, suggesting a relationship between anergy and Grail expression. On the other hand, however, the anti-CD3+anti-CD28-stimulated population has an even higher percentage of CD4<sup>+</sup> T cells expressing Grail than the ionomycin-stimulated population and also a considerably higher percentage of CD4<sup>+</sup> T cells expressing Grail than either the naïve or anti-CD3-stimulated populations, which have essentially equivalent percentages of CD4<sup>+</sup> T cells expressing Grail. Moreover, in CD4<sup>+</sup>Grail<sup>+</sup> T cells, Grail is expressed most highly in such cells from the anti-CD3+anti-CD28 and ionomycin+PMA-stimulated populations (**Figure 3.19B**). Thus, there does not appear to be a correlation between either the percentage of cells expressing Grail or alternatively, the total expression levels of Grail in such cells and their functional outcome. These total expression results translate into peripheral expression (**Figure 3.19C**), with the ionomycin- and the anti-CD3+anti-CD28-stimulated populations containing the highest proportion of cells expressing Grail at their periphery than ionomycin+PMA- and anti-CD3-stimulated populations, respectively. As for intensity of expression within the cells, again it is the cells cultured with priming stimuli (anti-CD3+anti-CD28 and ionomycin+PMA) that express Grail the most, while anti-CD3 and ionomycin alone render only a slightly higher Grail expression than that of the naïve CD4<sup>+</sup> T cells (**Figure 3.19B**). The intensity of Grail expression within the cells' periphery (**Figure 3.19D**) is a reflection of this trend as once again the cells grown with priming stimuli are the ones that express Grail the most in the periphery. These data were corroborated by representative images of Grail positive cells (**Figure 3.20**) as whilst unstimulated CD4<sup>+</sup> T cells exhibited diffuse Grail expression, stimulated cells showed a more intense and peripheral Grail location with highest expression shown under conditions of priming (anti-CD3+anti-CD28 and ionomycin+PMA); results from the

ionomycin+PMA population should be interpreted with some caution as the cells appear to be undergoing apoptosis.

By the 40 h time point, however, Grail expression is reduced under all conditions tested. Nevertheless, at 40 h post stimulation (**Figure 3.21**) anti-CD3-stimulated CD4<sup>+</sup> T cells were found to have the highest proportion of cells expressing Grail, higher than anti-CD3+anti-CD28-stimulated CD4<sup>+</sup> T cells (18% versus 11%, respectively), an inverse situation to that observed at 20 h suggesting that conflicting data with the literature may reflect the differential kinetics observed. Likewise, for the stimuli affecting the calcium pathway directly, again an inverse pattern to that observed at 20 h is seen, with the population undergoing priming having a higher proportion of CD4<sup>+</sup> T cells positive for Grail than the population undergoing anergy (**Figure 3.21A**). This trend is reflected in the proportion of CD4<sup>+</sup> T cells expressing Grail within the periphery (**Figure 3.21C**) with anti-CD3-stimulated CD4<sup>+</sup> T cells also expressing more Grail than anti-CD3+anti-CD28-stimulated CD4<sup>+</sup> T cells while ionomycin+PMA-stimulated CD4<sup>+</sup> T cells express more Grail than ionomycin-stimulated CD4<sup>+</sup> T cells (**Figure 3.21B**). Within the periphery, however there is not much difference in terms of Grail intensity expression between different conditions (**Figure 3.21D**). Nevertheless, although there is no clear correlation between Grail expression and priming or tolerance, there appears to be inverse patterns not only of expression but also subcellular location elicited by the differential stimuli.

### ***3.1.4 Distribution of the E3 ubiquitin-protein ligase-expressing cells according to the cell cycle stage***

As the above studies suggested that the expression profile of E3 ligases differed throughout the kinetics of the induction and priming, it was decided to correlate E3 ligase expression with cell cycle progression in the two populations in an attempt to determine if there were distinct expression patterns in G0/G1 arrest (associated with anergy) Vs S and G2/M phases (associated with priming). Indeed, as described in section 2.9.1.2, LSC can be used to assess the cell cycle stage of individual T cells and correlate this with signalling and/or phenotypic markers. Thus, cells were stained with DAPI to detect nuclear DNA and anti-CD4 and anti-E3 ligase to locate T cells and the intracellular protein of interest. By measuring the max pixel (which correlates with DNA concentration) and integral (which correlates to total quantity of DNA) values of DAPI it is possible to obtain a dot plot distribution of the population of cells which allows determination of their cell cycle status.

Firstly, analysis of cell cycle status of CD4<sup>+</sup> T cells under the differential conditions of induction of priming and tolerance were examined at 20 and 40 h. CD4<sup>+</sup> T cells were gated and their DAPI max pixel VS integral values plotted, analysed and graphed (**Figure 3.22**). For this set of experiments cells in S and G2/M phases and newly-formed daughter cells were grouped together in one group called “Mitotic” cells. After 20 h of *in vitro* culture most (over 50%) of the CD4<sup>+</sup> T cells were in the G0/G1 stage of the cell cycle, regardless of the stimulus (**Figure 3.22A**). Only around 10% of the various populations exhibited apoptosis at this time-point, although the naïve CD4<sup>+</sup> T cells (“no stimulus”) tended towards a higher, but not statistically significant, proportion of apoptotic cells (above 20%). Moreover, consistent with the idea that cells need to be activated in the induction phase of both priming and tolerance, similar proportions of the cells from each group were mitotic at this time-point.

However, and perhaps consistent with DNA synthesis data (**Figure 3.1**), at the 40 h time point (**Figure 3.22B**) some differences do appear. Cells stimulated with anti-CD3 are predominantly apoptotic with the majority of the remainder arrested in G0/G1 and only a small proportion advancing through the cell cycle. By contrast, the majority of population stimulated with anti-CD3+ anti-CD28 were advancing through the cell cycle and tended to show protection from apoptosis and growth arrest. The ionomycin-stimulated population appears to be overwhelmingly arrested in G0/G1 but perhaps surprisingly, the proportion of cells in apoptosis is just 10% and a considerable proportion (35%) are still mitotic. Rather unexpectedly, the ionomycin+PMA-stimulated population had a very high proportion of cells in apoptosis (44%) and equal percentages of cells arrested in G0/G1 and progressing through the cell cycle; one would expect more cells in the mitotic stages of the cell cycle but it may be possible the intensity of the stimulus might have been too much for the cells for such a prolonged period.

#### **3.1.4.1 Cbl-b**

Consistent with the findings that, at least in the early stages (20 h) of induction of priming and tolerance, all the cells showed a similar profile of cell cycle progression, it appeared that in general CD4<sup>+</sup>Cbl-b<sup>+</sup> T cells from all conditions exhibited similar cell cycle status (**Figure 3.23A**). Interestingly, however, Cbl-b<sup>+</sup> cells from the population of cells stimulated with anti-CD3+ anti-CD28 do show a considerable higher proportion of their cells in G0/G1 (42%) than any of the other populations, perhaps suggesting that expression of Cbl-b antagonises progression of primed cells. Nevertheless, these results

seem to suggest that, regardless of the stimulus, most of the Cbl-b<sup>+</sup> cells are mitotic at this time-point.

It is also noteworthy to stress that the level of expression of Cbl-b in a cell does not change according to the stage of the cell cycle as much as the proportion of cells expressing it within a population (**Figure 3.23B**). However, mitotic cells do seem to express more Cbl-b than G0/G1 cells (there were too few CD4<sup>+</sup>Cbl-b<sup>+</sup> cells undergoing apoptosis to make conclusions about Cbl-b expression intensity in apoptotic cells). Perhaps rather surprisingly, anti-CD3+anti-CD28-stimulated cells seem to express most Cbl-b in the mitotic stages. Thus, high levels of Cbl-b expression per se do not appear to dictate cell cycle arrest and indeed, when total CD4<sup>+</sup> T cells in each cell cycle stage are screened for Cbl-b expression, mitotic cells show, by far, the highest proportion of Cbl-b-expressing cells (**Figure 3.23C**). Thus, very few (less than 10%, regardless of the stimulus) CD4<sup>+</sup> apoptotic cells are Cbl-b<sup>+</sup>. The same holds true for cells in G0/G1 with the following exceptions: naïve (no stimulus) and anti-CD3+anti-CD28-stimulated populations have 17% and 34%, respectively, of their CD4<sup>+</sup> T cells expressing Cbl-b. As for mitotic cells, as stated above, there is a high percentage of CD4<sup>+</sup> T cells positive for Cbl-b (above 35%, regardless of the nature of stimulation) but the naïve population (81%) and the anti-CD3+anti-CD28 population (74%) have the highest proportion of Cbl-b<sup>+</sup> cells within the CD4 positives.

Analysis of the expression of Cbl-b according to cell cycle stage at 40 h of *in vitro* culture revealed similar profiles (**Figure 3.24**) as again the majority of CD4<sup>+</sup>Cbl-b<sup>+</sup> cells are found in the mitotic stages (**Figure 3.24A**) regardless of the nature of the stimulus. Perhaps, consistent with the cell cycle analysis data (**Figure 3.22B**), the ionomycin+PMA-stimulated population has a high proportion of cells in apoptosis (25%) whilst all populations have only about 10% of Cbl-b<sup>+</sup> cells in G0/G1 phase with the exception of anti-CD3+anti-CD28-stimulated cells with just 1%. Again, the level of expression of Cbl-b in a cell does not appear to change much according to the stage of the cell cycle or the stimuli (**Figure 3.24B**); nonetheless, mitotic anti-CD3- and ionomycin+PMA-stimulated cells seem to express it more. Finally, analysis of the CD4<sup>+</sup> cells in each stage of the cell cycle again reveals that few of these are Cbl-b<sup>+</sup> with most of the Cbl-b<sup>+</sup> cells being mitotic (**Figure 3.24C**).

#### 3.1.4.2 Itch

The expression of Itch was correlated with the cell cycle status of CD4<sup>+</sup> T cells during induction of priming and tolerance (**Figure 3.25**). Analysis of the CD4<sup>+</sup>Itch<sup>+</sup>

cells revealed that for the naïve (unstimulated) population, the highest percentage of these CD4<sup>+</sup>Itch<sup>+</sup> cells were in G0/G1 (51%) while the rest were, rather surprisingly, mitotic (33%) or consistent with their lack of signalling, apoptotic (16%) (**Figure 3.25A**). Similarly, CD4<sup>+</sup>Itch<sup>+</sup> cells from the anergic (anti-CD3) and primed (anti-CD3+anti-CD28) populations were predominantly found in G0/G1 (64% and 77%, respectively) while the rest of the CD4<sup>+</sup>Itch<sup>+</sup> cells were mainly mitotic (35% and 20%) and very few were apoptotic (1% and 3%). Rather surprisingly therefore, for the populations of cells stimulated via the calcium pathway (ionomycin and ionomycin+PMA), CD4<sup>+</sup>Itch<sup>+</sup> T cells were mainly mitotic (67% and 65%, respectively) with some also arrested in G0/G1 (30% and 32%) but only a few were found to be apoptotic (3% and 3%). Moreover, analysis of the level of expression of Itch in CD4<sup>+</sup>Itch<sup>+</sup> cells revealed that generally, for each condition tested, Itch expression increased with cell cycle progression rather than peaking in G0/G1, the stage most associated with anergy. Nevertheless, expression was highest in the ionomycin-treated cells and this stimulus has classically been associated with the role of E3 ligases in anergy (**Figure 3.25B**).

When the proportion of all CD4<sup>+</sup> T cells in each cell cycle stage was examined for Itch expression, while for anergy and priming induction via the TCR there was a peak of Itch-positive T cells in the G0/G1 phase, for the calcium-based stimuli Itch-positive T cells were more associated with mitosis than growth arrest. Thus, whilst 64% of unstimulated CD4<sup>+</sup> T cells in G0/G1 phase are Itch<sup>+</sup> those from the anti-CD3 and anti-CD3+anti-CD28 populations are even more so (94% and 92%, respectively), while the G0/G1 populations of CD4<sup>+</sup> T cells stimulated with ionomycin and ionomycin+PMA only have 13% and 8%, respectively, of Itch<sup>+</sup> cells (**Figure 3.25C**). As for mitotic cells, naïve, anti-CD3- and anti-CD3+anti-CD28-stimulated CD4<sup>+</sup> T cell populations also all exhibit a high proportion of Itch<sup>+</sup> cells (over 70%) while ionomycin- and ionomycin-stimulated populations have 35% and 42%, respectively, of Itch-positive CD4<sup>+</sup> T cells. As for apoptotic cells, naïve, anti-CD3- and anti-CD3+anti-CD28-stimulated CD4<sup>+</sup> T cell populations have once again a high proportion of Itch<sup>+</sup> cells (over 30%) while ionomycin- and ionomycin-stimulated populations have less than 7% of Itch-positive CD4<sup>+</sup> T cells. Collectively therefore, at this time point, Itch expression did not appear to correlate with functional outcome, but rather with the nature of the stimuli used.

Furthermore, analysis at the 40 h time point, revealed that for all conditions tested, most of the CD4<sup>+</sup>Itch<sup>+</sup> cells were found in the mitotic stages (**Figure 3.26A**). Indeed, of the CD4<sup>+</sup>Itch<sup>+</sup> cells from the population stimulated with ionomycin, the highest

proportion of these cells is in mitosis (69%) and the smallest proportion in apoptosis (3%). Similarly, apart from high levels of Itch in ionomycin-induced apoptotic cells, again Itch expression tends to increase with cell cycle progression (**Figure 3.26B**). Moreover, analysis of the total CD4<sup>+</sup> populations in each cell cycle stage revealed that mitotic cells showed the highest proportion of Itch<sup>+</sup> regardless of the stimulus (**Figure 3.26C**). Unlike at 20 h, unstimulated, anti-CD3- and anti-CD3+anti-CD28-stimulated CD4<sup>+</sup> cells arrested in G0/G1 are not predominantly Itch<sup>+</sup>, and neither are the ionomycin- and ionomycin+PMA-stimulated ones, perhaps suggesting that these cells were transiting rather than being arrested in G0/G1. Thus, taken together, if anything such single cell analysis would suggest that Itch expression is more associated with mitosis than cell cycle arrest, at least during this induction phase where both anergic and priming cells need to go through an activation stage.

### 3.1.4.3 Grail

The expression of Grail according to cell cycle stage of CD4<sup>+</sup> T cells at 20 h was also quantified (**Figure 3.27**). In this case, the CD4<sup>+</sup>Grail<sup>+</sup> cells of the ionomycin-stimulated population were found to be spread roughly evenly between all the cell cycle stages (**Figure 3.27A**). By contrast, all the other populations had less than 2% of the CD4<sup>+</sup>Grail<sup>+</sup> T cells undergoing apoptosis and all of them had more CD4<sup>+</sup>Grail<sup>+</sup> cells in the G0/G1 than in the mitotic phases. Generally, however, mitotic cells were found to express more Grail than cells in other stages (**Figure 3.27B**), although those from the ionomycin+PMA group were the only ones not to show an increase in Grail expression from G0/G1 to mitotic phases. CD4<sup>+</sup> T cells stimulated with anti-CD3+anti-CD28 appeared to express more Grail at all cell cycle stages than CD4<sup>+</sup> T cells from any of the other functional conditions. Perhaps of interest, the vast majority of CD4<sup>+</sup> T cells in G0/G1 were positive for Grail, regardless of the stimuli (**Figure 3.27C**). The vast majority of CD4<sup>+</sup> T cells in the mitotic phases were also positive for Grail, with there being one exception in the form of the T cells stimulated with anti-CD3+anti-CD28, of which less than half were positive for Grail. As for apoptotic cells, there is a high percentage of Grail-positive CD4<sup>+</sup> cells in the populations stimulated with anti-CD3+anti-CD28 and ionomycin (87% and 86%, respectively), a reasonable percentage in the unstimulated population (40%), and a very small percentage in the populations stimulated with anti-CD3 and ionomycin+PMA (8% and 7%, respectively).

Again however, any association of this E3 ligase with G0/G1 observed at 20 h presumably reflected cells transiting this stage as, at 40 h, apart from the anti-CD3+anti-

CD28-stimulated population, in all other populations the majority of CD4<sup>+</sup>Grail<sup>+</sup> cells are in the mitotic stages (**Figure 3.28A**). Indeed, in both anti-CD3- and ionomycin-stimulated populations there is a higher proportion of CD4<sup>+</sup>Grail<sup>+</sup> cells in the mitotic stages than in the corresponding priming stimulus populations (anti-CD3+anti-CD28 and ionomycin+PMA) whilst for the anti-CD3+anti-CD28-stimulated population, most of the CD4<sup>+</sup>Grail<sup>+</sup> cells are apoptotic (62%). The low proportion of CD4<sup>+</sup>Grail<sup>+</sup> cells in G0/G1 is also something to take in consideration (26%, 15%, 3% and 21% for the anti-CD3-, anti-CD3+anti-CD28-, ionomycin- and ionomycin+PMA-stimulated populations, respectively) and again expression levels of Grail generally appear to increase with cell cycle progression (**Figure 3.28B**). Finally, analysis of the total CD4<sup>+</sup> T cells in each cell cycle phase revealed that at 40 h, almost all of the anti-CD3-, anti-CD3+anti-CD28- and ionomycin+PMA-stimulated mitotic CD4<sup>+</sup> T cells are positive for Grail (**Figure 3.28C**) whereas only 19% of the ionomycin-stimulated mitotic CD4<sup>+</sup> T cells are positive for Grail. Moreover, an even lower proportion of ionomycin-stimulated cells in G0/G1 were Grail positive. Collectively, therefore, these data do not support a correlation expression of Grail and cell cycle arrest contributing to the induction of anergy.

### ***3.1.5 Analysis of the expression of E3 ubiquitin-protein ligases in the induction phase of anergy and priming, in vivo***

To investigate whether similar patterns of E3 ubiquitin-protein ligases expression are found during induction of tolerance and priming in response to antigen *in vivo*, Cbl-b, Itch, Smurf1 and Smurf2 expression was examined in antigen-specific CD4<sup>+</sup> T cells in lymph node tissue, in the context of a systemic model of antigen-specific priming and tolerance [30, 265-267]. Thus, 24 h after adoptive transfer of antigen-specific DO11.10 TCR T cells, recipient mice received OVA<sub>323-339</sub> peptide *i.v.*, either alone or together with LPS to induce systemic tolerance or priming, respectively (**Figure 3.29A**). The efficacy of these regimes was confirmed by assessing the clonal expansion (**Figure 3.29B**) of DO11.10 TCR T cells in the mesenteric lymph nodes, 0, 3, 5 and 10 days after primary exposure to the antigen. In addition, the proliferative (**Figure 3.29C**) and cytokine production (**Figure 3.29D**) recall responses of such antigen-specific CD4<sup>+</sup> T cells from peripheral lymph nodes were assessed at D10 *ex vivo*.

The peak of antigen-specific clonal expansion of the CD4<sup>+</sup> T cells was observed, at D3 after immunisation in both the tolerised and primed groups (**Figure 3.29B**), as previously reported [265, 266]. As expected, there was no major clonal expansion in the naïve group during the time-course and, at all times after primary immunisation, there

was significantly higher clonal expansion in the tissues harvested from primed compared to tolerised mice, as also shown previously [265, 284]. By D10, clonal expansion in the immunised groups had dropped to below that of the naïve group.

After re-stimulation with OVA<sub>323-339</sub> *in vitro*, T cells from tolerised mice also showed reduced proliferation (**Figure 3.29C**) and IFN $\gamma$  production (**Figure 3.29D**) relative to T cells from primed mice. T cells from naïve mice proliferated significantly more than the tolerised group but less than the primed group. The same trend is observable for IFN $\gamma$  production, although no longer on a significant scale. Collectively, these data show that i.v. administration of OVA<sub>323-339</sub> with or without LPS as an adjuvant, induced priming and tolerance, respectively, *in vivo*.

### 3.1.5.1 Cbl-b

The *in vitro* studies in the previous sections pointed towards an upregulation of Cbl-b in priming CD4<sup>+</sup> T cells rather than anergising CD4<sup>+</sup> T cells; but the question remained how this would translate into an *in vivo* antigen-specific situation.

As described before, in this study, 24 h after adoptive transfer of antigen-specific DO11.10 TCR T cells, recipient mice received OVA<sub>323-339</sub> peptide i.v., either alone or together with LPS to induce systemic tolerance or priming, respectively. At D5 after immunisation, PLNs were harvested and prepared for immunohistochemistry. D5 was chosen as by then enough time had passed to allow induction of tolerance and priming and at the same time there was still a significant difference in clonal expansion of DO11.10 T cells between tolerised and primed groups (**Figure 3.29B**).

The tissue sections were stained for DO11.10 TCR T cells (red; KJ1-26<sup>+</sup> T cells) and Cbl-b (blue) expression. The LSC was used to quantify Cbl-b expression in such antigen-specific T cells within the lymph node tissue. Representative images of these tissue sections (**Figure 3.30A and B**) showed that, consistent with its ubiquitous expression in haematopoietic cells [177, 180, 202, 285, 286], Cbl-b expression was detected throughout the lymph node section and not only KJ1-26<sup>+</sup> T cells. In contrast to the *in vitro* data using anti-CD3 $\pm$ anti-CD28 to induce anergy and priming, analysis of the proportion of DO11.10 T cells expressing Cbl-b (**Figure 3.30C**) showed that a similar proportion of these cells *in vivo* were Cbl-b positive but that a higher percentage of DO11.10 T cells from tolerised mice were found to be expressing Cbl-b than DO11.10 T cells from primed mice (8.9% and 3.8%, respectively) however, this is not statistically significant. Also on the same trend, it is noteworthy to mention that the tolerised mice also exhibit higher levels of Cbl-b expression in the KJ1-26<sup>+</sup>Cbl-b<sup>+</sup> cells

than the primed mice (**Figure 3.30B**) though, once again, this is not statistically significant.

### 3.1.5.2 Itch

The *in vitro* studies (sections 3.1.2 and 3.1.3.2) pointed towards an upregulation of Itch protein expression in anergising and priming CD4<sup>+</sup> T cells when compared to unstimulated CD4<sup>+</sup> T cells; differences between anergising and priming cells were minimal, but could this situation be somewhat different in the *in vivo* induction phase?

As described before, for the *in vivo* induction phase of tolerance and priming, at D5 after immunisation, PLNs were harvested and prepared for immunohistochemistry. The tissue sections were stained for DO11.10 TCR T cells (KJ1-26<sup>+</sup> T cells) and Itch, and the LSC was used to quantify Itch expression in T cells within the lymph node tissue. Again, imaging revealed that Itch expression (blue) was not restricted to DO11.10 TCR T cells (red) but rather is expressed by cells throughout the LN section (**Figure 3.31A and B**), although Itch expression seems more concentrated in some cells/patches of cells of the section. In this case, in keeping with the *in vitro* data, both tolerised and primed mice were found to be expressing Itch in a high percentage of DO11.10 T cells (34.4% and 35.8%, respectively), but there was no significant difference between the two groups of mice (**Figure 3.31C**). Also, the intensity of Itch expression in KJ1-26<sup>+</sup>Itch<sup>+</sup> cells appears to be similar for both tolerised and primed groups (**Figure 3.31D**).

### 3.1.5.3 Smurf1

The Western blotting data revealed Smurf1 could potentially be involved in anergy and priming induction so some of the D5 PLN tissue was also stained for DO11.10 TCR T cells (KJ1-26<sup>+</sup> T cells) and Smurf1, and LSC used to quantify Smurf1 expression in T cells within the lymph node tissue. Representative images of the tolerised and primed tissue sections show Smurf1 expression in many cells of the lymph node and not only in KJ1-26<sup>+</sup> cells (**Figure 3.32A and B**). Indeed, only a small percentage of KJ1-26<sup>+</sup> T cells express Smurf1 (**Figure 3.32C**), and this number does not vary much between the tolerised and primed groups (9.2% and 8.2%, respectively) and although Smurf1 appears to be expressed more highly in primed KJ1-26<sup>+</sup>Smurf1<sup>+</sup> cells than tolerised KJ1-26<sup>+</sup>Smurf1<sup>+</sup>, this is not statistically significant (**Figure 3.32D**).

#### 3.1.5.4 Smurf2

The Western blotting data also suggested a potential upregulation during priming induction, *in vitro*, of Smurf2. Thus, using D5 PLN tissue obtained from the systemic model of antigen-specific priming and tolerance described before, DO11.10 TCR T cells (KJ1-26<sup>+</sup> T cells) and Smurf2 were stained for, and LSC used to quantify Smurf2 expression in these antigen-specific T cells. Again, imaging revealed that Smurf2 is expressed throughout the lymph node, in KJ1-26<sup>+</sup> and non-KJ1-26<sup>+</sup> cells alike, in both tolerised (**Figure 3.33A**) and primed (**Figure 3.33B**) mice. However, Smurf2 is expressed in a higher percentage of tolerised KJ1-26<sup>+</sup> T cells than primed KJ1-26<sup>+</sup> T cells (10.7% and 6.5%, respectively; **Figure 3.33C**) and at higher levels (**Figure 3.33D**). Despite neither of these data are statistically significant, they are different from the data observed in the Western blotting analysis of *in vitro* anergy and priming induction. It remains a possibility Smurf2 might be involved in the tolerance or priming decision albeit its kinetics might change considerably.

## 3.2 The maintenance phase of anergy and priming in CD4<sup>+</sup> T cells

To characterise differential signalling events in the maintenance phase of anergy and priming an *in vitro* system of antigen-specific T cell re-stimulation was developed. T cell anergy or priming was induced in primary antigen-specific DO11.10 T cells by TCR engagement or by TCR engagement with appropriate co-stimulation as described previously [49, 130, 257]. Briefly, to do this, lymph node single cell suspensions, in which typically 30-40 % of the lymphocytes were CD4<sup>+</sup>DO11.10<sup>+</sup> T cells, were cultured for 2 d with plate-bound anti-CD3 antibody or with plate-bound anti-CD3 antibody and anti-CD28 antibody. These cells were then washed, re-plated and rested for an additional 2 d in fresh medium, before being re-stimulated with LPS-matured DCs which had been pulsed with or without OVA<sub>323-339</sub> (referred to from now on as LPS-matured, OVA-loaded DCs and LPS-matured DCs, respectively) (**Figure 3.34**). The DO11.10 T cells are transgenic for the TCR, which recognises the OVA<sub>323-339</sub> peptide.

### ***3.2.1 Functional analysis of DO11.10 T cells in the maintenance phase of anergy and priming***

To confirm maintenance of anergic or primed responses by CD4 positive, DO11.10 T cells even after re-stimulation, the functional hallmarks associated with these two behaviours were probed. Thus, naïve, anergised and primed DO11.10 T cells were first assessed for their ability to produce IL-2 in response to re-stimulation by FACS analysis of intracellular cytokine staining (**Figure 3.35A**). This revealed that less anergic CD4<sup>+</sup>KJ1-26<sup>+</sup> T cells expressed intracellular IL-2 after re-stimulation with LPS-matured DCs than naïve CD4<sup>+</sup>KJ1-26<sup>+</sup> T cells after stimulation with the same LPS-matured DCs. Most revealing is the fact there is no difference in IL-2-expression between the anergic CD4<sup>+</sup>KJ1-26<sup>+</sup> cells re-stimulated with LPS-matured DCs or LPS-matured, OVA-loaded DCs. As for the primed T cells, after re-stimulation with LPS-matured, OVA-loaded DCs, there is an increase in the percentage of CD4<sup>+</sup>KJ1-26<sup>+</sup> cells expressing IL-2 intracellularly, consistent with primed T cell behaviour.

The quantity of IL-2 secreted to the medium was also measured (**Figure 3.35B**). Re-stimulating any of the three populations of T cells (naïve, anergised and primed) with LPS-matured DCs without antigen does not elicit strong IL-2 production. The culture media supernatants from anergised T cells re-stimulated with LPS-matured, OVA-loaded DCs also failed to show any measurable levels of IL-2. However, naïve T cells did produce and secrete IL-2 into the culture medium and primed T cells did so to an even higher degree, after re-stimulation with LPS-matured, OVA-loaded DCs. Thus, compared to the naïve and primed T cells, the anergised T cells revealed a defect in IL-2 production in response to antigen. Taking this in consideration with the intracellular IL-2 levels (**Figure 3.35A**) there is a strong indication the population of “anergised” T cells had indeed become anergic and, when re-stimulated they not only failed to produce IL-2 in response to antigen but actually blocked its production and secretion.

Once IL-2 is produced, it binds to its specific receptor complex (IL-2R) thus triggering T cell proliferation [287]. Consistent with the IL-2 data, out of the three populations of T cell re-stimulated with LPS-matured, OVA-loaded DCs, the primed population proliferated the most, the naïve population proliferated well and the anergised population exhibited vestigial proliferation (**Figure 3.35C**). This proliferative unresponsiveness can be overcome by supplementing the T cells with exogenous IL-2, as this bypasses the need for co-stimulation [52, 130]. In **Figure 3.35D**, the defective proliferation was found to be partly rescued by the addition of exogenous IL-2

(recombinant IL-2 [rIL-2]), as rIL-2 coupled with LPS-matured, OVA-loaded DCs co-culture increased the proliferation of the anergic T cells to the same order of magnitude of proliferation exhibited by primed T cells in the absence of IL-2 (**Figure 3.35C**). However, this joint stimulation of the anergic T cells still yields less proliferation of similarly stimulated naïve T cells and even less proliferation than the similarly stimulated primed T cells (**Figure 3.35D**). In the absence of (re-)stimulation with LPS-matured, OVA-loaded DCs, of the three T cell populations cultured with rIL-2 alone, major proliferation was only detected in the primed but not naïve or anergic groups (**Figure 3.35D**). Indeed, the proliferation level of these primed T cells is in the same order of magnitude as the one observed for naïve T cells stimulated with rIL-2 coupled with LPS-matured, OVA-loaded DCs co-culture.

### ***3.2.2 Analysis of the expression of E3 ubiquitin-protein ligases in the maintenance phase of anergy and priming***

To start the analysis of E3 ubiquitin-proteins expression levels in T cells in the maintenance phase of anergy and priming, Western blotting assays were first conducted. Cells were extracted, stimulated *in vitro* to induce anergy or priming and then re-stimulated to mimic the maintenance phase of anergy or priming, as described before in the Materials and Methods chapter. As a first step, total cell protein of the co-cultures was extracted and analysed for the expression of relevant proteins (**Figure 3.36**).

The membrane was first blotted for PLC $\gamma$ -1, as this would give an indication of the activation status of the cells. Of the T cell populations which were not re-stimulated with antigen, the expression of PLC $\gamma$ -1 is highest in the anti-CD3+anti-CD28-stimulated cells (**Figure 3.37**) confirming our previous findings (section 3.1.2) that anti-CD3+anti-CD28-stimulated cells became activated and, hence primed whilst the relatively reduced levels found in anti-CD3-treated cells reflected their anergic status. Following re-stimulation with LPS-matured, OVA-loaded DCs, PLC $\gamma$ -1 is also most highly expressed in the anti-CD3+anti-CD28-stimulated cells (primed T cells). However anti-CD3-stimulated cells (anergic) appear to have upregulated their PLC $\gamma$ -1 expression compared to unstimulated cells (naïve), denoting there was some activation of these anergic T cells after re-stimulation.

In the absence of re-stimulation with antigen, Cbl-b and Smurf2 were found to be most highly expressed in the primed T cells and least in the naïve cells. Both exhibit a ladder effect possibly due to ubiquitination: Smurf2, unlike Smurf1, did not exhibit this

ladder pattern in the earlier experiments focusing on the first 48 h of the induction phase, and hence perhaps this potential regulation is the result of prolonged *in vitro* culture ( $\pm 120$  h). As for Itch, Smurf1 and Grail, these are all expressed most highly in the naïve cells; Smurf1 and Grail exhibit the same expression levels in anergic and primed T cells while Itch is expressed at a higher level in the primed relative to the anergic populations of cells as seen in the induction phase experiments previously (section 3.1.2). Smurf1 once again exhibits a ladder pattern; however, the big difference is the high expression levels of these proteins in naïve cells relative to the primed and anergic populations at this 20 h time point of the maintenance phase; perhaps prolonged *in vitro* culture induces their downregulation in anergic and primed T cells. By contrast, all of T cell populations express very high levels of Ikaros, without much difference of expression between them.

Following re-stimulation with LPS-matured, OVA-loaded DCs, the protein levels of Itch, Cbl-b, Smurf1, Smurf2 and Ikaros appear to be similar in both primed and anergic populations and there appears to be slightly less Grail expression in the primed relative to the anergic populations. Again, Cbl-b and Smurf2 exhibit an extended ladder pattern. Ikaros, is expressed more strongly in primed and anergic T cells than naïve T cells, though it may be the case (comparing with the non-re-stimulated T cells) that after re-stimulation all T cell populations downregulate Ikaros, being the naïve T cells the ones which downregulate it the most.

The total protein lysates were also tested for the presence of ubiquitinated proteins (**Figure 3.38**). Globally, the ubiquitination of proteins (**Figure 3.38A**) appears to be most strong in the re-stimulated anergic T cells, with the primed T cells showing higher level than either primary antigen responses (naïve) or any of the non-antigen-re-stimulated populations. Assessment of the prevalence of mono- and poly-ubiquitinated proteins (**Figure 3.38B**) also showed that re-stimulated anergic and primed T cells do seem to express mono- and poly-ubiquitinated proteins more intensely than naïve T cells although the levels of K63-linked polyubiquitinated proteins are roughly comparable in the three re-stimulated populations, albeit perhaps to a slightly lower extent in the primed population (**Figure 3.38C**).

The analysis of E3 ubiquitin-proteins expression levels in the maintenance phase of anergy and priming was extended to Western blotting analysis of the antigen-specific KJ1-26<sup>+</sup> T cells co-cultured with OVA-loaded, LPS-matured DCs. Briefly, cells were extracted from LNs, stimulated *in vitro* to induce anergy or priming before being re-stimulated to mimic the maintenance phase of anergy or priming, as described above.

Here two methods to induce anergy were used: by means of TCR ligation (via immobilised anti-CD3 antibody) and by means of a direct increase of intracellular  $\text{Ca}^{2+}$  levels (via ionomycin). PLC $\gamma$ -1 protein levels were confirmed to be reduced in the ionomycin-induced anergic T cells (not shown). After 20 h of re-stimulation with OVA-loaded, LPS-matured DCs, KJ1-26<sup>+</sup> T cells were harvested and MACS-purified. Both the positive fraction of antigen-specific KJ1-26<sup>+</sup> T cells and the negative fraction of non-KJ1-26<sup>+</sup> T cells were collected. The total cell protein was extracted from both fractions and analysed for the expression of relevant proteins (**Figure 3.39**).

The membrane was blotted for DO11.10 TCR in order to check the efficacy of the MACS isolation (**Figure 3.40**). As expected, all lanes loaded with protein extracts from the KJ1-26<sup>+</sup> T cell fractions blotted positive for this transgenic TCR while none of the lanes loaded with protein extracts from the residual cell fractions did. The MACS isolation was thus effective in enriching antigen-specific T cells and served as an additional loading control for these populations. The two populations of anergic KJ1-26<sup>+</sup> T cells expressed roughly the same amount of Erk with the primed KJ1-26<sup>+</sup> T cells exhibiting slightly less. Taking this in consideration, Itch, Cbl-b and Grail expression appears to be quite comparable in anergic and primed KJ1-26<sup>+</sup> T cells, although it may be slightly less in the primed population relative to the two populations of anergic cells. Rather surprisingly, Traf6 doesn't seem to be expressed by these cells in the maintenance phase. On the other hand, Ikaros is expressed most by primed KJ1-26<sup>+</sup> T cells, at slightly lower levels in TCR ligation-induced anergic T cells, whilst ionomycin-induced anergic T cells have substantially less Ikaros expression. Another point regarding Ikaros is that it is expressed more highly in the KJ1-26<sup>+</sup> T cells fraction relative to the non-KJ1-26<sup>+</sup> cells fraction, unlike all other proteins tested on this panel, suggesting that it may be preferentially expressed by CD4<sup>+</sup> T cells.

APCs, namely DCs, but also some non-transgenic CD4<sup>+</sup> T cells, should make up most of the non-KJ1-26<sup>+</sup> cells fraction. From the point of view of bi-directional signalling between antigen-specific T cells and their APCs, it is interesting to point out that Itch and Traf6 are expressed most highly in the non-KJ1-26<sup>+</sup> population co-cultured with the primed cells while Grail is expressed the least in these cells (**Figure 3.40**). Interestingly, the Itch, Cbl-b and Grail bands reveals different profiles between the ionomycin- and anti-CD3-induced anergic populations suggesting they may elicit similar functional responses by different routes.

### ***3.2.3 Analysis of the expression of E3 ubiquitin-protein ligases in the maintenance phase of anergy and priming at the single-cell level***

The above Western blotting analysis of antigen-specific CD4<sup>+</sup> T cells in the maintenance phase of priming and tolerance not only required extremely large numbers of cells, and hence mice, to generate the minimum protein levels, but also introduced potential confounding artefacts by the requirement to purify the cells subsequent to stimulation. Also, although it provided information of the populations of cells as a whole, it did not allow analysis of the behaviour and protein expression patterns of individual cells. LSC analysis allows this, so, in the next set of experiments, naïve, anergic and primed T cells were re-stimulated to promote the maintenance phase and analysed via LSC.

#### **3.2.3.1 Arf6**

LSC provides analysis of the “primed” and “anergic” populations at the single cell level: however, not all cells in the anti-CD3-stimulated population will be anergic nor will all cells in the anti-CD3+anti-CD28-stimulated group be primed. Despite exhaustive characterisation of phenotype over the years, there are no clear markers of primed versus tolerised cells and, thus, the lack of definitive markers for the functional states of priming and anergy may obscure some differential E3 ubiquitin-protein ligase expression patterns between these cohorts of cells. However, in human anergic T cells, ADP-ribosylation factor-6 (Arf6) is reported to be predominantly localised at the plasma membrane while in primed T cells it is scattered throughout internal structures such as endosomes and the cytoplasm [288]. Arf6 is a member of the Arf family of GTPases involved in membrane traffic and regulation of the cortical actin cytoskeleton [289-291]; this regulation is mediated in coordination with Rac1 and RhoA, more specifically, activation of Arf6 downregulates Rho signalling [292].

During antigen recognition, the filaments of cytoskeletal actin form a scaffold for signalling complexes, allowing the activation of signalling cascades; they also initiate molecular movement on the surface of the T cells, allowing the organisation of SMACs [293]. The GTP-bound form of Arf6 localises predominantly at the plasma membrane and is associated with inhibition of Erk 1/2 activation, of IL-2 transcription and of proliferation; it is thought GTP-Arf6 accomplishes these effects by inhibition of TCR-mediated reorganisation of polymerised actin whereas the GDP-bound form of Arf6 is scattered throughout the cytoplasm [291, 294]. Arf6 is therefore a potential marker for

assessing the current activation state of T cells, at the single cell level and hence it was explored whether membrane localisation of Arf6 could be used to identify anergic cells in our antigen-specific model of the maintenance of priming and tolerance.

Thus, as before, DO11.10 T cells were extracted, stimulated *in vitro* to induce anergy or priming before being re-stimulated with antigen to mimic the maintenance phase of anergy or priming. Cells were then stained for nuclear DNA, DO11.10 TCR and Arf6 and initial visual inspection of the slides did not reveal any differential location between anergic and primed T cells; indeed many DO11.10 T cells did not appear to be expressing Arf6 but in those expressing it, regardless of being anergic or primed cells, Arf6 was localised in the plasma cell membrane (not shown). LSC quantification confirmed that not all DO11.10 T cells express Arf6 (**Figure 3.41A**) but, interestingly, the percentage of cells expressing it increases after re-stimulation with peptide-pulsed DCs (compared to LPS-matured DCs only). Similarly, the percentage of DO11.10 T cells positive for Arf6 in the periphery also increases after re-stimulation with peptide-pulsed DCs (compared to LPS-matured DCs only), but this is regardless of whether the cells are naïve, anergic or primed (**Figure 3.41C**). Moreover, in terms of the levels of Arf6 expression per cell there is not much difference between naïve, anergic and primed cells, but in all of these populations Arf6 is more intensely expressed after re-stimulation with LPS-matured, OVA-loaded DCs than with LPS-matured DCs (**Figure 3.41B**). Paradoxically, in the periphery, Arf6 appears to be more intensely expressed in anergic and primed cells after re-stimulation with LPS-matured DCs, not LPS-matured, OVA-loaded DCs (**Figure 3.41D**) whereas for the naïve cells there are no differences of Arf6 expression between either ways of re-stimulation. From the previous work on human T cells [288] one was expecting anergic T cells to express more Arf6 in the periphery (plasma cell membrane location) than primed T cells; this is not the case in the event of LPS-matured, OVA-loaded DCs re-stimulation and, as such, Arf6 location can not be used as a marker for anergy in DO11.10 TCR T cells.

### 3.2.3.2 Ubiquitination

Firstly, total cell ubiquitination levels of the three populations were assessed after re-stimulation (**Figure 3.42**). Briefly, DO11.10 T cells were extracted, stimulated *in vitro* to induce anergy or priming before being re-stimulated with antigen to mimic the maintenance phase of anergy or priming. Cells were then stained for nuclear DNA, DO11.10 TCR and ubiquitin and the levels of protein ubiquitination in KJ1-26<sup>+</sup> T cells quantified by LSC as described in the Materials and Methods chapter. This showed that

the total levels of ubiquitination of proteins does not vary much after 1 h of re-stimulation with antigen between the conditions tested (**Figure 3.42A**), either in terms of global expression or reflecting expression at the cell periphery (**Figure 3.42C**), albeit there appears to be a slight reduction in all cases in response to antigen. There is a similar pattern after 20 h of re-stimulation with respect to total expression (**Figure 3.42B**). At the cell periphery however, anergic cells re-stimulated with LPS-matured, OVA-loaded DCs have their proteins more intensely ubiquitinated than either naïve or primed T cells and, perhaps more importantly, one can see re-stimulation with LPS-matured, OVA-loaded DCs induced protein ubiquitination to higher levels than re-stimulation with only LPS-matured DCs (**Figure 3.42D**). Representative images (**Figure 3.43**) of naïve DO11.10 TCR T cells after 20 h of re-stimulation are shown which indicate that protein ubiquitination can be found all over the cell, though most cells exhibit it most intensely at the periphery of the cells. In some cells ubiquitinated proteins appear to be concentrated in one or two poles, where co-localisation with the TCR is apparent.

### 3.2.3.3 Cbl-b

Modulation of expression of Cbl-b in DO11.10 TCR T cells was also analysed during the maintenance phases of anergy and priming. After 1 h of co-culture with LPS-matured, OVA-loaded DCs (**Figure 3.44**), the primed population of KJ1-26<sup>+</sup> T cells has the highest proportion of cells expressing Cbl-b, although this is low and only slightly higher than that of the naïve and anergic populations which are comparable (**Figure 3.44A**). Moreover, analysis of the MFI of Cbl-b expression of KJ1-26<sup>+</sup>Cbl-b<sup>+</sup> cells showed no difference amongst the different T cell populations (**Figure 3.44B**), meaning that the cells which are expressing Cbl-b express it at the same level regardless of whether they are naïve, anergic or primed. The proportion of KJ1-26<sup>+</sup> T cells expressing Cbl-b at the periphery is very low for all populations, though again primed T cells have the highest proportion (**Figure 3.44C**). Interestingly, however, with respect to the levels of expression of Cbl-b in KJ1-26<sup>+</sup>Cbl-b<sup>+</sup> T cells at the periphery, Cbl-b is expressed most highly at the periphery of anergic T cells and at lower, but comparable levels in the naïve and primed populations (**Figure 3.44D**).

After 20 h of co-culture with LPS-matured, OVA-loaded DCs (**Figure 3.45**), it is the primed population of KJ1-26<sup>+</sup> T cells that once again has the highest proportion of cells expressing Cbl-b (**Figure 3.45A**). Both anergic and primed cells have a much higher proportion of cells expressing Cbl-b than naïve cells, indicating that Cbl-b has

been induced in these two T cell populations. This is also true for Cbl-b expression at the periphery (**Figure 3.45C**). Although the mean total levels of Cbl-b expression do not change as much, primed cells express more Cbl-b than naïve and anergic cells that have roughly the same amount (**Figure 3.45B**) and this difference is exacerbated at the cell periphery (**Figure 3.45D**).

#### 3.2.3.4 Itch

Analysis of Itch expression during the maintenance phases of priming and tolerance revealed that at 1 h following re-stimulation by antigen of naïve, anergic and primed populations, primed KJ1-26<sup>+</sup> T cells have upregulated Itch expression and exhibit the highest proportion of cells positive for Itch (**Figure 3.46A**). By contrast, the naïve and the anergic populations exhibit comparable lower proportions of Itch-positive cells irrespective of whether they have been exposed to antigen or not. The level of expression of Itch in KJ1-26<sup>+</sup>Itch<sup>+</sup> T cells is also highest in primed T cells re-stimulated with LPS-matured, OVA-loaded DCs (**Figure 3.46B**). Indeed, even primed T cells re-stimulated with LPS-matured DCs in the absence of antigen express more Itch than naïve and anergic populations, which have comparable levels of Itch regardless of the re-stimulation. Moreover, this general pattern is also observed when examining the levels of expression of Itch at the periphery of the cells (**Figure 3.46D**). Thus, re-stimulation (**Figure 3.46C**) with LPS-matured, OVA-loaded DCs increases the proportion of KJ1-26<sup>+</sup> T cells positive for Itch at the periphery of primed T cells compared to that observed with the naïve and anergic populations, and which exhibit comparable percentages of KJ1-26<sup>+</sup> T cells expressing Itch at the cell surface. However, the anergic population is the only one which has the same proportion of KJ1-26<sup>+</sup> T cells expressing Itch at the periphery in the presence and absence of antigen since both naïve and primed populations have a higher proportion of KJ1-26<sup>+</sup> T cells expressing Itch at the cell surface following challenge with LPS-matured, OVA-loaded DCs. Imaging of the cells confirmed that following challenge with antigen, primed cells exhibited the highest levels of Itch expression and this was predominantly restricted to the cell periphery (**Figure 3.47**). Interestingly, in some naïve cells, Itch could be found concentrated in one or two focal points at the periphery of the cell.

By contrast, after 20 h of *in vitro* re-stimulation with LPS-matured, OVA-loaded DCs the proportion of KJ1-26<sup>+</sup>Itch<sup>+</sup> T cells has increased in all populations but, this increase is particularly dramatic in the case of the primed and anergic populations. Nevertheless, as seen at the earlier time point, the primed T cells are the ones with the

highest proportion while naïve cells are the ones with the lowest percentage of KJ1-26<sup>+</sup> cells positive for Itch (**Figure 3.48A**). This pattern translates well into peripheral expression (**Figure 3.48C**) and also with respect to the levels of expression of Itch in KJ1-26<sup>+</sup>Itch<sup>+</sup> T cells, both in terms of throughout the whole cell (**Figure 3.48B**) as well as at the periphery (**Figure 3.48D**). To corroborate these data, Itch expression was also quantified via flow cytometry (**Figure 3.48E**) and in general terms, the flow cytometry results match those from the LSC, albeit the proportions of T cells positive for Itch are slightly different. Imaging of Itch expression in the three groups of cells (**Figure 3.49**) revealed that Itch is expressed throughout the entire cell but is mostly concentrated in the periphery, probably in the plasma cell membrane with naïve T cells expressing the lowest levels of Itch. Interestingly, it appears that there may be some Itch expression in the nucleus, particularly in anergic cells, at this time point. Also, many primed cells showed a more diffuse, albeit intense, localisation of Itch in the periphery, perhaps in vesicles.

#### ***3.2.4 Distribution of the E3 ubiquitin-protein ligase-expressing cells according to the cell cycle stage***

It has been hypothesised that unresponsiveness of anergic T cells (as measured by IL-2 production and proliferation) could involve cell death and/or cell growth arrest [295]. To assess the relative roles of these mechanisms in the maintenance phase of anergy, cell cycle progression in the different T cell populations was investigated using LSC, as described in the Materials and Methods chapter. Briefly, naïve, anergic and primed DO11.10 TCR antigen-specific T cells were re-stimulated with LPS-matured DCs loaded with OVA<sub>323-339</sub>, before being stained with DAPI and the KJ1-26 antibody.

After 1 h of re-stimulation (**Figure 3.50A**) the majority (>50%) of naïve and primed cells are found in the G0/G1 cell cycle phase. Although cells of the anergic population are also mostly found in the G0/G1 phase (41%), a considerable number of them are undergoing apoptosis (25%). Moreover, by 20 h of re-stimulation (**Figure 3.50B**) the anergic T cells are mostly either undergoing apoptosis (35%) or are arrested in G0/G1 (42%). On the other hand, the primed T cells are predominantly undergoing mitosis (26%) or indeed already generated newly-formed daughter cells (NFDCs) (47%). As for the naïve population, these cells are mostly in G0/G1 (48%) and S (26%) phases. These findings confirm that the different *in vitro* culture regimes induce T cell priming or anergy that is long-lasting and maintained following rechallenge with

antigen. They also suggest that, at the population level, anergy involves both the induction of cell cycle arrest and apoptosis.

As with the induction phase of anergy and priming, it was decided to correlate E3 ubiquitin-protein ligase expression with cell cycle progression in naïve, anergic and primed populations of antigen-specific T cells in an attempt to find distinct expression patterns in G0/G1 arrest (associated with anergy) Vs S and G2/M phases (associated with priming).

#### 3.2.4.1 Cbl-b

After 1 h of re-stimulation with LPS-matured, OVA-loaded DCs, most of KJ1-26<sup>+</sup> that were Cbl-b<sup>+</sup> from naïve, anergic and primed populations were found in the NFDCs stage (57, 55 and 41%, respectively) (**Figure 3.51A**). However, KJ1-26<sup>+</sup>Cbl-b<sup>+</sup> cells from the primed population could also be found with high prevalence in the S phase (45%) while KJ1-26<sup>+</sup>Cbl-b<sup>+</sup> cells from naïve and anergic populations are found at lower prevalences throughout the G0/G1, S and G2/M phases. Interestingly, the level of expression of Cbl-b also changes according to the stage of the cell cycle (**Figure 3.51B**), as there is higher expression of Cbl-b at the stages of cell cycle associated with division (S and G2/M phases) and perhaps consistent with their increased proliferative capacity relative to anergic cells, naïve and primed cells seem to express the most Cbl-b in the G2/M phase. Moreover, when KJ1-26<sup>+</sup> T cells in each cell cycle stage are screened for Cbl-b expression, mitotic cells (cells in S, G2/M and NFDCs) show, by far, the highest proportion of Cbl-b-expressing cells (**Figure 3.51C**). In the mitotic stages naïve, anergic and primed populations all have above 70% of their cells positive for Cbl-b. Only cells from the naïve population undergoing apoptosis were found to express Cbl-b, and these only constituted a low percentage of such apoptotic cells.

Analysis of the expression of Cbl-b according to cell cycle stage after 20 h of re-stimulation revealed that about 40% of KJ1-26<sup>+</sup> cells in all populations are in S phase although a considerable proportion of such cells from the naïve and primed populations are also found in G0/G1(**Figure 3.52A**). On the other hand, the anergic KJ1-26<sup>+</sup> T cells positive for Cbl-b are mostly to be found in the NFDC (35%) or S phases (45%), with the occasional apoptotic, G0/G1 and G2/M phase cells. Again, generally, the level of expression of Cbl-b is lowest in apoptotic and G0/G1-arrested cells (**Figure 3.52B**). Naïve cells have Cbl-b most strongly expressed in S and G2/M phases while primed cells exhibit strong expression of Cbl-b in S, G2/M and NFDC phases.

Finally, analysis of all the KJ1-26<sup>+</sup> cells in each stage of the cell cycle reveals that the majority of these cells in mitotic stages are Cbl-b-positive whilst, apart from the primed cells which are likely to be transiting rather than arrested in G0/G1, a lower proportion of those in the G0/G1 phases are Cbl-b<sup>+</sup> (**Figure 3.52C**). Rather surprisingly therefore, the primed population has a higher percentage of Cbl-b<sup>+</sup> cells in apoptosis than either the naïve or anergic populations.

Thus, and as previously observed in the induction phase, high levels of Cbl-b expression per se do not appear to dictate cell cycle arrest but rather appear to be associated with proliferation.

#### 3.2.4.2 Itch

Similarly, the expression of Itch was correlated with the cell cycle status of KJ1-26<sup>+</sup> T cells after 1 h of re-stimulation with LPS-matured, OVA-loaded DCs (**Figure 3.53**) revealing that about 30-40% of KJ1-26<sup>+</sup> cells expressing Itch, in all populations, are in S phase although a considerable proportion of such cells from the naïve population are apoptotic (44%) with only a few cells in G0/G1, G2/M or NFDC stages (**Figure 3.53A**). By contrast, the primed KJ1-26<sup>+</sup> T cells positive for Cbl-b are mostly found in the NFDC (43%) and S phases (37%), whilst the anergic KJ1-26<sup>+</sup>Itch<sup>+</sup> cells can be found as apoptotic (11%), G0/G1 (39%), S (44%) and as newly-formed daughter cells (6%). Moreover, such analysis revealed that there is a lower expression of Itch in apoptotic and G0/G1-arrested cells compared to the mitotic stages, regardless of the stimulus (**Figure 3.53B**). The naïve population had the most Itch intensity of expression in NFDCs, closely followed by the anergic population of cells (cells in S, G2/M and NFDCs). Consistent with this indication that Itch expression is also correlating with cell cycle progression, when the proportion of KJ1-26<sup>+</sup> T cells in each cell cycle stage was examined for Itch expression (**Figure 3.53C**), it was revealed all NFDCs (100%), regardless of the stimulus, were positive for Itch. However, it should be noted that apart from apoptotic cells and those of the primed G2/M population all other stages also showed high proportions of the cells to be Itch<sup>+</sup>, irregardless of their functional status.

Further analysis of the cell cycle distribution of Itch, this time after 20 h of re-stimulation with LPS-matured, OVA-loaded DCs revealed that the majority of primed KJ1-26<sup>+</sup>Itch<sup>+</sup> cells are in S phase (55%) (**Figure 3.54A**). Naïve and anergic KJ1-26<sup>+</sup>Itch<sup>+</sup> cells are mainly found in G0/G1 (45 and 40%, respectively) and while, perhaps consistent with their relative proliferative capacities, naïve KJ1-26<sup>+</sup>Itch<sup>+</sup> cells can also be found in considerable amounts in the S phase (32%), the remainder of anergic KJ1-

26<sup>+</sup>Itch<sup>+</sup> cells are most commonly found as apoptotic cells (37%). As seen in the 1 h time-point and in the induction phase, KJ1-26<sup>+</sup>Itch<sup>+</sup> cells have a lower expression of Itch in apoptotic and G0/G1-arrested cells, which tends to increase with progression in the cell cycle, regardless of the origin of the population (naïve or anergic or primed) (**Figure 3.54B**). Moreover, analysis of the KJ1-26<sup>+</sup> populations in each cell cycle stage revealed that NFDCs showed the highest proportion of Itch<sup>+</sup> regardless of the stimulus (**Figure 3.54C**). With progression in the cell cycle, the primed population displays an increase in the proportion of KJ1-26<sup>+</sup> cells positive for Itch, whereas the anergic population is the one which has the highest proportion of G0/G1 phase KJ1-26<sup>+</sup> cells positive for Itch.

Thus, taken together, this single-cell analysis suggests that, although Itch is expressed more intensely in the advanced stages of the cell cycle, in the population of anergic cells Itch expression could be related to apoptotic and G0/G1 KJ1-26<sup>+</sup> T cells.

### ***3.2.5 Analysis of the expression of E3 ubiquitin-protein ligases in the maintenance phase of anergy and priming, in vivo***

The experiments investigating the roles of E3 ubiquitin-protein ligases in the maintenance phases of anergy and priming *in vitro* suggested similarities between the two states, namely upregulation of Cbl-b and Itch when compared to a naïve population of T cells. To determine whether this was also the case *in vivo*, 24 h after adoptive transfer of DO11.10 TCR transgenic T cells, mice were immunised with OVA<sub>323-339</sub> peptide i.v., either alone or together with LPS to induce systemic tolerance or priming, respectively (**Figure 3.55A**). Seven days after this primary immunisation, recipient mice were challenged with OVA<sub>323-339</sub> + LPS i.v. and their LNs harvested 24 h later in order to examine the expression of E3 ligases in the maintenance phase of tolerance and priming.

The LNs were sectioned and stained for DO11.10 TCR T cells and B cells. The number of DO11.10 TCR T cells per LN section was quantified by the LSC in naïve, tolerised and primed tissue. Primed tissue has more transgenic T cells than naïve and tolerised tissue sections, as one would expect since the primed transgenic cells should proliferate more than naïve and tolerised cells after re-stimulation with OVA<sub>323-339</sub> + LPS (**Figure 3.55B**). In addition, generation of tissue maps by LSC allowed identification of the B cell-rich (follicles) and T cell (paracortex) areas, as described in section 2.9.2 (**Figure 2.8**) and this approach was used to identify the localisation of the transgenic T cells in the LN, establishing whether they could be found on the follicles or

the paracortex. The number of KJ1-26<sup>+</sup> T cells in either location was divided by the total number of KJ1-26<sup>+</sup> T cells in the LN section and the data plotted in **Figure 3.55C**. As expected, the proportion of DO11.10 TCR T cells present in the follicles is significantly lower than the proportion of those present in the paracortex, for naïve, tolerised and primed transgenic T cells, as expected. Interestingly, it has been shown that in the primary response to antigen, more primed than tolerised T cells migrate into the follicles as apparently tolerised T cells are defective in their ability to migrate to the B cell rich areas and hence, provide B cell help [265, 284]. However, in an *in vivo* model of oral tolerance [267, 296], tolerised antigen-specific T cells re-challenged with a priming stimulus *in vivo* were shown to be able to enter B cell follicles while remaining unable to provide B cell help. In fact, this is also what appears to happen here in this systemic model of tolerance maintenance, as there were no significant differences in the proportion of antigen-specific T cells present in the follicular areas between the tolerised and the primed groups, following secondary antigenic challenge (**Figure 3.55C**).

### 3.2.5.1 Cbl-b

Following the secondary antigenic challenge, LNs were harvested, sectioned and stained for DO11.10 TCR transgenic T cells (red), B cells (green) and Cbl-b (blue). The expression of Cbl-b in the antigen-specific T cells in LNs of naïve, tolerised and primed mice was then examined *in situ* by LSC (**Figure 3.56**), as described in section 2.9.2. Consistent with the *in vitro* data, although not significant, there appears to be higher expression of Cbl-b, both in terms of the proportion of antigen-specific T cells and levels of expression in such Cbl-b<sup>+</sup> cells, in the primed relative to tolerised mice. Perhaps surprisingly, however, there is a higher percentage of naïve KJ1-26<sup>+</sup> T cells expressing Cbl-b than either tolerised or primed KJ1-26<sup>+</sup> T cells (**Figure 3.56A**). Moreover, these naïve KJ1-26<sup>+</sup>Cbl-b<sup>+</sup> cells express Cbl-b significantly more highly than the tolerised cells, which have comparable levels of Cbl-b expression with primed cells (**Figure 3.56B**). Images of these LN sections indicate that, consistent with its ubiquitous expression in haematopoietic cells [177, 180, 202, 285, 286], Cbl-b expression occurs in cells throughout the LN, spanning paracortical and follicular areas, DO11.10 T cells and non-DO11.10 T cells alike in naïve (**Figure 3.56C**), tolerised (**Figure 3.56D**) and primed (**Figure 3.56E**) LN sections alike.

Consistent with the finding that re-challenge with a priming stimulus abrogates the block in follicular migration of tolerised T cells, there was no difference in the

proportional distribution of KJ1-26<sup>+</sup>Cbl-b<sup>+</sup> cells per follicles and paracortex, comparing the different groups, while obviously in all groups more KJ1-26<sup>+</sup>Cbl-b<sup>+</sup> cells could be found in the paracortex than the follicles (**Figure 3.57A**). In other words, localisation of KJ1-26<sup>+</sup>Cbl-b<sup>+</sup> cells mirrors the distribution of all KJ1-26<sup>+</sup> T cells. Moreover, KJ1-26<sup>+</sup>Cbl-b<sup>+</sup> cells from all groups expressed comparable levels of Cbl-b (although the naïve cells appeared to exhibit a slightly higher expression of Cbl-b than tolerised or primed cells) regardless of follicular or paracortical location (although, paracortical-localised antigen-specific T cells exhibit a slightly higher expression of Cbl-b than follicular-localised ones) (**Figure 3.57B**). Nonetheless, differences were observed in terms of percentage of KJ1-26<sup>+</sup> T cells expressing Cbl-b (**Figure 3.57C**). Thus, the naïve population of KJ1-26<sup>+</sup> T cells in the paracortex have a significantly higher percentage of cells positive for Cbl-b than the tolerised population of KJ1-26<sup>+</sup> T cells in the paracortex. The general trend is that the naïve population of KJ1-26<sup>+</sup> T cells, either in the paracortex or the follicles, has a higher percentage of cells positive for Cbl-b than either the tolerised or primed populations.

### 3.2.5.2 Itch

Following the same procedure as for the detection of Cbl-b expression in the maintenance phase of tolerance and priming *in vivo*, LNs were sectioned, stained for DO11.10 TCR transgenic T cells (red), B cells (green) and Itch (blue), and analysed for Itch expression with the LSC and fluorescent microscopy (**Figure 3.58**). Here, unlike what was observed in the *in vitro* maintenance phase experiments, the primed population of KJ1-26<sup>+</sup> T cells appeared to exhibit a lower percentage of cells positive for Itch than either the naïve or tolerised populations, although these differences did not prove significant (**Figure 3.58A**). Moreover, in terms of levels of expression of Itch in KJ1-26<sup>+</sup>Itch<sup>+</sup> cells, there are no apparent differences between the three populations (**Figure 3.58B**). Imaging of the LN sections again reveals Itch expression throughout all cells in the LN, in the follicles and in the paracortex, independently of the naïve (**Figure 3.58C**), tolerised (**Figure 3.58D**) or primed (**Figure 3.58E**) status of the tissue.

Analysis of the percentage of KJ1-26<sup>+</sup> T cells expressing Itch according to LN localisation was also carried out (**Figure 3.59A**). The proportion of KJ1-26<sup>+</sup> T cells expressing Itch in the follicles is the same for the naïve, tolerised and primed groups. However, not only is the proportion of naïve KJ1-26<sup>+</sup> T cells expressing Itch higher in the paracortical-located than the follicular-located transgenic T cells, but this percentage of naïve KJ1-26<sup>+</sup> T cells expressing Itch in the paracortex is higher than the percentage

of tolerised KJ1-26<sup>+</sup> T cells expressing Itch in the paracortex and significantly higher than the percentage of primed KJ1-26<sup>+</sup> T cells expressing Itch in the paracortex. Nevertheless, in terms of levels of expression of Itch, all KJ1-26<sup>+</sup>Itch<sup>+</sup> cells, regardless of the functional group or LN localisation, are expressing Itch at comparable levels (**Figure 3.59B**).

### 3.2.5.3 Grail

Grail expression was also assessed *in situ*, in the maintenance phase. Thus, following the secondary antigenic challenge, LNs were harvested, sectioned and stained for DO11.10 TCR transgenic T cells, B cells and Grail. The expression of Grail in antigen-specific T cells in LNs of naïve, tolerised and primed mice was then examined by LSC, as described in section 2.9.2. This revealed that Grail is also expressed in a higher percentage of naïve KJ1-26<sup>+</sup> T cells than tolerised or primed KJ1-26<sup>+</sup> T cells (**Figure 3.60A**). Moreover, Grail is also expressed at lower levels in KJ1-26<sup>+</sup> T cells from tolerised relative to both naïve and primed mice (**Figure 3.60B**).

Analysis of the proportion of KJ1-26<sup>+</sup> T cells expressing Grail according to their follicular/paracortical localisation (**Figure 3.61A**) revealed that globally, there are no significant differences amongst the different populations, although the general trend is that, regardless of the population, a higher percentage of the antigen-specific T cells located in the follicles express Grail than those in the paracortex. Interestingly, however, the naïve and the primed DO11.10 TCR T cells localised in the follicles express significantly more Grail than their tolerised counterparts (**Figure 3.61B**) whilst there is no such difference between naïve, primed and tolerised DO11.10 TCR T cells located on the paracortex.

**Figure 3.1: Induction of anergy and priming in T cells.**

CD4<sup>+</sup> T cells were extracted from lymph nodes (LNs) and purified, after which they were cultured *in vitro* in the absence or presence of the indicated stimuli in order to induce anergy or priming (A). Cells were tested for functional hallmarks such as activation (B) and proliferation (C). Activation of CD4<sup>+</sup> T cells was measured after 20 h of *in vitro* culture: cells were washed and stained for CD4 and CD69 (early activation marker). The mean fluorescence intensity (MFI) of the cells was measured via flow cytometry and the MFI plotted as fold increase of the MFI of naïve CD4<sup>+</sup> T cells (the MFI value of naïve CD4<sup>+</sup> T cells was taken as basal and assigned the “1” value). Proliferation of CD4<sup>+</sup> T cells was measured by means of counts per minute (cpm) of [<sup>3</sup>H]thymidine incorporation in newly-synthesised DNA after 48 h of *in vitro* culture. The results shown are representative of at least two independent experiments.

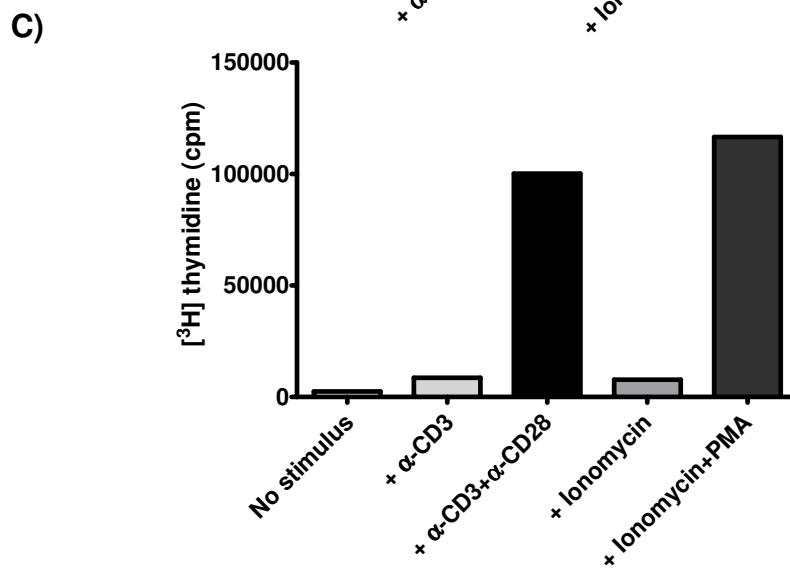
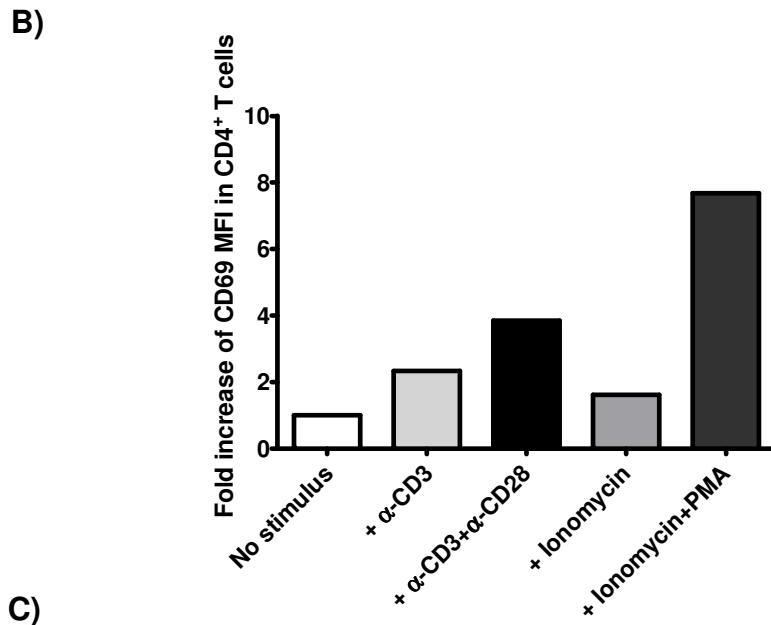
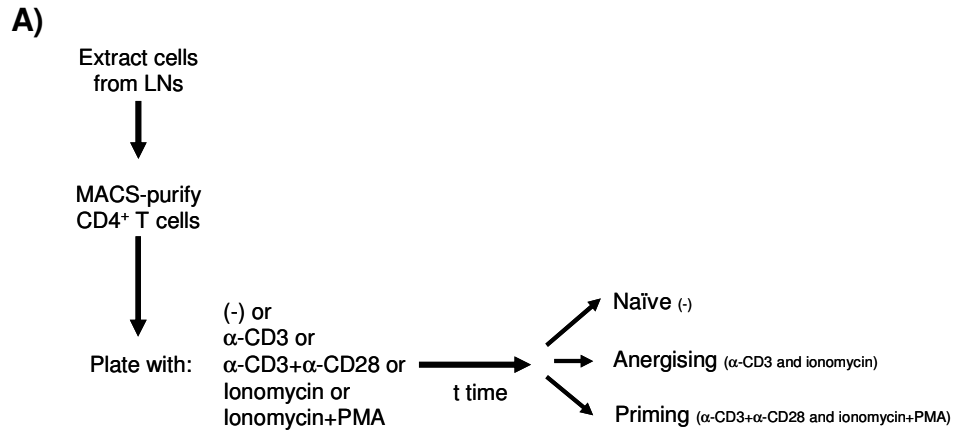
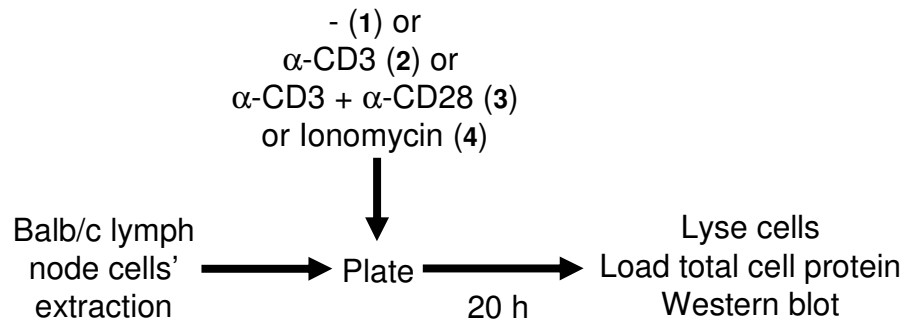


**Figure 3.2: Expression of E3 ubiquitin-protein ligases in T cells.**

Lymph nodes were extracted from BALB/c mice and mashed up. Viable T cells were cultured *in vitro* without stimuli (1) or in the presence of anti-CD3 antibody (2), or anti-CD3 and anti-CD28 antibodies (3), or ionomycin (4); cells were cultured for a total of 20 h, after which they were harvested and lysed (**A**). Total protein extracts were separated by SDS-PAGE and transferred onto a nitrocellulose membrane. The membrane was analysed by Western blotting for proteins of interest: it was blocked in 5% milk/ TBS-T for 1 h, washed 3 x 10 min with TBS-T, probed with primary antibody overnight in the cold room, washed 3 x 5 min with TBS-T, incubated with HRP-linked secondary antibody for 1 h, washed 3 x 5 min with TBS-T, incubated with ECL solution for 1 m, and developed. The membrane was then stripped and subsequently re-probed again, originating the profile observed in **B**. Total Erk 1/ 2 (44 and 42 KDa, respectively) was used as loading control (LC). Data are representative of at least two independent experiments.

**A)**



**B)**

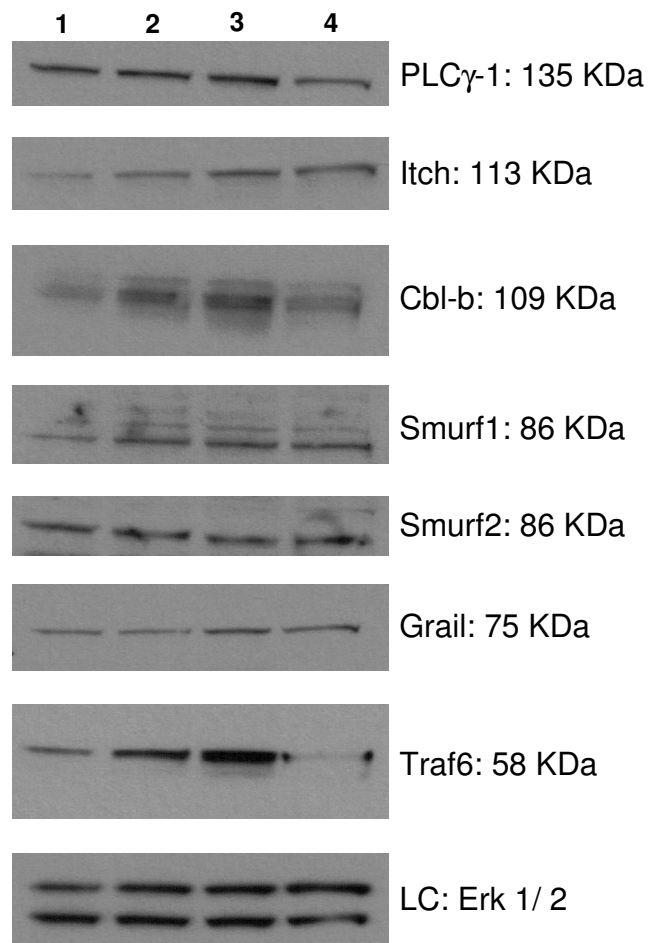
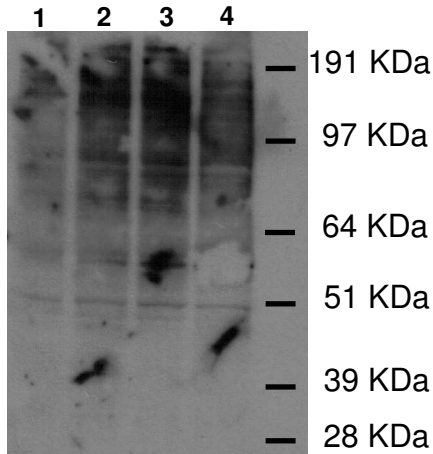


### **Figure 3.3: Ubiquitination of proteins in T cells.**

Lymph nodes were extracted from BALB/c mice and mashed up. Viable T cells were cultured *in vitro* without stimuli (1) or in the presence of anti-CD3 antibody (2), or anti-CD3 and anti-CD28 antibodies (3), or ionomycin (4); cells were cultured for a total of 20 h, after which they were harvested and lysed, as described in **Figure 3.2A**. Total protein extracts were separated by SDS-PAGE and transferred onto a nitrocellulose membrane. The membrane was analysed by Western blotting for all ubiquitinated conjugates and free ubiquitin (**A**): it was blocked in 5% milk/ TBS-T for 1 h, washed 3 x 10 min with TBS-T, probed with primary antibody overnight in the cold room, washed 3 x 5 min with TBS-T, incubated with HRP-linked secondary antibody for 1 h, washed 3 x 5 min with TBS-T, incubated with ECL solution for 1 m, and developed. The membrane was then stripped and subsequently re-probed again for mono- and poly-ubiquitinated conjugates (**B**), poly-ubiquitinated conjugates (**C**) and K63-linked poly-ubiquitinated conjugates (**D**). The loading control can be observed in **Figure 3.2B**. Data are representative of at least two independent experiments.

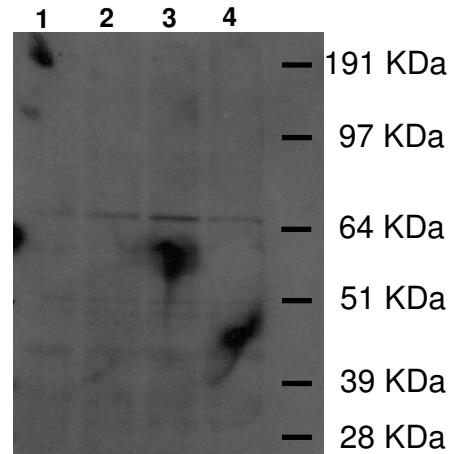
**A)**

All ubiquitinated  
conjugates and free  
ubiquitin



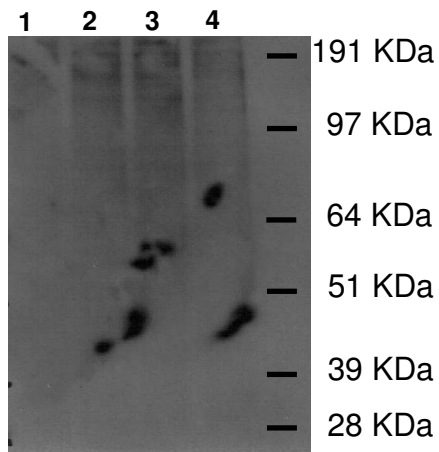
**B)**

Mono- and  
polyubiquitinated  
conjugates



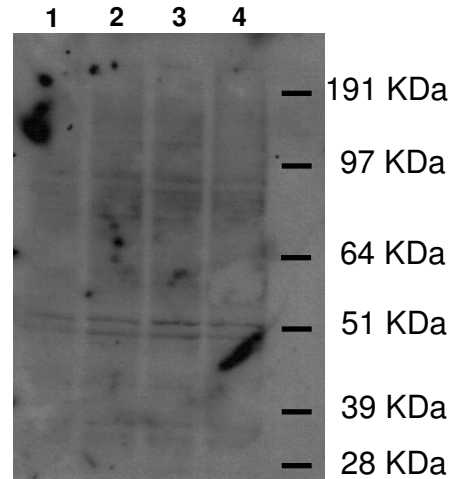
**C)**

Polyubiquitinated  
conjugates



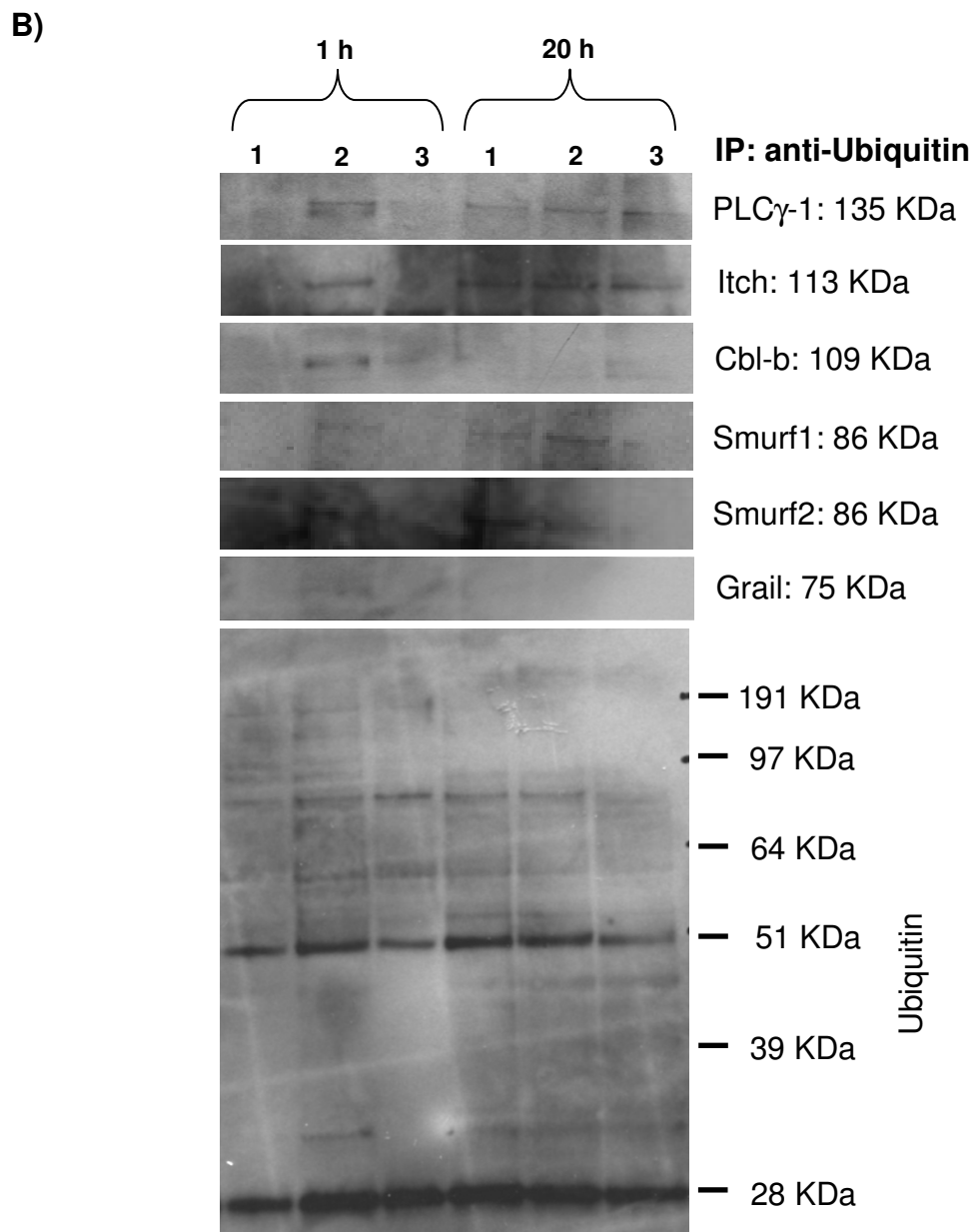
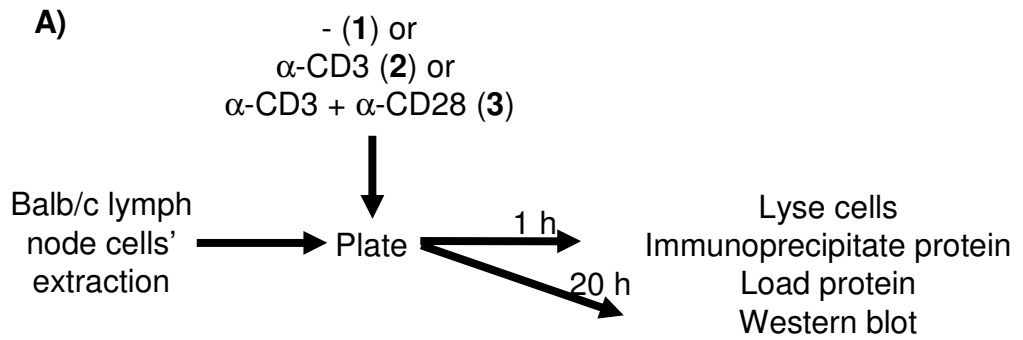
**D)**

K63-linked polyubiquitinated  
conjugates



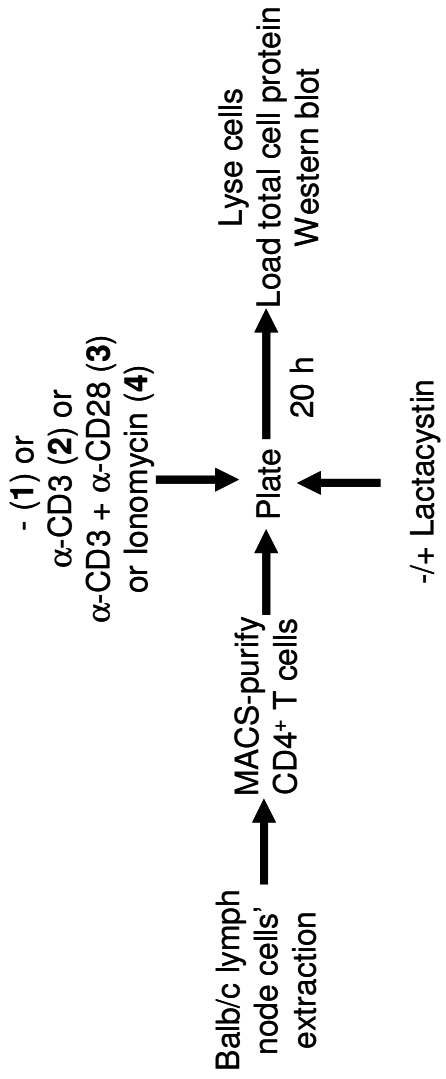
### **Figure 3.4: Immunoprecipitation of ubiquitin in T cells.**

Lymph nodes were extracted from BALB/c mice and mashed up. Viable T cells were cultured *in vitro* without stimuli (1) or in the presence of anti-CD3 antibody (2), or anti-CD3 and anti-CD28 antibodies (3); cells were cultured for 1 and 20 h, after which they were harvested and lysed; total protein extracts were extracted with anti-ubiquitin antibody; the immunoprecipitates were separated by SDS-PAGE and transferred onto a nitrocellulose membrane (**A**). The membrane was analysed by Western blotting for proteins of interest: it was blocked in 5% milk/ TBS-T for 1 h, washed 3 x 10 min with TBS-T, probed with primary antibody overnight in the cold room, washed 3 x 5 min with TBS-T, incubated with HRP-linked secondary antibody for 1 h, washed 3 x 5 min with TBS-T, incubated with ECL solution for 1 m, and developed. The membrane was then stripped and subsequently re-probed again, originating the profile observed in **B**. In the end, the membrane was probed with anti-ubiquitin antibody.



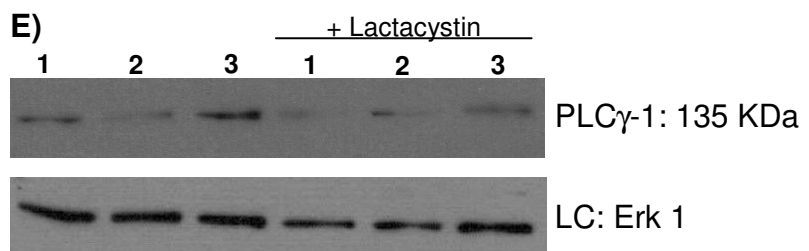
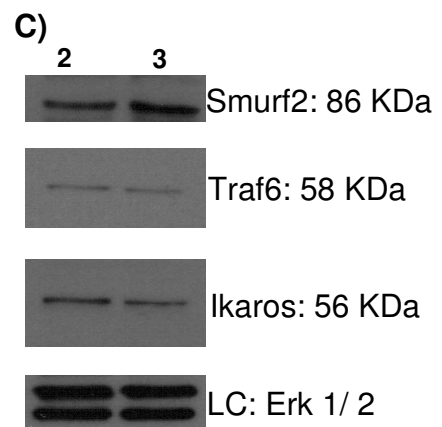
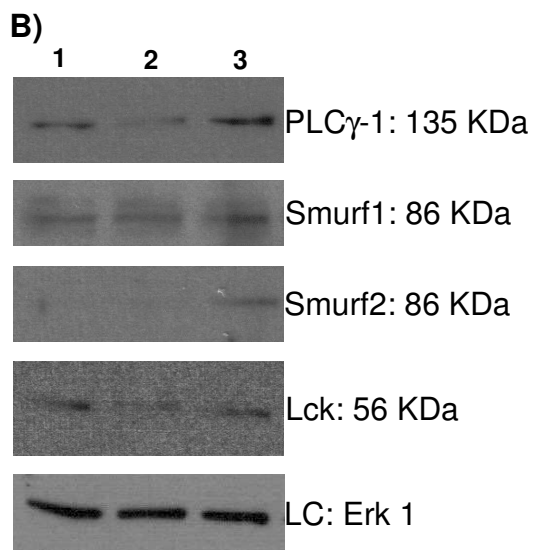
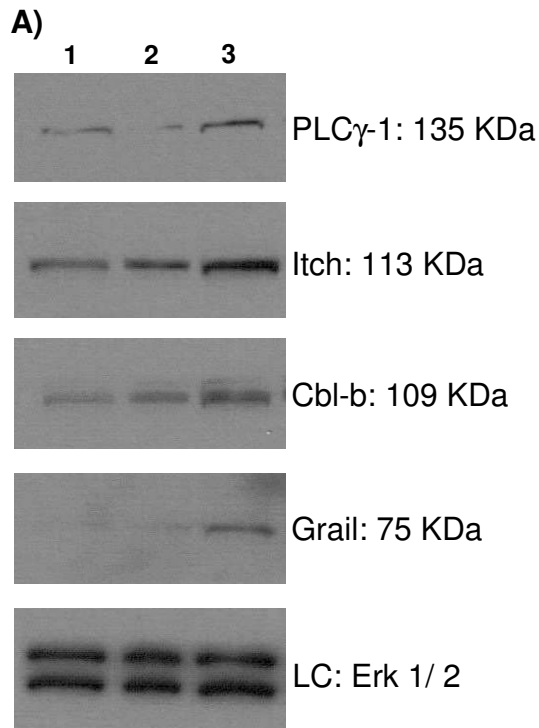
**Figure 3.5: Induction of anergy and priming in CD4<sup>+</sup> T cells.**

Lymph nodes were extracted from BALB/c mice and mashed up. The resulting cells were indirectly magnetically labelled and CD4<sup>+</sup> T cells were negatively selected. Viable CD4<sup>+</sup> T cells were cultured *in vitro* without stimuli (1) or in the presence of anti-CD3 antibody (2), or anti-CD3 and anti-CD28 antibodies (3), or ionomycin (4); lactacystin was added to a set of these T cell populations in order to inhibit proteasome function; cells were cultured for a total of 20 h, after which they were harvested and lysed. Total protein extracts were separated by SDS-PAGE and transferred onto a nitrocellulose membrane. The membrane was analysed by Western blotting for proteins of interest.



**Figure 3.6: Expression of E3 ubiquitin-protein ligases in CD4<sup>+</sup> T cells.**

Lymph nodes were extracted from BALB/c mice and mashed up. The resulting cells were indirectly magnetically labelled and CD4<sup>+</sup> T cells were negatively selected. Viable CD4<sup>+</sup> T cells were cultured *in vitro* without stimuli (1) or in the presence of anti-CD3 antibody (2), or anti-CD3 and anti-CD28 antibodies (3); where indicated lactacystin was added to the T cell culture; cells were cultured for a total of 20 h, after which they were harvested and lysed. Total protein extracts were separated by SDS-PAGE and transferred onto a nitrocellulose membrane. The membranes were analysed by Western blotting for proteins of interest: they were blocked in 5% milk/ TBS-T for 1 h, washed 3 x 10 min with TBS-T, probed with primary antibody overnight in the cold room, washed 3 x 5 min with TBS-T, incubated with HRP-linked secondary antibody for 1 h, washed 3 x 5 min with TBS-T, incubated with ECL solution for 1 m, and developed. The membranes were then stripped and subsequently re-probed again, originating the profile observed in **A**, **B**, **C** and **E**. Total Erk was used as loading control (LC). Data are representative of at least two independent experiments.

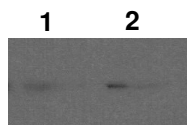


**Figure 3.7: Expression of E3 ubiquitin-protein ligases in CD4<sup>+</sup> T cells after proteasome inhibition.**

Lymph nodes were extracted from BALB/c mice and mashed up. The resulting cells were indirectly magnetically labelled and CD4<sup>+</sup> T cells were negatively selected. Viable CD4<sup>+</sup> T cells were cultured *in vitro* with the proteasome inhibitor lactacystin and without further stimuli (1) or in the presence of anti-CD3 antibody (2), or anti-CD3 and anti-CD28 antibodies (3), or ionomycin (4); cells were cultured for a total of 20 h, after which they were harvested and lysed. Total protein extracts were separated by SDS-PAGE and transferred onto a nitrocellulose membrane. The membranes were analysed by Western blotting for proteins of interest: they were blocked in 5% milk/ TBS-T for 1 h, washed 3 x 10 min with TBS-T, probed with primary antibody overnight in the cold room, washed 3 x 5 min with TBS-T, incubated with HRP-linked secondary antibody for 1 h, washed 3 x 5 min with TBS-T, incubated with ECL solution for 1 m, and developed. The membranes were then stripped and subsequently re-probed again, originating the profile observed in **A**, **B** and **C**. Total Erk was used as loading control (LC). Data are representative of at least two independent experiments.

**A)**

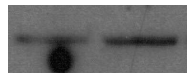
+ Lactacystin

PLC $\gamma$ -1: 135 KDa

Itch: 113 KDa



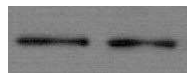
Smurf1: 86 KDa



Smurf2: 86 KDa



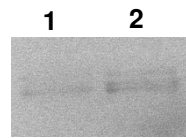
Lck: 56 KDa



LC: Erk 1

**B)**

+ Lactacystin



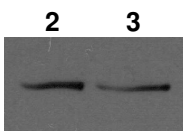
Cbl-b: 109 KDa



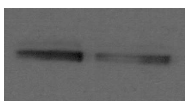
LC: Erk 1

**C)**

+ Lactacystin



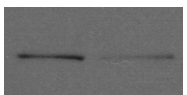
Itch: 113 KDa



Cbl-b: 109 KDa



Smurf2: 86 KDa



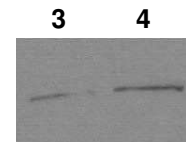
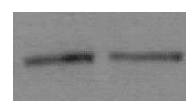
Grail: 75 KDa



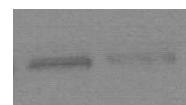
LC: Erk 1/2

**D)**

+ Lactacystin

PLC $\gamma$ -1: 135 KDa

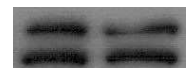
Itch: 113 KDa



Cbl-b: 109 KDa



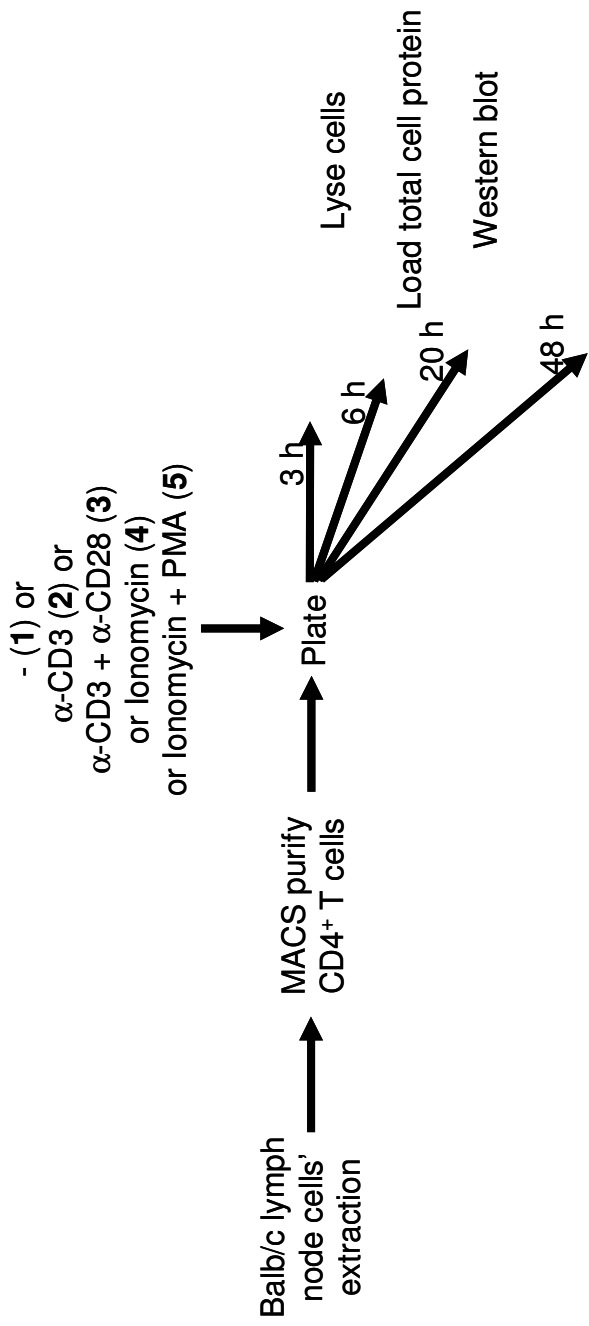
Grail: 75 KDa



LC: Erk 1/2

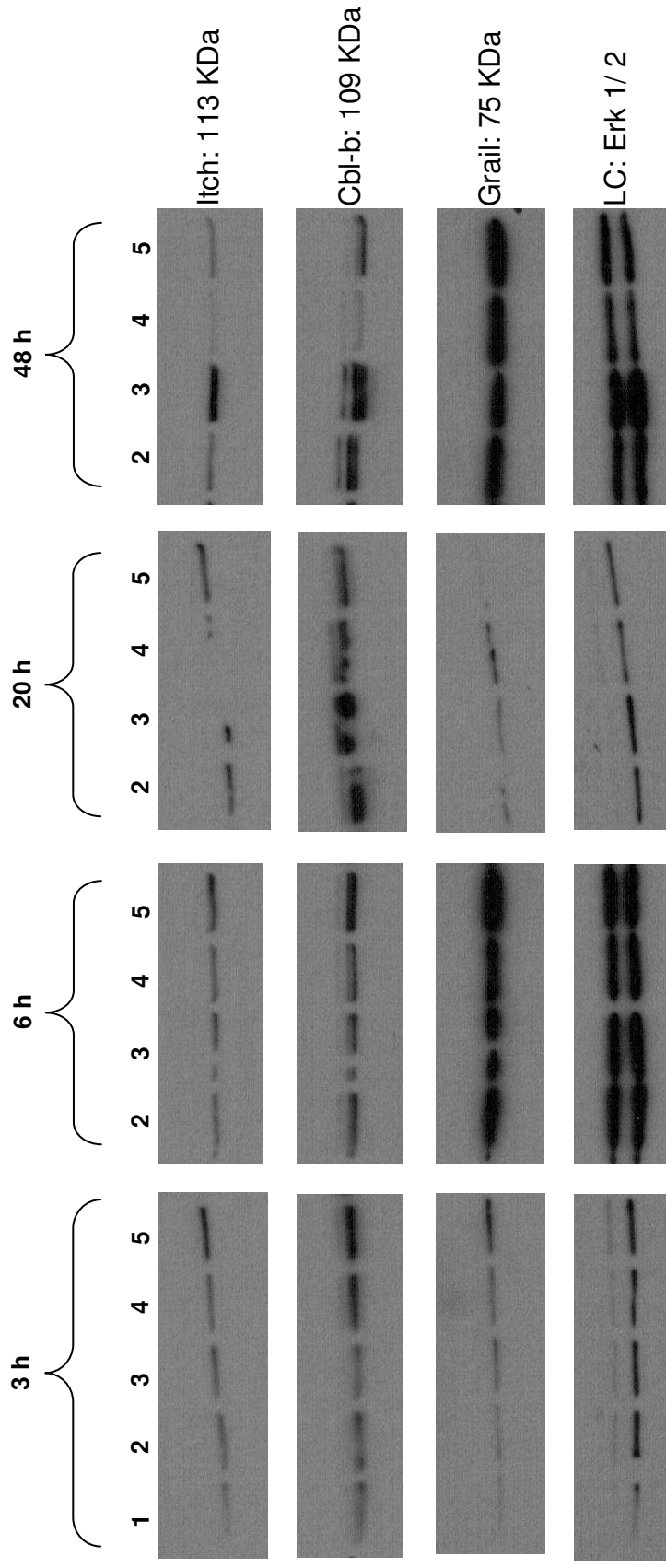
**Figure 3.8: Inducing anergy and priming in CD4<sup>+</sup> T cells.**

Lymph nodes were extracted from BALB/c mice and mashed up. The resulting cells were indirectly magnetically labelled and CD4<sup>+</sup> T cells were negatively selected. Viable CD4<sup>+</sup> T cells were cultured *in vitro* without stimuli (1) or in the presence of anti-CD3 antibody (2), or anti-CD3 and anti-CD28 antibodies (3), or ionomycin (4), or ionomycin and PMA (5); cells were cultured for 3, 6, 20 and 48 h, after which they were harvested and lysed. Total protein extracts were separated by SDS-PAGE and transferred onto a nitrocellulose membrane. The membrane was analysed by Western blotting for proteins of interest.



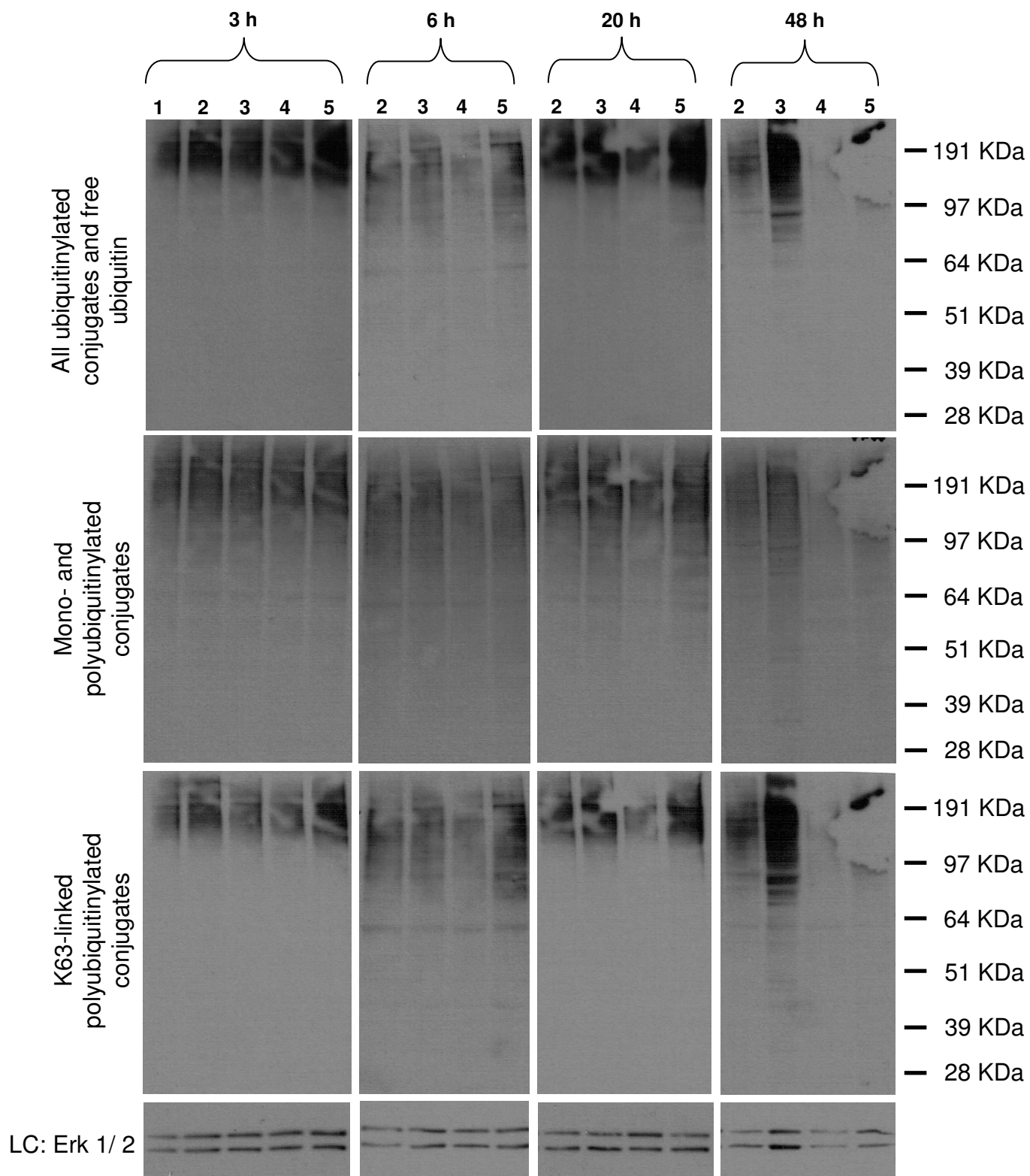
**Figure 3.9: Expression of E3 ubiquitin-protein ligases in anergising and priming CD4<sup>+</sup> T cells.**

Lymph nodes were extracted from BALB/c mice and mashed up. The resulting cells were indirectly magnetically labelled and CD4<sup>+</sup> T cells were negatively selected. Viable CD4<sup>+</sup> T cells were cultured *in vitro* without stimuli (1) or in the presence of anti-CD3 antibody (2), or anti-CD3 and anti-CD28 antibodies (3), or ionomycin (4), or ionomycin and PMA (5); cells were cultured for 3, 6, 20 and 48 h, after which they were harvested and lysed. This figure was generated from two separate experiments, one comprising the 3 and 20 h time points, and the other comprising the 6 and the 48 h time points. Total protein extracts were separated by SDS-PAGE and transferred onto a nitrocellulose membrane. The membrane was analysed by Western blotting for proteins of interest: it was blocked in 5% milk/ TBS-T for 1 h, washed 3 x 10 min with TBS-T, probed with primary antibody overnight in the cold room, washed 3 x 5 min with TBS-T, incubated with HRP-linked secondary antibody for 1 h, washed 3 x 5 min with TBS-T, incubated with ECL solution for 1 m, and developed. The membrane was then stripped and subsequently re-probed again. Total Erk was used as loading control (LC).



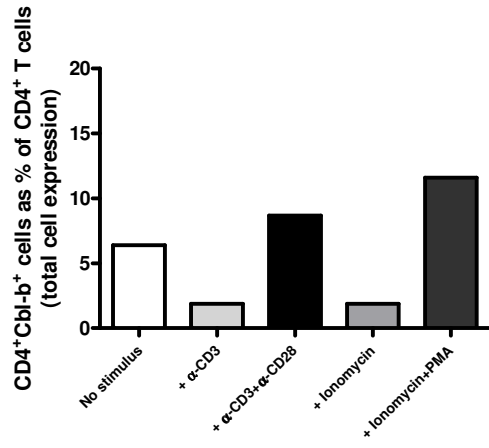
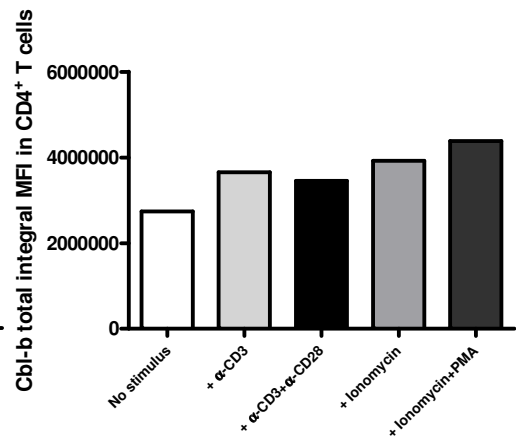
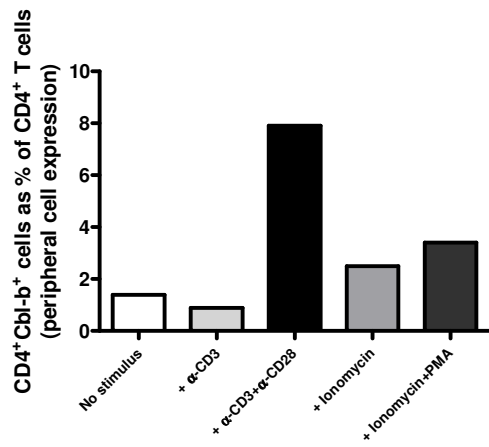
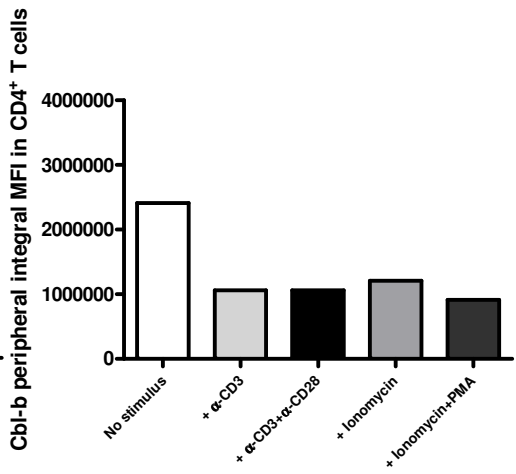
**Figure 3.10: Expression of ubiquitinated proteins in anergising and priming CD4<sup>+</sup> T cells.**

Lymph nodes were extracted from BALB/c mice and mashed up. The resulting cells were indirectly magnetically labelled and CD4<sup>+</sup> T cells were negatively selected. Viable CD4<sup>+</sup> T cells were cultured *in vitro* without stimuli (1) or in the presence of anti-CD3 antibody (2), or anti-CD3 and anti-CD28 antibodies (3), or ionomycin (4), or ionomycin and PMA (5); cells were cultured for 3, 6, 20 and 48 h, after which they were harvested and lysed. Total protein extracts were separated by SDS-PAGE and transferred onto a nitrocellulose membrane. The membrane was analysed by Western blotting for proteins of interest: it was blocked in 5% milk/ TBS-T for 1 h, washed 3 x 10 min with TBS-T, probed with primary antibody overnight in the cold room, washed 3 x 5 min with TBS-T, incubated with HRP-linked secondary antibody for 1 h, washed 3 x 5 min with TBS-T, incubated with ECL solution for 1 m, and developed. The membrane was then stripped and subsequently re-probed again. Total Erk was used as loading control (LC).



**Figure 3.11: Quantification of Cbl-b expression in CD4<sup>+</sup> T cells after 20 h of *in vitro* stimulation.**

CD4<sup>+</sup> T cells were extracted from lymph nodes, purified, cultured *in vitro* in the absence or presence of the indicated stimuli for 20 h, washed, cytocentrifuged, stained for nuclear DNA (DAPI; blue), CD4 (red) and Cbl-b (green) and Cbl-b expression in CD4<sup>+</sup> T cells quantified with the LSC as described in the Materials and Methods chapter. Firstly, all events were sorted on their nuclear staining (“cells”) and from these CD4<sup>+</sup> T cells were gated. **A)** shows the percentage of CD4<sup>+</sup> T cells that are positive for Cbl-b out of the whole population of CD4<sup>+</sup> T cells, in terms of total cell expression. **B)** shows the mean fluorescence intensity (MFI) of Cbl-b expression in those CD4<sup>+</sup> T cells that are also positive for Cbl-b in terms of total cell expression. **C)** shows the proportion of CD4<sup>+</sup> T cells that are positive for Cbl-b out of the whole population of CD4<sup>+</sup> T cells, in terms of peripheral cell expression. **D)** shows MFI of Cbl-b expression in those CD4<sup>+</sup> T cells that are also positive for Cbl-b in terms of peripheral cell expression.

**A)****B)****C)****D)**

**Figure 3.12: Visualisation of Cbl-b expression in CD4<sup>+</sup> T cells after 20 h of *in vitro* stimulation.**

CD4<sup>+</sup> T cells were extracted from lymph nodes, purified, cultured *in vitro* in the absence or presence of the indicated stimuli for 20 h, washed, cytocentrifuged and stained for nuclear DNA (DAPI; blue), CD4 (red) and Cbl-b (green). Fluorescence was visualised using an Olympus BX50 fluorescent microscope and images captured and merged (x40 objectives). Cells were identified by nuclear staining with the DNA dye DAPI (blue). The expression of Cbl-b was determined with an  $\alpha$ -Cbl-b-specific antibody coupled to tyramide amplification and the fluorochrome Alexa Fluor 488 (AF488 - green). Staining of CD4 co-receptor (also by means of an  $\alpha$ -CD4-specific antibody coupled to tyramide amplification and the fluorochrome Alexa Fluor 647 [AF647 – red]) allowed locating the cell plasma membrane. Merging these three images results in the far right image – “Merge”.

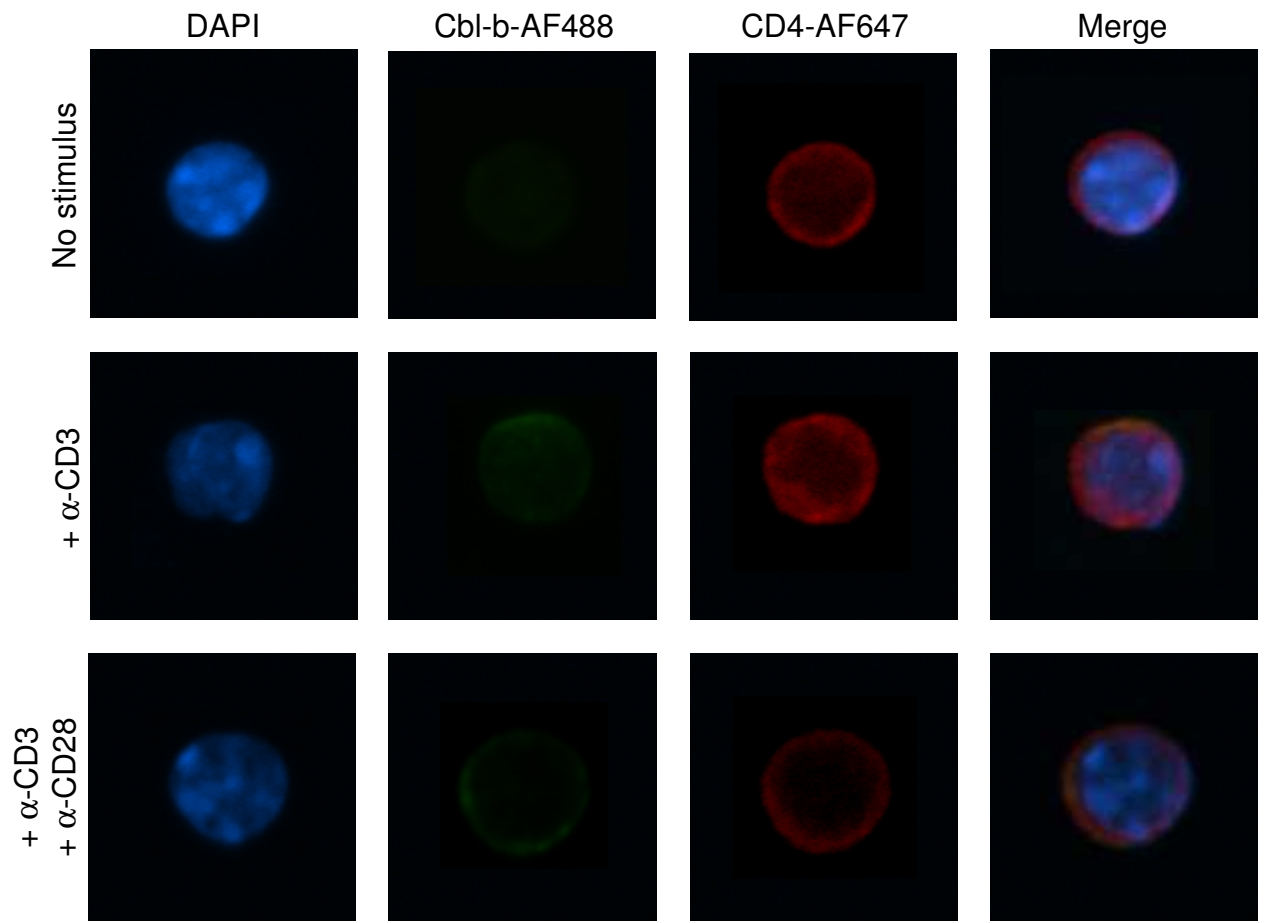
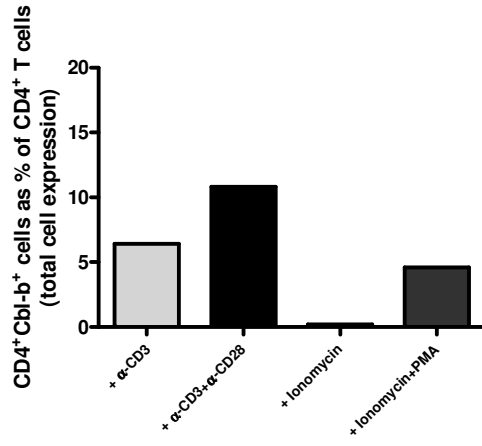


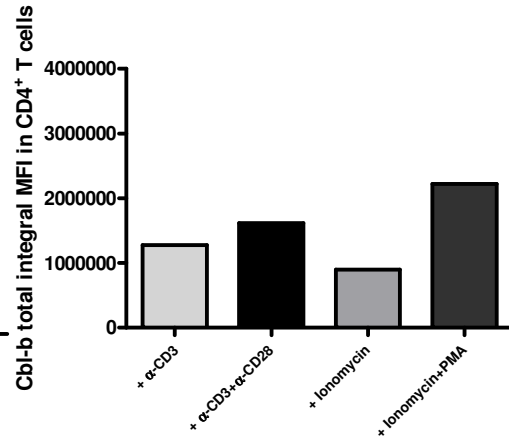
**Figure 3.13: Quantification of Cbl-b expression in CD4<sup>+</sup> T cells after 40 h of *in vitro* stimulation.**

CD4<sup>+</sup> T cells were extracted from lymph nodes, purified, cultured *in vitro* in the presence of the indicated stimuli for 40 h, washed, cytocentrifuged, stained for nuclear DNA (DAPI; blue), CD4 (red) and Cbl-b (green) and Cbl-b expression in CD4<sup>+</sup> T cells quantified with the LSC as described in the Materials and Methods chapter. Firstly, all events were sorted on their nuclear staining (“cells”) and from these CD4<sup>+</sup> T cells were gated. **A)** shows the percentage of CD4<sup>+</sup> T cells that are positive for Cbl-b out of the whole population of CD4<sup>+</sup> T cells, in terms of total cell expression. **B)** shows the mean fluorescence intensity (MFI) of Cbl-b expression in those CD4<sup>+</sup> T cells that are also positive for Cbl-b in terms of total cell expression. **C)** shows the proportion of CD4<sup>+</sup> T cells that are positive for Cbl-b out of the whole population of CD4<sup>+</sup> T cells, in terms of peripheral cell expression. **D)** shows MFI of Cbl-b expression in those CD4<sup>+</sup> T cells that are also positive for Cbl-b in terms of peripheral cell expression.

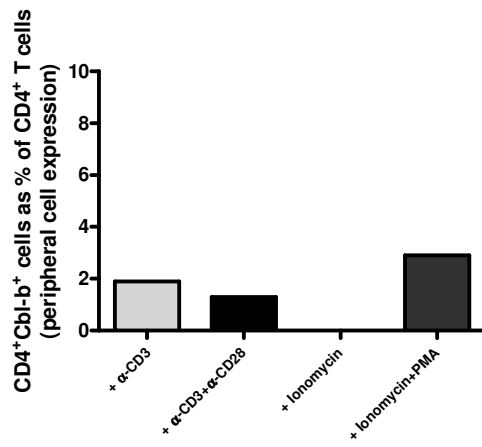
**A)**



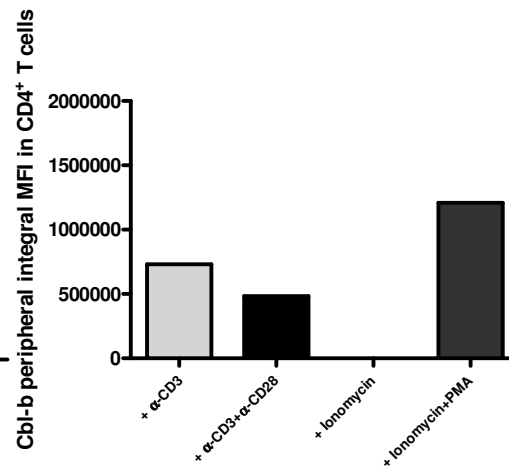
**B)**



**C)**

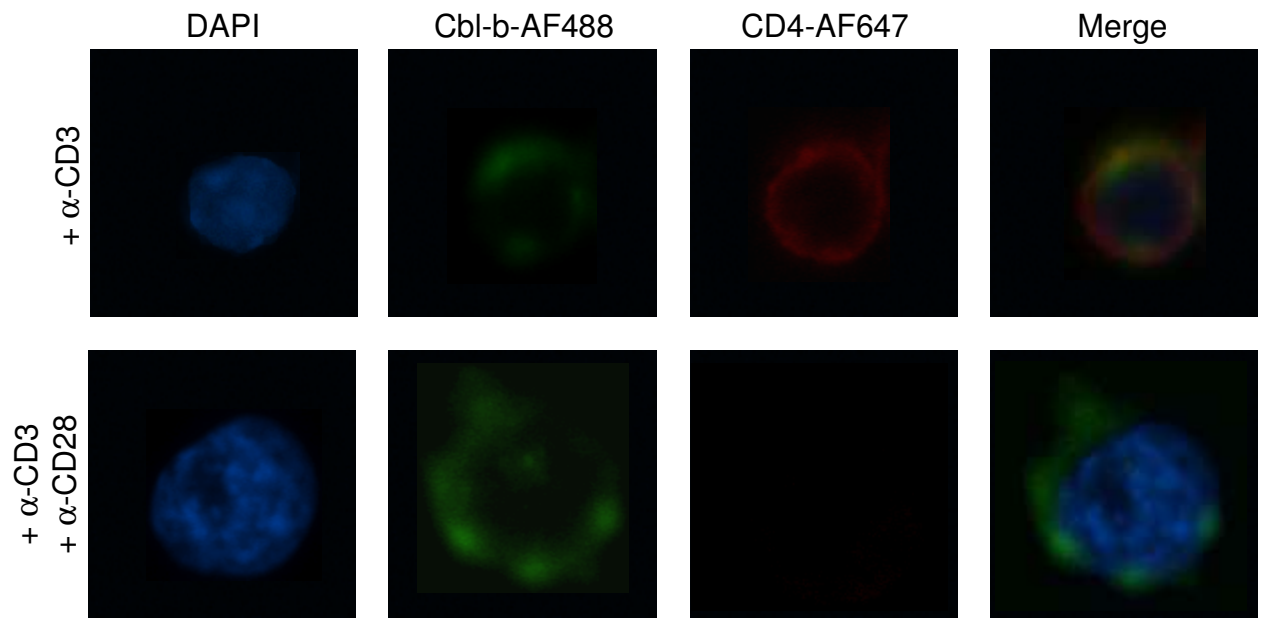


**D)**



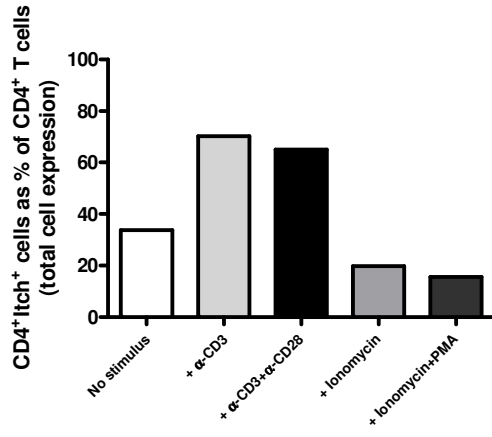
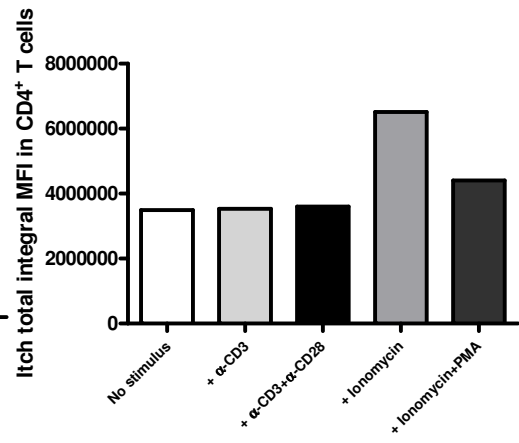
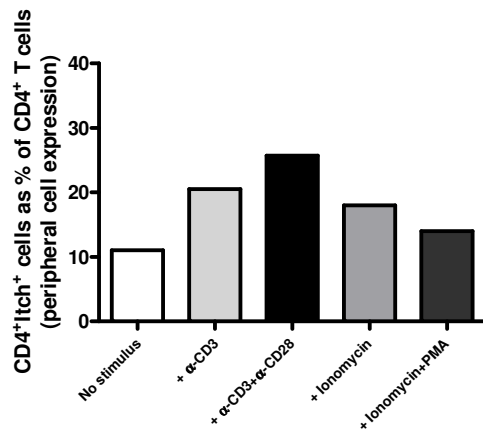
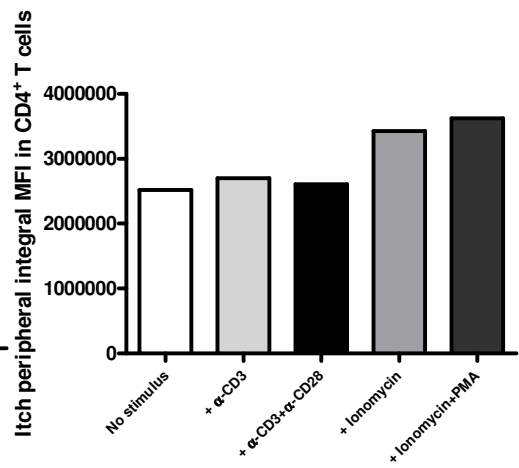
**Figure 3.14: Visualisation of Cbl-b expression in CD4<sup>+</sup> T cells after 40 h of *in vitro* stimulation.**

CD4<sup>+</sup> T cells were extracted from lymph nodes, purified, cultured *in vitro* in the absence or presence of the indicated stimuli for 40 h, washed, cytocentrifuged and stained for nuclear DNA (DAPI; blue), CD4 (red) and Cbl-b (green). Fluorescence was visualised using an Olympus BX50 fluorescent microscope and images captured and merged (x40 objectives). Cells were identified by nuclear staining with the DNA dye DAPI (blue). The expression of Cbl-b was determined with an  $\alpha$ -Cbl-b-specific antibody coupled to tyramide amplification and the fluorochrome Alexa Fluor 488 (AF488 - green). Staining of CD4 co-receptor (also by means of an  $\alpha$ -CD4-specific antibody coupled to tyramide amplification and the fluorochrome Alexa Fluor 647 [AF647 – red]) allowed locating the cell plasma membrane. Merging these three images results in the far right image – “Merge”.



**Figure 3.15: Quantification of Itch expression in CD4<sup>+</sup> T cells after 20 h of *in vitro* stimulation.**

CD4<sup>+</sup> T cells were extracted from lymph nodes, purified, cultured *in vitro* in the presence of the indicated stimuli for 20 h, washed, cytocentrifuged, stained for nuclear DNA (DAPI; blue), CD4 (red) and Itch (green) and Itch expression in CD4<sup>+</sup> T cells quantified with the LSC as described in the Materials and Methods chapter. Firstly, all events were sorted on their nuclear staining (“cells”) and from these CD4<sup>+</sup> T cells were gated. **A)** shows the percentage of CD4<sup>+</sup> T cells that are positive for Itch out of the whole population of CD4<sup>+</sup> T cells, in terms of total cell expression. **B)** shows the mean fluorescence intensity (MFI) of Itch expression in those CD4<sup>+</sup> T cells that are also positive for Itch in terms of total cell expression. **C)** shows the proportion of CD4<sup>+</sup> T cells that are positive for Itch out of the whole population of CD4<sup>+</sup> T cells, in terms of peripheral cell expression. **D)** shows MFI of Itch expression in those CD4<sup>+</sup> T cells that are also positive for Itch in terms of peripheral cell expression.

**A)****B)****C)****D)**

**Figure 3.16: Visualisation of Itch expression in CD4<sup>+</sup> T cells after 20 h of *in vitro* stimulation.**

CD4<sup>+</sup> T cells were extracted from lymph nodes, purified, cultured *in vitro* in the absence or presence of the indicated stimuli for 20 h, washed, cytocentrifuged and stained for nuclear DNA (DAPI; blue) and Itch (green). Fluorescence was visualised using an Olympus BX50 fluorescent microscope and images captured and merged (x40 objectives). Cells were identified by nuclear staining with the DNA dye DAPI (blue). The expression of Itch was determined with an  $\alpha$ -Itch-specific antibody coupled to tyramide amplification and the fluorochrome Alexa Fluor 488 (AF488 - green). Merging these two images results in the far right image - "Merge".

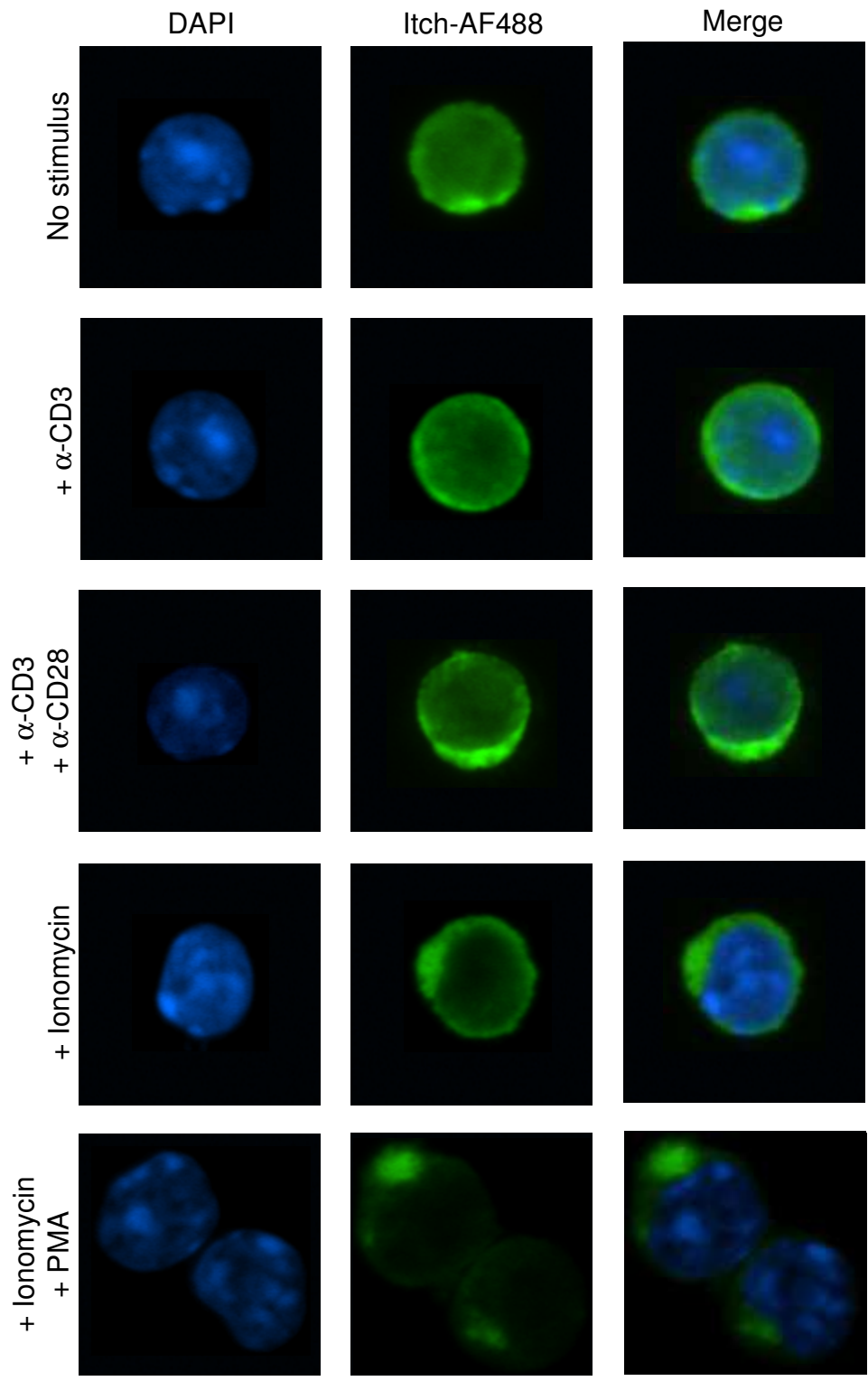
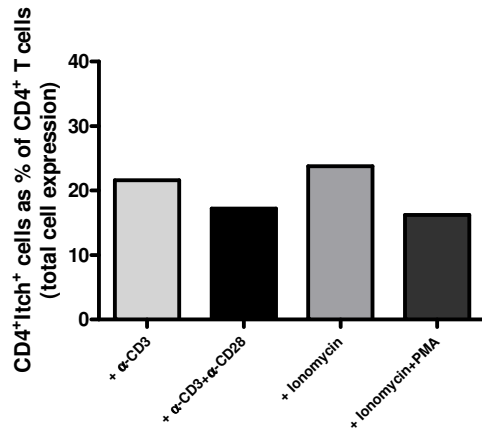


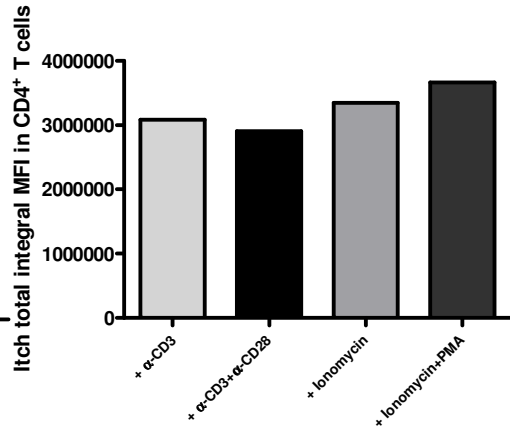
**Figure 3.17: Quantification of Itch expression in CD4<sup>+</sup> T cells after 40 h of *in vitro* stimulation.**

CD4<sup>+</sup> T cells were extracted from lymph nodes, purified, cultured *in vitro* in the presence of the indicated stimuli for 40 h, washed, cytocentrifuged, stained for nuclear DNA (DAPI; blue), CD4 (red) and Itch (green) and Itch expression in CD4<sup>+</sup> T cells quantified with the LSC as described in the Materials and Methods chapter. Firstly, all events were sorted on their nuclear staining (“cells”) and from these CD4<sup>+</sup> T cells were gated. **A)** shows the percentage of CD4<sup>+</sup> T cells that are positive for Itch out of the whole population of CD4<sup>+</sup> T cells, in terms of total cell expression. **B)** shows the mean fluorescence intensity (MFI) of Itch expression in those CD4<sup>+</sup> T cells that are also positive for Itch in terms of total cell expression. **C)** shows the proportion of CD4<sup>+</sup> T cells that are positive for Itch out of the whole population of CD4<sup>+</sup> T cells, in terms of peripheral cell expression. **D)** shows MFI of Itch expression in those CD4<sup>+</sup> T cells that are also positive for Itch in terms of peripheral cell expression.

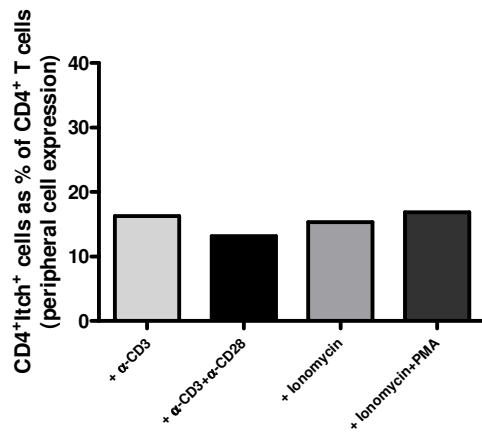
**A)**



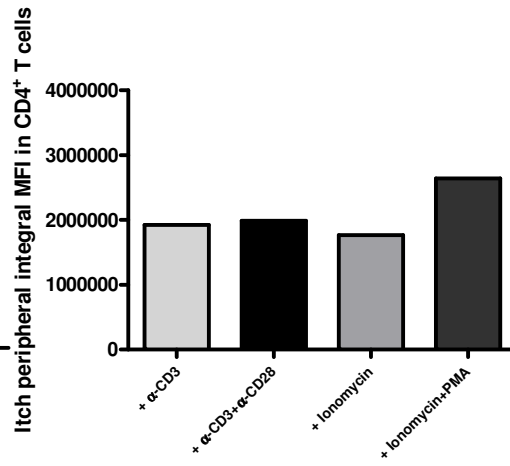
**B)**



**C)**

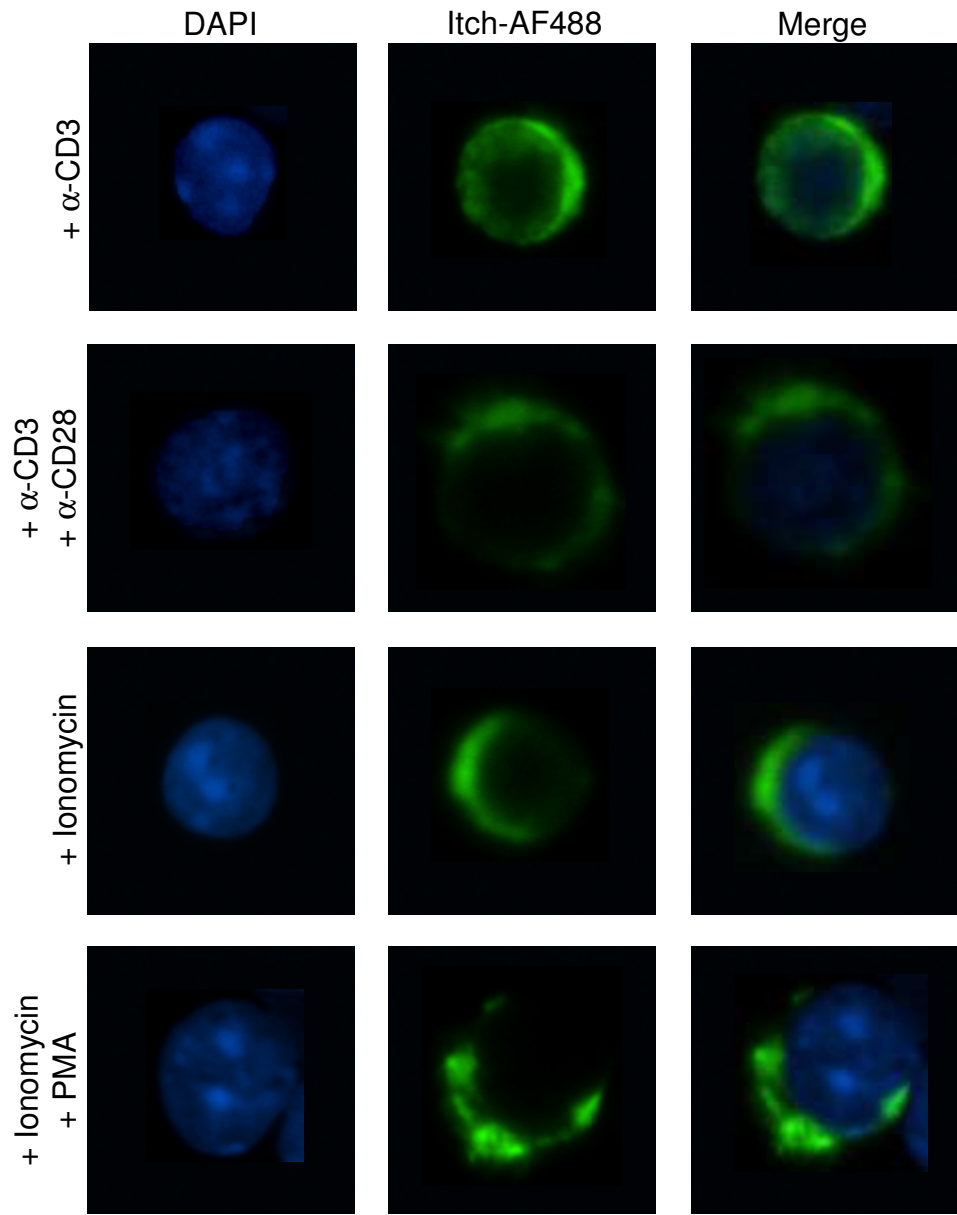


**D)**



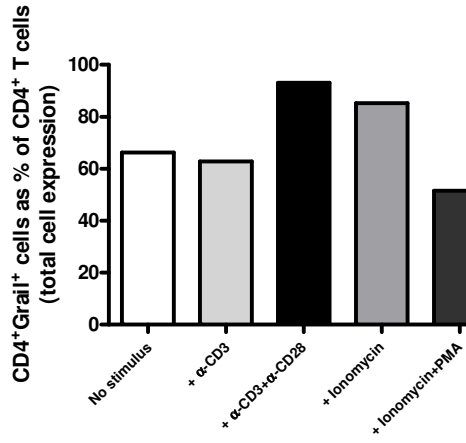
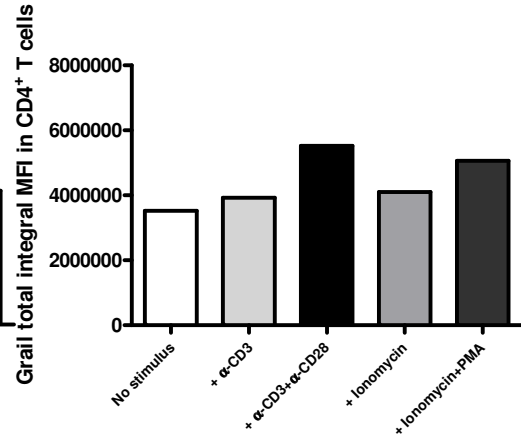
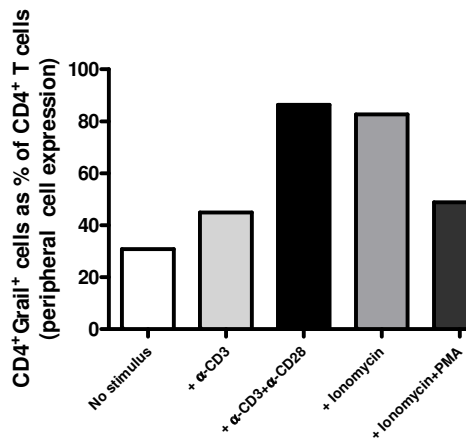
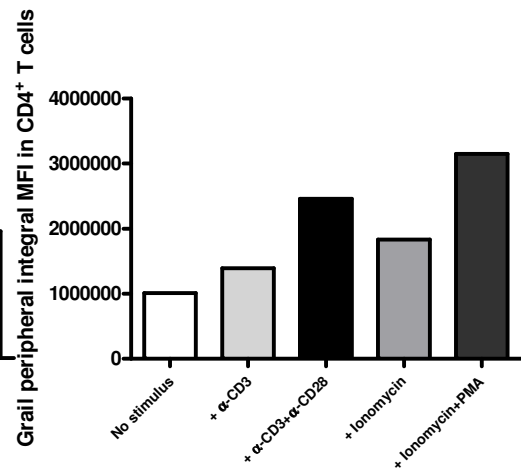
**Figure 3.18: Visualisation of Itch expression in CD4<sup>+</sup> T cells after 40 h of *in vitro* stimulation.**

CD4<sup>+</sup> T cells were extracted from lymph nodes, purified, cultured *in vitro* in the absence or presence of the indicated stimuli for 40 h, washed, cytocentrifuged and stained for nuclear DNA (DAPI; blue) and Itch (green). Fluorescence was visualised using an Olympus BX50 fluorescent microscope and images captured and merged (x40 objectives). Cells were identified by nuclear staining with the DNA dye DAPI (blue). The expression of Itch was determined with an  $\alpha$ -Itch-specific antibody coupled to tyramide amplification and the fluorochrome Alexa Fluor 488 (AF488 - green). Merging these two images results in the far right image - "Merge".



**Figure 3.19: Quantification of Grail expression in CD4<sup>+</sup> T cells after 20 h of *in vitro* stimulation.**

CD4<sup>+</sup> T cells were extracted from lymph nodes, purified, cultured *in vitro* in the presence of the indicated stimuli for 20 h, washed, cytocentrifuged, stained for nuclear DNA (DAPI; blue), CD4 (red) and Grail (green) and Itch expression in CD4<sup>+</sup> T cells quantified with the LSC as described in the Materials and Methods chapter. Firstly, all events were sorted on their nuclear staining (“cells”) and from these CD4<sup>+</sup> T cells were gated. **A)** shows the percentage of CD4<sup>+</sup> T cells that are positive for Grail out of the whole population of CD4<sup>+</sup> T cells, in terms of total cell expression. **B)** shows the mean fluorescence intensity (MFI) of Grail expression in those CD4<sup>+</sup> T cells that are also positive for Grail in terms of total cell expression. **C)** shows the proportion of CD4<sup>+</sup> T cells that are positive for Grail out of the whole population of CD4<sup>+</sup> T cells, in terms of peripheral cell expression. **D)** shows MFI of Grail expression in those CD4<sup>+</sup> T cells that are also positive for Grail in terms of peripheral cell expression.

**A)****B)****C)****D)**

**Figure 3.20: Visualisation of Grail expression in CD4<sup>+</sup> T cells after 20 h of *in vitro* stimulation.**

CD4<sup>+</sup> T cells were extracted from lymph nodes, purified, cultured *in vitro* in the absence or presence of the indicated stimuli for 20 h, washed, cytocentrifuged and stained for nuclear DNA (DAPI; blue), CD4 (red) and Grail (green). Fluorescence was visualised using an Olympus BX50 fluorescent microscope and images captured and merged (x40 objectives). Cells were identified by nuclear staining with the DNA dye DAPI (blue). The expression of Grail was determined with an  $\alpha$ -Grail-specific antibody coupled to tyramide amplification and the fluorochrome Alexa Fluor 488 (AF488 - green). Staining of CD4 co-receptor (also by means of an  $\alpha$ -CD4-specific antibody coupled to tyramide amplification and the fluorochrome Alexa Fluor 647 [AF647 - red]) allowed locating the cell plasma membrane. Images of representative cells were chosen on the basis of their Grail staining. Merging these three images results in the far right image - "Merge".

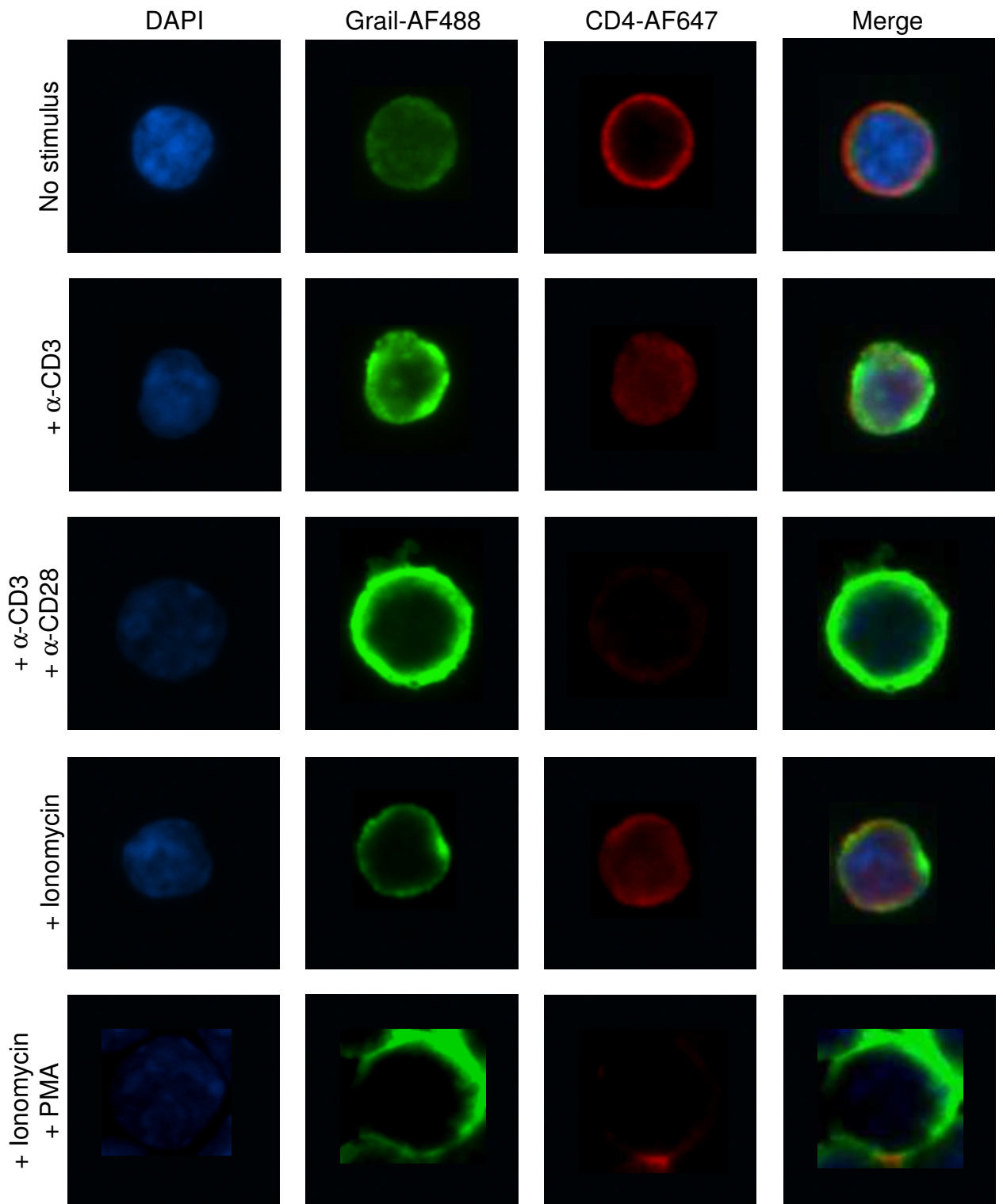
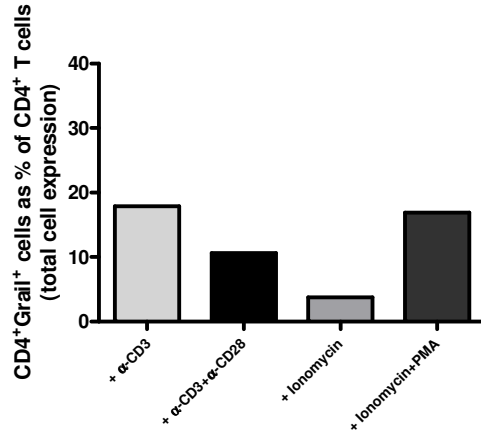


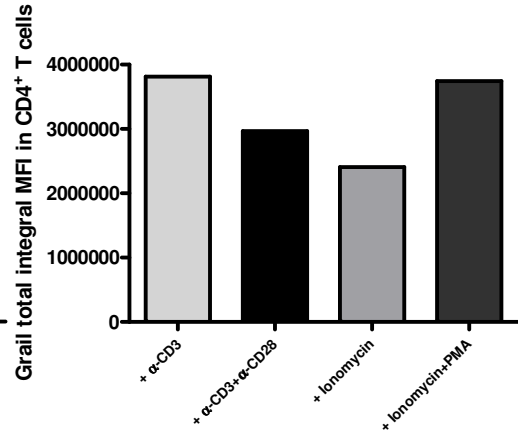
**Figure 3.21: Quantification of Grail expression in CD4<sup>+</sup> T cells after 40 h of *in vitro* stimulation.**

CD4<sup>+</sup> T cells were extracted from lymph nodes, purified, cultured *in vitro* in the presence of the indicated stimuli for 40 h, washed, cytocentrifuged, stained for nuclear DNA (DAPI; blue), CD4 (red) and Grail (green) and Itch expression in CD4<sup>+</sup> T cells quantified with the LSC as described in the Materials and Methods chapter. Firstly, all events were sorted on their nuclear staining (“cells”) and from these CD4<sup>+</sup> T cells were gated. **A)** shows the percentage of CD4<sup>+</sup> T cells that are positive for Grail out of the whole population of CD4<sup>+</sup> T cells, in terms of total cell expression. **B)** shows the mean fluorescence intensity (MFI) of Grail expression in those CD4<sup>+</sup> T cells that are also positive for Grail in terms of total cell expression. **C)** shows the proportion of CD4<sup>+</sup> T cells that are positive for Grail out of the whole population of CD4<sup>+</sup> T cells, in terms of peripheral cell expression. **D)** shows MFI of Grail expression in those CD4<sup>+</sup> T cells that are also positive for Grail in terms of peripheral cell expression.

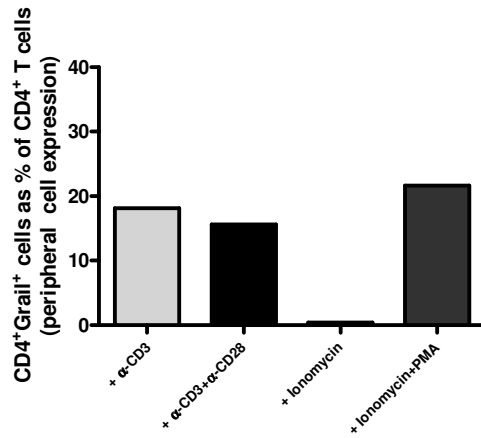
**A)**



**B)**



**C)**



**D)**

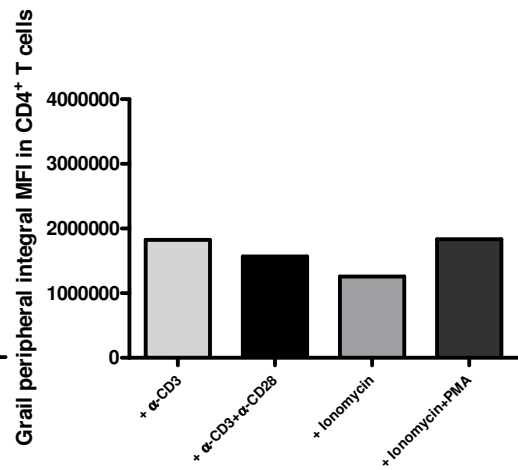
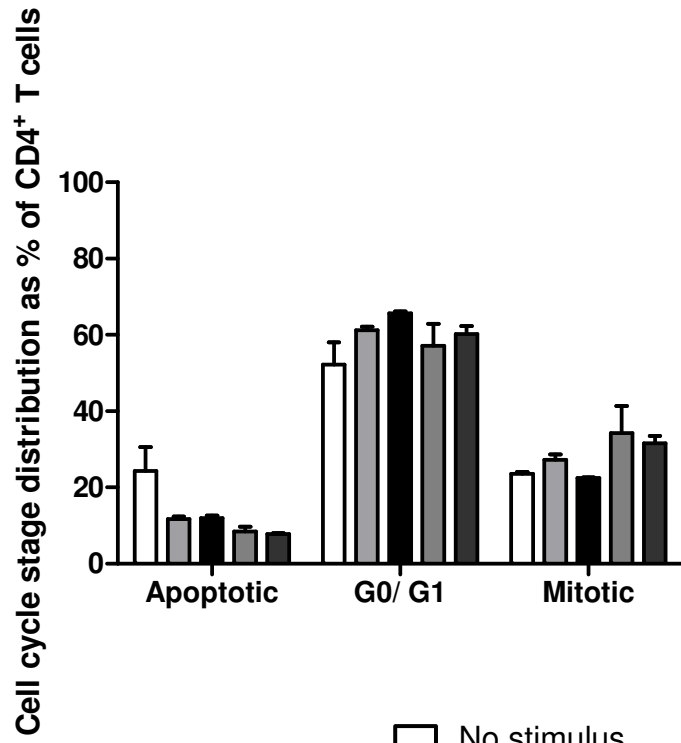


**Figure 3.22: Analysis of cell cycle stage distribution in CD4<sup>+</sup> T cells.**

CD4<sup>+</sup> T cells were extracted from lymph nodes, purified, cultured *in vitro* in the absence or presence of the indicated stimuli for 20 h (A) or 40 h (B), washed, cytocentrifuged, stained for the nucleus and CD4 (plus further label with adequate fluorochrome). The slides were analysed in the LSC: CD4<sup>+</sup> T cells were gated, their DAPI max pixel Vs integral values plotted and adequate regions drawn matching the different cell cycle stages. Values are presented as percentage of CD4<sup>+</sup> T cells in a particular cell cycle stage out of the whole population of CD4<sup>+</sup> T cells, for that particular stimulus. Some stimulated populations were normalised to 100%. Cells in S phase, G2/M phase and newly-formed daughter cells were grouped together in one group called “Mitotic” cells. The results shown are the mean ± SEM of triplicate slide staining and are representative of three independent experiments.

A)



B)

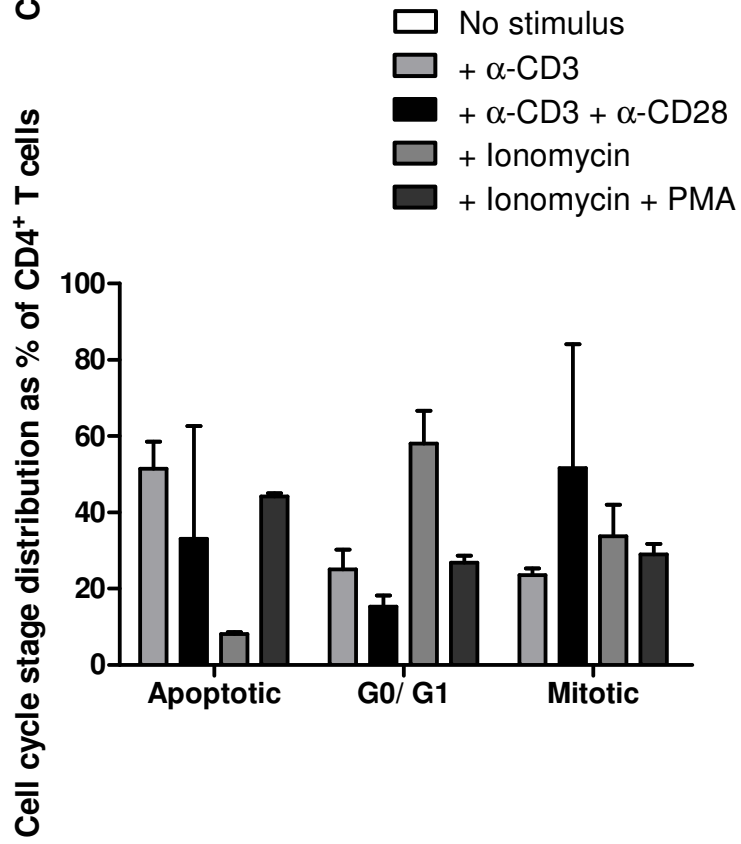


**Figure 3.23: Analysis of Cbl-b expression according to cell cycle stage in CD4<sup>+</sup> T cells after 20 h of *in vitro* stimulation.**

CD4<sup>+</sup> T cells were extracted from lymph nodes, purified, cultured *in vitro* in the presence of the indicated stimuli for 20 h, washed, cytocentrifuged, stained for nucleus, CD4 and Cbl-b (these were further labelled with adequate fluorochromes). The slides were analysed in the LSC. **A)** CD4<sup>+</sup> T cells were gated, Cbl-b<sup>+</sup> cells gated after this and their DAPI max pixel Vs integral values plotted. Values are presented as percentage of CD4<sup>+</sup>Cbl-b<sup>+</sup> T cells in a particular cell cycle stage out of the whole population of CD4<sup>+</sup>Cbl-b<sup>+</sup> T cells, for that particular stimulus. Some stimulated populations were normalised to 100%. **B)** CD4<sup>+</sup> T cells were gated, their DAPI max pixel Vs integral values plotted after this and cells within the different cell cycle stages checked for Cbl-b expression. Values are presented as MFI of Cbl-b of the CD4<sup>+</sup>Cbl-b<sup>+</sup> cells in a particular cell cycle stage. **C)** CD4<sup>+</sup> T cells were gated, their DAPI max pixel Vs integral values plotted after this and cells within the different cell cycle stages checked for Cbl-b expression. Values are presented as percentage of Cbl-b<sup>+</sup> cells out of the CD4<sup>+</sup> cells in a particular cell cycle stage.

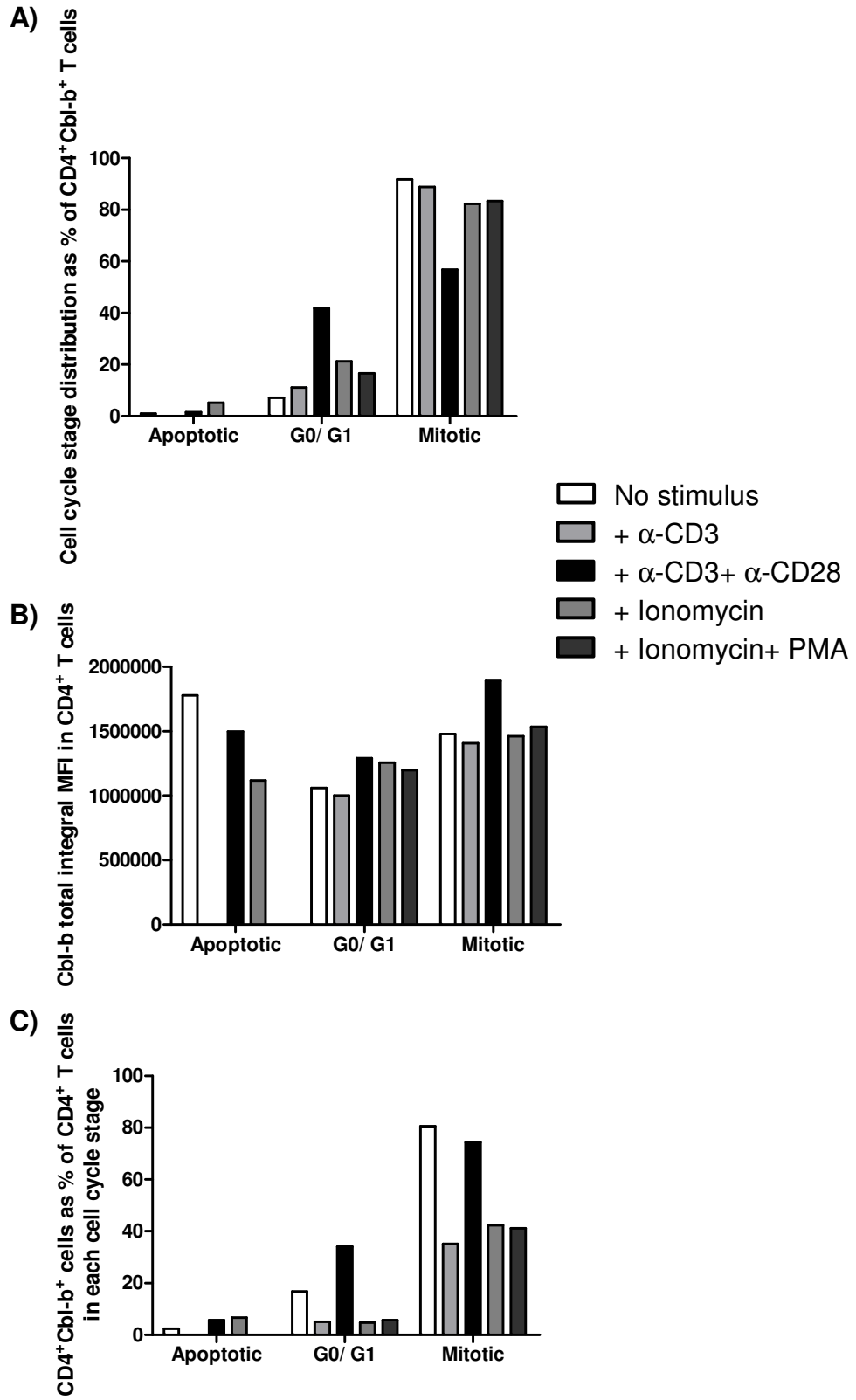


**Figure 3.24: Analysis of Cbl-b expression according to cell cycle stage in CD4<sup>+</sup> T cells after 40 h of *in vitro* stimulation.**

CD4<sup>+</sup> T cells were extracted from lymph nodes, purified, cultured *in vitro* in the presence of the indicated stimuli for 40 h, washed, cytocentrifuged, stained for nucleus, CD4 and Cbl-b (these were further labelled with adequate fluorochromes). The slides were analysed in the LSC. **A)** CD4<sup>+</sup> T cells were gated, Cbl-b<sup>+</sup> cells gated after this and their DAPI max pixel Vs integral values plotted. Values are presented as percentage of CD4<sup>+</sup>Cbl-b<sup>+</sup> T cells in a particular cell cycle stage out of the whole population of CD4<sup>+</sup>Cbl-b<sup>+</sup> T cells, for that particular stimulus. Some stimulated populations were normalised to 100%. **B)** CD4<sup>+</sup> T cells were gated, their DAPI max pixel Vs integral values plotted after this and cells within the different cell cycle stages checked for Cbl-b expression. Values are presented as MFI of Cbl-b of the CD4<sup>+</sup>Cbl-b<sup>+</sup> cells in a particular cell cycle stage. **C)** CD4<sup>+</sup> T cells were gated, their DAPI max pixel Vs integral values plotted after this and cells within the different cell cycle stages checked for Cbl-b expression. Values are presented as percentage of Cbl-b<sup>+</sup> cells out of the CD4<sup>+</sup> cells in a particular cell cycle stage.

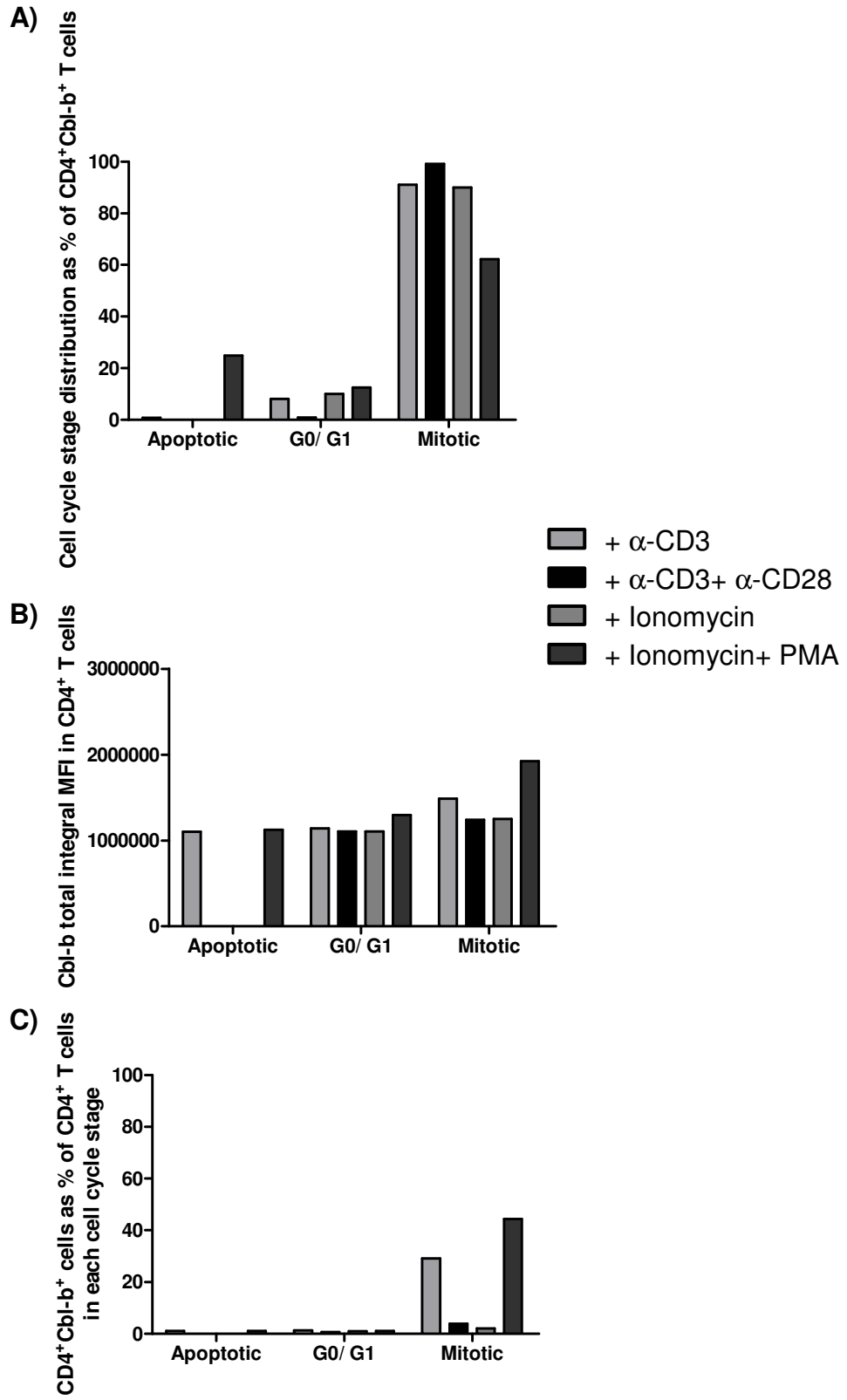


**Figure 3.25: Analysis of Itch expression according to cell cycle stage in CD4<sup>+</sup> T cells after 20 h of *in vitro* stimulation.**

CD4<sup>+</sup> T cells were extracted from lymph nodes, purified, cultured *in vitro* in the presence of the indicated stimuli for 20 h, washed, cytocentrifuged, stained for nucleus, CD4 and Itch (these were further labelled with adequate fluorochromes). The slides were analysed in the LSC. **A)** CD4<sup>+</sup> T cells were gated, Itch<sup>+</sup> cells gated after this and their DAPI max pixel Vs integral values plotted. Values are presented as percentage of CD4<sup>+</sup>Itch<sup>+</sup> T cells in a particular cell cycle stage out of the whole population of CD4<sup>+</sup>Itch<sup>+</sup> T cells, for that particular stimulus. Some stimulated populations were normalised to 100%. **B)** CD4<sup>+</sup> T cells were gated, their DAPI max pixel Vs integral values plotted after this and cells within the different cell cycle stages checked for Itch expression. Values are presented as MFI of Itch of the CD4<sup>+</sup>Itch<sup>+</sup> cells in a particular cell cycle stage. **C)** CD4<sup>+</sup> T cells were gated, their DAPI max pixel Vs integral values plotted after this and cells within the different cell cycle stages checked for Itch expression. Values are presented as percentage of Itch<sup>+</sup> cells out of the CD4<sup>+</sup> cells in a particular cell cycle stage.

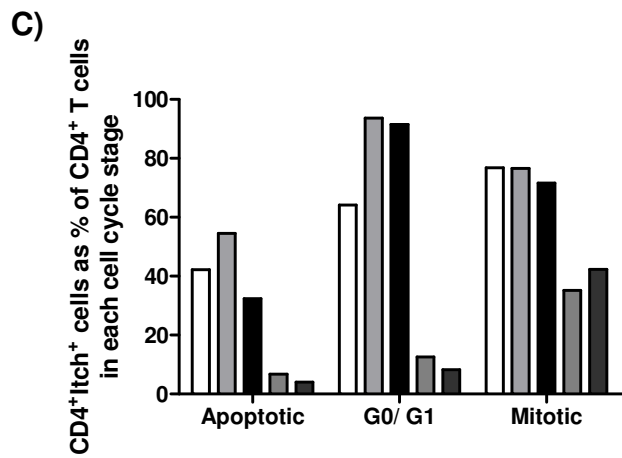
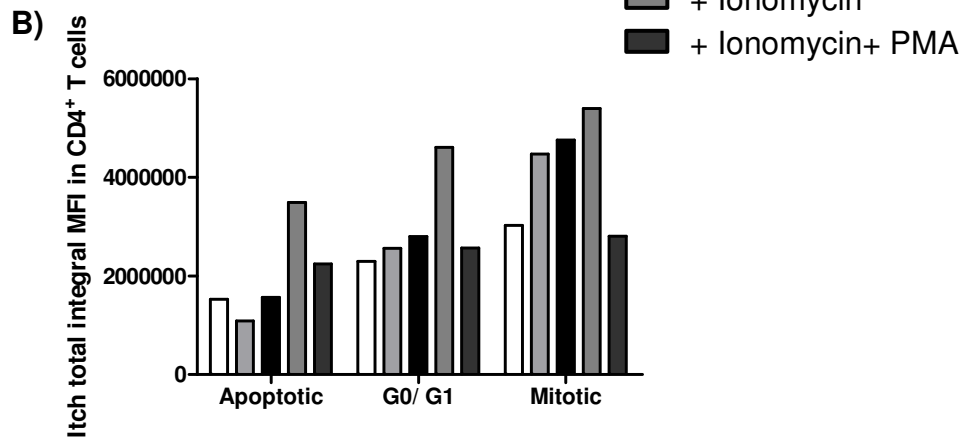
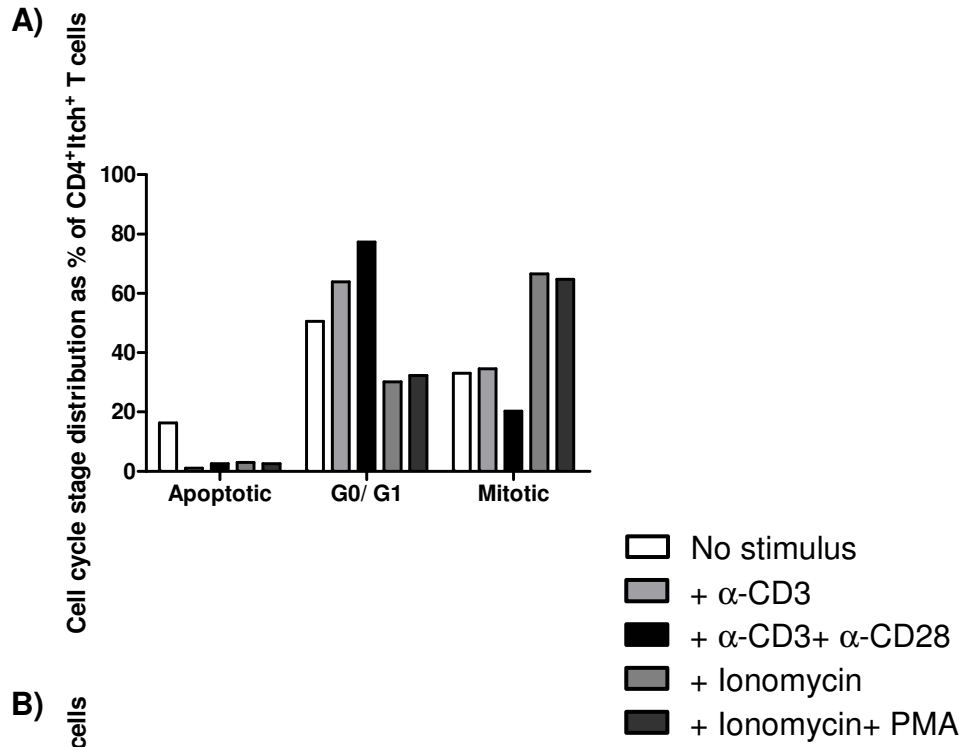
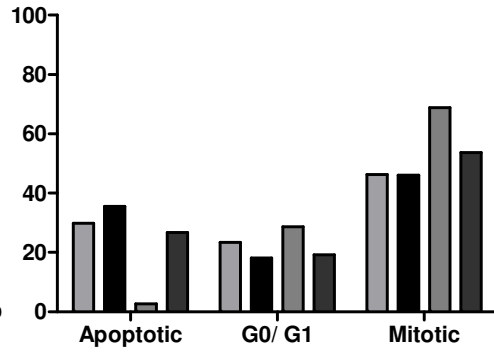


**Figure 3.26: Analysis of Itch expression according to cell cycle stage in CD4<sup>+</sup> T cells after 40 h of *in vitro* stimulation.**

CD4<sup>+</sup> T cells were extracted from lymph nodes, purified, cultured *in vitro* in the presence of the indicated stimuli for 40 h, washed, cytocentrifuged, stained for nucleus, CD4 and Itch (these were further labelled with adequate fluorochromes). The slides were analysed in the LSC. **A)** CD4<sup>+</sup> T cells were gated, Itch<sup>+</sup> cells gated after this and their DAPI max pixel Vs integral values plotted. Values are presented as percentage of CD4<sup>+</sup>Itch<sup>+</sup> T cells in a particular cell cycle stage out of the whole population of CD4<sup>+</sup>Itch<sup>+</sup> T cells, for that particular stimulus. Some stimulated populations were normalised to 100%. **B)** CD4<sup>+</sup> T cells were gated, their DAPI max pixel Vs integral values plotted after this and cells within the different cell cycle stages checked for Itch expression. Values are presented as MFI of Itch of the CD4<sup>+</sup>Itch<sup>+</sup> cells in a particular cell cycle stage. **C)** CD4<sup>+</sup> T cells were gated, their DAPI max pixel Vs integral values plotted after this and cells within the different cell cycle stages checked for Itch expression. Values are presented as percentage of Itch<sup>+</sup> cells out of the CD4<sup>+</sup> cells in a particular cell cycle stage.

A)

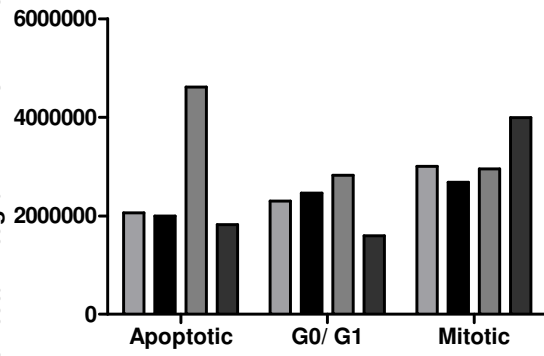
Cell cycle stage distribution as % of CD4<sup>+</sup>Itch<sup>+</sup> T cells



- +  $\alpha$ -CD3
- +  $\alpha$ -CD3+  $\alpha$ -CD28
- + Ionomycin
- + Ionomycin+ PMA

B)

Itch total integral MFI in CD4<sup>+</sup> T cells



C)

CD4<sup>+</sup>Itch<sup>+</sup> cells as % of CD4<sup>+</sup> T cells in each cell cycle stage

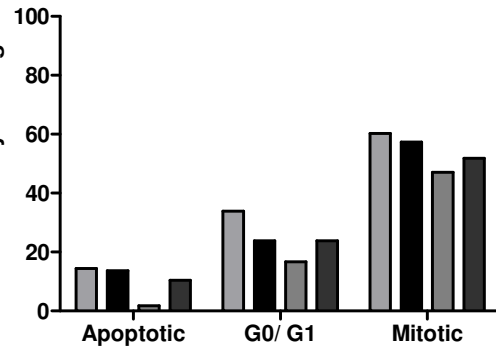


**Figure 3.27: Analysis of Grail expression according to cell cycle stage in CD4<sup>+</sup> T cells after 20 h of *in vitro* stimulation.**

CD4<sup>+</sup> T cells were extracted from lymph nodes, purified, cultured *in vitro* in the presence of the indicated stimuli for 20 h, washed, cytocentrifuged, stained for nucleus, CD4 and Grail (these were further labelled with adequate fluorochromes). The slides were analysed in the LSC. **A)** CD4<sup>+</sup> T cells were gated, Grail<sup>+</sup> cells gated after this and their DAPI max pixel Vs integral values plotted. Values are presented as percentage of CD4<sup>+</sup>Grail<sup>+</sup> T cells in a particular cell cycle stage out of the whole population of CD4<sup>+</sup>Grail<sup>+</sup> T cells, for that particular stimulus. Some stimulated populations were normalised to 100%. **B)** CD4<sup>+</sup> T cells were gated, their DAPI max pixel Vs integral values plotted after this and cells within the different cell cycle stages checked for Grail expression. Values are presented as MFI of Itch of the CD4<sup>+</sup>Grail<sup>+</sup> cells in a particular cell cycle stage. **C)** CD4<sup>+</sup> T cells were gated, their DAPI max pixel Vs integral values plotted after this and cells within the different cell cycle stages checked for Grail expression. Values are presented as percentage of Grail<sup>+</sup> cells out of the CD4<sup>+</sup> cells in a particular cell cycle stage.

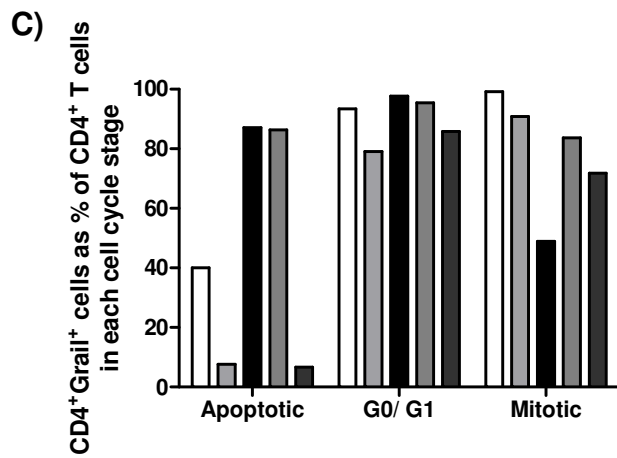
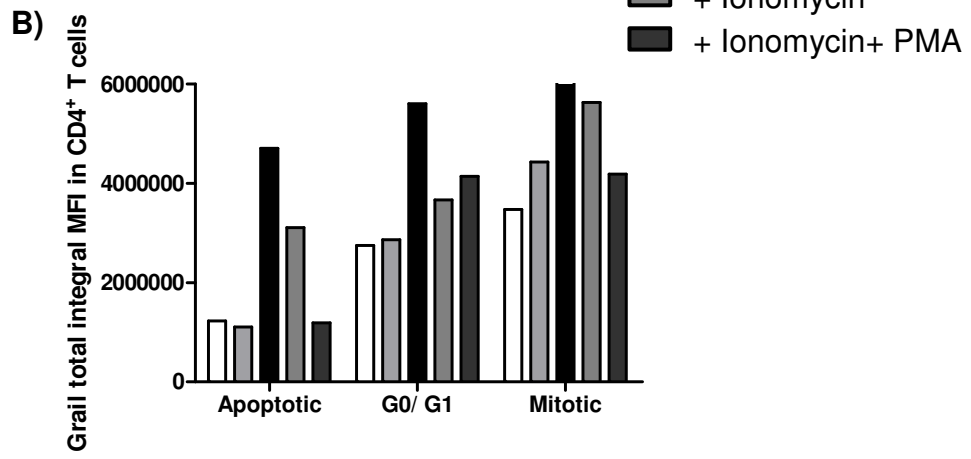
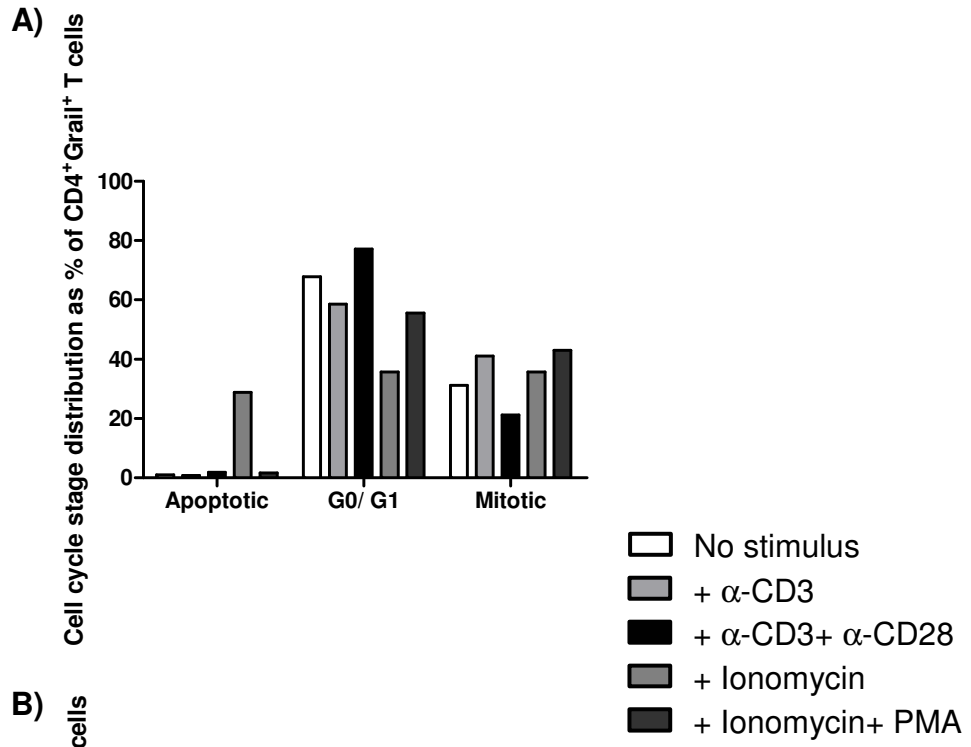


**Figure 3.28: Analysis of Grail expression according to cell cycle stage in CD4<sup>+</sup> T cells after 40 h of *in vitro* stimulation.**

CD4<sup>+</sup> T cells were extracted from lymph nodes, purified, cultured *in vitro* in the presence of the indicated stimuli for 40 h, washed, cytocentrifuged, stained for nucleus, CD4 and Grail (these were further labelled with adequate fluorochromes). The slides were analysed in the LSC. **A)** CD4<sup>+</sup> T cells were gated, Grail<sup>+</sup> cells gated after this and their DAPI max pixel Vs integral values plotted. Values are presented as percentage of CD4<sup>+</sup>Grail<sup>+</sup> T cells in a particular cell cycle stage out of the whole population of CD4<sup>+</sup>Grail<sup>+</sup> T cells, for that particular stimulus. Some stimulated populations were normalised to 100%. **B)** CD4<sup>+</sup> T cells were gated, their DAPI max pixel Vs integral values plotted after this and cells within the different cell cycle stages checked for Grail expression. Values are presented as MFI of Itch of the CD4<sup>+</sup>Grail<sup>+</sup> cells in a particular cell cycle stage. **C)** CD4<sup>+</sup> T cells were gated, their DAPI max pixel Vs integral values plotted after this and cells within the different cell cycle stages checked for Grail expression. Values are presented as percentage of Grail<sup>+</sup> cells out of the CD4<sup>+</sup> cells in a particular cell cycle stage.

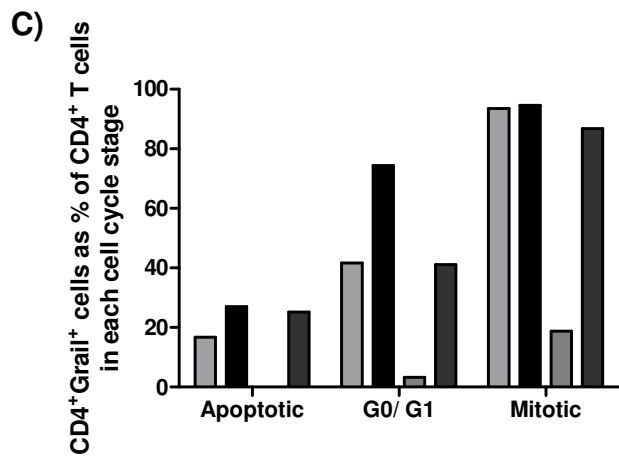
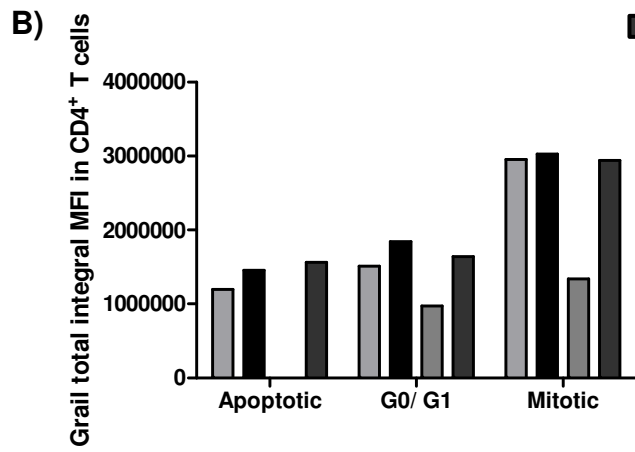
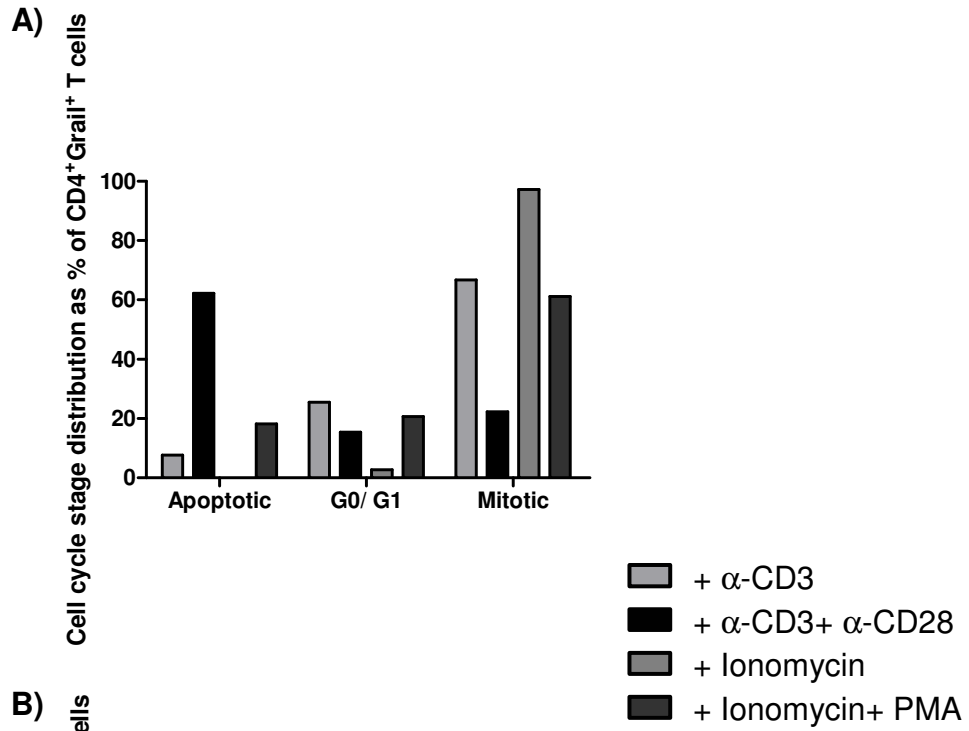


**Figure 3.29: Functional analysis of T cells from naïve, tolerised and primed mice.**

DO11.10 TCR transgenic T cells were adoptively transferred into naïve recipients 24 h prior to i.v. injection with sterile PBS (naïve), OVA<sub>323-339</sub> (tolerised) or OVA<sub>323-339</sub> + LPS (primed) (A). At D0, 3, 5 and 10 after immunisation MLNs were harvested and single cell suspensions were prepared and stained for CD4 and KJ1-26; the percentage of CD4<sup>+</sup>KJ1-26<sup>+</sup> T cells in the tissue was analysed by flow cytometry (B). At D10 after immunisation, PLNs were harvested and single cell suspensions were re-stimulated *in vitro* with or without antigen to assess proliferation (C) and IFN $\gamma$  production (D). Proliferation of CD4<sup>+</sup> T cells was measured by means of counts per minute (cpm) of [<sup>3</sup>H] thymidine incorporation in newly-synthesised DNA after 72 h of *in vitro* culture. The level of IFN $\gamma$  in culture supernatants was detected by ELISA at 48 h after re-stimulation *in vitro*. Both proliferation and IFN $\gamma$  production data are expressed as fold increase in signal from samples re-stimulated in the presence of antigen compared with the signal from those re-stimulated with media alone. Data represent mean  $\pm$  SD for three mice per group and each animal sample was performed in triplicate. Statistical significance was determined by one-way ANOVA (one way analysis of variance) followed by the Bonferroni post-test. Statistical significance was assumed when  $p \leq 0.05$ ; \* $\leq 0.05$ , \*\* $< 0.01$ .

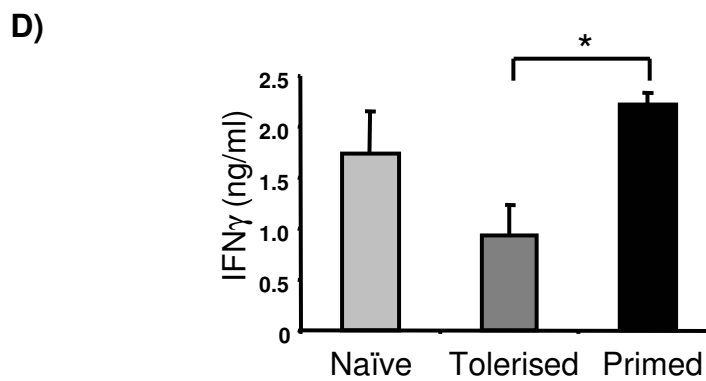
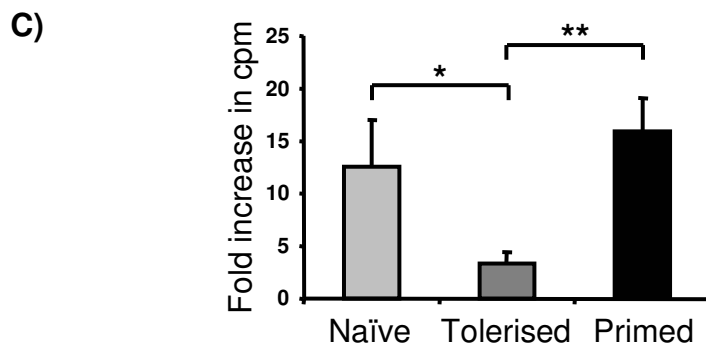
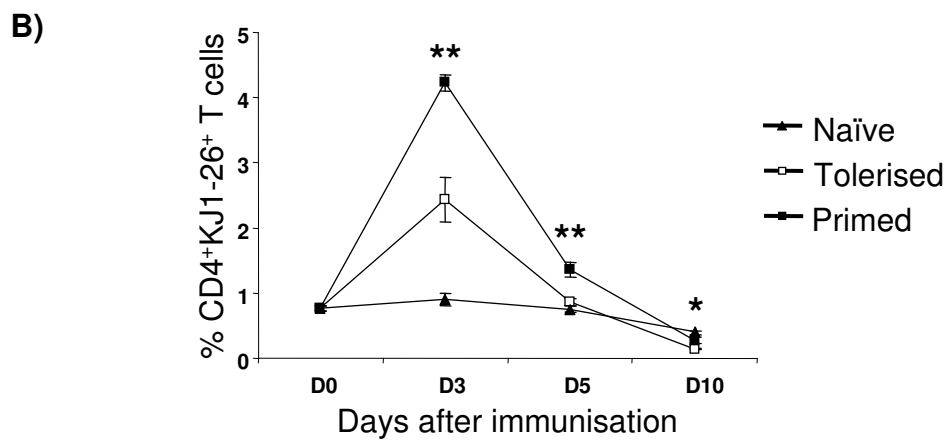
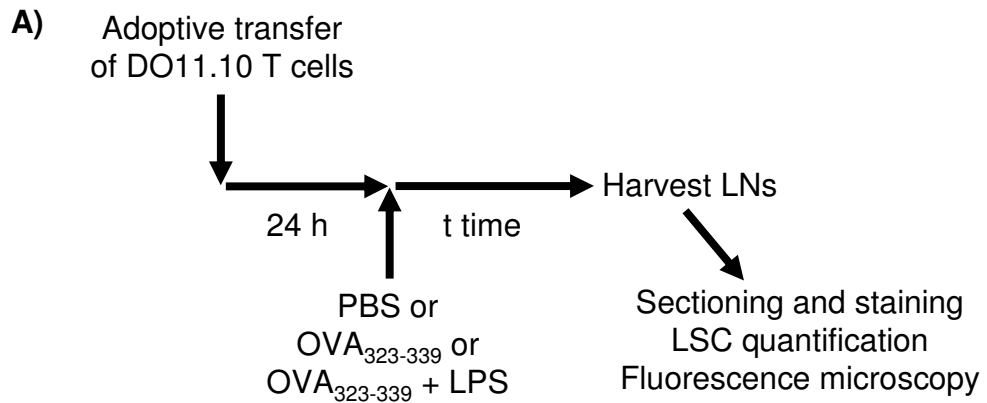
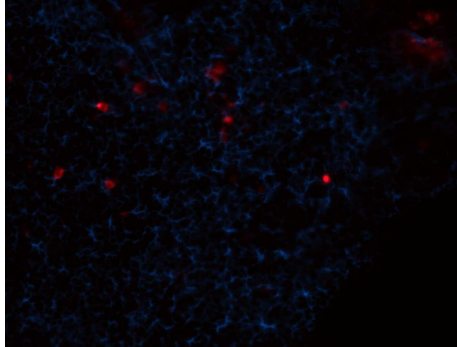


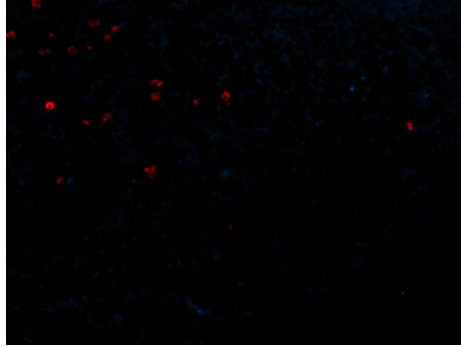
**Figure 3.30: Cbl-b expression in DO11.10 TCR transgenic T cells within the lymph node of tolerised and primed mice.**

DO11.10 TCR transgenic T cells were adoptively transferred into naïve recipients 24 h prior to i.v. injection with OVA<sub>323-339</sub> (tolerised) or OVA<sub>323-339</sub> + LPS (primed). At D5 after immunisation, PLNs were harvested and prepared for immunohistochemistry. Tissue sections were stained for DO11.10 TCR transgenic T cells (red) and Cbl-b (blue). Photographs were taken of the tolerised (**A**) and primed (**B**) tissue. Cbl-b expression in T cells was quantified with the LSC: KJ1-26<sup>+</sup> T cells were gated and the percentage of these cells expressing Cbl-b plotted (**C**); the MFI of Cbl-b in KJ1-26<sup>+</sup>Cbl-b<sup>+</sup> T cells was plotted in **D**. Data represent mean ± SEM for three mice per group. Student's unpaired t test analysis for two-tail p value was used.

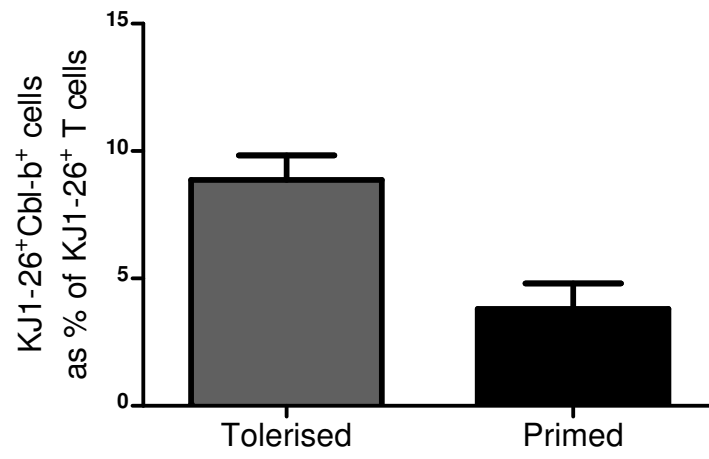
A)



B)



C)



D)

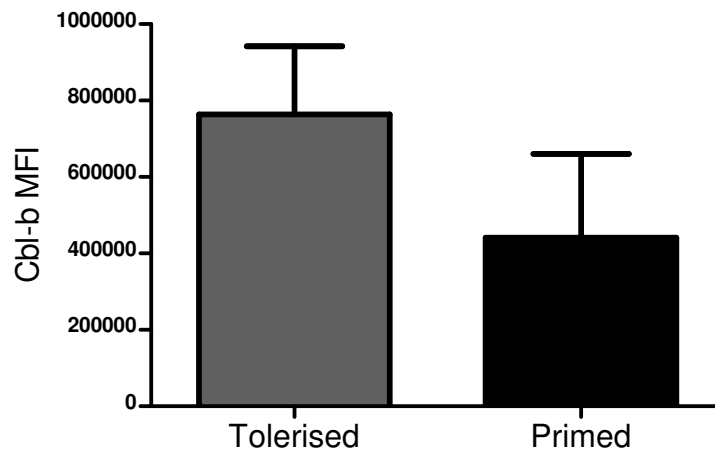
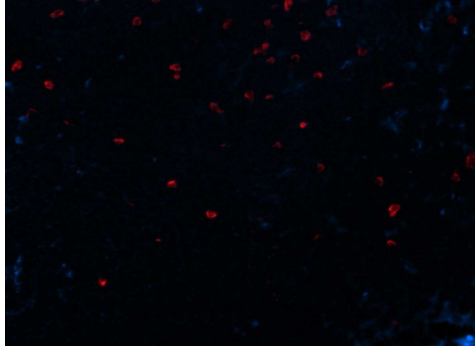


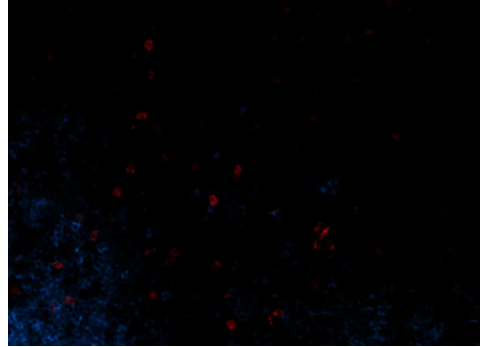
**Figure 3.31: Itch expression in DO11.10 TCR transgenic T cells within the lymph node of tolerised and primed mice.**

DO11.10 TCR transgenic T cells were adoptively transferred into naïve recipients 24 h prior to i.v. injection with OVA<sub>323-339</sub> (tolerised) or OVA<sub>323-339</sub> + LPS (primed). At D5 after immunisation, PLNs were harvested and prepared for immunohistochemistry. Tissue sections were stained for DO11.10 TCR transgenic T cells (red) and Itch (blue). Photographs were taken of the tolerised (**A**) and primed (**B**) tissue. Itch expression in T cells was quantified with the LSC: KJ1-26<sup>+</sup> T cells were gated and the percentage of these cells expressing Itch plotted (**C**); the MFI of Itch in KJ1-26<sup>+</sup>Itch<sup>+</sup> T cells was plotted in **D**. Data represent mean  $\pm$  SEM for three mice per group. Student's unpaired t test analysis for two-tail p value was used.

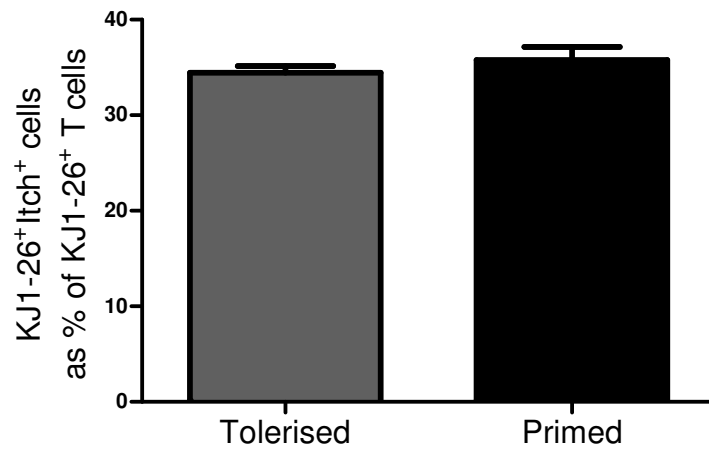
A)



B)



C)



D)

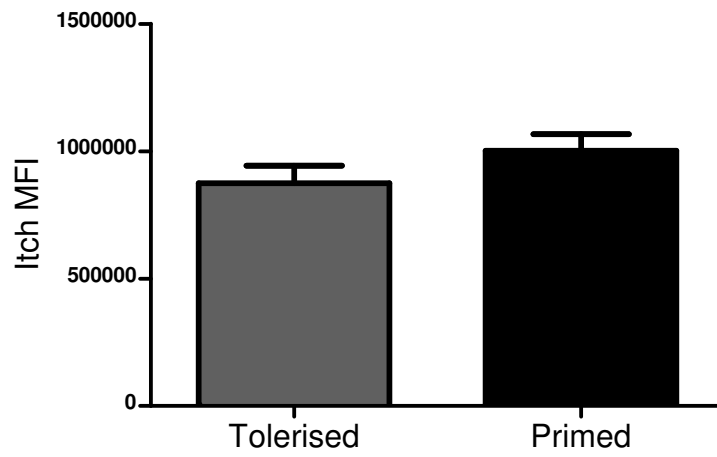


**Figure 3.32: Smurf1 expression in DO11.10 TCR transgenic T cells within the lymph node of tolerised and primed mice.**

DO11.10 TCR transgenic T cells were adoptively transferred into naïve recipients 24 h prior to i.v. injection with OVA<sub>323-339</sub> (tolerised) or OVA<sub>323-339</sub> + LPS (primed). At D5 after immunisation, PLNs were harvested and prepared for immunohistochemistry. Tissue sections were stained for DO11.10 TCR transgenic T cells (red) and Smurf1 (blue). Photographs were taken of the tolerised (**A**) and primed (**B**) tissue. Smurf1 expression in T cells was quantified with the LSC: KJ1-26<sup>+</sup> T cells were gated and the percentage of these cells expressing Smurf1 plotted (**C**); the MFI of Smurf1 in KJ1-26<sup>+</sup>Smurf1<sup>+</sup> T cells was plotted in **D**. Data represent mean ± SEM for three mice per group. Student's unpaired t test analysis for two-tail p value was used.

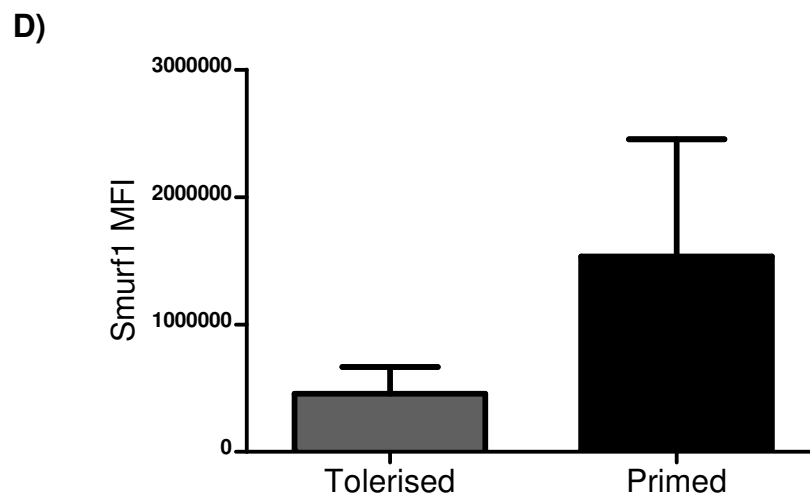
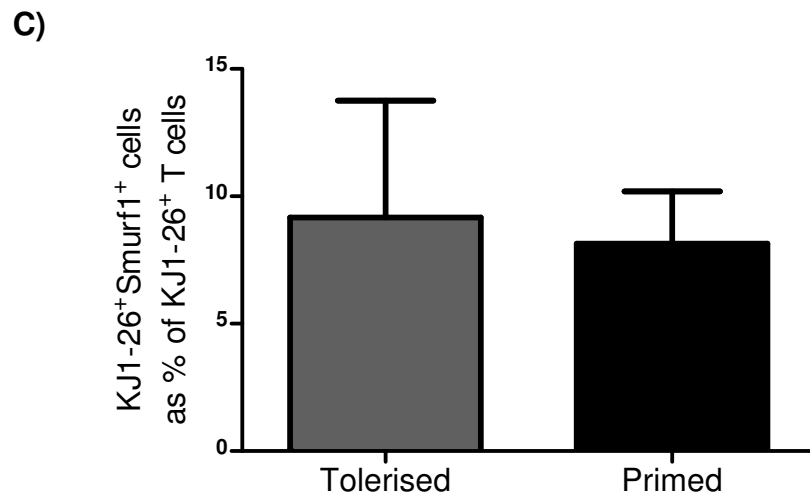
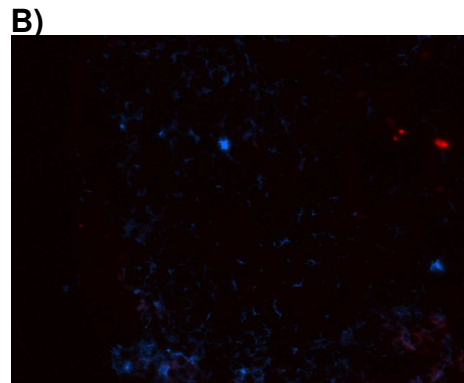
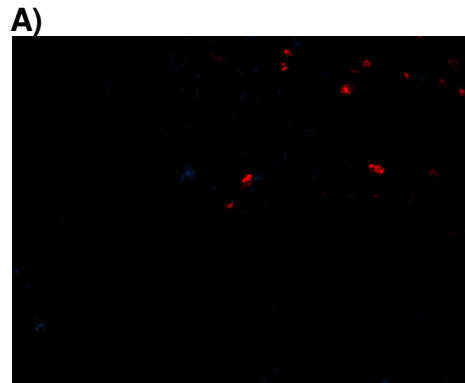
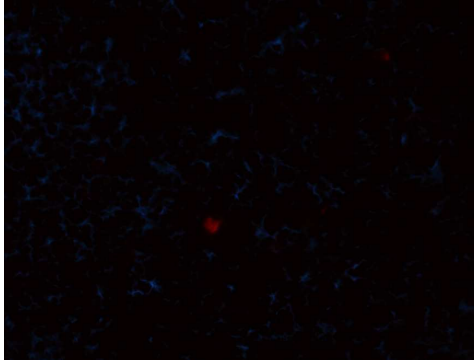


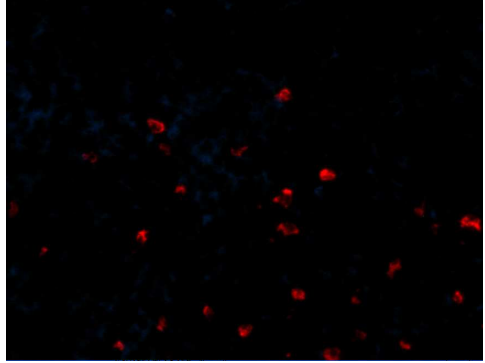
**Figure 3.33: Smurf2 expression in DO11.10 TCR transgenic T cells within the lymph node of tolerised and primed mice.**

DO11.10 TCR transgenic T cells were adoptively transferred into naïve recipients 24 h prior to i.v. injection with OVA<sub>323-339</sub> (tolerised) or OVA<sub>323-339</sub> + LPS (primed). At D5 after immunisation, PLNs were harvested and prepared for immunohistochemistry. Tissue sections were stained for DO11.10 TCR transgenic T cells (red) and Smurf2 (blue). Photographs were taken of the tolerised (**A**) and primed (**B**) tissue. Smurf2 expression in T cells was quantified with the LSC: KJ1-26<sup>+</sup> T cells were gated and the percentage of these cells expressing Smurf2 plotted (**C**); the MFI of Smurf2 in KJ1-26<sup>+</sup>Smurf2<sup>+</sup> T cells was plotted in **D**. Data represent mean ± SEM for three mice per group. Student's unpaired t test analysis for two-tail p value was used.

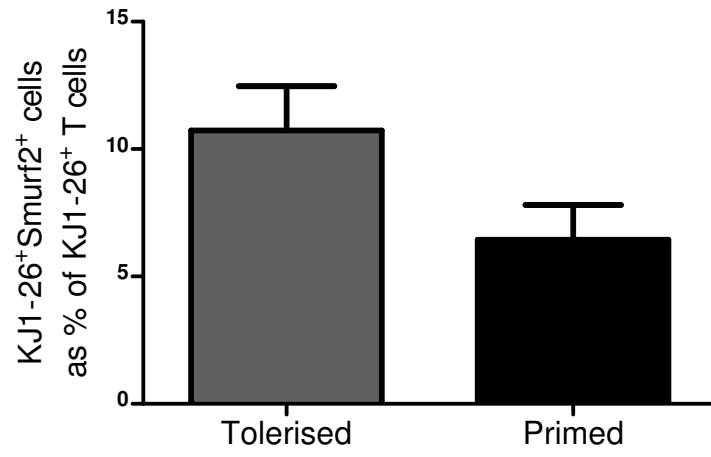
A)



B)



C)



D)

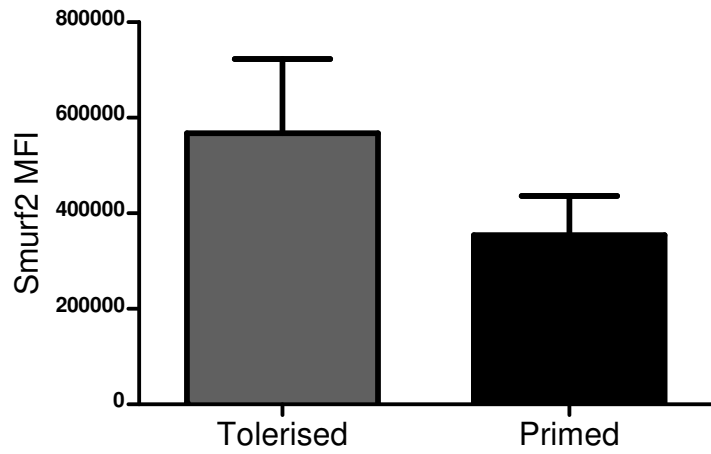


**Figure 3.34: Setting up antigen-specific T cells for anergy and priming analysis in the maintenance phase.**

DO11.10 T cells were extracted from lymph nodes and cultured *in vitro* in the presence of immobilised anti-CD3 antibody or immobilised anti-CD3 antibody and anti-CD28 antibody to induce anergy or priming, respectively. Excess antibody was washed off and the cells re-plated and rested for an additional 2 d in fresh medium. Naïve (freshly isolated), anergised and primed DO11.10 T cells were (re-)stimulated with LPS-matured DCs which had been pulsed with or without OVA<sub>323-339</sub> for the indicated time.

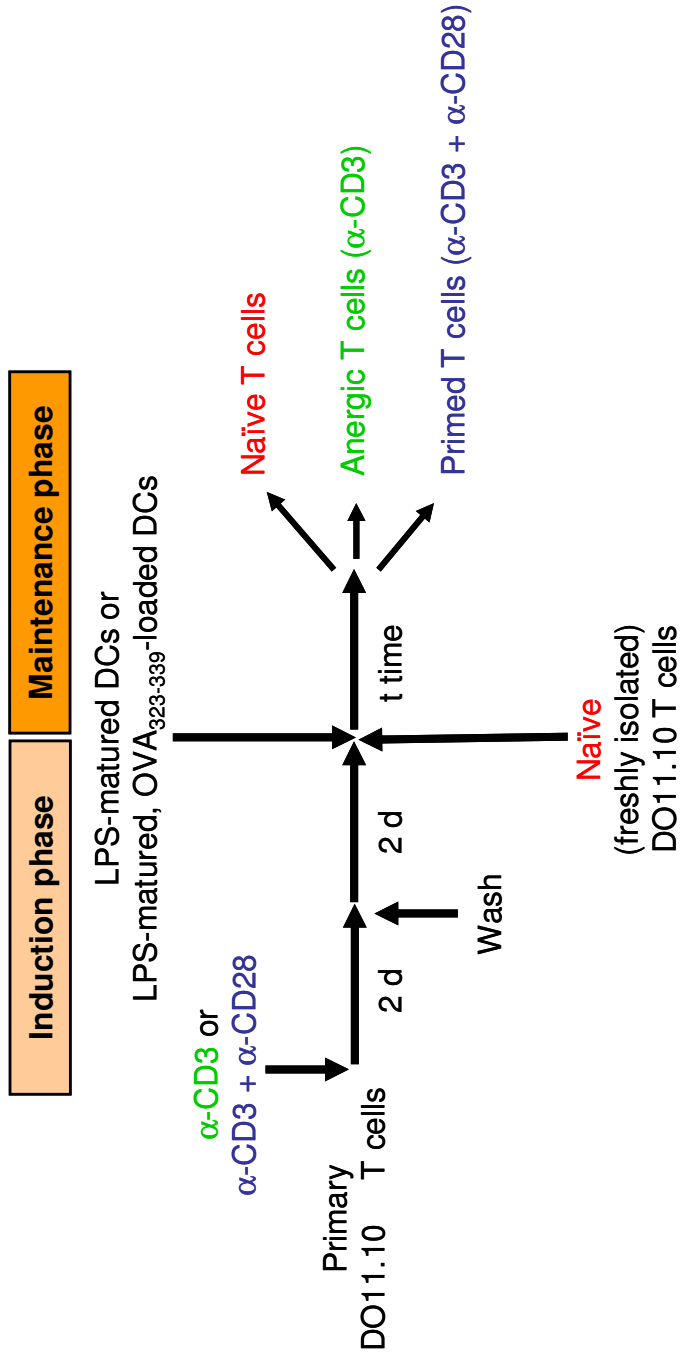


**Figure 3.35: Functional analysis of DO11.10 T cells in the maintenance phase of anergy and priming.**

T cells were tested for functional hallmarks such as IL-2 expression (**A** and **B**) and proliferation (**C** and **D**) at 20 and 48 h, respectively. DO11.10 T cells were anergised or primed *in vitro* via TCR activation by antibodies and subsequently re-stimulated with DCs to call the maintenance phase of either anergy or priming. **A)** Cells were washed and stained for CD4, DO11.10 TCR and IL-2; the percentage of CD4<sup>+</sup>KJ1-26<sup>+</sup> T cells expressing IL-2 was measured via flow cytometry in all populations of T cells and plotted as fold increase of the percentage of naïve CD4<sup>+</sup>KJ1-26<sup>+</sup> T co-cultured with LPS-matured DCs (the percentage of naïve CD4<sup>+</sup>KJ1-26<sup>+</sup> T expressing IL-2 was taken as basal and assigned the “1” value); results shown are representative of two independent experiments. **B)** Levels of IL-2 production were measured in the cultures’ supernatants by ELISA; the results shown are the mean ± SD of triplicate cultures and are representative of three independent experiments. **C and D)** Proliferation of DO11.10 T cells was measured by means of counts per minute (cpm) of [<sup>3</sup>H]thymidine incorporation in newly-synthesised DNA; the results shown are the mean ± SD of triplicate cultures and are representative of three independent experiments.

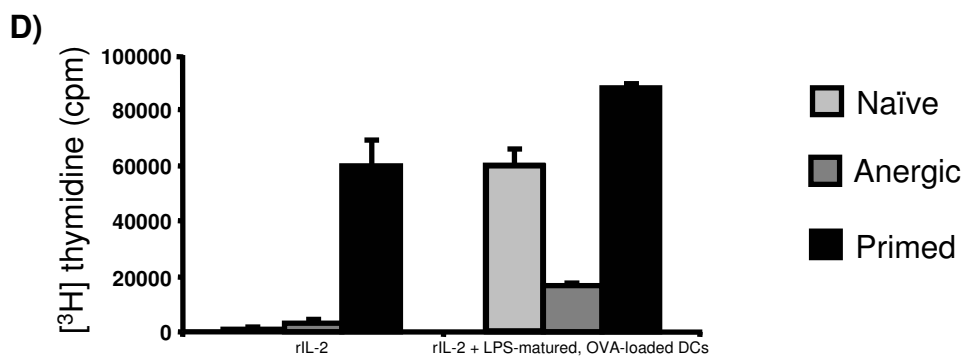
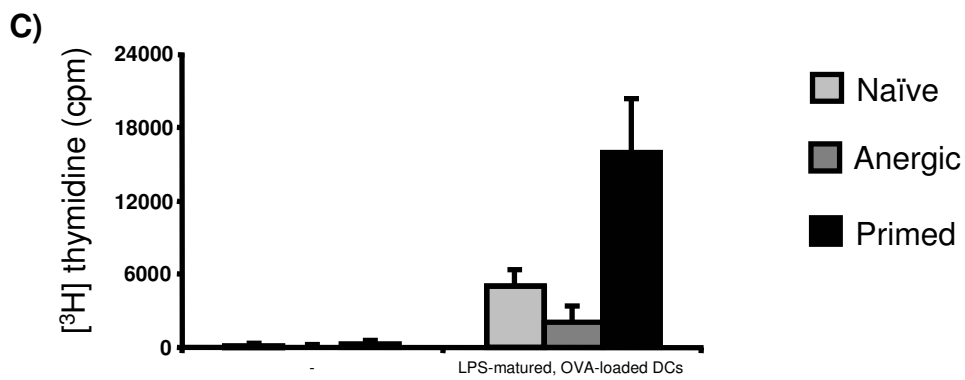
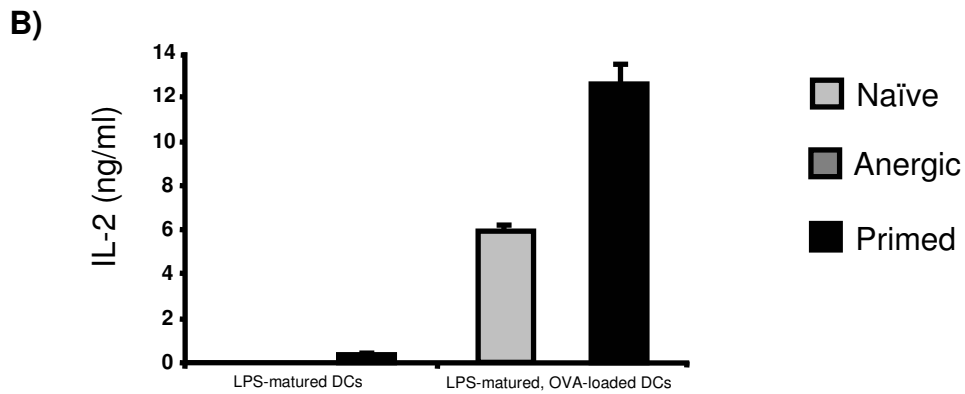
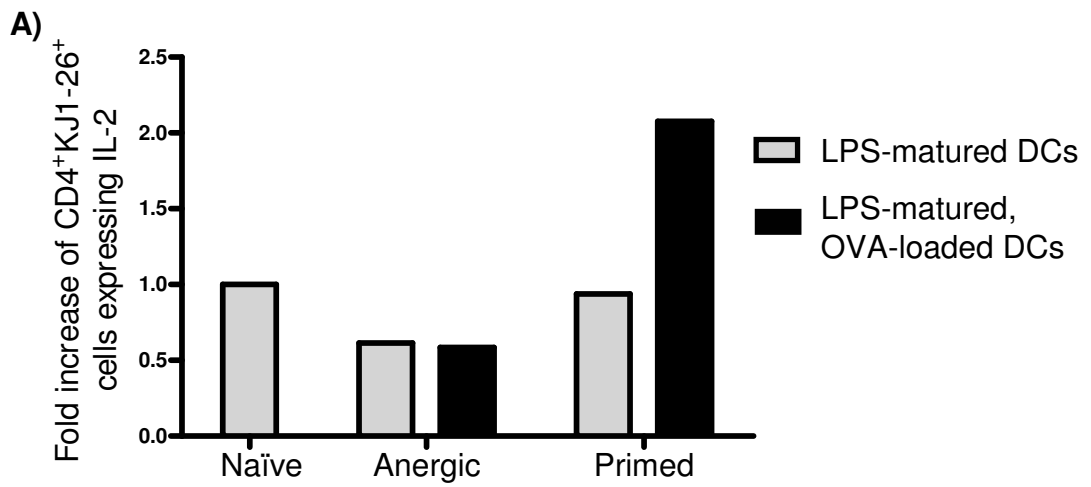


**Figure 3.36: Setting up DO11.10 TCR transgenic, antigen-specific T cells in the maintenance phases of anergy and priming for Western blotting analysis.**

Lymph nodes were extracted from DO11.10 mice on a BALB/c background and mashed up. The resulting cells were cultured *in vitro* with anti-CD3 antibody (2), or anti-CD3 and anti-CD28 antibodies (3) for 2 d. Excess antibody was washed off and the cells re-plated and rested for an additional 2 d in fresh medium. A set of naïve (1) (freshly isolated), anergic (2) and primed (3) T cells were co-cultured in fresh medium with LPS-matured DCs which had been pulsed with OVA<sub>323-339</sub>; the other set of T cell populations received only fresh medium. After 20 h, cells were harvested and lysed. Total protein extracts were separated by SDS-PAGE and transferred onto a nitrocellulose membrane. The membrane was analysed by Western blotting for proteins of interest.

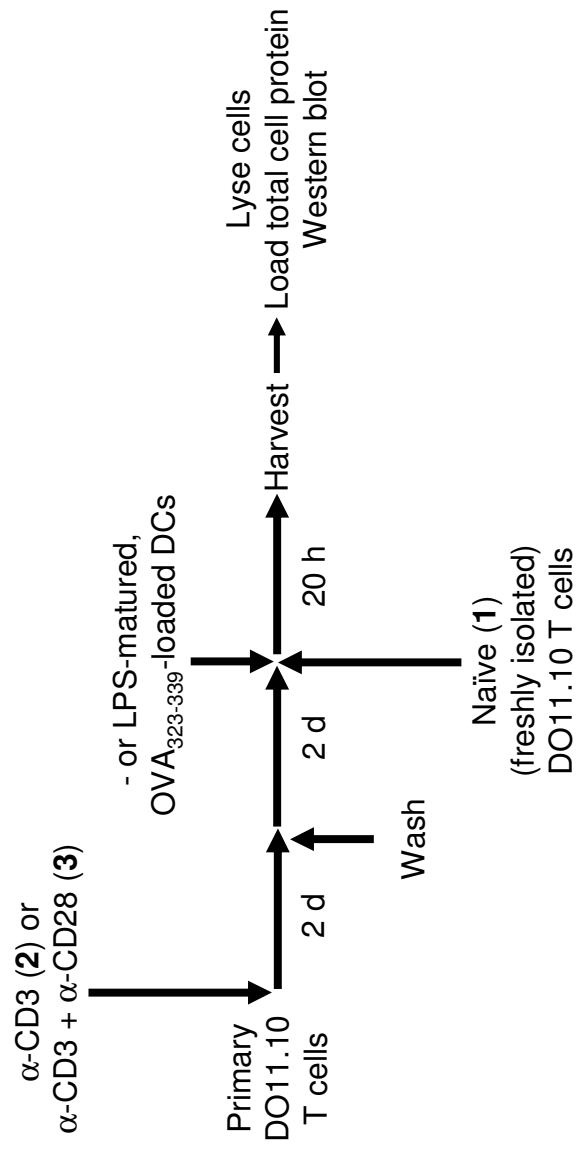


**Figure 3.37: Expression of E3 ubiquitin-protein ligases in the maintenance phase of anergic and primed T cells.**

Lymph nodes were extracted from DO11.10 mice on a BALB/c background and mashed up. The resulting cells were cultured *in vitro* with anti-CD3 antibody (2), or anti-CD3 and anti-CD28 antibodies (3) for 2 d. Excess antibody was washed off and the cells re-plated and rested for an additional 2 d in fresh medium. A set of naïve (1) (freshly isolated), anergic (2) and primed (3) T cells were co-cultured in fresh medium with LPS-matured DCs which had been pulsed with OVA<sub>323-339</sub>; the other set of T cell populations received only fresh medium. After 20 h, cells were harvested and lysed. Total protein extracts were separated by SDS-PAGE and transferred onto a nitrocellulose membrane. The membrane was analysed by Western blotting for proteins of interest: it was blocked in 5% milk/ TBS-T for 1 h, washed 3 x 10 min with TBS-T, probed with primary antibody overnight in the cold room, washed 3 x 5 min with TBS-T, incubated with HRP-linked secondary antibody for 1 h, washed 3 x 5 min with TBS-T, incubated with ECL solution for 1 m, and developed. The membrane was then stripped and subsequently re-probed again, originating the profile observed. Total Erk was used as loading control (LC).

+ LPS-matured,  
OVA<sub>323-339</sub>-loaded DCs

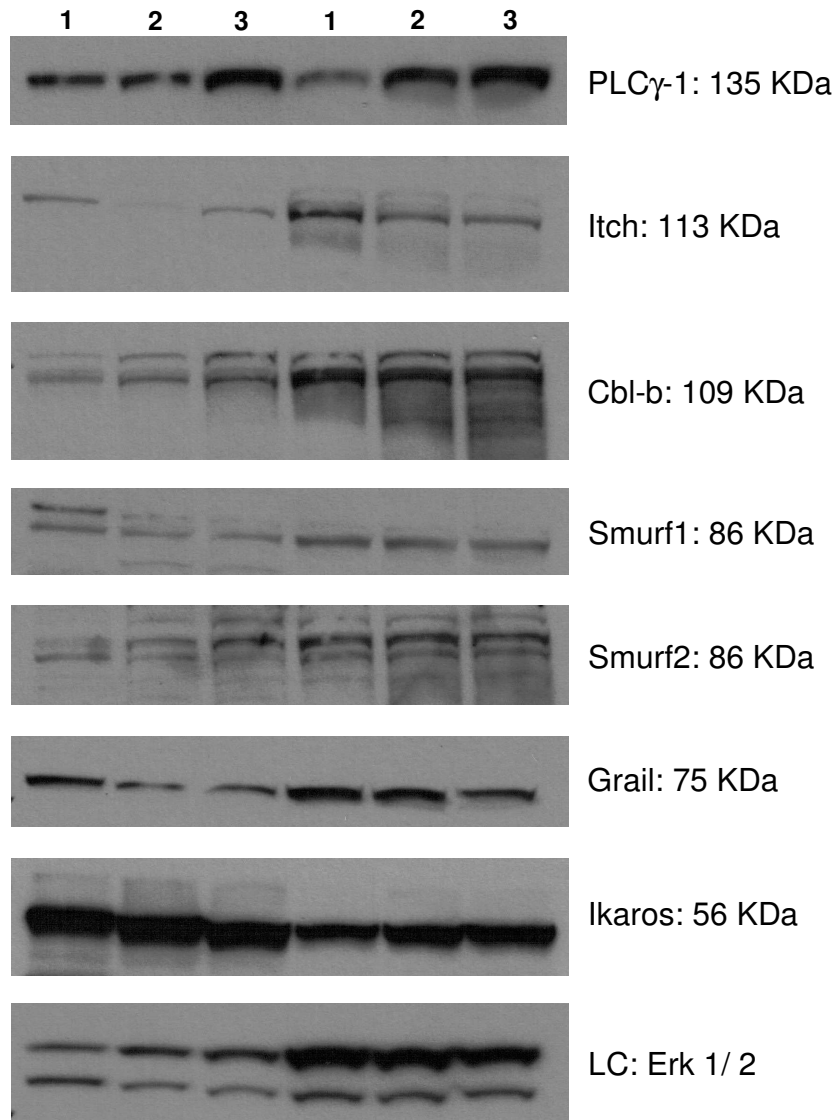


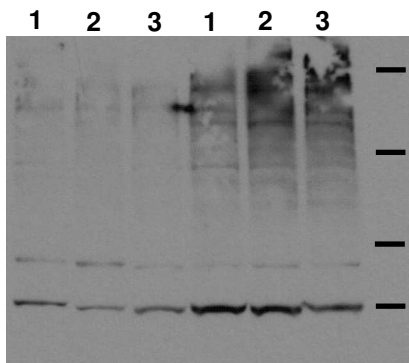
**Figure 3.38: Ubiquitination of proteins in the maintenance phase of anergic and primed T cells.**

Lymph nodes were extracted from DO11.10 mice on a BALB/c background and mashed up. The resulting cells were cultured *in vitro* with anti-CD3 antibody (2), or anti-CD3 and anti-CD28 antibodies (3) for 2 d. Excess antibody was washed off and the cells re-plated and rested for an additional 2 d in fresh medium. A set of naïve (1) (freshly isolated), anergic (2) and primed (3) T cells were co-cultured in fresh medium with LPS-matured DCs which had been pulsed with OVA<sub>323-339</sub>; the other set of T cell populations received only fresh medium. After 20 h, cells were harvested and lysed. Total protein extracts were separated by SDS-PAGE and transferred onto a nitrocellulose membrane. The membrane was analysed by Western blotting for all ubiquitinated conjugates and free ubiquitin (A): it was blocked in 5% milk/ TBS-T for 1 h, washed 3 x 10 min with TBS-T, probed with primary antibody overnight in the cold room, washed 3 x 5 min with TBS-T, incubated with HRP-linked secondary antibody for 1 h, washed 3 x 5 min with TBS-T, incubated with ECL solution for 1 m, and developed. The membrane was then stripped and subsequently re-probed again for mono- and poly-ubiquitinated conjugates (B) and K63-linked poly-ubiquitinated conjugates (C). The loading control can be observed in **Figure 3.39**.

**A)**

All ubiquitinated  
conjugates and free  
ubiquitin

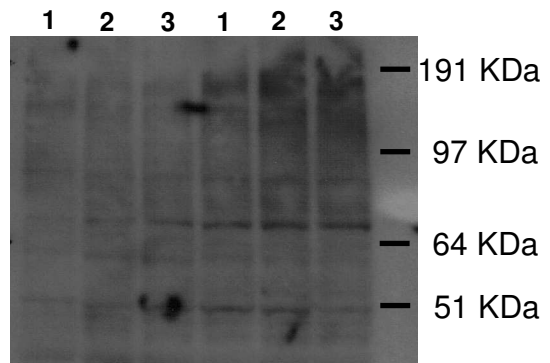
+ LPS-matured,  
OVA<sub>323-339</sub>-loaded DCs



**B)**

Mono- and  
polyubiquitinated  
conjugates

+ LPS-matured,  
OVA<sub>323-339</sub>-loaded DCs



**C)**

K63-linked polyubiquitinated  
conjugates

+ LPS-matured,  
OVA<sub>323-339</sub>-loaded DCs

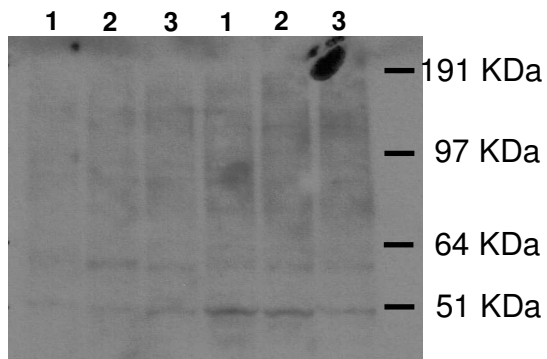


**Figure 3.39: Setting up DO11.10 TCR transgenic, antigen-specific T cells in the maintenance phases of anergy and priming for Western blotting analysis.**

Lymph nodes were extracted from DO11.10 mice on a BALB/c background and mashed up. The resulting cells were cultured *in vitro* with ionomycin (A), anti-CD3 antibody (B), or anti-CD3 and anti-CD28 antibodies (C) for 2 d. Cells were washed, replated and rested for an additional 2 d in fresh medium. Anergic (A and B) and primed (C) T cells were co-cultured in fresh medium with LPS-matured DCs which had been pulsed with OVA<sub>323-339</sub>. After 20 h, cells were harvested and DO11.10 TCR T cells indirectly magnetically labelled with the use of the KJ1-26 antibody. Both the positive fraction (KJ1-26<sup>+</sup> T cells) (+) and the negative fraction (non-KJ1-26<sup>+</sup> cells) (-) were collected and lysed. Total protein extracts were separated by SDS-PAGE and transferred onto a nitrocellulose membrane. The membrane was analysed by Western blotting for proteins of interest.



**Figure 3.40: Expression of E3 ubiquitin-protein ligases in the maintenance phase of anergic and primed DO11.10 TCR transgenic, antigen-specific T cells.**

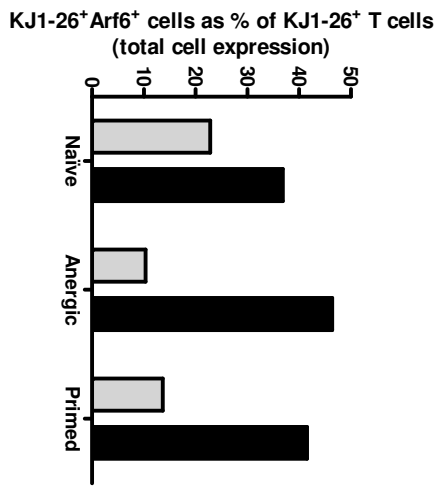
Lymph nodes were extracted from DO11.10 mice on a BALB/c background and mashed up. The resulting cells were cultured *in vitro* with ionomycin (A), anti-CD3 antibody (B), or anti-CD3 and anti-CD28 antibodies (C) for 2 d. Cells were washed, replated and rested for an additional 2 d in fresh medium. Anergic (A and B) and primed (C) T cells were co-cultured in fresh medium with LPS-matured DCs which had been pulsed with OVA<sub>323-339</sub>. After 20 h, cells were harvested and DO11.10 TCR T cells indirectly magnetically labelled with the use of the KJ1-26 antibody. Both the positive fraction (KJ1-26<sup>+</sup> T cells) (+) and the negative fraction (non-KJ1-26<sup>+</sup> cells) (-) were collected and lysed. Total protein extracts were separated by SDS-PAGE and transferred onto a nitrocellulose membrane. The membrane was analysed by Western blotting for proteins of interest: it was blocked in 5% milk/ TBS-T for 1 h, washed 3 x 10 min with TBS-T, probed with primary antibody overnight in the cold room, washed 3 x 5 min with TBS-T, incubated with HRP-linked secondary antibody for 1 h, washed 3 x 5 min with TBS-T, incubated with ECL solution for 1 m, and developed. The membrane was then stripped and subsequently re-probed again, originating the profile observed. Total Erk was used as loading control (LC).



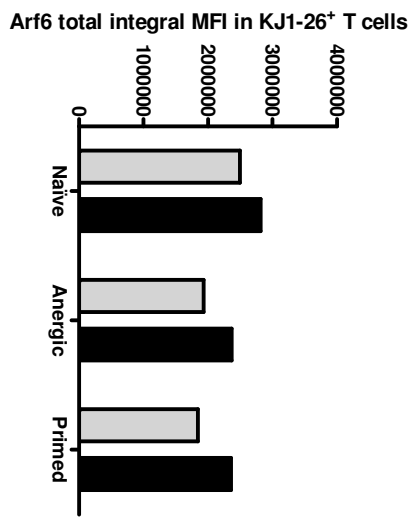
**Figure 3.41: Quantification of Arf6 expression in KJ1-26<sup>+</sup> T cells after 20 h of *in vitro* re-stimulation.**

DO11.10 T cells were extracted from lymph nodes and cultured *in vitro* in the presence of anti-CD3 or anti-CD3 and anti-CD28 antibodies to induce anergy or priming, respectively. Excess antibody was washed off and the cells re-plated and rested for an additional 2 d in fresh medium. Naïve (freshly isolated), anergised and primed DO11.10 T cells were (re-)stimulated with LPS-matured DCs which had been pulsed with or without OVA<sub>323-339</sub>. Cells were harvested, washed, cytocentrifuged, stained for nuclear DNA (DAPI), DO11.10 TCR and Arf6 and Arf6 expression in KJ1-26<sup>+</sup> T cells quantified with the LSC as described in the Materials and Methods chapter. Firstly, all events were sorted on their nuclear staining (“cells”) and from these KJ1-26<sup>+</sup> T cells were gated. **A)** shows the percentage of KJ1-26<sup>+</sup> T cells that are positive for Arf6 out of the whole population of KJ1-26<sup>+</sup> T cells, in terms of total cell expression. **B)** shows the mean fluorescence intensity (MFI) of Arf6 expression in those KJ1-26<sup>+</sup> T cells that are also positive for Arf6 in terms of total cell expression. **C)** shows the percentage of KJ1-26<sup>+</sup> T cells that are positive for Arf6 out of the whole population of KJ1-26<sup>+</sup> T cells, in terms of peripheral cell expression. **D)** shows MFI of Arf6 expression in those KJ1-26<sup>+</sup> T cells that are also positive for Arf6 in terms of peripheral cell expression. The results shown are representative of two independent experiments.

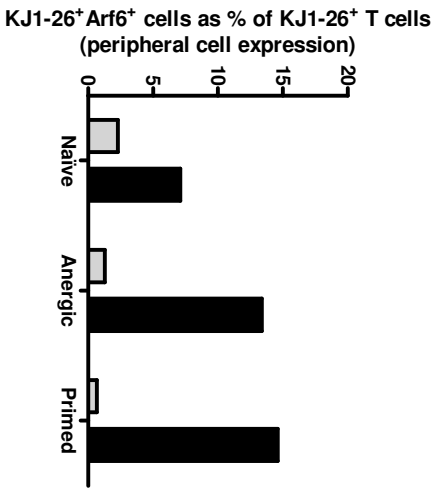
A)



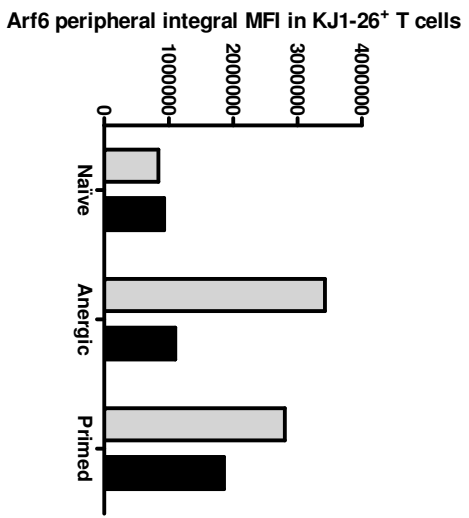
B)



C)



D)

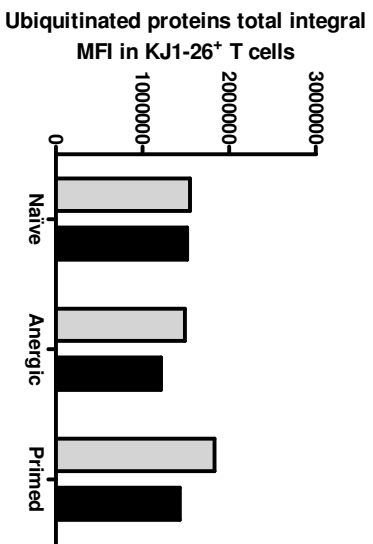


Re-stimulation with:  
□ LPS-matured DCs  
■ LPS-matured, OVA-loaded DCs

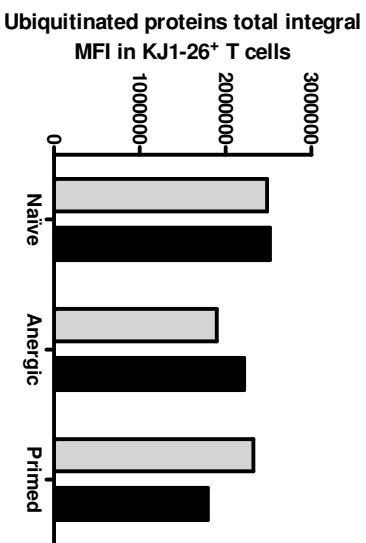
**Figure 3.42: Quantification of the ubiquitination of proteins in KJ1-26<sup>+</sup> T cells after *in vitro* re-stimulation.**

DO11.10 T cells were extracted from lymph nodes and cultured *in vitro* in the presence of anti-CD3 or anti-CD3 and anti-CD28 antibodies to induce anergy or priming, respectively. Excess antibody was washed off and the cells re-plated and rested for an additional 2 d in fresh medium. Naïve (freshly isolated), anergised and primed DO11.10 T cells were (re-)stimulated with LPS-matured DCs which had been pulsed with or without OVA<sub>323-339</sub>. Cells were harvested, washed, cytocentrifuged, stained for nuclear DNA (DAPI), DO11.10 TCR and ubiquitin and the levels of protein ubiquitination in KJ1-26<sup>+</sup> T cells quantified with the LSC as described in the Materials and Methods chapter. Firstly, all events were sorted on their nuclear staining (“cells”) and from these KJ1-26<sup>+</sup> T cells were gated. **A)** shows the mean fluorescence intensity (MFI) of ubiquitinated proteins in the whole KJ1-26<sup>+</sup> T cells after 1 h of co-culture with DCs. **B)** shows the MFI of ubiquitinated proteins in the whole KJ1-26<sup>+</sup> T cells after 20 h of co-culture with DCs. **C)** shows the MFI of ubiquitinated proteins in the periphery of KJ1-26<sup>+</sup> T cells after 1 h of co-culture with DCs. **D)** shows the MFI of ubiquitinated proteins in the periphery of KJ1-26<sup>+</sup> T cells after 20 h of co-culture with DCs. The results shown are representative of three independent experiments.

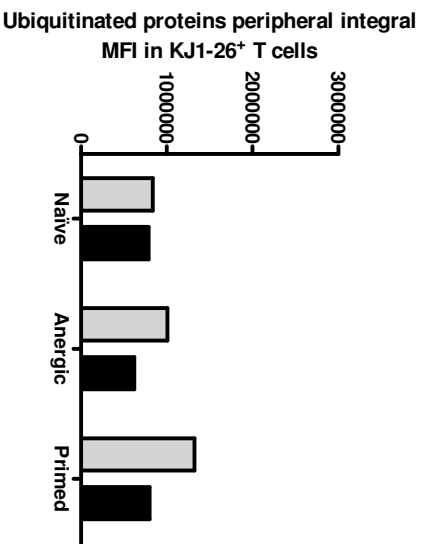
A)



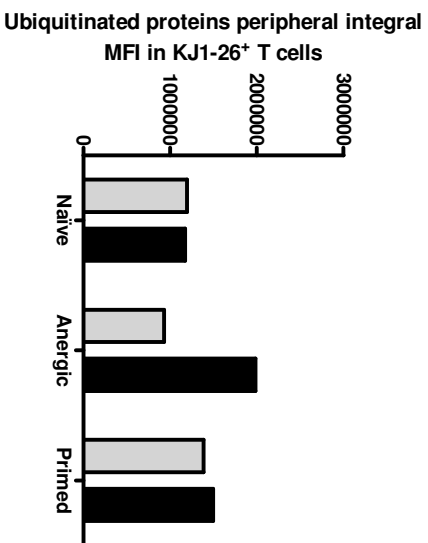
B)



C)



D)



Re-stimulation with:

- LPS-matured DCs
- LPS-matured, OVA-loaded DCs

**Figure 3.43: Visualisation of ubiquitinated proteins in KJ1-26<sup>+</sup> T cells after 20 h of *in vitro* re-stimulation.**

DO11.10 T cells were extracted from lymph nodes and cultured *in vitro* in the presence of anti-CD3 or anti-CD3 and anti-CD28 antibodies to induce anergy or priming, respectively. Excess antibody was washed off and the cells re-plated and rested for an additional 2 d in fresh medium. Naïve (freshly isolated), anergised and primed DO11.10 T cells were (re-)stimulated with LPS-matured DCs which had been pulsed with or without OVA<sub>323-339</sub> for 20 h. Cells were harvested, washed, cytocentrifuged, stained for nuclear DNA (DAPI; blue), DO11.10 TCR (red) and ubiquitin (green). Fluorescence was visualised using an Olympus BX50 fluorescent microscope and images captured and merged (x40 objectives). Cells were identified by nuclear staining with the DNA dye DAPI (blue). The ubiquitination of proteins was determined with an  $\alpha$ -ubiquitin-specific antibody coupled to tyramide amplification and the fluorochrome Alexa Fluor 488 (AF488 - green). Staining of the DO11.10 TCR (also by means of an  $\alpha$ -DO11.10-specific antibody [KJ1-26] coupled to tyramide amplification and the fluorochrome Alexa Fluor 647 [AF647 – red]) allowed locating the cell plasma membrane. Merging these three images results in the far right image – “Merge”.

**Naïve T cells co-cultured with:**

LPS-matured,  
OVA<sub>323-339</sub>-loaded DCs

LPS-matured DCs

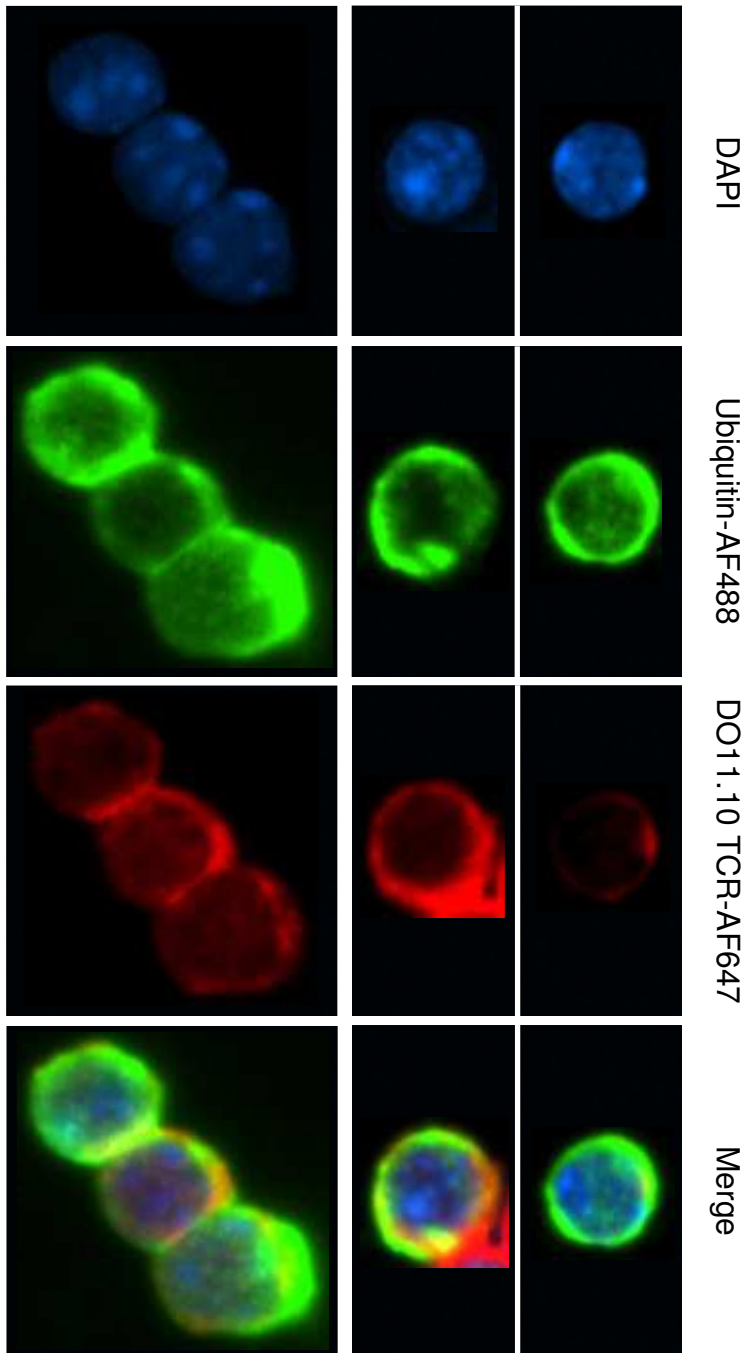
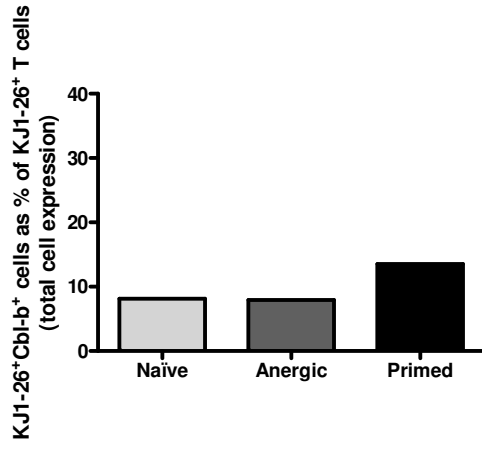


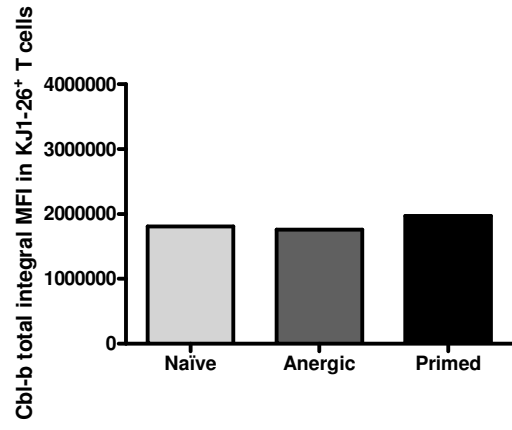
**Figure 3.44: Quantification of Cbl-b expression in KJ1-26<sup>+</sup> T cells after 1 h of *in vitro* re-stimulation.**

DO11.10 T cells were extracted from lymph nodes and cultured *in vitro* in the presence of anti-CD3 or anti-CD3 and anti-CD28 antibodies to induce anergy or priming, respectively. Excess antibody was washed off and the cells re-plated and rested for an additional 2 d in fresh medium. Naïve (freshly isolated), anergised and primed DO11.10 T cells were (re-)stimulated with LPS-matured DCs pulsed with OVA<sub>323-339</sub> for 1 h. Cells were harvested, washed, cytocentrifuged, stained for nuclear DNA (DAPI), DO11.10 TCR and Cbl-b and Cbl-b expression in KJ1-26<sup>+</sup> T cells quantified with the LSC as described in the Materials and Methods chapter. Firstly, all events were sorted on their nuclear staining (“cells”) and from these KJ1-26<sup>+</sup> T cells were gated. **A)** shows the percentage of KJ1-26<sup>+</sup> T cells that are positive for Cbl-b out of the whole population of KJ1-26<sup>+</sup> T cells, in terms of total cell expression. **B)** shows the mean fluorescence intensity (MFI) of Cbl-b expression in those KJ1-26<sup>+</sup> T cells that are also positive for Cbl-b in terms of total cell expression. **C)** shows the percentage of KJ1-26<sup>+</sup> T cells that are positive for Cbl-b out of the whole population of KJ1-26<sup>+</sup> T cells, in terms of peripheral cell expression. **D)** shows MFI of Cbl-b expression in those KJ1-26<sup>+</sup> T cells that are also positive for Cbl-b in terms of peripheral cell expression. The results shown are representative of three independent experiments.

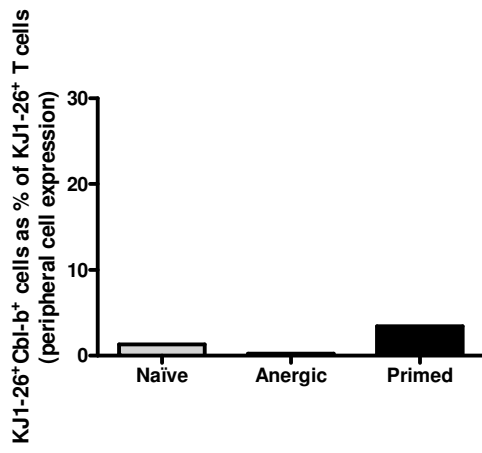
**A)**



**B)**



**C)**



**D)**

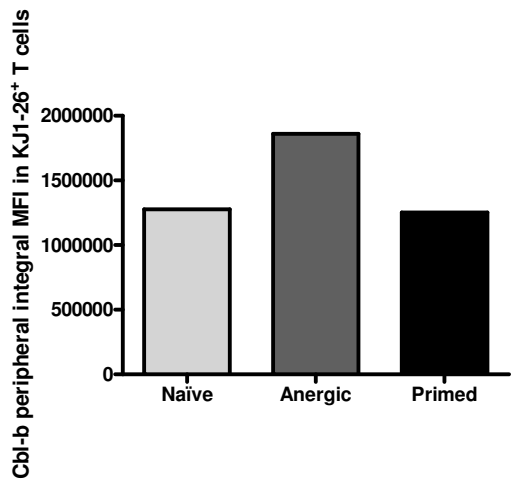
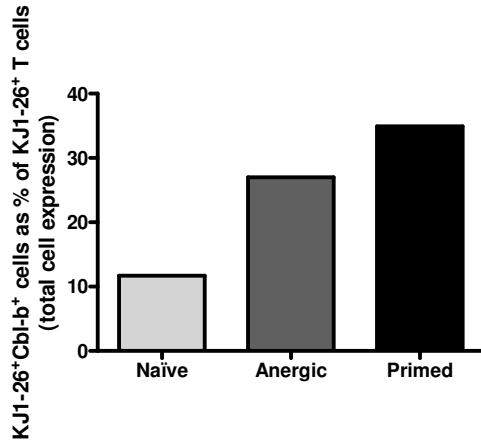


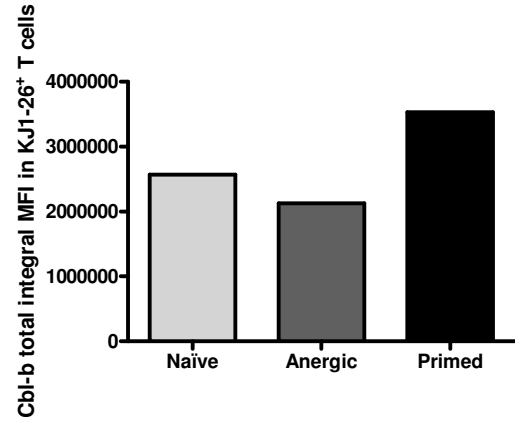
**Figure 3.45: Quantification of Cbl-b expression in KJ1-26<sup>+</sup> T cells after 20 h of *in vitro* re-stimulation.**

DO11.10 T cells were extracted from lymph nodes and cultured *in vitro* in the presence of anti-CD3 or anti-CD3 and anti-CD28 antibodies to induce anergy or priming, respectively. Excess antibody was washed off and the cells re-plated and rested for an additional 2 d in fresh medium. Naïve (freshly isolated), anergised and primed DO11.10 T cells were (re-)stimulated with LPS-matured DCs pulsed with OVA<sub>323-339</sub> for 20 h. Cells were harvested, washed, cytocentrifuged, stained for nuclear DNA (DAPI), DO11.10 TCR and Cbl-b and Cbl-b expression in KJ1-26<sup>+</sup> T cells quantified with the LSC as described in the Materials and Methods chapter. Firstly, all events were sorted on their nuclear staining (“cells”) and from these KJ1-26<sup>+</sup> T cells were gated. **A)** shows the percentage of KJ1-26<sup>+</sup> T cells that are positive for Cbl-b out of the whole population of KJ1-26<sup>+</sup> T cells, in terms of total cell expression. **B)** shows the mean fluorescence intensity (MFI) of Cbl-b expression in those KJ1-26<sup>+</sup> T cells that are also positive for Cbl-b in terms of total cell expression. **C)** shows the percentage of KJ1-26<sup>+</sup> T cells that are positive for Cbl-b out of the whole population of KJ1-26<sup>+</sup> T cells, in terms of peripheral cell expression. **D)** shows MFI of Cbl-b expression in those KJ1-26<sup>+</sup> T cells that are also positive for Cbl-b in terms of peripheral cell expression. The results shown are representative of three independent experiments.

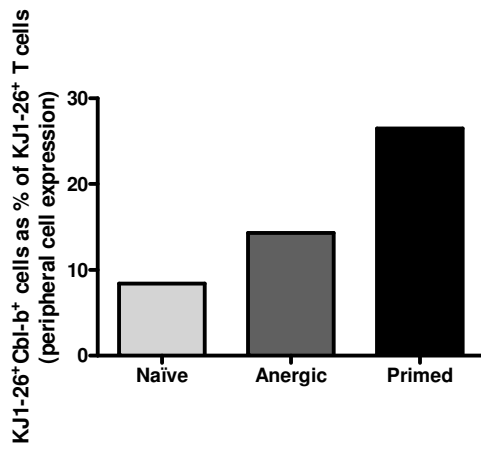
**A)**



**B)**



**C)**



**D)**

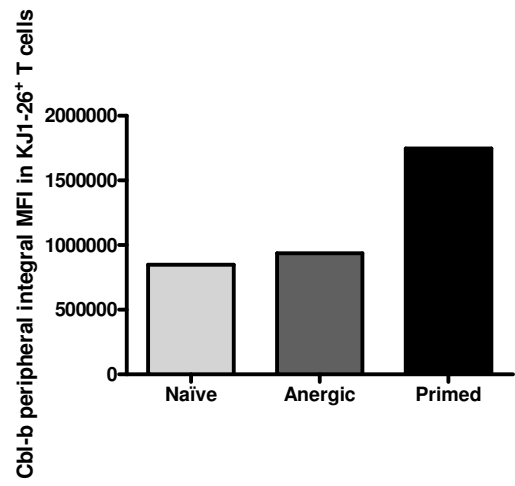
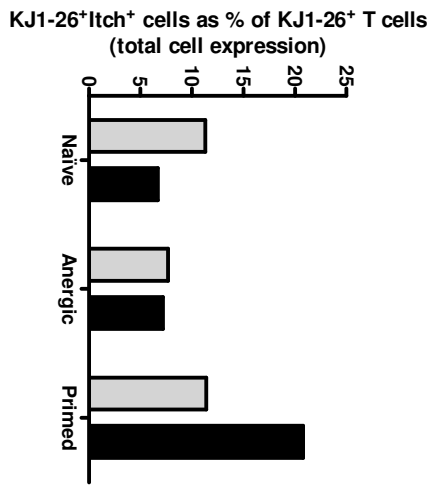


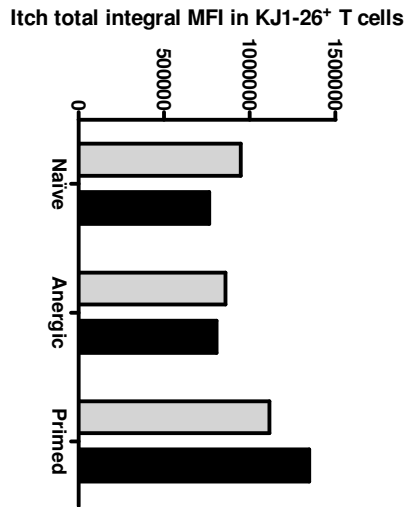
**Figure 3.46 Quantification of Itch expression in KJ1-26<sup>+</sup> T cells after 1 h of *in vitro* re-stimulation.**

DO11.10 T cells were extracted from lymph nodes and cultured *in vitro* in the presence of anti-CD3 or anti-CD3 and anti-CD28 antibodies to induce anergy or priming, respectively. Excess antibody was washed off and the cells re-plated and rested for an additional 2 d in fresh medium. Naïve (freshly isolated), anergised and primed DO11.10 T cells were (re-)stimulated with LPS-matured DCs which had been pulsed with or without OVA<sub>323-339</sub> for 1 h. Cells were harvested, washed, cytocentrifuged, stained for nuclear DNA (DAPI), DO11.10 TCR and Itch and Itch expression in KJ1-26<sup>+</sup> T cells quantified with the LSC as described in the Materials and Methods chapter. Firstly, all events were sorted on their nuclear staining (“cells”) and from these KJ1-26<sup>+</sup> T cells were gated. **A)** shows the percentage of KJ1-26<sup>+</sup> T cells that are positive for Itch out of the whole population of KJ1-26<sup>+</sup> T cells, in terms of total cell expression. **B)** shows the mean fluorescence intensity (MFI) of Itch expression in those KJ1-26<sup>+</sup> T cells that are also positive for Itch in terms of total cell expression. **C)** shows the percentage of KJ1-26<sup>+</sup> T cells that are positive for Itch out of the whole population of KJ1-26<sup>+</sup> T cells, in terms of peripheral cell expression. **D)** shows MFI of Itch expression in those KJ1-26<sup>+</sup> T cells that are also positive for Itch in terms of peripheral cell expression. The results shown are representative of three independent experiments.

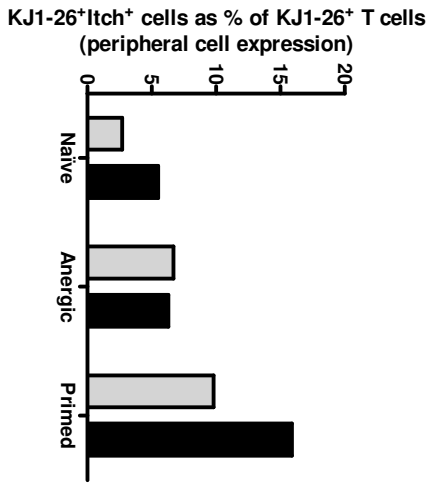
A)



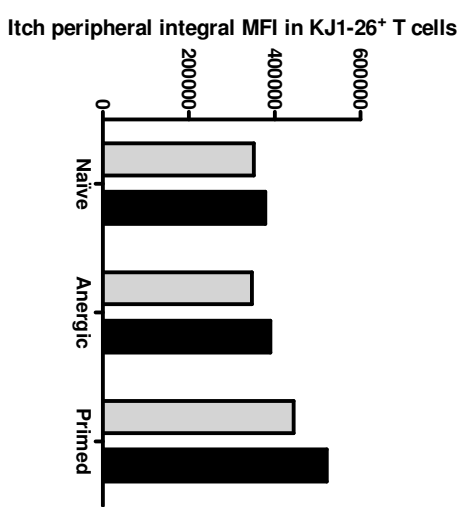
B)



C)



D)



Re-stimulation with:

- LPS-matured DCs
- LPS-matured, OVA-loaded DCs

**Figure 3.47: Visualisation of Itch expression in KJ1-26<sup>+</sup> T cells after 1 h of *in vitro* re-stimulation.**

DO11.10 T cells were extracted from lymph nodes and cultured *in vitro* in the presence of anti-CD3 or anti-CD3 and anti-CD28 antibodies to induce anergy or priming, respectively. Excess antibody was washed off and the cells re-plated and rested for an additional 2 d in fresh medium. Naïve (freshly isolated), anergised and primed DO11.10 T cells were (re-)stimulated LPS-matured DCs pulsed with OVA<sub>323-339</sub> for 1 h. Cells were harvested, washed, cytocentrifuged, stained for nuclear DNA (DAPI; blue) and Itch (green). Fluorescence was visualised using an Olympus BX50 fluorescent microscope and images captured and merged (x40 objectives). Cells were identified by nuclear staining with the DNA dye DAPI. The expression of Itch was determined with an  $\alpha$ -Itch-specific antibody coupled to tyramide amplification and the fluorochrome Alexa Fluor 488 (AF488 - green). Merging these two images results in the far right image – “Merge”.

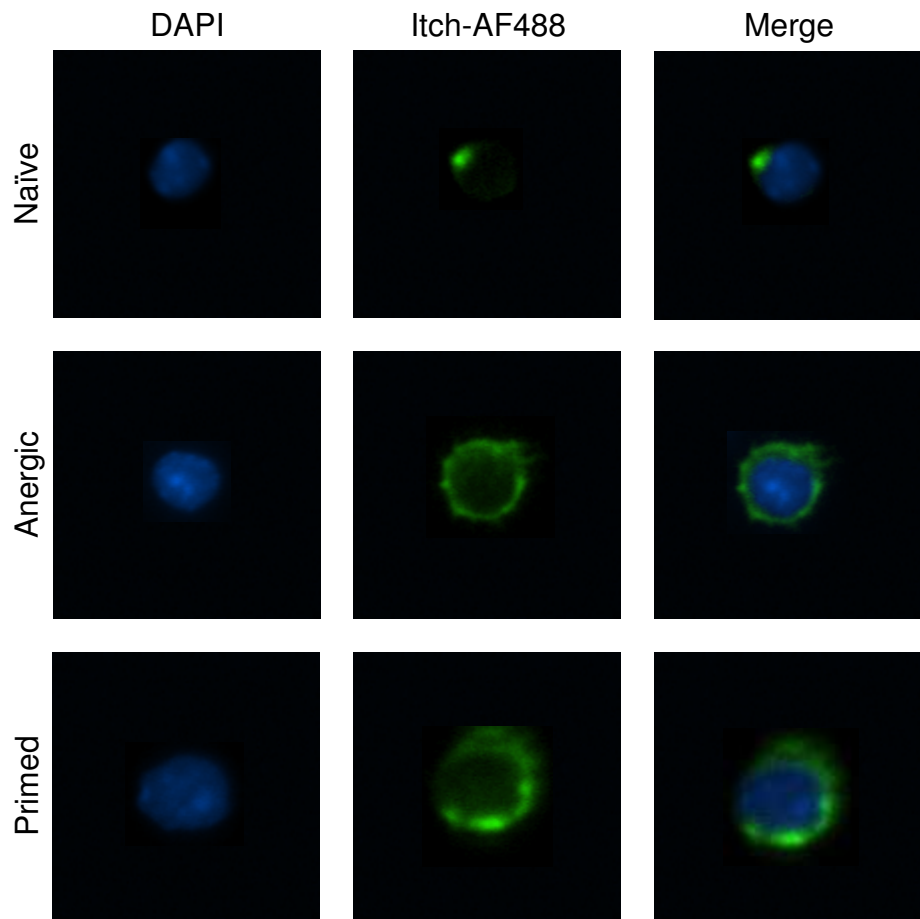
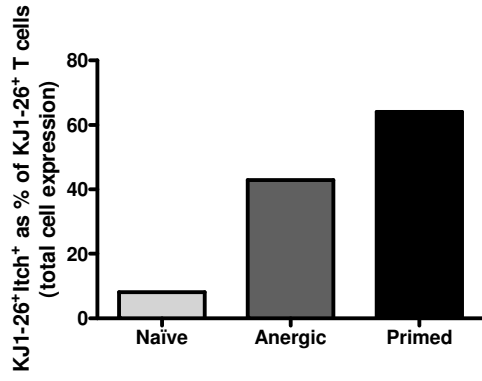


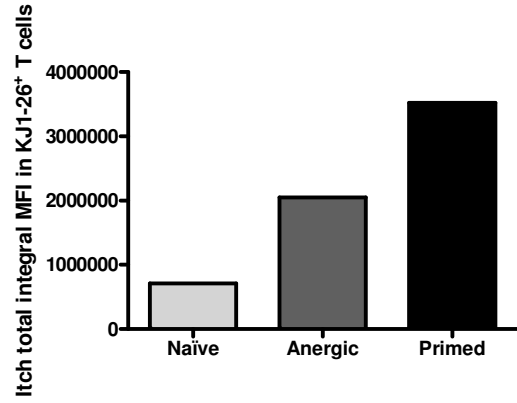
**Figure 3.48: Quantification of Itch expression in KJ1-26<sup>+</sup> T cells after 20 h of *in vitro* re-stimulation.**

DO11.10 T cells were extracted from lymph nodes and cultured *in vitro* in the presence of anti-CD3 or anti-CD3 and anti-CD28 antibodies to induce anergy or priming, respectively. Excess antibody was washed off and the cells re-plated and rested for an additional 2 d in fresh medium. Naïve (freshly isolated), anergised and primed DO11.10 T cells were (re-)stimulated with LPS-matured DCs which had been pulsed with or without OVA<sub>323-339</sub> for 20 h. **A, B, C and D)** T cells co-cultured with LPS-matured DCs pulsed with OVA<sub>323-339</sub> were harvested, washed, cytocentrifuged, stained for nuclear DNA (DAPI), DO11.10 TCR and Itch and Itch expression in KJ1-26<sup>+</sup> T cells quantified with the LSC as described in the Materials and Methods chapter. Firstly, all events were sorted on their nuclear staining (“cells”) and from these KJ1-26<sup>+</sup> T cells were gated. **A)** shows the percentage of KJ1-26<sup>+</sup> T cells that are positive for Itch out of the whole population of KJ1-26<sup>+</sup> T cells, in terms of total cell expression. **B)** shows the mean fluorescence intensity (MFI) of Itch expression in those KJ1-26<sup>+</sup> T cells that are also positive for Itch in terms of total cell expression. **C)** shows the percentage of KJ1-26<sup>+</sup> T cells that are positive for Itch out of the whole population of KJ1-26<sup>+</sup> T cells, in terms of peripheral cell expression. **D)** shows MFI of Itch expression in those KJ1-26<sup>+</sup> T cells that are also positive for Itch in terms of peripheral cell expression. **E)** Cells were fixed and stained for CD4, DO11.10 TCR and Itch; the percentage of CD4<sup>+</sup>KJ1-26<sup>+</sup> T cells expressing Itch was measured via flow cytometry. The results shown are representative of three independent experiments.

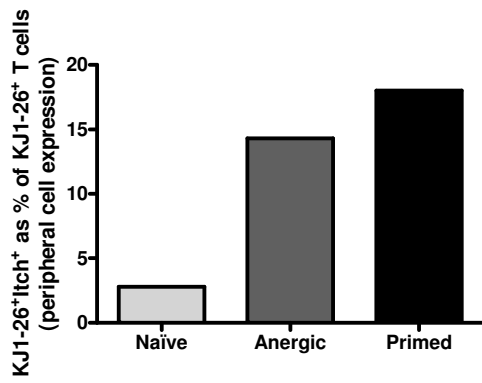
**A)**



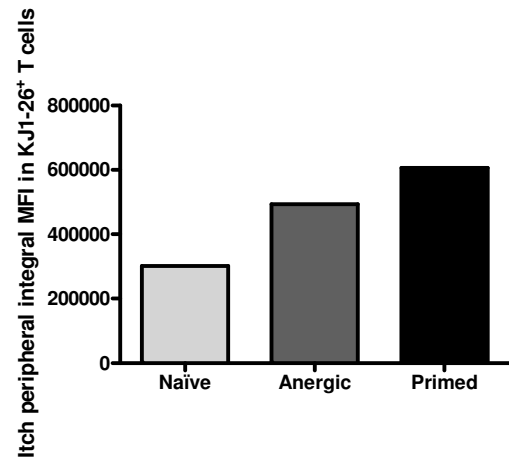
**B)**



**C)**



**D)**



**E)**

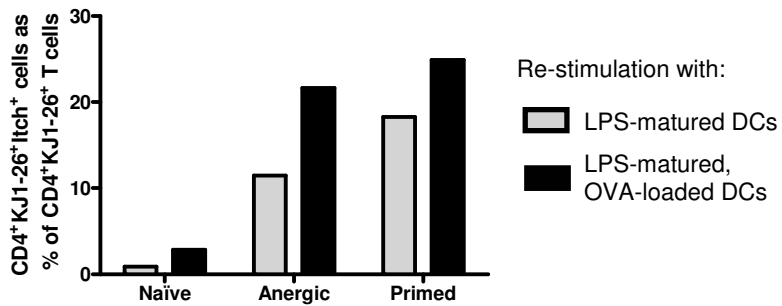


**Figure 3.49: Visualisation of Itch expression in KJ1-26<sup>+</sup> T cells after 20 h of *in vitro* re-stimulation.**

DO11.10 T cells were extracted from lymph nodes and cultured *in vitro* in the presence of anti-CD3 or anti-CD3 and anti-CD28 antibodies to induce anergy or priming, respectively. Excess antibody was washed off and the cells re-plated and rested for an additional 2 d in fresh medium. Naïve (freshly isolated), anergised and primed DO11.10 T cells were (re-)stimulated LPS-matured DCs pulsed with OVA<sub>323-339</sub> for 20 h. Cells were harvested, washed, cytocentrifuged, stained for nuclear DNA (DAPI; blue) and Itch (green). Fluorescence was visualised using an Olympus BX50 fluorescent microscope and images captured and merged (x40 objectives). Cells were identified by nuclear staining with the DNA dye DAPI. The expression of Itch was determined with an  $\alpha$ -Itch-specific antibody coupled to tyramide amplification and the fluorochrome Alexa Fluor 488 (AF488 - green). Merging these two images results in the far right image – “Merge”.

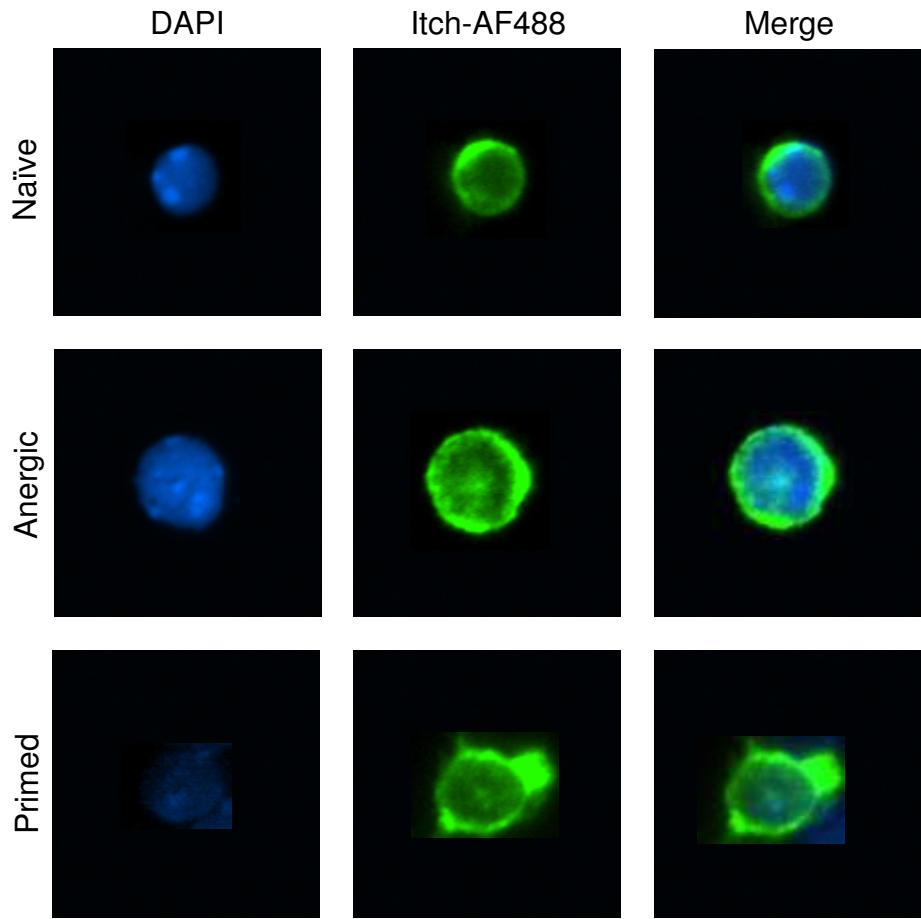
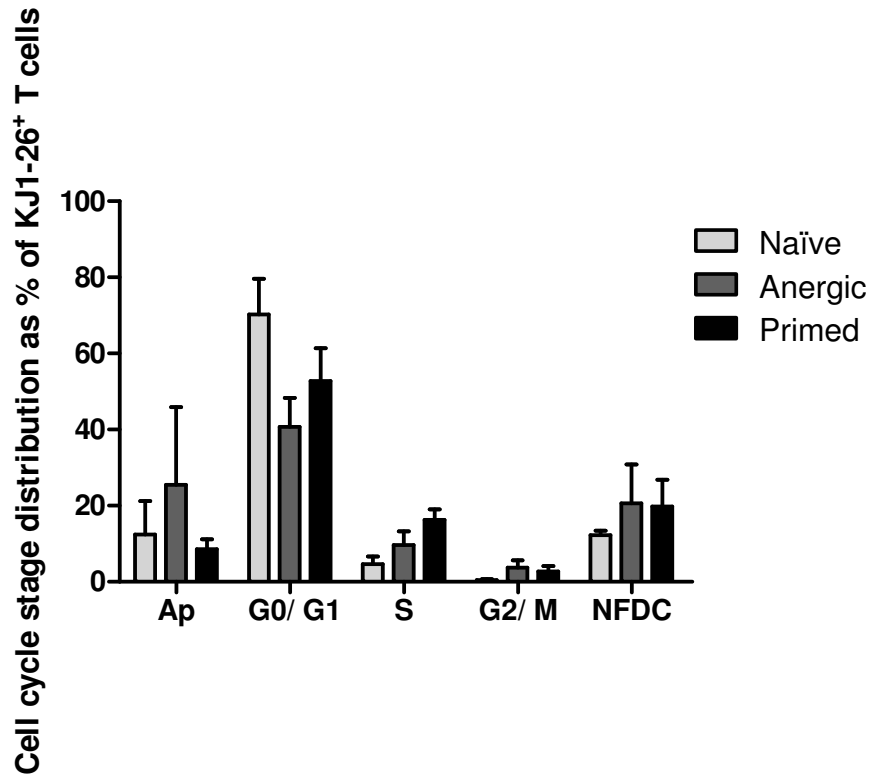


**Figure 3.50: Analysis of cell cycle stage distribution in KJ1-26<sup>+</sup> T cells after *in vitro* re-stimulation.**

DO11.10 T cells were extracted from lymph nodes and cultured *in vitro* in the presence of anti-CD3 or anti-CD3 and anti-CD28 antibodies to induce anergy or priming, respectively. Excess antibody was washed off and the cells re-plated and rested for an additional 2 d in fresh medium. Naïve (freshly isolated), anergised and primed DO11.10 T cells were (re-)stimulated LPS-matured DCs pulsed with OVA<sub>323-339</sub> for 1 h (A) or 20 h (B), washed, cytocentrifuged, stained for the nucleus and DO11.10 TCR (plus further label with adequate fluorochrome). The slides were analysed in the LSC: KJ1-26<sup>+</sup> T cells were gated, their DAPI max pixel Vs integral values plotted and adequate regions drawn matching the different cell cycle stages. Values are presented as percentage of KJ1-26<sup>+</sup> T cells in a particular cell cycle stage out of the whole population of KJ1-26<sup>+</sup> T cells, for that particular stimulus. Some stimulated populations were normalised to 100%. “Ap” stands for apoptotic cells and “NFDC” for newly-formed daughter cells. The results shown are the mean ± SEM of triplicate slide staining and are representative of three independent experiments.

A)



B)

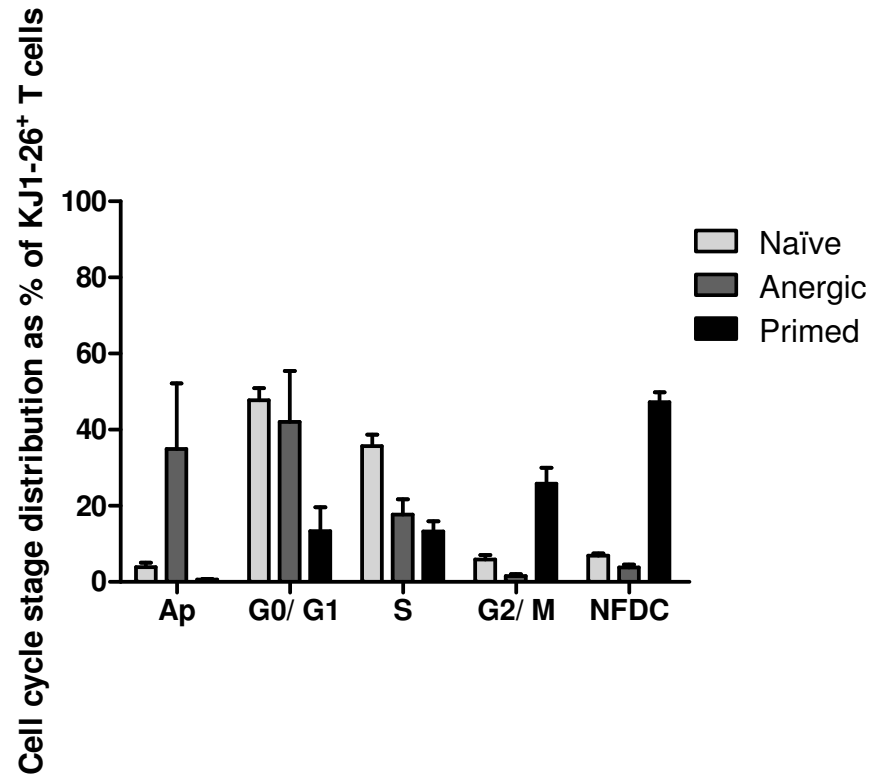
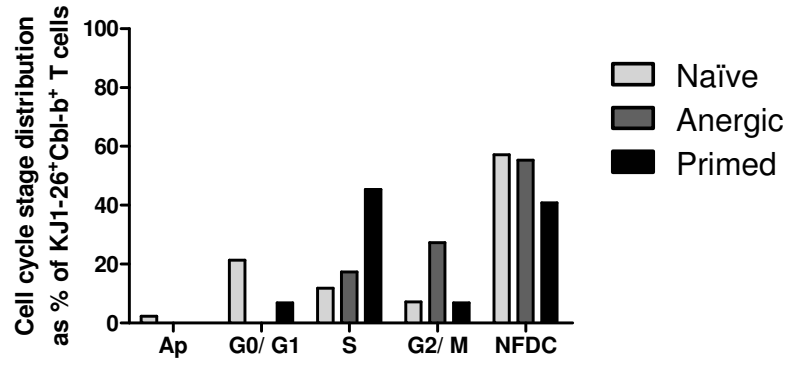


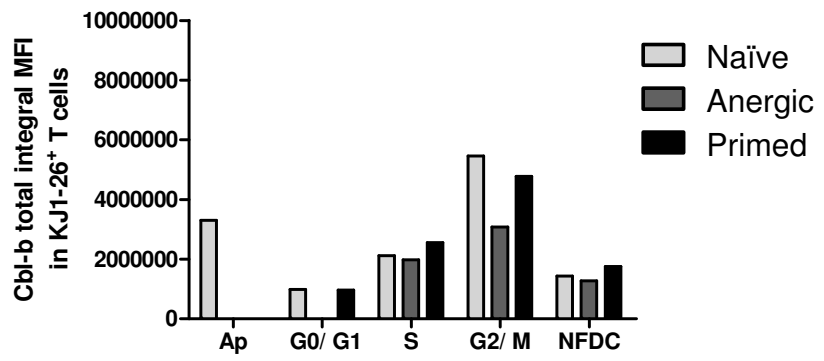
**Figure 3.51: Analysis of Cbl-b expression according to cell cycle stage in KJ1-26<sup>+</sup> T cells after 1 h of *in vitro* re-stimulation.**

DO11.10 T cells were extracted from lymph nodes and cultured *in vitro* in the presence of anti-CD3 or anti-CD3 and anti-CD28 antibodies to induce anergy or priming, respectively. Excess antibody was washed off and the cells re-plated and rested for an additional 2 d in fresh medium. Naïve (freshly isolated), anergised and primed DO11.10 T cells were (re-)stimulated LPS-matured DCs pulsed with OVA<sub>323-339</sub> for 1 h, washed, cytocentrifuged, stained for the nucleus, DO11.10 TCR and Cbl-b (these were further labelled with adequate fluorochromes). The slides were analysed in the LSC. **A)** KJ1-26<sup>+</sup> T cells were gated, Cbl-b<sup>+</sup> cells gated after this and their DAPI max pixel Vs integral values plotted. Values are presented as percentage of KJ1-26<sup>+</sup>Cbl-b<sup>+</sup> T cells in a particular cell cycle stage out of the whole population of KJ1-26<sup>+</sup>Cbl-b<sup>+</sup> T cells, for that particular stimulus. Some stimulated populations were normalised to 100%. **B)** KJ1-26<sup>+</sup> T cells were gated, their DAPI max pixel Vs integral values plotted after this and cells within the different cell cycle stages checked for Cbl-b expression. Values are presented as MFI of Cbl-b of the KJ1-26<sup>+</sup>Cbl-b<sup>+</sup> cells in a particular cell cycle stage. **C)** KJ1-26<sup>+</sup> T cells were gated, their DAPI max pixel Vs integral values plotted after this and cells within the different cell cycle stages checked for Cbl-b expression. Values are presented as percentage of Cbl-b<sup>+</sup> cells out of the KJ1-26<sup>+</sup> cells in a particular cell cycle stage.

A)



B)



C)

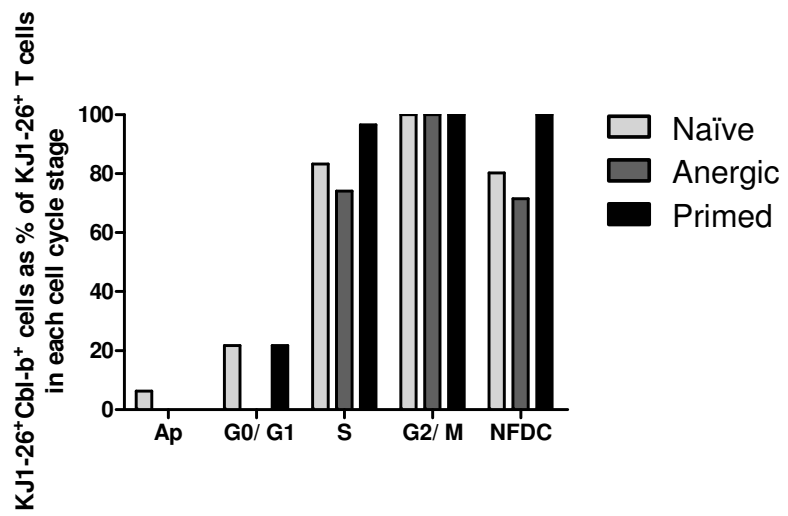
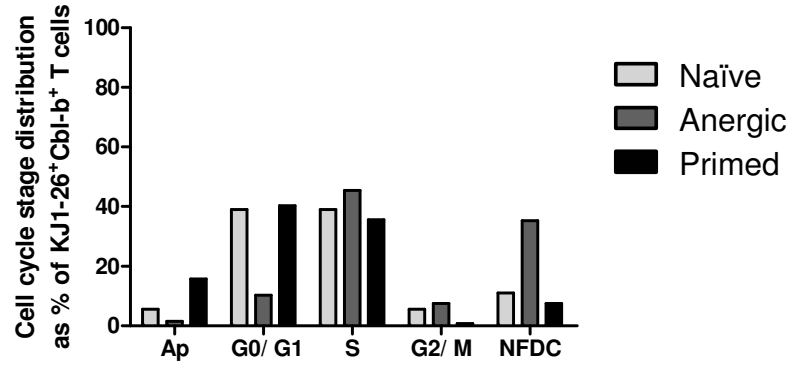


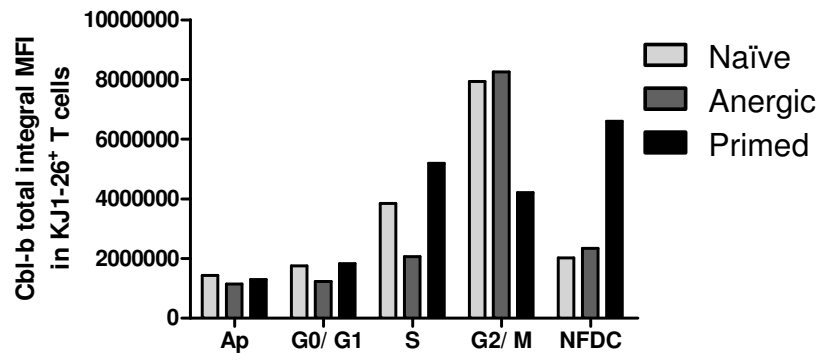
**Figure 3.52: Analysis of Cbl-b expression according to cell cycle stage in KJ1-26<sup>+</sup> T cells after 20 h of *in vitro* re-stimulation.**

DO11.10 T cells were extracted from lymph nodes and cultured *in vitro* in the presence of anti-CD3 or anti-CD3 and anti-CD28 antibodies to induce anergy or priming, respectively. Excess antibody was washed off and the cells re-plated and rested for an additional 2 d in fresh medium. Naïve (freshly isolated), anergised and primed DO11.10 T cells were (re-)stimulated LPS-matured DCs pulsed with OVA<sub>323-339</sub> for 20 h, washed, cytocentrifuged, stained for the nucleus, DO11.10 TCR and Cbl-b (these were further labelled with adequate fluorochromes). The slides were analysed in the LSC. **A)** KJ1-26<sup>+</sup> T cells were gated, Cbl-b<sup>+</sup> cells gated after this and their DAPI max pixel Vs integral values plotted. Values are presented as percentage of KJ1-26<sup>+</sup>Cbl-b<sup>+</sup> T cells in a particular cell cycle stage out of the whole population of KJ1-26<sup>+</sup>Cbl-b<sup>+</sup> T cells, for that particular stimulus. Some stimulated populations were normalised to 100%. **B)** KJ1-26<sup>+</sup> T cells were gated, their DAPI max pixel Vs integral values plotted after this and cells within the different cell cycle stages checked for Cbl-b expression. Values are presented as MFI of Cbl-b of the KJ1-26<sup>+</sup>Cbl-b<sup>+</sup> cells in a particular cell cycle stage. **C)** KJ1-26<sup>+</sup> T cells were gated, their DAPI max pixel Vs integral values plotted after this and cells within the different cell cycle stages checked for Cbl-b expression. Values are presented as percentage of Cbl-b<sup>+</sup> cells out of the KJ1-26<sup>+</sup> cells in a particular cell cycle stage.

A)



B)



C)

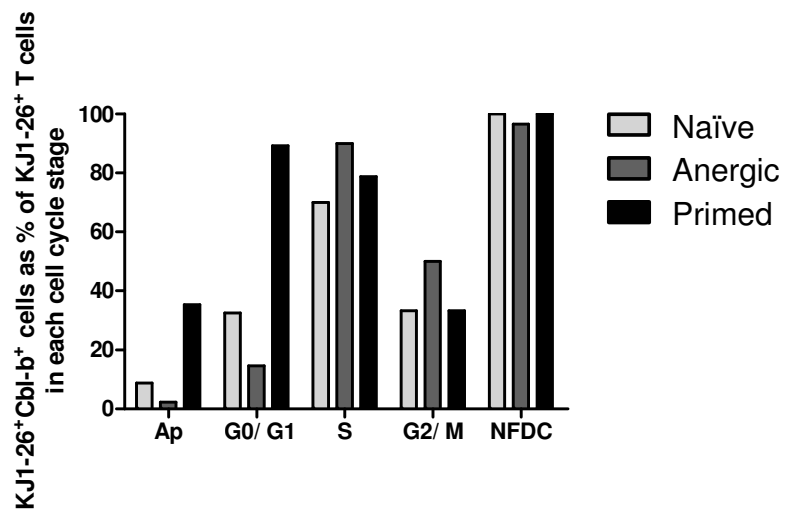
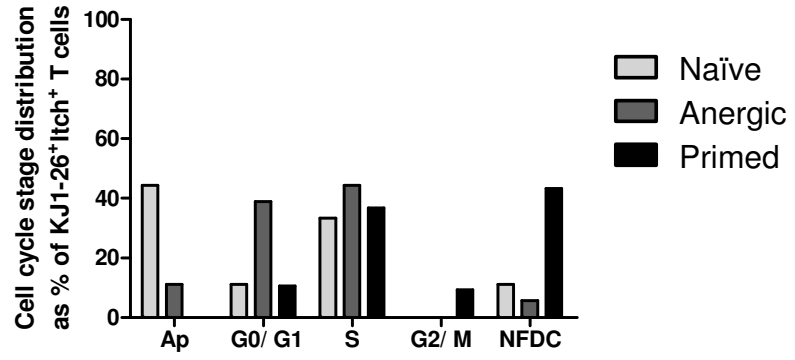


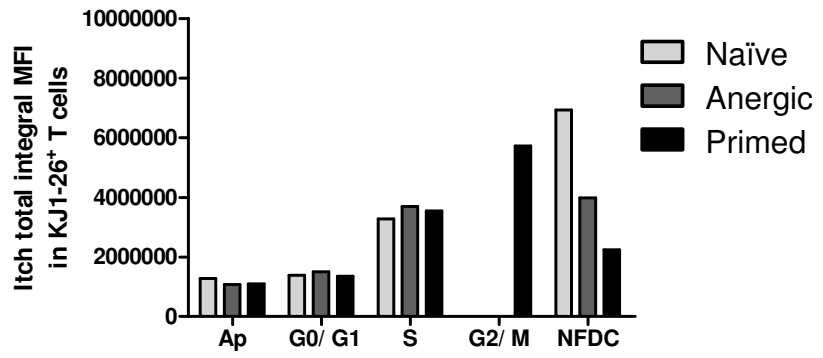
**Figure 3.53: Analysis of Itch expression according to cell cycle stage in KJ1-26<sup>+</sup> T cells after 1 h of *in vitro* re-stimulation.**

DO11.10 T cells were extracted from lymph nodes and cultured *in vitro* in the presence of anti-CD3 or anti-CD3 and anti-CD28 antibodies to induce anergy or priming, respectively. Excess antibody was washed off and the cells re-plated and rested for an additional 2 d in fresh medium. Naïve (freshly isolated), anergised and primed DO11.10 T cells were (re-)stimulated LPS-matured DCs pulsed with OVA<sub>323-339</sub> for 1 h, washed, cytocentrifuged, stained for the nucleus, DO11.10 TCR and Itch (these were further labelled with adequate fluorochromes). The slides were analysed in the LSC. **A)** KJ1-26<sup>+</sup> T cells were gated, Itch<sup>+</sup> cells gated after this and their DAPI max pixel Vs integral values plotted. Values are presented as percentage of KJ1-26<sup>+</sup>Itch<sup>+</sup> T cells in a particular cell cycle stage out of the whole population of KJ1-26<sup>+</sup>Itch<sup>+</sup> T cells, for that particular stimulus. Some stimulated populations were normalised to 100%. **B)** KJ1-26<sup>+</sup> T cells were gated, their DAPI max pixel Vs integral values plotted after this and cells within the different cell cycle stages checked for Itch expression. Values are presented as MFI of Itch of the KJ1-26<sup>+</sup>Itch<sup>+</sup> cells in a particular cell cycle stage. **C)** KJ1-26<sup>+</sup> T cells were gated, their DAPI max pixel Vs integral values plotted after this and cells within the different cell cycle stages checked for Itch expression. Values are presented as percentage of Itch<sup>+</sup> cells out of the KJ1-26<sup>+</sup> cells in a particular cell cycle stage.

A)



B)



C)

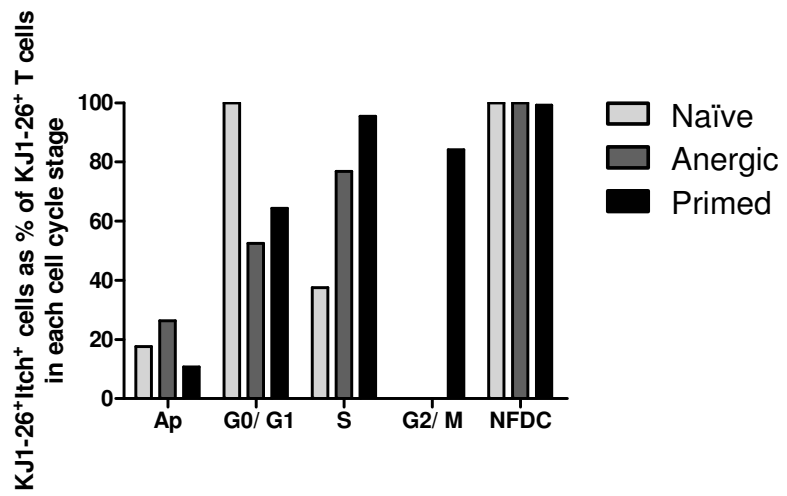
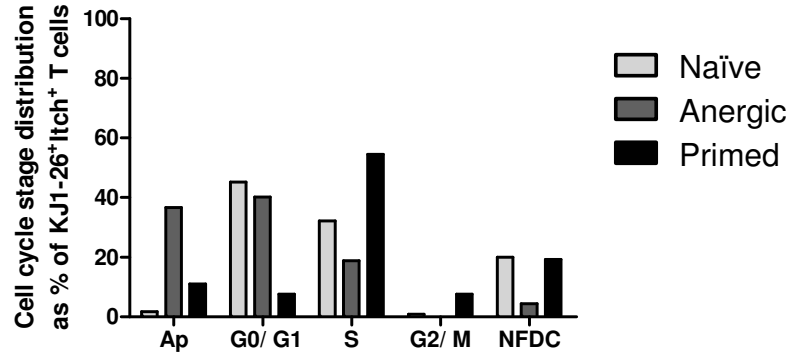


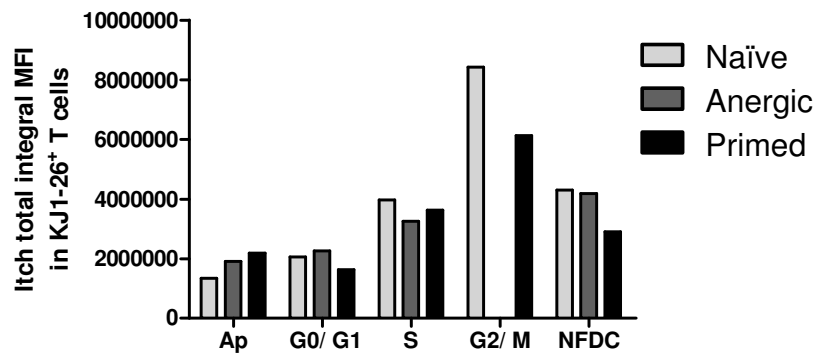
**Figure 3.54: Analysis of Itch expression according to cell cycle stage in KJ1-26<sup>+</sup> T cells after 20 h of *in vitro* re-stimulation.**

DO11.10 T cells were extracted from lymph nodes and cultured *in vitro* in the presence of anti-CD3 or anti-CD3 and anti-CD28 antibodies to induce anergy or priming, respectively. Excess antibody was washed off and the cells re-plated and rested for an additional 2 d in fresh medium. Naïve (freshly isolated), anergised and primed DO11.10 T cells were (re-)stimulated LPS-matured DCs pulsed with OVA<sub>323-339</sub> for 20 h, washed, cytocentrifuged, stained for the nucleus, DO11.10 TCR and Itch (these were further labelled with adequate fluorochromes). The slides were analysed in the LSC. **A)** KJ1-26<sup>+</sup> T cells were gated, Itch<sup>+</sup> cells gated after this and their DAPI max pixel Vs integral values plotted. Values are presented as percentage of KJ1-26<sup>+</sup>Itch<sup>+</sup> T cells in a particular cell cycle stage out of the whole population of KJ1-26<sup>+</sup>Itch<sup>+</sup> T cells, for that particular stimulus. Some stimulated populations were normalised to 100%. **B)** KJ1-26<sup>+</sup> T cells were gated, their DAPI max pixel Vs integral values plotted after this and cells within the different cell cycle stages checked for Itch expression. Values are presented as MFI of Itch of the KJ1-26<sup>+</sup>Itch<sup>+</sup> cells in a particular cell cycle stage. **C)** KJ1-26<sup>+</sup> T cells were gated, their DAPI max pixel Vs integral values plotted after this and cells within the different cell cycle stages checked for Itch expression. Values are presented as percentage of Itch<sup>+</sup> cells out of the KJ1-26<sup>+</sup> cells in a particular cell cycle stage.

A)



B)



C)

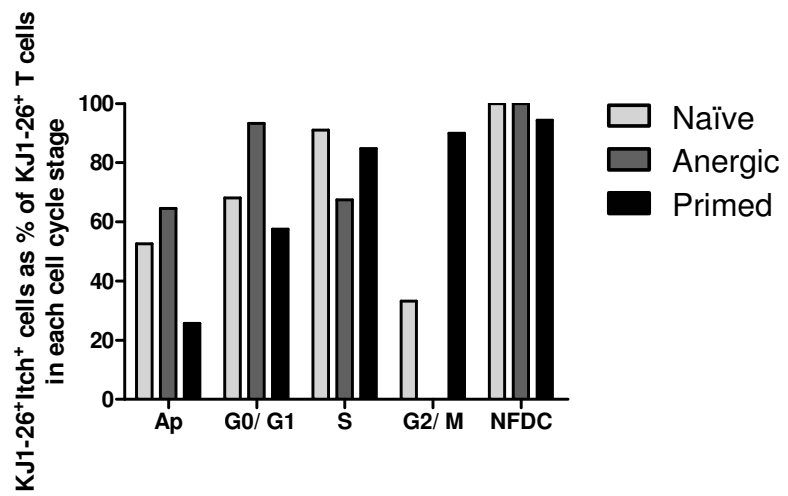
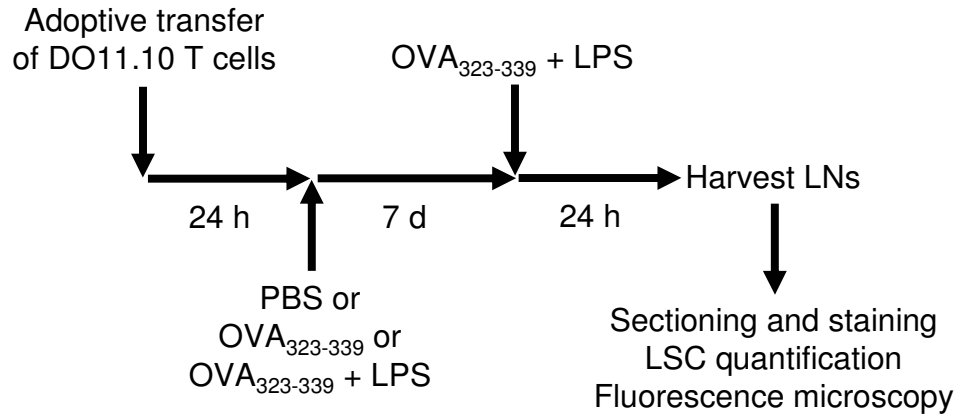


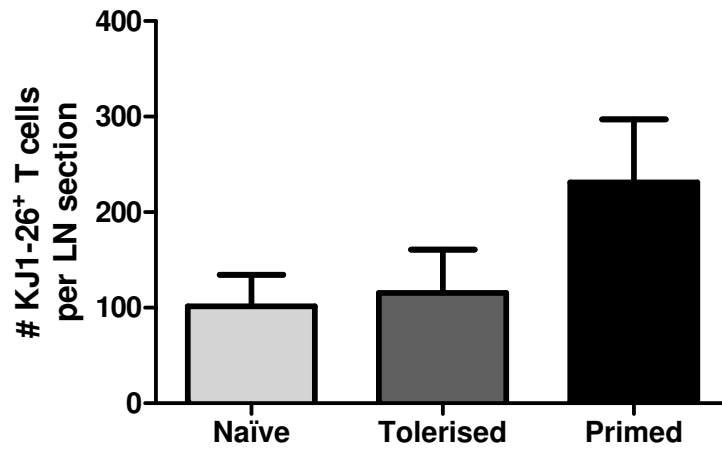
**Figure 3.55: The maintenance phase in tolerised and primed mice.**

DO11.10 TCR transgenic T cells were adoptively transferred into naïve recipients 24 h prior to i.v. injection with sterile PBS (naïve), OVA<sub>323-339</sub> (tolerised) or OVA<sub>323-339</sub> + LPS (primed); a secondary response was elicited by challenge with OVA<sub>323-339</sub> and LPS seven days later; PLNs were harvested 24 h after that and prepared for immunohistochemistry; tissue sections were stained for DO11.10 TCR transgenic T cells and B cells (**A**). **B**) The number of KJ1-26<sup>+</sup> T cells in each section was quantified by LSC. **C**) The LSC was used to identify the location of KJ1-26<sup>+</sup> T cells within the LN: B cell rich areas (follicles) and the B cell-free area (paracortex) were identified allowing the generation of a tissue map depicting the follicular and paracortical areas of the LN; KJ1-26<sup>+</sup> T cells were also identified, a map of their location also generated and the two maps fused, which allows quantification of KJ1-26<sup>+</sup> T cells in the context of follicular and paracortical location. Of the total number of KJ1-26<sup>+</sup> T cells in a section, the percentages which correspond to follicular and paracortical location were plotted. Data represent mean  $\pm$  SEM of three mice per group. Statistical significance was determined by one-way ANOVA (one way analysis of variance) followed by the Bonferroni post-test in **B**) and by regular two-way ANOVA (not repeated measures) followed by the Bonferroni post-test (to test significance of LN location for each stimulus; no interaction between the two variables [LN location Vs mice stimulation] was found) in **C**). Statistical significance was assumed when  $p \leq 0.05$ ; \* $\leq 0.05$ , \*\* $< 0.01$ ; \*\*\* $< 0.001$ .

A)



B)



C)

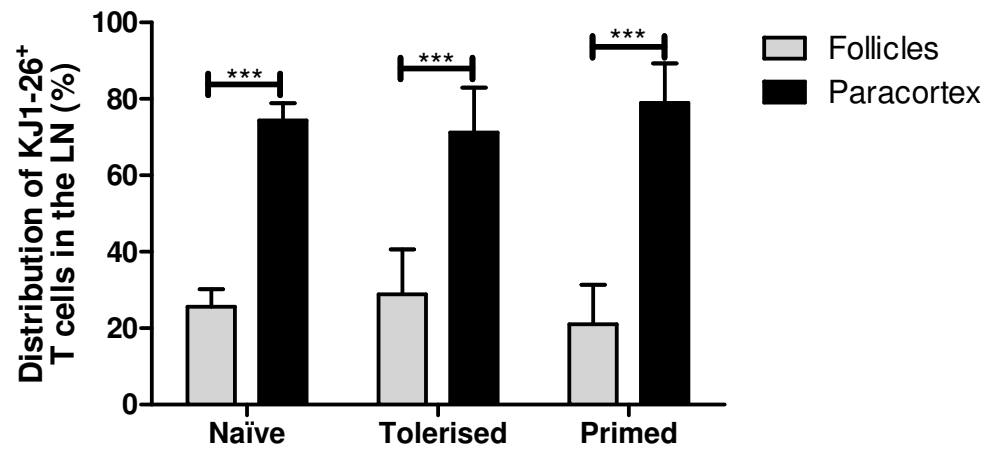
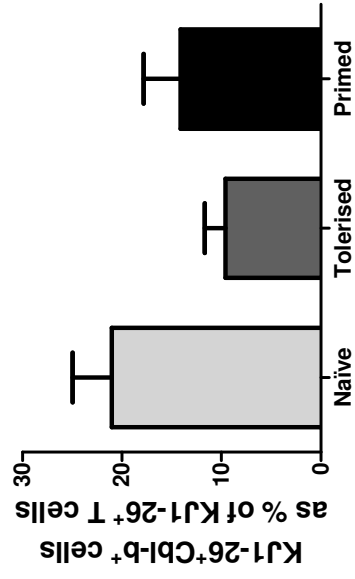


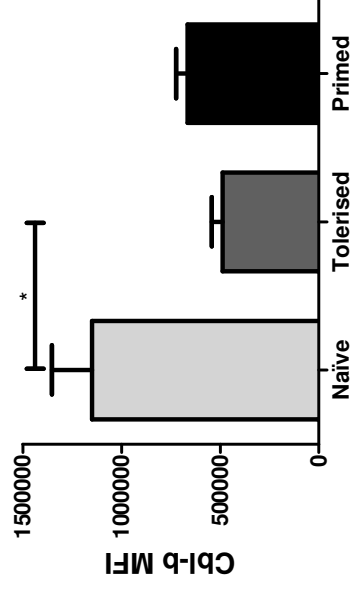
**Figure 3.56: Cbl-b expression in DO11.10 TCR transgenic T cells within the lymph node of tolerised and primed mice after re-stimulation.**

DO11.10 TCR transgenic T cells were adoptively transferred into naïve recipients 24 h prior to i.v. injection with sterile PBS (naïve), OVA<sub>323-339</sub> (tolerised) or OVA<sub>323-339</sub> + LPS (primed); a secondary response was elicited by challenge with OVA<sub>323-339</sub> and LPS seven days later; PLNs were harvested 24 h after that and prepared for immunohistochemistry. Tissue sections were stained for DO11.10 TCR transgenic T cells (red), B cells (green) and Cbl-b (blue). Cbl-b expression in DO11.10 T cells was quantified with the LSC: KJ1-26<sup>+</sup> T cells were gated and the percentage of these cells expressing Cbl-b plotted (**A**); the MFI of Cbl-b in KJ1-26<sup>+</sup>Cbl-b<sup>+</sup> T cells was plotted in **B**. Photographs were taken of the naïve (**C**), tolerised (**D**) and primed tissue (**E**). Data represent mean ± SEM of three mice per group. Statistical significance was determined by one-way ANOVA (one way analysis of variance) followed by the Bonferroni post-test. Statistical significance was assumed when  $p \leq 0.05$ ; \* $\leq 0.05$ , \*\* $< 0.01$ ; \*\*\* $< 0.001$ .

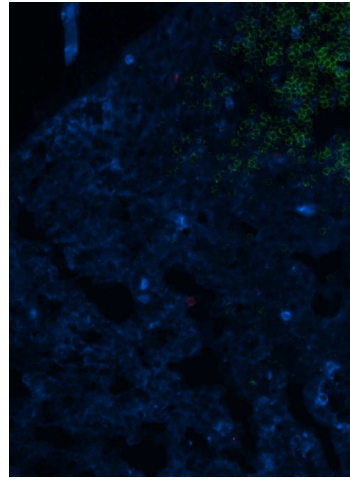
A)



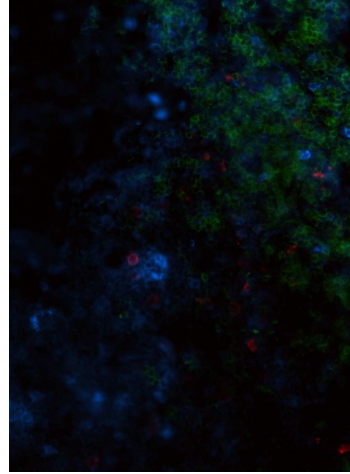
B)



C)



D)



E)

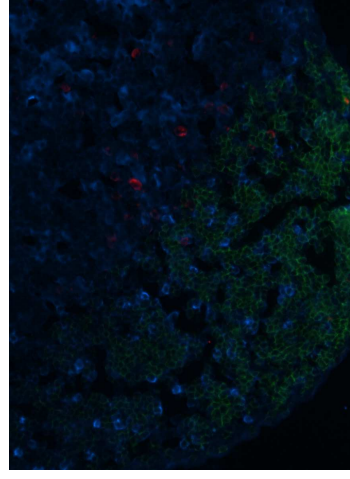
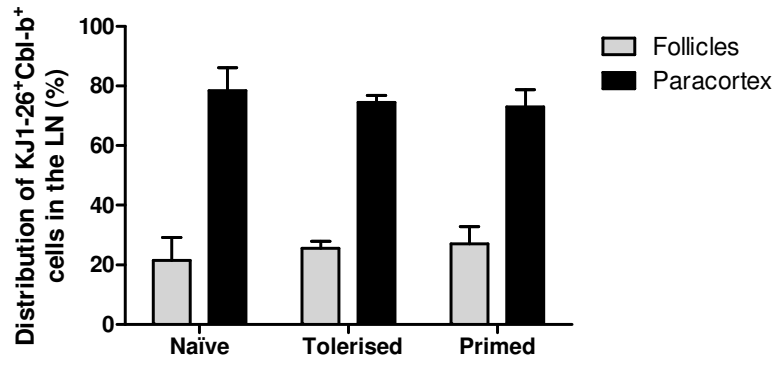


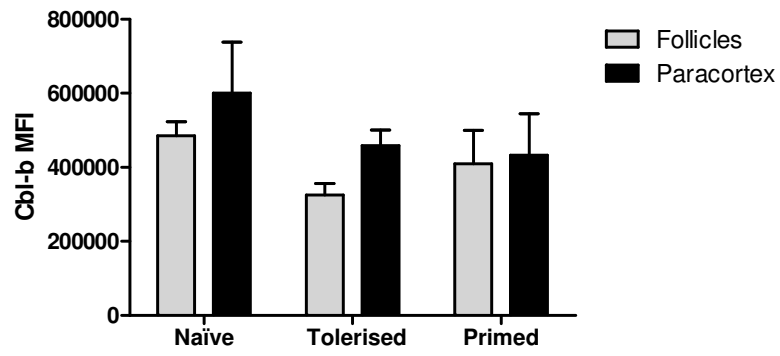
**Figure 3.57: Analysis of the effect of Cbl-b expression in DO11.10 T cells' migration into B cell follicles in tolerised and primed mice after re-stimulation.**

DO11.10 TCR transgenic T cells were adoptively transferred into naïve recipients 24 h prior to i.v. injection with sterile PBS (naïve), OVA<sub>323-339</sub> (tolerised) or OVA<sub>323-339</sub> + LPS (primed); a secondary response was elicited by challenge with OVA<sub>323-339</sub> and LPS seven days later; PLNs were harvested 24 h after that and prepared for immunohistochemistry; tissue sections were stained for DO11.10 TCR transgenic T cells, B cells and Cbl-b. The LSC was used to identify the location of KJ1-26<sup>+</sup> T cells within the LN and to quantify Cbl-b expression in the KJ1-26<sup>+</sup> T cells. **A)** Of the total number of KJ1-26<sup>+</sup>Cbl-b<sup>+</sup> cells in a section, the percentages which correspond to follicular and paracortical location were plotted. **B)** shows the mean fluorescence intensity (MFI) of Cbl-b expression in those KJ1-26<sup>+</sup> T cells that are also positive for Cbl-b. **C)** shows the the percentage of KJ1-26<sup>+</sup> T cells that are positive for Cbl-b out of the population of KJ1-26<sup>+</sup> T cells within that specific LN area. Data represent mean ± SEM of three mice per group. Statistical significance was determined by regular two-way ANOVA (not repeated measures) followed by the Bonferroni post-test (to test significance of the stimulus for each LN location). Statistical significance was assumed when  $p \leq 0.05$ ; \* $\leq 0.05$ , \*\* $< 0.01$ ; \*\*\* $< 0.001$ .

A)



B)



C)

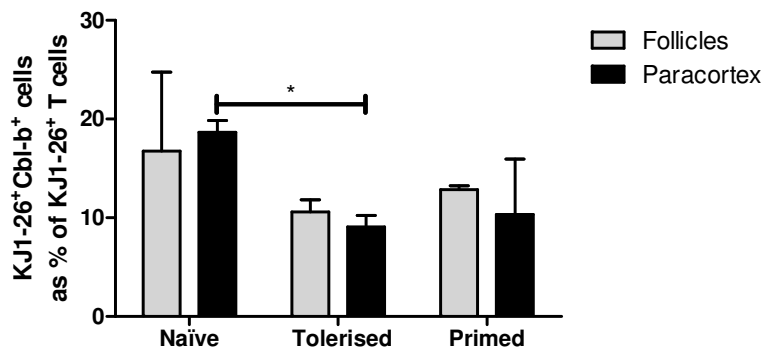
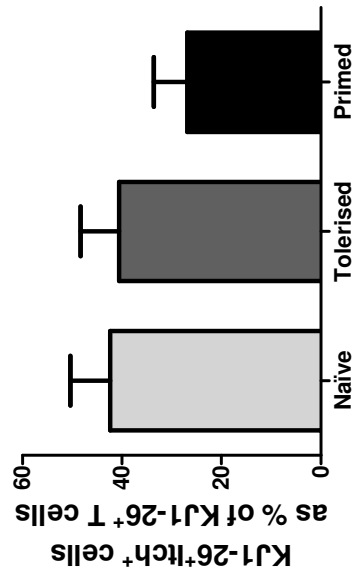


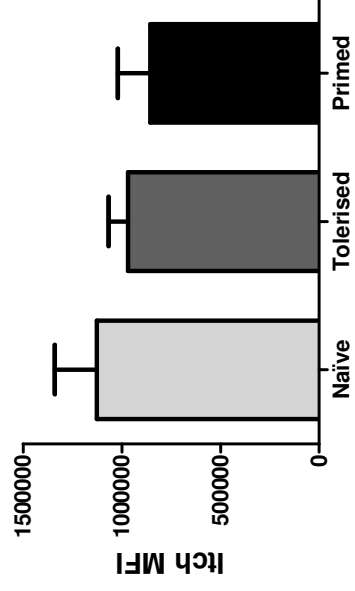
**Figure 3.58: Itch expression in DO11.10 TCR transgenic T cells within the lymph node of tolerised and primed mice after re-stimulation.**

DO11.10 TCR transgenic T cells were adoptively transferred into naïve recipients 24 h prior to i.v. injection with sterile PBS (naïve), OVA<sub>323-339</sub> (tolerised) or OVA<sub>323-339</sub> + LPS (primed); a secondary response was elicited by challenge with OVA<sub>323-339</sub> and LPS seven days later; PLNs were harvested 24 h after that and prepared for immunohistochemistry. Tissue sections were stained for DO11.10 TCR transgenic T cells (red), B cells (green) and Itch (blue). Itch expression in DO11.10 T cells was quantified with the LSC: KJ1-26<sup>+</sup> T cells were gated and the percentage of these cells expressing Itch plotted (**A**); the MFI of Itch in KJ1-26<sup>+</sup>Itch<sup>+</sup> T cells was plotted in **B**. Photographs were taken of the naïve (**C**), tolerised (**D**) and primed tissue (**E**). Data represent mean ± SEM of three mice per group. Statistical significance was determined by one-way ANOVA (one way analysis of variance) followed by the Bonferroni post-test. Statistical significance was assumed when  $p \leq 0.05$ ; \* $\leq 0.05$ , \*\* $< 0.01$ ; \*\*\* $< 0.001$ .

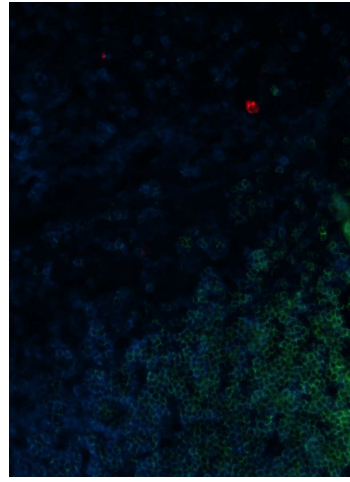
A)



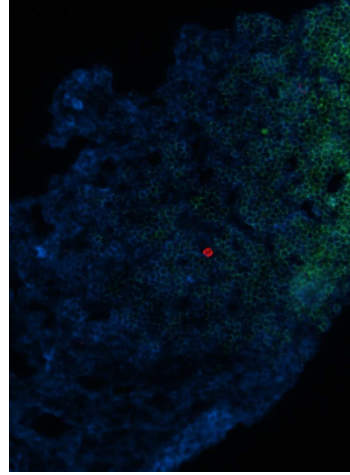
B)



C)



D)



E)

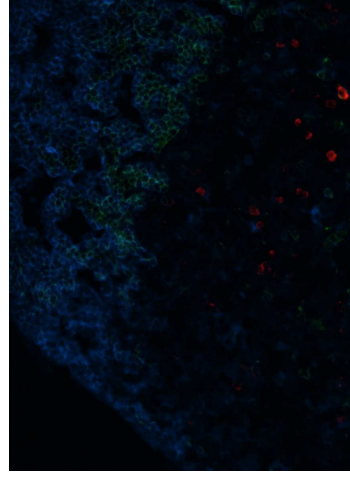
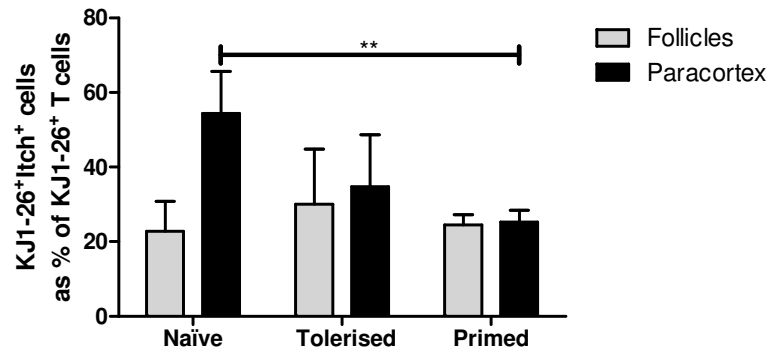


**Figure 3.59: Analysis of the effect of Itch expression in DO11.10 T cells' migration into B cell follicles in tolerised and primed mice after re-stimulation.**

DO11.10 TCR transgenic T cells were adoptively transferred into naïve recipients 24 h prior to i.v. injection with sterile PBS (naïve), OVA<sub>323-339</sub> (tolerised) or OVA<sub>323-339</sub> + LPS (primed); a secondary response was elicited by challenge with OVA<sub>323-339</sub> and LPS seven days later; PLNs were harvested 24 h after that and prepared for immunohistochemistry; tissue sections were stained for DO11.10 TCR transgenic T cells, B cells and Itch. The LSC was used to identify the location of KJ1-26<sup>+</sup> T cells within the LN and to quantify Itch expression in the KJ1-26<sup>+</sup> T cells. **A)** shows the percentage of KJ1-26<sup>+</sup> T cells that are positive for Itch out of the population of KJ1-26<sup>+</sup> T cells within that specific LN area. **B)** shows the mean fluorescence intensity (MFI) of Itch expression in those KJ1-26<sup>+</sup> T cells that are also positive for Itch. Data represent mean  $\pm$  SEM of three mice per group. Statistical significance was determined by regular two-way ANOVA (not repeated measures) followed by the Bonferroni post-test (to test significance of the stimulus for each LN location). Statistical significance was assumed when  $p \leq 0.05$ ; \* $\leq 0.05$ , \*\* $< 0.01$ ; \*\*\* $< 0.001$ .

A)



B)

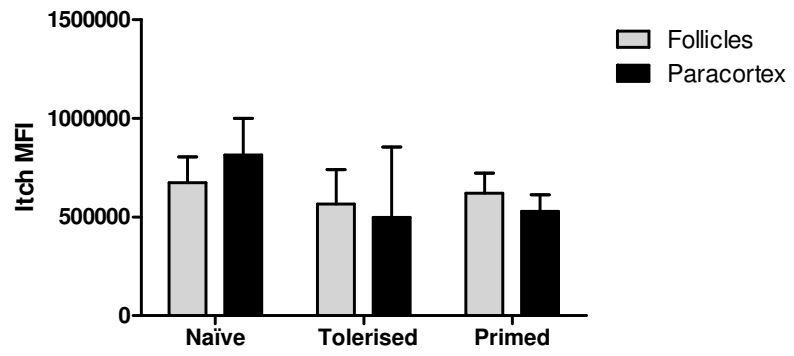
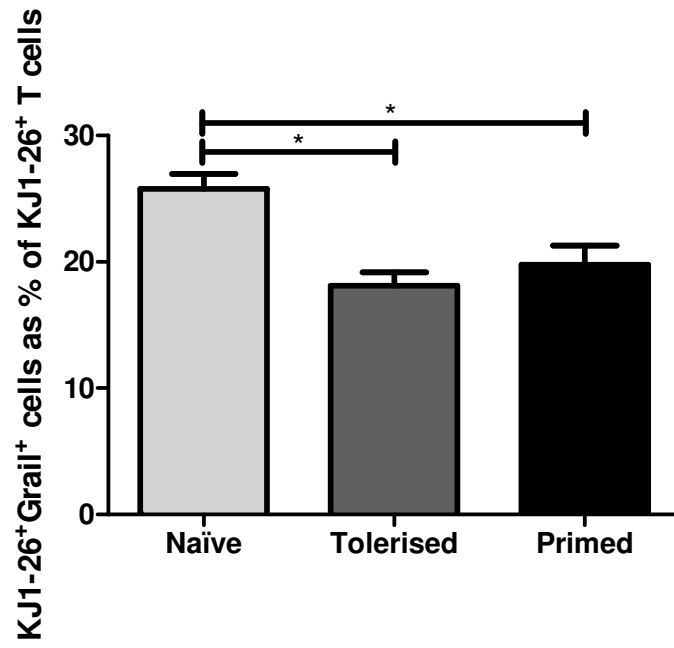


**Figure 3.60: Grail expression in DO11.10 TCR transgenic T cells within the lymph node of tolerised and primed mice after re-stimulation.**

DO11.10 TCR transgenic T cells were adoptively transferred into naïve recipients 24 h prior to i.v. injection with sterile PBS (naïve), OVA<sub>323-339</sub> (tolerised) or OVA<sub>323-339</sub> + LPS (primed); a secondary response was elicited by challenge with OVA<sub>323-339</sub> and LPS seven days later; PLNs were harvested 24 h after that and prepared for immunohistochemistry. Tissue sections were stained for DO11.10 TCR transgenic T cells, B cells and Grail. Grail expression in DO11.10 T cells was quantified with the LSC: KJ1-26<sup>+</sup> T cells were gated and the percentage of these cells expressing Grail plotted (**A**); the MFI of Grail in KJ1-26<sup>+</sup>Grail<sup>+</sup> T cells was plotted in **B**. Data represent mean ± SEM of three mice per group. Statistical significance was determined by one-way ANOVA (one way analysis of variance) followed by the Bonferroni post-test. Statistical significance was assumed when  $p \leq 0.05$ ; \* $\leq 0.05$ , \*\* $< 0.01$ ; \*\*\* $< 0.001$ .

A)



B)

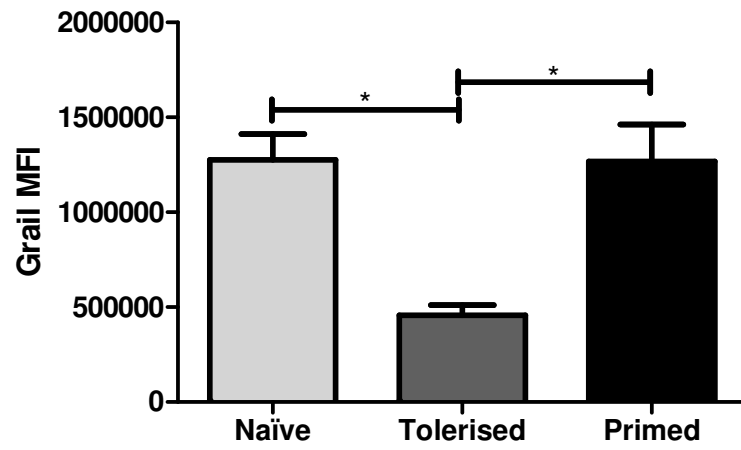
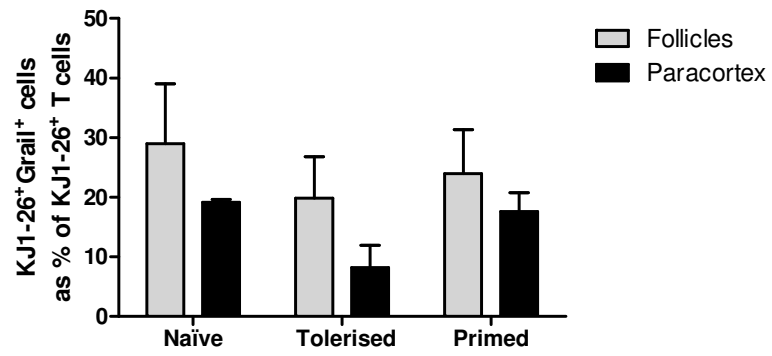


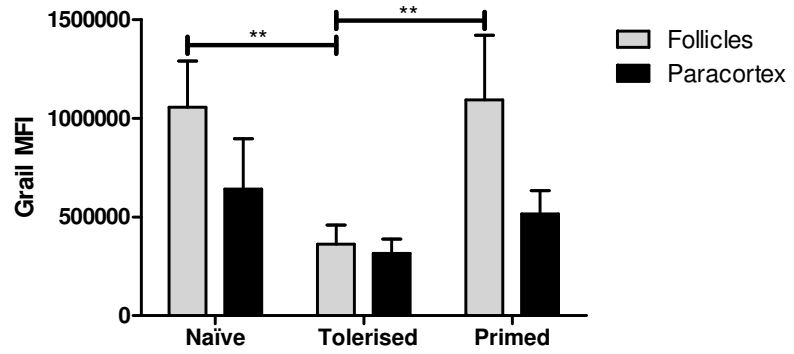
**Figure 3.61: Analysis of the effect of Grail expression in DO11.10 T cells' migration into B cell follicles in tolerised and primed mice after re-stimulation.**

DO11.10 TCR transgenic T cells were adoptively transferred into naïve recipients 24 h prior to i.v. injection with sterile PBS (naïve), OVA<sub>323-339</sub> (tolerised) or OVA<sub>323-339</sub> + LPS (primed); a secondary response was elicited by challenge with OVA<sub>323-339</sub> and LPS seven days later; PLNs were harvested 24 h after that and prepared for immunohistochemistry; tissue sections were stained for DO11.10 TCR transgenic T cells, B cells and Grail. The LSC was used to identify the location of KJ1-26<sup>+</sup> T cells within the LN and to quantify Itch expression in the KJ1-26<sup>+</sup> T cells. **A)** shows the percentage of KJ1-26<sup>+</sup> T cells that are positive for Grail out of the population of KJ1-26<sup>+</sup> T cells within that specific LN area. **B)** shows the mean fluorescence intensity (MFI) of Grail expression in those KJ1-26<sup>+</sup> T cells that are also positive for Grail. Data represent mean  $\pm$  SEM of three mice per group. Statistical significance was determined by regular two-way ANOVA (not repeated measures) followed by the Bonferroni post-test (to test significance of the stimulus for each LN location). Statistical significance was assumed when  $p \leq 0.05$ ; \* $\leq 0.05$ , \*\* $< 0.01$ ; \*\*\* $< 0.001$ .

A)



B)



CHAPTER 4  
DISCUSSION

## 4 DISCUSSION

### 4.1 Methods and results

This study focused on the analysis of expression of E3 ubiquitin-protein ligases by T cells after stimulation; in studying a plastic signal such as ubiquitination, it would have been desirable to have analysed more time points; furthermore, the elements involved in T cell signalling exhibit multiple levels of regulation, ranging from transcriptional, to translational, to posttranslational, all of these important aspects to investigate and all of them occurring in specific time-frames. However, due to practical reasons related to obtaining the biological material (e.g. cells and LNs) in quantities needed for the experimental procedures, only a limited number of time points could be chosen and these were selected relative to functional readouts. Naturally, in the process of such selection, some information about the system might not have been gathered. In addition, E3 ligases are known to be regulated not only by ubiquitination but also by phosphorylation by multiple pathways; a closer look at the phosphorylation status of the E3 ligases might have contributed to a better understanding of their activation state and hence clarified the potential role of E3s in targeting different substrates for ubiquitination, under different conditions. While the antibodies used throughout the Western blotting experiments reported here were shown to be specific, occasional technical glitches occurred such as air bubbles in the membrane and lanes with incomparable levels of protein; while in most cases the presence of air bubbles does not affect the global interpretation of any one blot, interpreting blots with lanes with differential levels of protein is much more difficult, and densitometry analysis of these blots would be of great help in validating the data. LSC allowed the *in situ* quantification of the expression of the E3 ligases in CD4<sup>+</sup> T cells; while generally the numbers of cells analysed were quite high, in some circumstances, such as in some of the stages of the cell cycle analysis, few cells were available for analysis and, as a result, these data are not as robust. Similarly, the *in vivo* experiments, both the induction and maintenance phases reflect one experiment, albeit with three mice per group.

## 4.2 Cbl-b

### 4.2.1 Induction

In the *in vitro* study of induction of priming and tolerance, Cbl-b was found to be upregulated in CD4<sup>+</sup> T cells after 20 h of TCR ligation, an effect that was potentiated when coupled with CD28 co-stimulation (**Figure 3.6**). Analysis of the expression of Cbl-b at the single-cell level at least partially confirmed these data as the priming CD4<sup>+</sup> T cell population, but not the anergising population, has a higher proportion of cells expressing Cbl-b than the unstimulated population (**Figure 3.11**). Moreover, at later time points Cbl-b is still more expressed in the anti-CD3+anti-CD28 priming population than in the anti-CD3 anergising population, as seen at 40 h via LSC (**Figure 3.13**) and at 48 h via Western blotting (**Figure 3.9**). Similarly, the *in vivo* study of the induction phase of tolerance and priming (**Figure 3.30**) revealed no significant differences between the two groups after 5 d of tolerance or priming induction in terms of proportion of antigen-specific T cells positive for Cbl-b or in terms of intensity of Cbl-b total protein expression per antigen-specific T cell; however in the *in vivo* system, although not significant, both parameters did tend to show slightly higher expression of Cbl-b in the tolerised group.

These findings are perhaps rather surprising as it has generally been reported that Cbl-b is most highly expressed in anergic cells [183] although a previous study had shown that, in splenic T cells stimulated *in vitro* with immobilised anti-CD3 antibody, Cbl-b expression decreases after 8 h to a barely noticeable intensity by 24 h, only recovering to the levels of the 8 h time point by 72 h [100]. Moreover, lower expression of Cbl-b in TCR/CD28 co-stimulated cells was expected as CD28 co-stimulation has been reported to induce greater proteasomal degradation than CD3 stimulation alone [185]. However, the proteasomal inhibitor data from our model of anti-CD3-mediated anergy of CD4<sup>+</sup> T cells suggest that increased proteasomal-mediated Cbl-b degradation takes place in anergic relative to that of naïve or primed cells (**Figure 3.7**). This effect requires TCR signalling as, while anergy induction by means of TCR ligation leads to accumulation of Cbl-b in proteasome-inhibited cells, anergy induction by means of direct Ca<sup>2+</sup> mobilisation fails to result in further substantial accumulation of Cbl-b (**Figure 3.7**), perhaps suggesting that Cbl-b expression is itself dynamically regulated by proteasomal degradation during antigen- but not ionomycin-mediated anergy and hence explaining the observed Cbl-b upregulation in ionomycin-anergised cells when

compared to unstimulated cells in the absence of proteasome inhibitors [183]. Interestingly, whilst Cbl-b is also more intensely expressed at 6 h in ionomycin+PMA-stimulated cells than cells stimulated with ionomycin alone, the opposite happens at 20 h (**Figure 3.9**). This latter finding is in keeping with a study which showed increased Cbl-b expression after ionomycin stimulation comparing to ionomycin+PMA and unstimulated cells after 24 h of stimulation in fetal liver chimeras of CD4<sup>+</sup> T cells [203].

A more recent study also found Cbl-b protein expression was upregulated after *in vitro* stimulation; curiously, although initially anti-CD3-stimulated cells expressed more Cbl-b than anti-CD3+anti-CD28-stimulated cells (4 and 8 h), in keeping with the results presented in this thesis, at later time-points (12, 24, 48 and 72 h) the reverse was true [297]. Indeed, in long-term ( $\pm$  120 h) *in vitro* culture experiments (**Figure 3.37**), priming LN cells were still expressing more Cbl-b than those undergoing anergy or naïve cells. Consistent with this, and counter to what was previously thought from Cbl-b knockout studies [182, 190, 193-195], Cbl-b may be involved in positive regulation of T cell activation, as a recent study showed it can associate and polyubiquitinate SHIP for proteasomal degradation [298]. However, most studies still point towards Cbl-b playing a role in the negative regulation of T cell activation, by means of dampening and/or terminating TCR signalling with such possible downstream targets as Vav, Akt, Erk, p38 and PLC $\gamma$ -1 [188, 193]. Cbl-b can also target TCR signalling directly, as loss of Cbl-b increased the phosphorylation of TCR $\zeta$  without affecting TCR degradation, leading to augmented T cell activation and spontaneous autoimmunity [221]; such direct regulation of TCR activity is achieved by polyubiquitinating TCR $\zeta$  via a K33 linkage, which reduces its association with Zap-70 [221]. Thus, these contradictory and counterregulatory effects of Cbl-b may be explained by a model that suggests that in the first 24 h Cbl-b contributes to reduce IL-2 production and IL-2R and CD71 expression by regulating TCR signalling (both in anti-CD3- and anti-CD3+CD28-stimulated CD4<sup>+</sup> T cells); after 24 h upregulation of Cbl-b may result not only in de-sensitisation of TCR signalling but also in preventing cell cycle progression and proliferation in the absence of antigen [297].

However, despite this model, to date Cbl-b expression had not been analysed in the context of cell cycle stage; this has now been done in this study using LSC. Perhaps arguing against the above model, however, after 20 h of stimulation a higher proportion of CD4<sup>+</sup>Cbl-b<sup>+</sup> cells could be found in the mitotic phases than in G0/G1, regardless of the nature of the stimulus (**Figure 3.23**). Interestingly, the population of cells stimulated with anti-CD3+anti-CD28 showed a considerable higher proportion of their CD4<sup>+</sup>Cbl-

b<sup>+</sup> cells in G0/G1 (42%) than any of the other populations, although it also seems to express Cbl-b more intensely in CD4<sup>+</sup>Cbl-b<sup>+</sup> cells in the mitotic stages. Moreover, analysis of the expression of Cbl-b according to cell cycle stage at 40 h of *in vitro* stimulation revealed similar profiles (**Figure 3.24**), as again the majority of CD4<sup>+</sup>Cbl-b<sup>+</sup> cells are found in the mitotic stages regardless of the nature of the stimulus. Though others have reported Cbl-b negatively regulating cell survival and late cell cycle progression (but not cell cycle entry) [196, 297], in these current data, high levels of Cbl-b expression per se do not appear to dictate cell cycle arrest.

#### 4.2.2 Maintenance

As Cbl-b has been reported to be involved in modulating TCR ligation and CD28 co-stimulation signalling in the maintenance phase of anergy and priming [193], as well as being upregulated in anergic T cells following ionomycin re-stimulation [193], Cbl-b expression was next assessed in the maintenance phase of anergic and primed cells. Again in this *in vitro* model, after 20 h of re-stimulation with LPS-matured, OVA-loaded DCs, Cbl-b levels appear to be similar in anergic and primed LN cells (**Figure 3.37**) and anergic and primed KJ1-26<sup>+</sup> T cells (**Figure 3.40**), as determined by Western blotting. Indeed, single cell analysis by LSC shows that, while Cbl-b expression is upregulated in the anergic and primed populations, it is the primed population of KJ1-26<sup>+</sup> T cells that has the highest proportion of cells expressing Cbl-b and the primed KJ1-26<sup>+</sup> T cells have the most intense expression of Cbl-b (**Figure 3.45**). Interestingly, after just 1 h of co-culture with LPS-matured, OVA-loaded DCs, the primed population of KJ1-26<sup>+</sup> T is already shown to be upregulating Cbl-b when compared to naïve and anergic cells (**Figure 3.44**). Also interesting, while Cbl-b is expressed most highly at the periphery of anergic T cells after 1 h of re-stimulation (**Figure 3.44**), after 20 h it is the primed T cells that express Cbl-b more intensely at the periphery (**Figure 3.45**). These data may therefore point towards different kinetics in the regulation of Cbl-b expression and consequent differential mechanisms of action of this E3 ligase in the maintenance phase of priming versus tolerance; as Cbl-b appears to be concentrated in the periphery of anergic cells at early time points this would be consistent with its roles in blocking early CD28-mediated signalling in anergic T cells, namely by downregulating PKC $\theta$  and p85 $\alpha$  [183, 190, 191] and by interfering with IS activity [208]. Also, later on, the primed cells express Cbl-b more intensely at the periphery which is consistent with Cbl-b's involvement in dampening TCR ligation+CD28-costimulation signalling in order to prevent hyperreactivity; this can be achieved by

downregulating the TCR, PLC $\gamma$ -1, Vav, Akt, Erk and/or p38 [188, 193, 221], or, at least in the induction phase by inhibiting cell cycle progression [297].

Expression of Cbl-b was analysed in the naïve, anergic and primed populations of T cells and correlated with cell cycle stage after 20 h of (re-)stimulation with LPS-matured, OVA-loaded DCs (**Figure 3.52**). Consistent with the data from the induction phase experiments, which showed that KJ1-26<sup>+</sup>Cbl-b<sup>+</sup> T cells undergoing priming could be found mainly in the G0/G1 phase at this time point, the “naïve” population - which is effectively undergoing antigen-driven priming - also shows a high and equivalent proportion of their KJ1-26<sup>+</sup>Cbl-b<sup>+</sup> cells in G0/G1. In fact, both the naïve and the primed population have roughly the same proportion of their KJ1-26<sup>+</sup>Cbl-b<sup>+</sup> T cells in G0/G1 (~40%), which is a higher proportion than that of the equivalent anergic population. Interestingly, and like what happens during the induction phase, generally, the level of expression of Cbl-b is lowest in apoptotic and G0/G1-arrested cells, regardless of stimulus (**Figure 3.52**). Although the three populations have roughly the same proportion of their KJ1-26<sup>+</sup>Cbl-b<sup>+</sup> T cells in the S phase (~40%), the anergic population is the one with the highest percentage of KJ1-26<sup>+</sup>Cbl-b<sup>+</sup> T NFDCs (35%). As seen in the induction phase therefore, high levels of Cbl-b expression *per se* do not appear to dictate cell cycle arrest (one might think they might actually be associated with proliferation in anergic cells). However, expression of Cbl-b in re-stimulated primed antigen-specific T cells is predominantly associated with the G0/G1 stage and might contribute to a G1/S block associated with homeostatic regulation.

Following secondary antigenic challenge *in vivo*, and consistent with the *in vitro* data, although not significant, if anything there appears to be higher expression of Cbl-b, both in terms of the proportion of antigen-specific T cells and levels of expression in such Cbl-b<sup>+</sup> cells, in the primed relative to tolerised mice (**Figure 3.56**). Perhaps reflecting this, after challenge with antigen, there is a higher percentage of KJ1-26<sup>+</sup> T cells from the naïve population expressing Cbl-b and higher levels of Cbl-b expression in such Cbl-b<sup>+</sup> cells compared to either the re-stimulated tolerised or primed mice (**Figure 3.56**). Also, this primary response population of KJ1-26<sup>+</sup> T cells in the paracortex has a significantly higher percentage of cells positive for Cbl-b than that of the equivalent tolerised population of KJ1-26<sup>+</sup> T cells (**Figure 3.57**).

In fact, the general trend is that the naïve population of KJ1-26<sup>+</sup> T cells undergoing a primary priming response, either in the paracortex or the follicles, has a higher percentage of cells positive for Cbl-b and a higher intensity of expression of Cbl-b than either the tolerised or primed populations (**Figure 3.57**). Moreover, analysis of

Cbl-b expression *in vivo* does not show a clear correlation between this parameter and differential function in terms of the maintenance phases of tolerance or priming, *in vivo*. Hence, its functions may lie more in the direction of TCR signal modulation rather than promotion/maintenance of anergy. Similarly, Cbl-b expression does not appear to correlate with a particular LN location of antigen-specific T cells, regardless of their activation/functional status. Indeed, it may be that Cbl-b is more involved in holding T cells in check by preventing excess activation rather being involved as a selective agent for anergy promotion/enforcement.

If T cells without functioning Cbl-b [123] and Cbl-b<sup>-/-</sup> T cells are susceptible to anergy [196], and taking into account the above data provided by this thesis, why does Cbl-b deficiency predispose toward autoimmunity [194, 195]? Part of the explanation may relate to the increased resistance of Cbl-b<sup>-/-</sup> T cells to dominant/extrinsic peripheral tolerance factors such as TGF- $\beta$  and T<sub>reg</sub> cells [197, 198]. Also, Cbl-b is also expressed in other tissues [174] and immune cells [175, 177, 179], whose functions might contribute to tolerance induction. Another potential factor may be that Cbl-b is involved in regulating the transition from the DN stage in developing thymocytes [299] and thus Cbl-b knockout mice bear developmentally-compromised T cells. Additionally, because self-reactive T cells can express effector functions transiently while they are undergoing peripheral tolerance [109, 300], the augmented initial expansion observed in Cbl-b<sup>-/-</sup> T cells immediately following self-antigen recognition could result in a greater amount of effector functions just because there are now more self-reactive cells even though the effector activities of individual T cells are not enhanced. Finally, one has to consider the different nature of the “anergy” condition *in vivo* and *in vitro*; considering that proliferation is a critical determinant in regulating anergy *in vitro* [49], but not *in vivo* [301], and that Cbl-b regulates proliferation [194, 195], it is perhaps less surprising that Cbl-b may play a more critical role in regulating anergy in experimental models *in vitro* than *in vivo*. However Cbl-b may act as a more general and less anergy-specific gatekeeper of lymphocyte activation, nonetheless targeting different substrates in response to functionally different stimuli to ensure that immune tolerance is properly maintained. Understanding such mechanisms may therefore benefit therapeutic intervention in human autoimmune diseases.

## 4.3 Itch

### 4.3.1 Induction

As with Cbl-b, the data presented in this thesis suggest that Itch is upregulated, as evidenced by Western blotting (**Figure 3.6 and 3.9**) and LSC (**Figure 3.15**), in CD4<sup>+</sup> T cells undergoing induction of both priming and anergy, when compared to naïve cells; however, CD4<sup>+</sup> T cells undergoing priming appear to express more Itch than those being anergised. This upregulation occurs in T cells regardless of the nature of the stimulus, ie, whether it involves TCR ligation by means of antibody or direct mobilisation of Ca<sup>2+</sup> by a pharmacological agent; the pathway(s) that leads to such upregulation therefore probably requires Ca<sup>2+</sup> flux and calcineurin in both cases, as previously reported for ionomycin-mediated anergy of a T cell line [183]. However, distinct signals may also be involved as when CD4<sup>+</sup> T cells are stimulated by the pharmacological agents this induces increased intensity of Itch expression in CD4<sup>+</sup>Itch<sup>+</sup> cells while TCR ligation results in an increased percentage of cells which express Itch (**Figure 3.15**). The studies with the *in vivo* model for induction of tolerance and priming confirmed expression of Itch in tolerised and primed antigen-specific T cells, although no significant differences between the two groups after 5 d of tolerance or priming induction in terms of proportion of antigen-specific T cells positive for Itch or in terms of intensity of total Itch protein expression per antigen-specific T cell could be found (**Figure 3.30**). This further strengthens the view that Itch plays roles in T cell signalling other than in just the context of anergy. In fact, as described in the Introduction section, Itch expression and activity favours T<sub>H</sub>1 differentiation by targeting the T<sub>H</sub>2-driving transcription factor JunB for degradation; this occurs after TCR ligation plus CD28 co-stimulation-mediated Jnk activation, which in turn activates Itch [226, 228]. It is also thought Itch-mediated degradation of JunB and c-Jun can suppress AP-1 formation and thus contribute to anergy [222], although the signalling inputs that would lead to Itch activation will have to be different since CD28 co-stimulation would not lead to anergy. One such differential signalling input could be CTLA-4-mediated, promoting anergy and leading to Itch activation [231]. Itch is most likely therefore to be involved in signalling in both priming and tolerance of T cells, although the pathways which lead to its activity in each case will impart different functional outcomes.

While Itch activity can be modulated by kinases [226, 228, 229], this is not the only way to regulate Itch. In fact, Itch proteasomal degradation has been reported

following a process in which Itch polyubiquitinates itself [302] and consistent with this, association between Itch and the ubiquitin protease FAM/USP9X was shown to prevent Itch degradation [302]. Moreover, another study in human cell lines, showed that auto-polyubiquitination of Itch via K29-linked chains, leads to its lysosomal degradation [303]. In the present study, after proteasome inhibition, Itch accumulates more in CD4<sup>+</sup> T cells undergoing anergy (anti-CD3) than priming (anti-CD3+anti-CD28) (**Figure 3.7**); as Itch appears to be more expressed in priming than anergising cells in the absence of proteasome inhibition, these data suggest that TCR ligation-mediated Itch upregulation is a very dynamic process reflecting a high turnover of Itch while the less dynamic process observed under conditions of CD28 co-stimulation ultimately results in stronger Itch expression at this time point. Curiously, T cells undergoing ionomycin-induced anergy do not display increased accumulation of Itch after proteasomal inhibition (**Figure 3.7**), giving rise to the possibility that Itch is not being dynamically regulated or alternatively, any such degradation of Itch is lysosome-mediated.

Itch has been recently implicated in cell survival [304], albeit in a non-T cell related context; Itch was shown to ubiquitinate Bid, a pro-apoptotic protein of the Bcl-2 family involved in death receptor-mediated apoptosis [305], targeting it to the proteasome and decreasing cellular apoptosis [304]. The expression of Itch in this context during priming and tolerance of T cells had not been analysed before and so to address whether the higher expression of Itch in primed cells reflected a role for this E3 ligase in promoting survival, we correlated Itch expression with apoptosis and cell cycle progression. Interestingly, these data show that only a low percentage of CD4<sup>+</sup>Itch<sup>+</sup> cells from the unstimulated population are apoptotic (16%), and the other populations have even a lower percentage of their CD4<sup>+</sup>Itch<sup>+</sup> cells in apoptosis (less than 5%) after 20 h of *in vitro* stimulation (**Figure 3.25**). However, by 40 h of stimulation although the percentage of non-apoptotic CD4<sup>+</sup>Itch<sup>+</sup> cells is still higher than the percentage of apoptotic CD4<sup>+</sup>Itch<sup>+</sup> cells in all populations, the proportion of CD4<sup>+</sup>Itch<sup>+</sup> T cells has increased substantially in response to all stimuli apart from ionomycin (**Figure 3.26**). These data may indicate Itch is not working as a mediator of cell survival in TCR-mediated signalling and may reflect the finding that at 20 h, the highest proportion of CD4<sup>+</sup>Itch<sup>+</sup> cells from the naïve (unstimulated), anergic (anti-CD3) and primed (anti-CD3+anti-CD28) groups could be found in the G0/G1 phase, perhaps indicating their growth arrest prior to commitment to apoptosis. By contrast, the highest percentage of CD4<sup>+</sup>Itch<sup>+</sup> T cells from the ionomycin and ionomycin+PMA groups at 20 h could be found in the mitotic stages (**Figure 3.25**) and by 40 h all stimuli yielded a higher

proportion of CD4<sup>+</sup>Itch<sup>+</sup> cells in the mitotic stages (**Figure 3.26**); moreover, Itch intensity of expression also seemed to increase with cell cycle progression regardless of the functional outcome of the population, at least at 20 h (**Figure 3.25**). Taken together these data reveal that the mechanism used to prime or anergise T cells (antibodies Vs pharmacological agents) influences the kinetics of Itch expression in a population of T cells, depending on the cell cycle stage. Also, regardless of functional outcome of the population, Itch expression is more associated with mitosis than cell cycle arrest, and least associated with apoptosis.

### **4.3.2 Maintenance**

The studies analysing the maintenance phase show that just after 1 h of (re-) stimulation by antigen primed KJ1-26<sup>+</sup> T cells are already upregulating Itch while the naïve and the anergic populations exhibit comparable lower proportions of Itch-positive cells irrespective of whether they have been exposed to antigen or not (**Figure 3.46**). By 20 h following (re-)stimulation by antigen, both anergic and primed populations were found to be upregulating Itch expression, when compared to the naïve population (**Figure 3.48**). Therefore, it seems that in the maintenance phase, like in the induction phase, priming induces Itch expression more strongly than anergy. As Itch expression was observed to be upregulated at the periphery of anergic and primed cells, compared to naïve cells (**Figure 3.48**), part of this effect could be due to the reported relocation of Itch from the cytoplasm to endocytic vesicles observed in anergic cells re-stimulated with antigen [183]. Interestingly, the primed cells showed foci of concentrated Itch expression in the periphery, which is consistent with Itch being expressed in endocytic vesicles (**Figure 3.49**). However, naïve cells also express Itch at the periphery and the upregulation in anergic cells could merely reflect a higher intensity of expression in this area rather than relocation, as Itch is known to be strongly associated with endocytic vesicles [306]; the present data cannot rule out the possibility that relocation occurs, although it might not necessarily be a hallmark of Itch-mediated maintenance of anergy.

Correlation of Itch expression with cell cycle stage after re-stimulation with antigen revealed Itch to be expressed more intensely in KJ1-26<sup>+</sup>Itch<sup>+</sup> cells in the advanced stages of cell cycle, regardless of the functional status of the population both at the 1 h (**Figure 3.53**) and the 20 h (**Figure 3.54**) time points; these results are similar to the ones observed for the induction phase. Also similar is the fact Itch expression is least associated with apoptosis. What is clearly different from the induction phase is the distribution of KJ1-26<sup>+</sup>Itch<sup>+</sup> cells according to cell cycle stage; in the maintenance

phase naïve, anergic and primed populations exhibit differential distribution profiles of KJ1-26<sup>+</sup>Itch<sup>+</sup> T cells, indicating that the functional status of the cell may be an important factor in the maintenance phase of priming and anergy; in fact, under these conditions, in the anergic population Itch expression could indeed be related to apoptotic and G0/G1 T cells.

Following secondary antigenic challenge *in vivo*, and unlike the *in vitro* data, no upregulation of Itch was observed in either the tolerised or primed tissues, compared to the naïve tissue (**Figure 3.58**), as all groups have equivalent percentages of KJ1-26<sup>+</sup>Itch<sup>+</sup> cells and equivalent Itch intensity of expression in those KJ1-26<sup>+</sup>Itch<sup>+</sup> cells. There were also no significant differences in terms of intensity of Itch expression according to LN localisation between naïve, anergic or primed KJ1-26<sup>+</sup> cells (**Figure 3.59**). However, the percentage of antigen-stimulated naïve KJ1-26<sup>+</sup> T cells expressing Itch is higher in those cells located in the paracortex relative to the follicles and it is also higher than either tolerised or primed KJ1-26<sup>+</sup> T cells, irrespective of the LN location. This is an interesting result as these naïve T cells are undergoing a primary priming response and hence should migrate into B cell follicles. While these cells do indeed migrate into the follicles as much as re-challenged tolerised and primed cells (**Figure 3.55**), perhaps the higher percentage of Itch-positive KJ1-26<sup>+</sup> T cells observed in the paracortex suggests that these cells are being signalled not to migrate into the follicles by an Itch-dependent homeostatic mechanism to control hyperreactivity of the induction of priming. Indeed, a role for Itch in preventing unwarranted expansion of B cells has already been described [224], although these were not conventional LN B cells.

As suggested by the results in the present study, there is increasing evidence from the literature that the involvement of Itch in regulating T cell anergy is not straightforward. For example, a recent study has shown that siRNA-mediated knockdown of Itch leads to a downregulation of IFN $\gamma$  and IL-2 mRNA after re-stimulation [231] a finding that is rather counterintuitive given that an upregulation of the production of these two cytokines might have been expected in the absence of a protein which promotes anergy. However, deficiency of Itch is known to favour T<sub>H</sub>2 differentiation [222] (in the *in vivo* model used in the studies reported in this thesis, stimulation of the transgenic antigen-specific T cells gives rise to a mixed T<sub>H</sub>1/T<sub>H</sub>2 phenotype) and as such, under these conditions other effector cytokines than IFN- $\gamma$  and IL-2 could be favoured. Itch has also been shown to mediate K29-polyubiquitination of Deltex1, targeting it to the lysosome [303] and Deltex1, which is a transcription target of NFAT, is reported to be upregulated in T cells undergoing anergy where it is thought

to inhibit their activation by promoting optimum expression of Cbl-b via interaction with Egr2 [307]. Again, therefore, Itch-mediated degradation of Deltex1 would seem to be counterproductive for anergy induction.

Thus, in the light of the high expression of Itch exhibited by primed cells in this study together with previously published reports of the induction of anergy in Itch-defective T cells [183, 231], it is necessary to question whether Itch is a factor for T cell anergy. If not, how is it possible to explain the severe autoimmune phenotype of the itchy mice [210-212]? Certainly, part of the inflammation observed in those mice was caused by lymphocyte-independent dysregulation of the innate immune system [213] as well as the resistance of Itch<sup>-/-</sup> T cells to undergo anergy in response to T<sub>reg</sub>-mediated inhibition and to TGF- $\beta$  treatment [218]. Additionally, Itch has also been reported to be involved in dampening the signal in priming T cells [223], and as such even properly primed Itch-deficient T cells could become hyperreactive, contributing to the autoimmune phenotype. Finally, Itch can influence T cell differentiation and polarisation [222], and hence its deficiency alters the balance between the clones of effector T<sub>H</sub> cells further contributing to the autoimmune phenotype. Having said that, Itch is expressed in both the induction and maintenance phases of T cell anergy and, under such conditions, has been shown to act to prevent the activation of the transcriptional program leading up to T cell priming [183]. Thus, Itch can drive T cell anergy but this is not its exclusive role; Itch acts in the context of TCR signalling, both in the context of T cell priming and T cell anergy. Coupled with its role in T cell differentiation, Itch appears to act as a fine regulator of T cell responses.

Itch is also of importance for the modulation of the human immune system, as can be seen from the recent description of the first human phenotype associated with Itch deficiency [308]. Those patients, who have a mutation resulting in truncation of Itch, display morphologic and developmental abnormalities and may develop a multisystemic autoimmune disease characterised by cell infiltration of the lungs, liver and gut [308]. The fact that not all of these Itch-deficient patients have severe autoimmune disease suggests the involvement of other modifiers, either genetic or environmental, in promoting quiescence, although the activity of other ubiquitin-protein ligases was not sufficient to restore a normal phenotype [308]. As such, the study of Itch modulation of the immune system may yet result in potential human beneficial therapeutic intervention.

## 4.4 Grail

### 4.4.1 Induction

Grail is expressed in LN cells and, in contrast to what was expected, was found to be upregulated in CD4<sup>+</sup> T cells undergoing priming, compared to those from either the unstimulated or anergic groups of cells after 20 h of stimulation (**Figures 3.2 and 3.6**). However, proteasome inhibition leads to Grail accumulation in anti-CD3-induced anergic cells but not primed cells suggesting that Grail may have been expressed at higher levels transiently during the processes leading to induction of anergy (**Figure 3.7**). Nevertheless, these data taken together point towards TCR ligation leading to Grail upregulation and CD28 co-stimulation preventing its proteasome-mediated degradation, thus keeping Grail expression high in primed T cells, at the 20 h time point. As Grail expression has been associated to anergy induction [233] and also reported to be high in naïve T cells [235], these results were not expected. However, a recent study showed that priming CD4<sup>+</sup> T cells with anti-CD3+anti-CD28 only leads to Grail downregulation after 20 h [248]. This downregulation was found to be dependent on CD28 co-stimulation and required for T cell proliferation and IL-2 production [248]. For full Grail downregulation however, IL-2R signalling via STAT5, Akt and mTOR is needed [248] which, at the 20 h time point of the *in vitro* system used in the studies reported in this thesis, would not yet have achieved full strength.

Interestingly, after 48 h of stimulation, Grail was found to be expressed more in anti-CD3-stimulated cells than in anti-CD3+anti-CD28-stimulated cells (**Figure 3.9**), in agreement with the above study reporting Grail downregulation after 20 h that is maintained until at least the 48 h time point following anti-CD3+anti-CD28-mediated priming of CD4<sup>+</sup> T cells [248]. By contrast, ionomycin+PMA-stimulated cells express Grail more intensely than cells stimulated with ionomycin alone, at 3 and 6 h of *in vitro* culture, though at 20 h the opposite happens (**Figure 3.9**). Interestingly, at 20 h in ionomycin-treated cells, Grail is not being downregulated by proteasome degradation (**Figure 3.7**). The expression of Grail at the single cell level after 20 h of stimulation was also quantified by the LSC (**Figure 3.19**), revealing a lower proportion of ionomycin+PMA-stimulated CD4<sup>+</sup> T cells expressing Grail than any other populations, consistent with the Western blotting findings (**Figure 3.9**). Also consistent with the Western blotting findings, the anti-CD3+anti-CD28-stimulated population has a higher proportion of cells expressing Grail and a higher intensity of Grail expression per Grail-

positive cell than anti-CD3-stimulated cells (**Figure 3.19**). It is clear from these data that anergising cells via TCR ligation or via direct  $\text{Ca}^{2+}$  mobilisation has very different consequences on Grail regulation and on the kinetics of Grail regulation, despite similar functional outcomes. Although the high expression at early time points may be surprising at first, it has been shown recently that ionomycin+PMA stimulus can indeed induce strong Grail expression; thus, in primary murine  $\text{T}_{\text{H}1}$  cells stimulated with ionomycin+PMA, *Grail* expression was found to be activated by direct binding of NFAT dimers to the *Grail* promoter [309]. Also in this study, ionomycin-mediated anergy induction in primary murine  $\text{T}_{\text{H}1}$  cells, also increased NFAT dimers binding to the *Grail* promoter [309], agreeing with the findings of the present study that E3 ligases are similarly regulated, at least during the early stages of induction of both priming and tolerance.

Interestingly, fluorescence imaging of these populations of cells revealed the biggest difference lies between unstimulated (naïve) and stimulated (regardless of stimulus) cells as unstimulated  $\text{CD4}^{+}$  T cells have a rather diffuse Grail expression and stimulated cells have a more intense and peripheral Grail expression (**Figure 3.20**). This is consistent with Grail being reported as an endosomal protein [233], though evidence for relocation to the endosomes can not really be concluded from these fluorescent microscopy images.

At the 40 h time point in our single-cell analysis of Grail expression, Grail expression was found to be higher in anti-CD3- than in anti-CD3+anti-CD28-stimulated  $\text{CD4}^{+}$  T cells (**Figure 3.21**), in agreement with the Western blotting data regarding the kinetics of Grail expression as well as with the study which reported that Grail downregulation after 20 h was maintained until at least 48 h [248].

Regulation of Grail appears to be transcriptional, translational and posttranslational as another recent study reported Grail mRNA expression by naïve  $\text{CD4}^{+}$  T cells was upregulated 2 d after *in vitro* stimulation with anti-CD3, peaking at D3; however, although stimulation with anti-CD3+anti-CD28 also upregulated Grail mRNA expression at D2, by D3 these levels were reduced [236]. What the different data are showing is that Grail upregulation is not exclusive to anergic cells, as previously thought; in fact, the differential upregulation of Grail proposed for anergic versus primed cells takes considerable time (~2 d). Moreover, Grail is dynamically synthesised and degraded according to different stimuli; the timing and extent to which these occur is of further assistance to the final functional outcome of the cell. For example, recent work has shown that Grail can have an effect on the activation status of

Erk in primed T cells: after 30 min of TCR ligation and co-stimulation, Grail<sup>-/-</sup> splenic naïve CD4<sup>+</sup> T cells showed more phosphorylated and total Erk than wt cells, while no differences were found at the level of calcineurin or NFAT expression [235]. Also very interestingly, it has been reported that anti-CD3-stimulated (anergising) Grail<sup>-/-</sup> CD4<sup>+</sup> T cells expressed less Lck, Zap70 and PKC $\theta$  than wt cells at 24 h (there was no difference between wt and Grail<sup>-/-</sup> naïve populations of cells) [236], which would place Grail as a positive regulator of these proteins during the first 24 h of anergy induction, an apparent contradiction as Lck, Zap70 and PKC $\theta$  are involved in the promotion of proliferation and cytokine production. Of course, the process of anergy induction does lead initially to the clonal expansion of T cells [109], so these results are not completely irreconcilable.

A role for Grail in cell cycle arrest or apoptosis induction has not yet been described. Similarly, Grail expression has not been analysed according to the different cell cycle stages. Using the LSC it was possible to achieve this, at the single-cell level. After 20 h of stimulation Grail was found to be expressed more intensely in mitotic cells than cells in any other stages while a higher proportion of CD4<sup>+</sup>Grail<sup>+</sup> cells could be found in the G0/G1 than in the mitotic phases, regardless of the nature of the stimulus (**Figure 3.27**). This would appear to indicate Grail is not really involved in regulating T cell anergy or priming via cell cycle regulation. In fact, any association of Grail with G0/G1 observed at 20 h presumably reflected cells transiting through this stage as, at 40 h, apart from the anti-CD3+anti-CD28-stimulated population, in all other populations the majority of CD4<sup>+</sup>Grail<sup>+</sup> cells are in the mitotic stages (**Figure 3.28**). However, the high proportion of CD4<sup>+</sup>Grail<sup>+</sup> cells from the anti-CD3+anti-CD28-stimulated population which can be found in apoptosis at 40 h, coupled with the high intensity of Grail expression in CD4<sup>+</sup>Grail<sup>+</sup> cells in both apoptotic and G0/G1 phases at 20 h does contribute to the idea that Grail may act to dampen T cell activation, preventing hyper-responsiveness under priming conditions. Though evidence for Grail promoting direct induction of apoptosis has not yet been demonstrated - to the contrary, T<sub>H</sub>1, T<sub>H</sub>2 and T<sub>H</sub>17 populations of Grail<sup>-/-</sup> splenic CD4<sup>+</sup> T cells actually had less viability after 5 d of *in vitro* stimulation than Grail<sup>+/+</sup> cells [235] - both anti-CD3- and anti-CD3+anti-CD28-stimulated Grail<sup>-/-</sup> CD4<sup>+</sup> T cells exhibited enhanced proliferation and IL-2 and IFN $\gamma$  production when compared to similarly-stimulated wt cells [235, 236]. Again, collectively, these data seem to suggest Grail is involved, as a negative modulator, in the control of T cell activation. However, Grail deficiency is not enough to completely suppress the requirement for CD28 co-stimulation as anergising Grail<sup>-/-</sup> CD4<sup>+</sup> T cells

still exhibited less proliferation and cytokine production than wt priming cells [235, 236].

In terms of how Grail could modulate T cell activation, as mentioned above, this could be initiated via the downregulation of total and phosphorylated Erk, which takes place within 30 min of TCR ligation and co-stimulation [235]. It is also interesting, in the context of the differential results obtained in the present study, to point out that, from the functional point of view it is not equivalent to study the effect of Grail in anti-CD3+anti-CD28- and ionomycin+PMA-mediated priming cells as Grail<sup>-/-</sup> splenic naïve CD4<sup>+</sup> T cells showed higher proliferation during anti-CD3+anti-CD28 stimulation than wt cells, while ionomycin+PMA-stimulated Grail-deficient cells did not [235]. As Grail is usually associated with hyporesponsiveness and can probably assist in preventing hyperresponsiveness, it is interesting to note that such ionomycin+PMA stimulation does not lead to a differential functional outcome in wt and Grail<sup>-/-</sup> T cells when the data here (**Figure 3.9**) and that of others [309] did show upregulation of Grail in ionomycin+PMA-stimulated cells. This is reminiscent of what was observed during anergy induction, that is, that direct Ca<sup>2+</sup> mobilisation has different consequences for Grail expression regulation and function than TCR ligation-mediated Ca<sup>2+</sup> mobilisation - not only in anergy induction but also in priming.

#### **4.4.2 Maintenance**

After prolonged *in vitro* culture, naïve LN cells express more Grail than anergic or primed cells (**Figure 3.37**), perhaps indicative of their resting state and potential consequent induction of apoptosis due to lack of selection signals. Moreover, the experiments studying the maintenance phase of anergy and priming show that after re-stimulation with LPS-matured, OVA-loaded DCs, naïve and anergic LN cells from DO11.10 mice upregulate Grail expression more than primed cells (**Figure 3.37**), the further upregulation during the maintenance phase of anergy relative to that of priming being unlike what happens in the similar stage of the induction phases of these functional outcomes. Indeed, anergised DO11.10 TCR-transgenic T cells (either via ionomycin or TCR ligation in the absence of co-stimulation) express higher levels of Grail than primed DO11.10 T cells after re-stimulation with LPS-matured, OVA-loaded DCs (**Figure 3.40**). In fact Grail protein has previously been shown to be downregulated in the maintenance phase of primed CD4<sup>+</sup> T cells, after 24 h of anti-CD3+anti-CD28 re-stimulation, rather than with antigen as in the present study [310]; Grail was shown to ubiquitinate and degrade CD83 via the proteasome on CD4<sup>+</sup> T cells

anergised with ionomycin and re-stimulated with anti-CD3+anti-CD28 antibodies [310]. Downregulation of CD83, which is also expressed in DCs and mediates intercellular interactions between DCs and T cells, led to reduced proliferation and production of IL-2 and IL-17 [310].

So, Grail protein levels in each population appear to depend not only on the nature of the stimulus but also on whether that population of T cells is undergoing induction or maintaining a previously achieved functional state.

In the *in vivo* model of tolerance maintenance, after antigenic challenge Grail was expressed in a higher percentage of naïve DO11.10 TCR transgenic T cells undergoing a primary response than in tolerised or primed cells maintaining their differential functional outcomes to secondary challenge (**Figure 3.60**). This was interesting as at this time point, Grail was least expressed in tolerised DO11.10 TCR transgenic T cells, in contrast to what was suggested by the Western blotting data convey from the *in vitro* maintenance phase experiments, in which primed DO11.10 TCR transgenic T cells expressed the least Grail. These differences may reflect different kinetics of the *in vitro* and *in vivo* tolerance mediators.

Regarding the functionality of *in vivo* primed and tolerised T cells, it is hypothesised these tolerant T cells, once in the follicles, remain incapable of providing B cell help, unlike the primed T cells [267, 296]. As indicated by the present study, re-challenge of tolerised T cells induces their migration into B cell follicles as much as re-challenge of primed T cells (**Figure 3.55**). However, a higher percentage of DO11.10 TCR T cells located in the follicles express Grail than those in the paracortex (**Figure 3.61**); also, the antigen-specific T cells found in the follicles express more Grail than those found in the paracortex; this might hint towards the preference of Grail expression in T cells migrating into the follicles. Indeed, recent work has suggested that Grail is involved in the formation of the follicles, though there, retroviral expression of Grail in bone marrow chimeric mice was associated with diminished lymphoid follicle formation [245] while here Grail is associated with T cell presence in the follicular areas. The relatively downregulated expression of Grail detected in tolerised compared to naïve and primed DO11.10 TCR T cells localised in the follicles could, on the other hand, potentially implicate a role for Grail in capacitating T cells to provide B cell help, as there could be a threshold of Grail intensity of expression, that once reached would enable B cell help.

It would not be surprising that the cells termed “naïve” in this experiment would indeed also be providing B cell help as, for them antigen challenge comes as the

primary stimulus and they should be undergoing priming after that. This would implicate Grail as a promoter of T cell activation, a function which, so far, has not been described for Grail.

## 4.5 Smurfs

Smurf1 is expressed in naïve CD4<sup>+</sup> T cells and CD4<sup>+</sup> T cells during primary stimulation (**Figure 3.6**). The presence of a ladder of Smurf1 bands, coupled with the finding of co-precipitation of Smurf1 with ubiquitin (**Figure 3.4**) suggests Smurf1 is ubiquitinated and/or associated with ubiquitin-containing proteins. Smurf1 can ubiquitinate target proteins [250] and be itself ubiquitinated [254]; in either case, the ubiquitinated target is downmodulated. In anergising T cells, proteasome inhibition does lead to Smurf1 accumulation (**Figure 3.7**) and thus, it might be the case that whilst TCR ligation upregulates Smurf1, lack of CD28 co-stimulation does not prevent its proteasomal degradation. The *in vivo* study of the induction phase of tolerance and priming (**Figure 3.32**) revealed no significant differences between the two groups in terms of proportion of OVA peptide TCR-specific T cells positive for Smurf1 or in terms of intensity of total protein expression per OVA peptide TCR-specific T cell, although this last parameter did show slightly more intense expression of Smurf1 in the primed group, consistent with the Western blotting data. Likewise, the expression of Smurf1 after re-stimulation (maintenance phase) is roughly equivalent in anergic and primed cells (**Figure 3.37**).

Smurf2 is also expressed in CD4<sup>+</sup> T cells, but appears to be upregulated by priming stimuli (**Figure 3.6**). As proteasome inhibition leads to increased Smurf2 accumulation in anergised, but not naïve or primed, T cells (**Figure 3.7**), this may suggest that, *in vitro*, TCR ligation leads to Smurf2 upregulation and CD28 co-stimulation prevents its degradation by inhibiting its proteasomal degradation, thus keeping Smurf2 expression high in priming T cells. Alternatively, the proteasome inhibition data may reflect a transient high anergising signal via the TCR at an earlier time point. However, in our model of *in vivo* tolerance and priming induction, no significant differences between the tolerised and primed antigen-specific T cells were found after 5 d of stimulation (**Figure 3.33**). Also, after *in vitro* re-stimulation of DO11.10 cells, naïve, anergic and primed populations expressed the same amount of Smurf2 (**Figure 3.37**). It might be the case Smurf2 helps the establishment of signalling events leading to effective T cell priming; once this is accomplished Smurf2 expression

would return to its basal levels, a proposal perhaps consistent with the *in vitro* proteasomal inhibition data. Smurf2 could in fact assist in the signalling events leading to T cell priming by degrading Rap1 [249], as Rap1 accumulation in anergic T cells has been linked to inhibition of Erk activation [48, 131]. When T cell priming had taken place, Smurf2 could ubiquitinate itself, targeting its expression back to basal levels [253]; this could explain the ladder pattern observed in the long term *in vitro*-cultured naïve, anergic and primed cells. Smurf2 has also been found to be involved in downregulating TGF- $\beta$  signalling via ubiquitination of the TGF- $\beta$  receptor, leading to enhanced T cell activity [252, 311]. This is potentially interesting as it is thought experimental setups used for anergy induction can partly lead to T<sub>reg</sub> differentiation and T<sub>reg</sub>-mediated suppression, which can depend on TGF- $\beta$  signalling. In this case, Smurf2 would act to prevent T<sub>reg</sub>-mediated suppression of activated cells. Smurf2 has also been reported to be able to ubiquitinate and degrade Smurf1, adding another level of complexity to the mechanism [254].

## 4.6 Other potential anergy markers

Despite exhaustive characterisation of phenotype over the years, there is still no clear marker exclusive to anergic T cells. This is an issue that prevents not only recognition of the state of activation of T cells *in vivo* but which also limits the analysis potential of a number of *in vitro* experimental systems. Moreover, two major mechanisms of peripheral tolerance, cell-intrinsic anergy and the dominant tolerance afforded by T<sub>regs</sub>, can be co-ordinately induced by the exposure of T cells to antigen administered in a tolerogenic context, as shown by oral or intravenous administration of peptide, which upregulated both antigen-specific anergic T cells and CD4<sup>+</sup>CD25<sup>+</sup> T<sub>reg</sub> populations [30, 312, 313].

As most of the *in vitro* experimental systems rely on priming and anergising populations of cells and reading the collective output, single-cell analysis can be tricky since not all cells in an anergised population will be anergic. However single-cell analysis can be used to search for an anergy marker common and exclusive to all anergic cells.

For example, human anergic T cells were reported to exhibit differential localisation of Arf6 according to the activation state of T cells: in the plasma membrane, in anergic cells; and scattered throughout endosomes and the cytoplasm, in primed cells [288]. However, in our antigen-specific model of the maintenance of priming and

tolerance, Arf6 total protein levels or localisation could not be used to distinguish anergic from primed cells (**Figure 3.41**).

#### 4.6.1 *Traf6*

The expression of the adaptor protein Traf6, which promotes the activation of NF- $\kappa$ B in its capacity as an E3 ubiquitin-protein ligase [70, 71], was found to be upregulated in priming LN cells and highly reduced in ionomycin-induced anergising LN cells (**Figure 3.2**). However, in purified CD4<sup>+</sup> T cells only minimal differences were found although under conditions of anti-CD3-induced anergy, cells tended to express more Traf6 than primed cells (**Figure 3.6**). The idea of Traf6 as a positive mediator of T cell priming – derived from its role in the activation of the IKK complex, leading to translocation of NF- $\kappa$ B to the nucleus [71, 73] – could thus not be confirmed. Interestingly, and perhaps consistent with the present results, King *et al* [314], showed that Traf6 is actually required for anergy induction in T cells. According to their report, the loss of Traf6 restored the ability of CD28<sup>-/-</sup> T cells to proliferate and produce IL-2; consistent with this, Traf6- $\Delta$ T T cells showed resistance to anergising stimuli; and, interestingly, resistance to anti-CD3-mediated anergy induction was co-related with decreased mRNA and protein expression of Cbl-b [314]. So, it appears that, while Traf6 can promote IKK activation by means of K63 ubiquitination [315], leading to NF- $\kappa$ B activation, it can also have a role in anergy induction. Data from **Figure 3.6** can support both these apparently contradictory roles of Traf6, as it shows Traf6 is being expressed in both anergising and priming CD4<sup>+</sup> T cells; this would imply Traf6 is carrying out different functions according to context, which would require additional regulatory mechanisms, possibly posttranslational ones, behind this potential change of role; such mechanisms remain to be elucidated.

Since Traf6- $\Delta$ T T cells were resistant to the induction of anergy, the maintenance phase of anergy could not be assessed [314]. Data from **Figure 3.40** do not help to elucidate this point, as the KJ1-26<sup>+</sup> antigen-specific T cells were shown not to express Traf6, regardless of the functional state; perhaps this is an indication that Traf6 plays a secondary role in this phase. On the other hand, Traf6 is expressed in the cells from the non-KJ1-26<sup>+</sup> fraction, in which DCs will be found most abundantly. As Traf6 has been reported to be expressed in DCs, where it regulates the critical processes required for maturation, activation, and development [316], this finding does not come as a surprise. In DCs, proteasome-mediated degradation of Traf6 has been shown to inhibit pro-

inflammatory cytokine production [317] and, consistent with this role of Traf6 in promoting immune responses, Traf6 expression in the non-KJ1-26<sup>+</sup> fraction is differential as Traf6 is expressed most highly in the population co-cultured with the primed T cells (**Figure 3.40**).

#### 4.6.2 Ikaros

Ikaros expression was found only to be slightly upregulated after 20 h of anti-CD3-mediated anergy induction relative to that of priming CD4<sup>+</sup> T cells (**Figure 3.6**), a difference that was maintained until 120 h of the induction processes in LN cells (**Figure 3.37**). At the 120 h time point however, naïve, anergic and primed LN cells all expressed very high levels of Ikaros and, interestingly, after re-stimulation, Ikaros was expressed more strongly in primed and anergic T cells than naïve T cells, though it may be the case that relative to the non-re-stimulated T cells, that after re-stimulation all T cell populations downregulate Ikaros, the naïve T cells simply being the ones that downregulate it the most. Nevertheless, Ikaros is clearly expressed the most by primed KJ1-26<sup>+</sup> T cells, at slightly lower levels in TCR ligation-induced anergic T cells, although ionomycin-induced anergic T cells exhibit substantially less Ikaros expression (**Figure 3.40**).

While the induction phase results are somewhat within the parameters of the expected, as Thomas *et al* [119] had previously reported CD4<sup>+</sup> T cells with reduced Ikaros activity to be resistant to clonal anergy, the maintenance phase data are somewhat more intriguing. Moreover, the slight differences observed in the induction phase might be related to the way Ikaros function is controlled, and this does not seem to rely mostly on protein expression. Thus, Thomas *et al* [119] found that naïve, primed and anergic CD4<sup>+</sup> T cells expressed comparable amounts of Ikaros protein isoforms and that Ikaros binds to the *Il2* promoter/enhancer in resting CD4<sup>+</sup> T cells, meaning Ikaros can mediate anergy even when present at comparable levels to those expressed in naïve cells, and hence it is the regulation of the transcriptional repressor activity that is likely to take prime stage for anergy induction.

Thomas *et al* [119] did not look at what happens in the maintenance phase; in the present data Ikaros is more highly expressed in antigen-specific primed T cells than anergic ones, while one would expect that in anergic T cells Ikaros transcriptional repressor activity would be higher than in primed T cells. This is not necessarily contradictory as the function of Ikaros has been proven to be controlled by a multitude of mechanisms.

Ikaros function is controlled by posttranslational modification. For instance, Ikaros can be subject to SUMOylation, which does not alter its DNA-binding activity, but rather inhibits its association with co-repressor complexes [318]. Therefore, differential SUMOylation, a posttranslational modification which consists in the addition of the UBL SUMO to the target protein, in anergic Vs primed cells could alter the constituents of Ikaros complexes that bind to the *Ii2* promoter, and impact on the repressive capacity of Ikaros at this locus.

Ikaros has also been shown to be phosphorylated by CK2 in response to mitogenic signals, a posttranslational modification which inhibits Ikaros DNA binding activity allowing G1/S progression [319]. Moreover, Ikaros can be de-phosphorylated by PP1, resulting in its stabilisation and preventing its degradation [320]. The activity of Ikaros depends therefore on a delicate balance of two opposing signalling pathways and this balance can be shifted depending on differential extracellular signals such as co-stimulation from CD28 or IL-2R, translating into differential signalling events, say differential phosphorylation occurring under anergic versus primed conditions. Curiously, Ikaros can also form complexes with ubiquitin in the nucleus, and these are responsible for targeting Ikaros to the proteasome, for degradation [320].

Perhaps more interestingly, Ikaros can also promote gene activation [321]. This is accomplished by association with Brg-1, a catalytic subunit of the SWI/SNF nucleosome complex, while its role in gene repression is mediated by association with the histone deacetylase-containing complexes NuRD and Sin3 [322, 323]. The function(s) associated with Ikaros upregulation after re-stimulation of primed T cells remain therefore to be determined but as a marker for anergic cells, simple analysis of Ikaros expression can not be used.

## 4.7 Ubiquitination

Analysis of the ubiquitination status of total protein lysates does not reveal many differences between CD4<sup>+</sup> T cells undergoing priming and anergy (**Figure 3.10**). Both populations of cells show similar bands of ubiquitinated proteins, with a similar intensity. However, the kinetics of ubiquitination in response to the different stimuli are distinct as intensity of ubiquitination changes throughout the time points. These data do not conflict with those of a previous study showing upregulation of total protein ubiquitination in a T<sub>H</sub>1 cell line undergoing ionomycin-induced anergy, when compared to unstimulated cells [183], as such anergic cells were not compared to primed ones. As

ubiquitination is involved in TCR signalling in many ways, namely also in signalling pathways leading to T cell priming, measuring total levels in such a context is not necessarily informative. Rather it is more important to assess the status of some selected targets, which are crucial for the signalling pathways they are involved in. In this regard, immunoprecipitation of ubiquitin-containing complexes revealed co-precipitation of some E3s and PLC $\gamma$ -1 (**Figure 3.4**), suggesting ubiquitination as a possible modulation factor in the expression of PLC $\gamma$ -1 in the context of anergy induction in responses to anti-CD3, as has been described for ionomycin-induced anergy of T cells [183].

The kinetics and differential patterns and intensities of ubiquitinated proteins, observed in primed and anergic cells resulting from TCR signalling imply a rapid and dynamic upregulation and downregulation of proteins. For instance, the ubiquitination process at the IS can be detected as soon as 5 min after T cell-APC conjugate formation and it is maintained for up to at least 30 min [324]. In the IS, it is thought the TCR:CD3 complex is a prime target for regulation by ubiquitination [278] and its ubiquitination appears to be mediated both by Cbl-b and Itch [221], with effector proteins downstream from the TCR ubiquitinated later.

Analysing the expression of K63-linked polyubiquitinated proteins did reveal some potentially interesting differences between naïve (unstimulated) and the primed (anti-CD3+anti-CD28) and tolerised (anti-CD3) groups (**Figure 3.3**). The use of antibodies that specifically recognise a particular ubiquitin linkage is very useful in determining the potential regulatory mechanism involving that protein. For example, the HWA4C4 monoclonal antibody specifically recognises K63-linked polyubiquitin chains but not any other isopeptide-linked polyubiquitin or monoubiquitin and can be used for detection of proteins in whole lysates via Western blotting [325]. Obviously it will recognise all the K63-linked polyubiquitinated proteins in the whole cell lysate, displaying the pattern of K63-linked polyubiquitinated proteins. Whilst K48-linked polyubiquitination typically leads to protein degradation by the 26S proteasome, monoubiquitination and K63-linked polyubiquitination are usually associated with proteasome-independent regulatory processes [326]. It is interesting to note though, that K63-linked polyubiquitination can also lead to proteasomal degradation [327, 328], although this is not the usual outcome; instead it can promote downmodulation by targeting proteins to the endocytic pathway, where they can be recycled back to function or degraded in the lysosome [159].

One way of investigating which proteins are being degraded in the proteasome is to block it. Accumulation of polyubiquitinated proteins is a consequence of inhibition of proteasomal protein degradation and is observed as soon as 1 h after lactacystin treatment, reaching its peak after 16 h [329]. However this accumulation of proteins due to proteasome inhibition affects cell function; for instance, it induces apoptosis of activated human CD4<sup>+</sup> T cells compared to unstimulated cells and those cells surviving proteasome inhibition undergo inhibition of proliferation by induction of p27<sup>kip1</sup>-mediated G1 phase cell cycle arrest [329]; re-stimulated cells also proliferate less when treated with proteasome inhibitors [329]; moreover, production of IFN $\gamma$ , IL-4 and IL-5 production in human CD4<sup>+</sup> T cells activated by DCs was suppressed after proteasome inhibition [329]. The mechanism involved in this cytokine production suppression is actually of relevance for anergic T cells as it was found it was due to inhibition of activation and nuclear translocation of NFAT [329], a transcription factor reported to be involved in the upregulation of anergy factors [114]. Thus, while allowing studying the mechanism of regulation of critical components of the anergic program, proteasome inhibition can also influence it. Here, in the studies of the role of proteasome-mediated degradation in the expression of critical intermediaries in T cell anergy and priming (**Figure 3.7**), generally less protein was found in those cells treated with lactacystin than those which were not, an effect which could be related to induction of apoptosis/growth arrest. However, all the E3s sought for analysis could be found being expressed in these proteasome-inhibited cells, and as discussed above, some exhibited differential behaviour regarding the anergising or priming stimuli.

Finally, the study of the maintenance phase revealed that ubiquitination may develop a more prominent role in maintaining the anergic phenotype rather than the primed one. While the levels of ubiquitinated proteins do not vary much between the three populations after just 1 h of re-stimulation, after 20 h of re-stimulation there is an increase in protein ubiquitination in the periphery of anergic KJ1-26<sup>+</sup> T cells re-stimulated with LPS-matured, OVA-loaded DCs, compared to any of the other populations (**Figure 3.42**). Also, analysis of protein ubiquitination by Western blotting revealed that after re-stimulation of LN cells, the anergic population had the most intense protein ubiquitination (**Figure 3.38**).

## 4.8 E3 ubiquitin-protein ligases in the context of T cell anergy

Taken together, these results indicate that upregulation of E3 ligase expression is not exclusive to anergising and anergic T cells as previously thought [183], as priming and primed T cells also exhibit upregulation of these proteins, and, as such, inference about their expression can not be used as marker for anergic T cells. As the evidence for the role of E3s in the regulation of signal transduction pathways leading up to or maintaining anergy is increasing [116, 183, 236], so is the evidence for the role of E3s in the modulation of the activity of primed cells [193, 223, 241].

Another interesting point of discussion relates to the interactions between different E3s and, more specifically, whether there is cooperation or redundancy in their actions in the context of TCR signalling downmodulation. In defence of the unique function hypothesis, several studies, which focused on the phenotype of the knockout of a single E3 ligase [193-195, 222, 236], reported naïve T cells as being hyperresponsive to stimulation. However, as studies relying on the manipulation of a particular gene tend to overemphasize its function in a response, these mice could have developed a generic lower activation threshold which could lead to a more robust response after the induction of anergy regardless of the function of that particular molecule. In fact, some E3s have been shown to target the same substrates - for instance Cbl-b, Itch and Grail all ubiquitinate the TCR [221, 236] - and that is an indication that some degree of functional redundancy exists. However, while many E3 ubiquitin-protein ligases seem active after TCR stimulation (**Figure 3.4**), differences in the turnover rate of some of the E3s suggest some may act later or have a more short-term action in the induction of anergy than others, while also affecting different cellular processes. It is yet to be established which of these E3 ubiquitin-protein ligases are responsible for the long-term selective blocks preventing IL-2 production, though possibly some kind of cooperation between them takes place. Indeed, some of the processes regulated by E3s in T cell anergy do seem dependent on functional interactions between various anergy factors, such that all must work together to maintain T cells in the tolerant state. For instance, Grail and Cbl-b may be mechanistically linked through Cbl-b downregulation of Akt phosphorylation; a decrease in Akt phosphorylation decreases mTOR activation, abrogating otubain 1 protein expression and thus resulting in the upregulation of Grail and inhibition of cell proliferation. The nature of such cooperation is also up for discussion; some E3s have been shown to interact directly, as seen for example in Itch-mediated ubiquitination of Cbl-b [205], while other forms of interaction have also been

reported which are more indirect: for example, Itch can also inhibit upregulation of Cbl-b in the absence of anergy-inducing conditions by ubiquitinating Deltex1 [303, 307].

The modulation of the activity of these E3 ubiquitin-protein ligases is of paramount importance for their timely action in the induction of anergy. Interestingly, this can be achieved via ubiquitination (**Figure 3.7**). As mentioned before, for example, Itch can ubiquitinate Cbl-b targeting it for proteasomal degradation, but there are also reports of self-ubiquitination with regulatory value for Itch [302, 303], Grail [247], Smurf1 [254] and Smurf2 [253].

## **4.9 Dissecting the mechanisms underlying differential signalling in anergy and priming**

PLC $\gamma$ -1 is one of the key effectors of TCR signalling [55] promoting, via intermediaries, the Ca<sup>2+</sup> flux and Ras-Erk pathway activation that are required for T cell priming [14]. TCR signalling in the absence of CD28 co-stimulation results in Ca<sup>2+</sup> flux but impaired Ras-Erk pathway activation, leading to T cell anergy [45, 114]. While PLC $\gamma$ -1 is required for T cell priming, during the induction of anergy its expression and activity are downregulated [111, 183], indicating that it is one of the key targets of the anergy inducing program. We therefore initially used total expression of PLC $\gamma$ -1 as a way to assess the effectiveness of the different stimuli in inducing differential functional outcomes on T cells via Western blotting. Consistent with this proposal, PLC $\gamma$ -1 expression was found to be upregulated during priming and downregulated in T cells undergoing anergy when comparing to unstimulated naïve CD4<sup>+</sup> T cells (**Figures 3.2 and 3.6**). After prolonged T cell culture ( $\pm$  120 h), primed T cells still expressed more PLC $\gamma$ -1 than unstimulated or anergic cells (**Figure 3.37**) and, after re-stimulation, the primed cells continued to express more PLC $\gamma$ -1 than anergic cells (**Figure 3.37**). These (and other) data confirmed that the different stimuli were inducing the desired outcomes while also showing PLC $\gamma$ -1 protein expression changes according to the functional outcome of the cell.

To address the mechanisms underlying this modulation of protein expression it was found that PLC $\gamma$ -1 co-precipitates with ubiquitin as early as within 1 h during induction of anergy but not priming (**Figure 3.4**). By 20 h, cells undergoing both anergy and priming show substantial PLC $\gamma$ -1 co-precipitation with ubiquitin, suggesting this protein is being regulated by ubiquitination, as had been previously suggested [183].

While ubiquitination of PLC $\gamma$ -1 at early time points seems associated with anergy induction, later ubiquitination seems common to both anergising and priming cells, and hence possibly reflects dampening of TCR signalling, thus preventing T cell hyperreactivity. To address whether ubiquitination of PLC $\gamma$ -1 could be targeting it for proteasomal degradation, experiments were repeated in the presence of proteasome inhibitors (**Figure 3.7**); while previous work had shown that ubiquitination-mediated degradation of PLC $\gamma$ -1 occurred via the lysosome as evidenced by the failure of the proteasome inhibitor MG132 to result in PLC $\gamma$ -1 accumulation [183], the present study found that at least some PLC $\gamma$ -1 is being degraded in the proteasome in cells undergoing anergy, after 20 h stimulation (**Figure 3.7**).

Other crucial effectors in TCR signalling which have been reported to be downregulated during anergy induction (compared to priming induction) are PKC $\theta$  and Lck [183]. While PKC $\theta$  downregulation in the context of anergy induction appears to be mediated by monoubiquitination and to be mostly proteasome-independent, Lck downregulation has been reported as dependent on ubiquitin but, depending on context, as either proteasome-dependent or cysteine protease-dependent [282, 283]. As seen in **Figure 3.7**, evidence for proteasome-mediated degradation of Lck was not found in this study.

Although progress has been made in identifying potential targets of differential signalling, the majority of work in this field has been carried out *in vitro* using T cell lines or purified T cells using biochemical analysis which takes no account of cell-cell interactions and physiological microenvironment. *In situ* examination of signalling in T cells primed and tolerised *in vivo* will therefore reflect more accurately the molecular mechanisms underlying tolerance induction and maintenance. Different ways to induce *in vivo* anergy have been used to study T cell signalling, namely administration of peptide i.v. and feeding whole protein [111, 330]. However, *in vitro* studies require quite different methods for inducing tolerance than those more physiological mechanisms used in *in vivo* anergy induction and this might help explain the apparently conflicting data generated from comparison of both types of experiments as the different methods might be inducing different kinds of tolerance.

In fact, the cellular response leading to anergy in the *in vitro* models has indeed been reported to be quite distinct from what occurs during the development of *in vivo* anergy. *In vitro* anergy typically develops in less than 1 day [49, 116] and in the process CD4<sup>+</sup> T cells have been reported not to enter cell cycle [52], while *in vivo* anergy induced by peripheral self-antigen is preceded by a proliferative phase, which goes on

for a few days [118]. Moreover, the *in vivo* studies describe a defect in  $\text{Ca}^{2+}$ -mediated translocation of NFAT into the nucleus that has been proposed to be caused by downregulation of  $\text{PLC}\gamma\text{-1}$  activation, whilst normal activation of Erk is observed [331], although in not all *in vivo* studies [131]; by contrast, *in vitro* anergy is characterised by normal  $\text{Ca}^{2+}$  mobilisation but impaired Ras-Erk pathway activation [123, 183]. Some have argued that the discrepancies observed in *in vitro* and *in vivo* models of anergy show that *in vitro* clonal anergy (commonly induced via treatment with anti-CD3 or ionomycin) and *in vivo* adaptive tolerance (usually induced using antigen in protein or peptide form) are two distinct biochemical states [260]. Both types of tolerance models result in reduced transcription of IL-2 and proliferation, but the defects in TCR-mediated signalling occur in different signalling cascades.

Thus, in adaptive tolerance, T cells appear to exhibit impaired phosphorylation of ZAP-70, LAT and  $\text{PLC}\gamma\text{-1}$  leading to decreased  $\text{Ca}^{2+}$  mobilisation whereas clonal anergy appears to be predominantly mediated by defects in the Ras-Erk pathway (which can also occur in adaptive tolerance [131], with little or no defects in the  $\text{Ca}^{2+}$ -NFAT pathway). Thus, this concept of distinct biochemical states leading to the same functional outcome (T cell anergy), can help explain why some of *in vivo* responses differ from those observed *in vitro*. For instance, no significant differences were found between tolerised and primed transgenic T cells in terms of expression of Cbl-b, Itch, Smurf1 and Smurf2 in the *in vivo* tolerance induction model while the *in vitro* experiments showed otherwise. Moreover, although most of the *in vitro* experiments related to a 20 h time point whilst the *in vivo* studies predominantly analysed LN tissue at 5 d after stimulus, the differences between anergic and primed cells were generally maintained in the long-term ( $\pm 120$  h) *in vitro* culture experiments (**Figure 3.37**) suggesting that such differences did not simply reflect kinetics. Given the above *in vivo* data, it is therefore interesting to note that no detectable difference in the development of adaptive tolerance, as measured by cell number and cytokine production, was found between Cbl-b-deficient  $\text{CD4}^+$  T cells and wt cells [260].

As mentioned above, even within the literature of *in vitro* T cell anergy, different anergy-inducing protocols produce different signalling outcomes. The most popular *in vitro* anergy-inducing methods involve stimulation of the T cells with immobilised anti-CD3 antibodies or stimulation with ionomycin; whilst in the first case ligation of the TCR (which leads to  $\text{Ca}^{2+}$  mobilisation and subsequent NFAT activation) to mimic antigen-stimulation occurs [49], in the second case  $\text{Ca}^{2+}$  mobilisation is promoted directly [259]. In either case, there is no co-stimulation and  $\text{Ca}^{2+}$ -NFAT signalling

induces a limited set of anergy-associated genes, distinct from genes induced in the productive immune response [116]. However, as ionomycin bypasses TCR ligation, the initial steps in T cell anergy are also omitted, steps in which Lck, ZAP-70, LAT, PLC $\gamma$ -1 and the TCR itself have been found to be downregulated. It is not difficult to speculate that they themselves might be involved in the regulation of expression of E3 ubiquitin-protein ligases, thus helping explaining the conflicting data regarding the two *in vitro* tolerance induction models. Similarly, the strong, unregulated mobilisation of intracellular calcium and calcium influx triggered by ionomycin may initiate a distinct transcriptional programme to that dictated by PLC $\gamma$ -1 signalling.

While T cell anergy is commonly associated with lack of cytokine production, this might not simply be due to a defect in synthesis and/or secretion but rather, also reflect disruption of the cell-cell interactions in microenvironments observed in priming. For instance, in a T cell population undergoing anergy induction, although some cells will develop an apoptotic program, anergic T cells are also thought to have impaired migration, or at least impaired B cell help capability. Many factors play a role in controlling cell numbers, namely by regulating cell cycle progression: for example, the G1/S checkpoint inhibitor Smad3 is a critical effector downstream of p27<sup>kip1</sup>, which has been implicated in the induction of tolerance [332]. Also important is the control of cellular growth; for example, as glucose uptake is limiting in T cell activation [333], CD28 co-stimulation is required to maximally increase its uptake through Akt-dependent and Akt-independent pathways which lead to elevated glucose transporter Glut1 expression and traffic to the cell surface [333]. A key protein in the decision between priming and anergy, mTOR integrates the inputs of co-stimulatory signals, determining the outcome of TCR engagement [334]; antigen recognition in the setting of mTOR activation leads to full immune responses, whereas recognition in the setting of mTOR inhibition results in quiescence [334]. The PI3K-Akt-mTOR pathway is necessary for IL-2 production and proliferation [334]; however, these two functional hallmarks of primed cells can be uncoupled one from the other, with IL-2 production appearing to be a more accurate determinant of priming [334].

As discussed above, Cbl-b, Itch and Grail are involved in many different ways in the regulation of the immune response, from T<sub>reg</sub>-mediated suppression [200, 238] to T cell differentiation [222], and their regulatory role is not even restricted to the modulation of T cell responses. In terms of differential gene upregulation/downregulation in anergic Vs priming T cells, previous work using gene chip analysis has shown that very few genes are differentially transcriptionally regulated

between these two populations of cells [335, 336], indicating that regulation of this system is either dependent on a handful of genes or that posttranslational regulatory mechanisms play a much more prominent role. E3 ubiquitin-protein ligases have been postulated to be induced in anergic T cells to modulate the activity and/or expression of other crucial proteins by ubiquitination. However, the data presented here suggest that upregulation of Cbl-b, Itch and Grail is not exclusive to T cells undergoing or maintaining anergy, on the contrary, it can be exacerbated by a co-stimulatory priming stimulus. The question regarding their role in anergy and priming therefore still remains and may be explained by increasing evidence that Cbl-b, Itch and Grail can modulate different proteins and can interact with each other. Thus, further studies regarding their kinetics of expression and activity – and, if they are to exist, the identification of exclusive targets in anergic and primed cells – can further assist in elucidating their differential roles in these two very distinct functional T cell outcomes. Furthermore, they will also shed light on the regulation of associated but general cellular processes, such as apoptosis, cell cycle progression and migration.

Ideally, an anergic program should be able to modulate all these cellular processes as well as cytokine production and others such as B-T cell cooperation. How can this be achieved? A stable difference in the gene expression profile between naïve and primed or anergic T cells could be achieved through ubiquitin modification translating into an increase in turnover of signalling mediators involved in the T cell response, thereby establishing a persistent unresponsive state in anergy. One of the attractive features of this mechanism is that signalling mediators would only require downmodulation when activated. One possibility for such E3-mediated driving of anergy involves cooperation between Cbl-b and Itch, resulting in the ubiquitination of the TCR, PLC $\gamma$ -1 and PKC $\theta$  and subsequent internalisation into an endocytic vesicle which, following Itch signalling, would be targeted to the lysosomes for degradation. Grail, which resides in the endosomal membrane, could also synergise with these effectors to further enhance protein ubiquitination. It is an interesting question whether any or all of these proteins remain active in anergic cells in the absence of antigenic challenge or whether they are rapidly upregulated only upon re-stimulation. Assessment of the prevalence of the E3s over longer periods in this study ( $\pm$  120 h) shows that they are still present in anergic and primed cells, which means they could be actively contributing to the enforcement of the anergy program even in the absence of re-exposure to antigen.

## 4.10 Summary

The data presented here, of which a brief summary can be found in **Table 4.1**, indicate that expression and/or upregulation of Cbl-b, Itch and Grail is not exclusive to T cells undergoing or maintaining anergy, as priming and primed T cells also exhibit not only expression but also upregulation of these proteins. By contrast, the data show that downregulation of PLC $\gamma$ -1 correlates nicely with anergy and, similarly that its upregulation correlates with priming; in anergising T cells, PLC $\gamma$ -1 downregulation was found to occur via the ubiquitin-proteasome pathway and, as others have implicated Itch and Cbl-b in the ubiquitination of PLC $\gamma$ -1, this is likely mediated by these two E3 ubiquitin-protein ligases.

After 20 h of stimulation, both priming and anergising populations of cells have higher expression of Cbl-b, Itch and Grail than the naïve population, which may point towards a role of these proteins in the downregulation or negative feedback inhibition of T cell activity. As Cbl-b, Itch and Grail have all been reported to downregulate TCR, this is a tempting mechanism through which such regulation could be achieved. Itch and Cbl-b can also downregulate PLC $\gamma$ -1, and in the context of CD28 co-stimulation, Itch can promote the ubiquitin-mediated degradation of Bcl10 (**Figure 4.1**). In the maintenance phase, although perhaps immediately after antigen re-stimulation Cbl-b, Itch and Grail might exert anergy-specific effects, at 20 h after re-stimulation of anergic and primed cells these E3 ubiquitin-protein ligases are again upregulated in both populations, which suggests they might again be involved in the homeostatic control of T cell activation. Potential targets for ubiquitin-mediated downregulation in the maintenance phase are, for Itch, the transcription factor Jun and Bcl10, for Grail, CD83, whilst all three can downregulate the TCR:CD3 complex.

These data therefore open up new possibilities with respect to the mechanisms modulating T cell activation which could contribute to the development of work on the identification of targets that are specifically downregulated in order to prevent hyperreactivity. Also of interest would be to understand the mechanism and context by which these E3 ubiquitin-protein ligases switch between roles, as this might help identify new anergy factors.

**Table 4.1: Summary of the results yielded by the main experimental approaches regarding the expression of Cbl-b, Itch and Grail.**

Induction										
WB (CD4 <sup>+</sup> T cells)					LSC* (CD4 <sup>+</sup> T cells)					
20 h			48 h			20 h			40 h	
	AN	PR	AN	PR	AN	PR	AN	PR	AN	PR
<b>Cbl-b</b>	↑	↑↑	+	++	↓	↑	+	↑	+	++
<b>Itch</b>	↑	↑↑	+	++	↑	↑	+	↑	+	+
<b>Grail</b>	↑	↑↑	++	+	-	↑	++	↑	++	+

\* In terms of % of E3-positive cells out of the CD4<sup>+</sup> T cells

- No difference to naïve cells

++ Expressed more than +

↓ Downregulated when compared to naïve cells

↑ Upregulated when compared to naïve cells

↑↑ Upregulated when compared to naïve cells and the other population

Maintenance										
WB (LN cells)					LSC* (KJ1-26 <sup>+</sup> T cells)					
20 h			20 h			24 h			<i>In vivo*</i>	
	AN	PR	AN	PR	AN	PR	AN	PR	AN	PR
<b>Cbl-b</b>	+	+	+	+	+	++	+	+	+	+
<b>Itch</b>	+	+	+	+	+	++	+	+	+	+
<b>Grail</b>	++	+	+	+	nd	nd	+	+	+	+

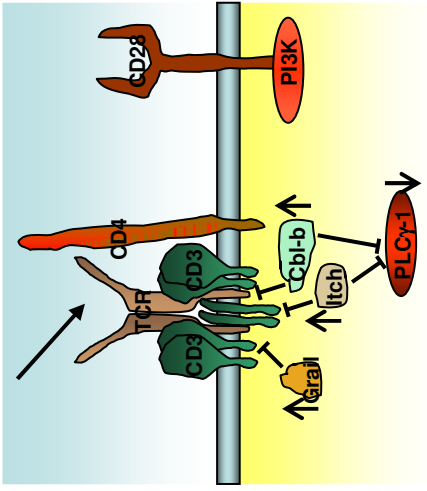
\* In terms of % of E3-positive cells out of the KJ1-26<sup>+</sup> T cells

nd No data

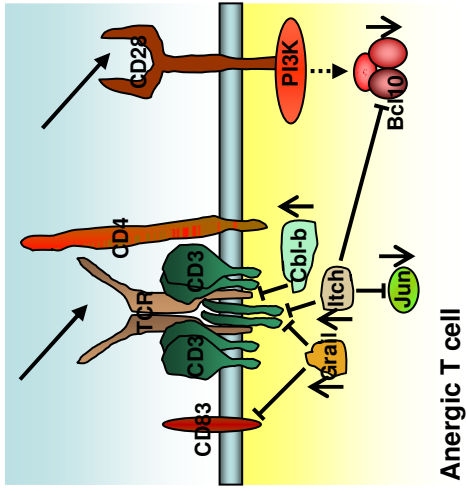
++ Expressed more than +

**Figure 4.1: Expression of Cbl-b, Itch and Grail after 20 h of stimulation and potential targets for their action in the downmodulation of T cell activity.**

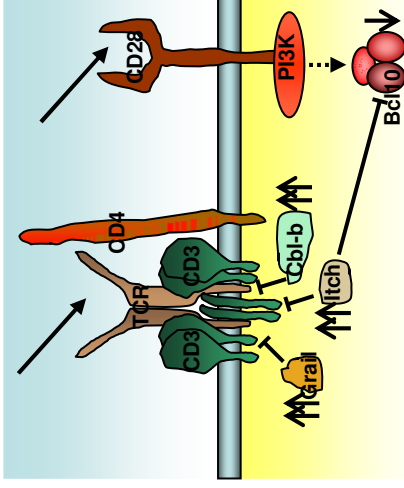
TCR ligation leads to upregulation of Cbl-b, Itch and Grail; Itch and Cbl-b can enforce the anergic programme by targeting PLC $\gamma$ -1 (and others) to the ubiquitin-proteasome pathway and Cbl-b, Itch and Grail can quench excess TCR signalling by downmodulating the TCR. TCR ligation coupled with CD28 co-stimulation leads to upregulation of Cbl-b, Itch and Grail; Itch can promote the ubiquitin-mediated degradation of Bcl10, quenching CD28-mediated signalling, and Cbl-b, Itch and Grail can quench excess TCR signalling by downmodulating the TCR. Re-stimulation of anergic cells with antigen leads to upregulation of Cbl-b, Itch and Grail; these E3 ubiquitin-protein ligases can quench excess TCR signalling by downmodulating the TCR whilst Grail can target CD83 and Itch can promote the ubiquitin-mediated degradation of Bcl10 and Jun. Re-stimulation of primed cells with antigen leads to upregulation of Cbl-b and Itch; these E3 ubiquitin-protein ligases can quench excess TCR signalling by downmodulating the TCR whilst Itch can promote the ubiquitin-mediated degradation of Bcl10 and Jun.



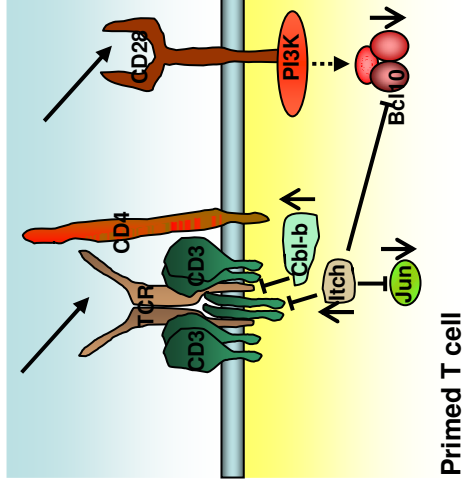
Naïve T cell



Anergic T cell



Naïve T cell



Primed T cell

## 5 References

1. Abbas AK and Janeway CA, Jr. **Immunology: improving on nature in the twenty-first century.** *Cell*, 2000, **100**(1): 129-38.
2. Murphy M, Travers P, and Walport M. **Janeway's Immunobiology.** 7<sup>th</sup> ed. 2008, New York: Garland Science. 887.
3. Janeway CA, Jr. **How the immune system works to protect the host from infection: a personal view.** *Proc Natl Acad Sci U S A*, 2001, **98**(13): 7461-8.
4. Lund FE, Garvy BA, Randall TD, and Harris DP. **Regulatory roles for cytokine-producing B cells in infection and autoimmune disease.** *Curr Dir Autoimmun*, 2005, **8**: 25-54.
5. Pennington DJ, Silva-Santos B, and Hayday AC. **Gammadelta T cell development--having the strength to get there.** *Curr Opin Immunol*, 2005, **17**(2): 108-15.
6. Godfrey DI, Stankovic S, and Baxter AG. **Raising the NKT cell family.** *Nat Immunol*, 2010, **11**(3): 197-206.
7. Mellman I and Steinman RM. **Dendritic cells: specialized and regulated antigen processing machines.** *Cell*, 2001, **106**(3): 255-8.
8. Kuby J, Goldsby R, Kindt T, and Osborne B. **Immunology.** 4<sup>th</sup> ed. 2000, New York: W.H.Freeman & Co Ltd. 670.
9. von Boehmer H. **Positive selection of lymphocytes.** *Cell*, 1994, **76**(2): 219-28.
10. Nossal GJ. **Negative selection of lymphocytes.** *Cell*, 1994, **76**(2): 229-39.
11. Schwartz RH. **Natural regulatory T cells and self-tolerance.** *Nat Immunol*, 2005, **6**(4): 327-30.
12. Agrewala JN, Brown DM, Lepak NM, Duso D, Huston G, and Swain SL. **Unique ability of activated CD4+ T cells but not rested effectors to migrate to non-lymphoid sites in the absence of inflammation.** *J Biol Chem*, 2007, **282**(9): 6106-15.
13. Nurieva R, Thomas S, Nguyen T, Martin-Orozco N, Wang Y, Kaja MK, Yu XZ, and Dong C. **T-cell tolerance or function is determined by combinatorial costimulatory signals.** *Embo J*, 2006, **25**(11): 2623-33.
14. Cronin SJ and Penninger JM. **From T-cell activation signals to signaling control of anti-cancer immunity.** *Immunol Rev*, 2007, **220**: 151-68.
15. Zheng W and Flavell RA. **The transcription factor GATA-3 is necessary and sufficient for Th2 cytokine gene expression in CD4 T cells.** *Cell*, 1997, **89**(4): 587-96.
16. Louten J, Boniface K, and de Waal Malefyt R. **Development and function of TH17 cells in health and disease.** *J Allergy Clin Immunol*, 2009, **123**(5): 1004-11.
17. Korn T, Bettelli E, Gao W, Awasthi A, Jager A, Strom TB, Oukka M, and Kuchroo VK. **IL-21 initiates an alternative pathway to induce proinflammatory T(H)17 cells.** *Nature*, 2007, **448**(7152): 484-7.
18. Nurieva R, Yang XO, Martinez G, Zhang Y, Panopoulos AD, Ma L, Schluns K, Tian Q, Watowich SS, Jetten AM, and Dong C. **Essential autocrine regulation by IL-21 in the generation of inflammatory T cells.** *Nature*, 2007, **448**(7152): 480-3.
19. Steinman L. **A brief history of T(H)17, the first major revision in the T(H)1/T(H)2 hypothesis of T cell-mediated tissue damage.** *Nat Med*, 2007, **13**(2): 139-45.
20. Wan YY. **Multi-tasking of helper T cells.** *Immunology*, 2010, **130**(2): 166-71.

21. Cahalan MD and Gutman GA. **The sense of place in the immune system.** *Nat Immunol*, 2006, **7**(4): 329-32.
22. Drayton DL, Liao S, Mounzer RH, and Ruddle NH. **Lymphoid organ development: from ontogeny to neogenesis.** *Nat Immunol*, 2006, **7**(4): 344-53.
23. Bajenoff M, Egen JG, Koo LY, Laugier JP, Brau F, Glaichenhaus N, and Germain RN. **Stromal cell networks regulate lymphocyte entry, migration, and territoriality in lymph nodes.** *Immunity*, 2006, **25**(6): 989-1001.
24. Mathis D and Benoist C. **Back to central tolerance.** *Immunity*, 2004, **20**(5): 509-16.
25. Walker LS and Abbas AK. **The enemy within: keeping self-reactive T cells at bay in the periphery.** *Nat Rev Immunol*, 2002, **2**(1): 11-9.
26. Borde M, Barrington RA, Heissmeyer V, Carroll MC, and Rao A. **Transcriptional basis of lymphocyte tolerance.** *Immunol Rev*, 2006, **210**: 105-19.
27. Kurts C, Sutherland RM, Davey G, Li M, Lew AM, Blanas E, Carbone FR, Miller JF, and Heath WR. **CD8 T cell ignorance or tolerance to islet antigens depends on antigen dose.** *Proc Natl Acad Sci U S A*, 1999, **96**(22): 12703-7.
28. Smith JA and Bluestone JA. **T cell inactivation and cytokine deviation promoted by anti-CD3 mAbs.** *Curr Opin Immunol*, 1997, **9**(5): 648-54.
29. Garside P and Mowat AM. **Oral tolerance.** *Semin Immunol*, 2001, **13**(3): 177-85.
30. Thorstenson KM and Khoruts A. **Generation of anergic and potentially immunoregulatory CD25+CD4 T cells in vivo after induction of peripheral tolerance with intravenous or oral antigen.** *J Immunol*, 2001, **167**(1): 188-95.
31. Zhang X, Izikson L, Liu L, and Weiner HL. **Activation of CD25(+)CD4(+) regulatory T cells by oral antigen administration.** *J Immunol*, 2001, **167**(8): 4245-53.
32. Piccirillo CA and Shevach EM. **Cutting edge: control of CD8+ T cell activation by CD4+CD25+ immunoregulatory cells.** *J Immunol*, 2001, **167**(3): 1137-40.
33. Takahashi T, Kuniyasu Y, Toda M, Sakaguchi N, Itoh M, Iwata M, Shimizu J, and Sakaguchi S. **Immunologic self-tolerance maintained by CD25+CD4+ naturally anergic and suppressive T cells: induction of autoimmune disease by breaking their anergic/suppressive state.** *Int Immunol*, 1998, **10**(12): 1969-80.
34. Fahlen L, Read S, Gorelik L, Hurst SD, Coffman RL, Flavell RA, and Powrie F. **T cells that cannot respond to TGF-beta escape control by CD4(+)CD25(+) regulatory T cells.** *J Exp Med*, 2005, **201**(5): 737-46.
35. Huber S, Schramm C, Lehr HA, Mann A, Schmitt S, Becker C, Protschka M, Galle PR, Neurath MF, and Blessing M. **Cutting edge: TGF-beta signaling is required for the in vivo expansion and immunosuppressive capacity of regulatory CD4+CD25+ T cells.** *J Immunol*, 2004, **173**(11): 6526-31.
36. Groux H, O'Garra A, Bigler M, Rouleau M, Antonenko S, de Vries JE, and Roncarolo MG. **A CD4+ T-cell subset inhibits antigen-specific T-cell responses and prevents colitis.** *Nature*, 1997, **389**(6652): 737-42.
37. Chen Y, Kuchroo VK, Inobe J, Hafler DA, and Weiner HL. **Regulatory T cell clones induced by oral tolerance: suppression of autoimmune encephalomyelitis.** *Science*, 1994, **265**(5176): 1237-40.
38. Moore KW, O'Garra A, de Waal Malefyt R, Vieira P, and Mosmann TR. **Interleukin-10.** *Annu Rev Immunol*, 1993, **11**: 165-90.
39. Lider O, Santos LM, Lee CS, Higgins PJ, and Weiner HL. **Suppression of experimental autoimmune encephalomyelitis by oral administration of**

- myelin basic protein. II. Suppression of disease and in vitro immune responses is mediated by antigen-specific CD8+ T lymphocytes.** *J Immunol*, 1989, **142**(3): 748-52.
40. Miller A, Lider O, Roberts AB, Sporn MB, and Weiner HL. **Suppressor T cells generated by oral tolerization to myelin basic protein suppress both in vitro and in vivo immune responses by the release of transforming growth factor beta after antigen-specific triggering.** *Proc Natl Acad Sci U S A*, 1992, **89**(1): 421-5.
  41. Grdic D, Hornquist E, Kjerrulf M, and Lycke NY. **Lack of local suppression in orally tolerant CD8-deficient mice reveals a critical regulatory role of CD8+ T cells in the normal gut mucosa.** *J Immunol*, 1998, **160**(2): 754-62.
  42. Joosten SA, van Meijgaarden KE, Savage ND, de Boer T, Triebel F, van der Wal A, de Heer E, Klein MR, Geluk A, and Ottenhoff TH. **Identification of a human CD8+ regulatory T cell subset that mediates suppression through the chemokine CC chemokine ligand 4.** *Proc Natl Acad Sci U S A*, 2007, **104**(19): 8029-34.
  43. Powell JD. **The induction and maintenance of T cell anergy.** *Clin Immunol*, 2006, **120**(3): 239-46.
  44. Green DR, Droin N, and Pinkoski M. **Activation-induced cell death in T cells.** *Immunol Rev*, 2003, **193**: 70-81.
  45. Fathman CG and Lineberry NB. **Molecular mechanisms of CD4+ T-cell anergy.** *Nat Rev Immunol*, 2007, **7**(8): 599-609.
  46. Alegre ML, Frauwirth KA, and Thompson CB. **T-cell regulation by CD28 and CTLA-4.** *Nat Rev Immunol*, 2001, **1**(3): 220-8.
  47. Lechler R, Chai JG, Marelli-Berg F, and Lombardi G. **T-cell anergy and peripheral T-cell tolerance.** *Philos Trans R Soc Lond B Biol Sci*, 2001, **356**(1409): 625-37.
  48. Boussiotis VA, Freeman GJ, Berezovskaya A, Barber DL, and Nadler LM. **Maintenance of human T cell anergy: blocking of IL-2 gene transcription by activated Rap1.** *Science*, 1997, **278**(5335): 124-8.
  49. Jenkins MK, Chen CA, Jung G, Mueller DL, and Schwartz RH. **Inhibition of antigen-specific proliferation of type 1 murine T cell clones after stimulation with immobilized anti-CD3 monoclonal antibody.** *J Immunol*, 1990, **144**(1): 16-22.
  50. Quill H and Schwartz RH. **Stimulation of normal inducer T cell clones with antigen presented by purified Ia molecules in planar lipid membranes: specific induction of a long-lived state of proliferative nonresponsiveness.** *J Immunol*, 1987, **138**(11): 3704-12.
  51. Chai JG and Lechler RI. **Immobilized anti-CD3 mAb induces anergy in murine naive and memory CD4+ T cells in vitro.** *Int Immunol*, 1997, **9**(7): 935-44.
  52. DeSilva DR, Urdahl KB, and Jenkins MK. **Clonal anergy is induced in vitro by T cell receptor occupancy in the absence of proliferation.** *J Immunol*, 1991, **147**(10): 3261-7.
  53. Zamoyska R, Basson A, Filby A, Legname G, Lovatt M, and Seddon B. **The influence of the src-family kinases, Lck and Fyn, on T cell differentiation, survival and activation.** *Immunol Rev*, 2003, **191**: 107-18.
  54. Salmond RJ, Filby A, Qureshi I, Caserta S, and Zamoyska R. **T-cell receptor proximal signaling via the Src-family kinases, Lck and Fyn, influences T-cell activation, differentiation, and tolerance.** *Immunol Rev*, 2009, **228**(1): 9-22.

55. Samelson LE. **Signal transduction mediated by the T cell antigen receptor: the role of adapter proteins.** *Annu Rev Immunol*, 2002, **20**: 371-94.
56. Huang F and Gu H. **Negative regulation of lymphocyte development and function by the Cbl family of proteins.** *Immunol Rev*, 2008, **224**: 229-38.
57. Manicassamy S, Gupta S, Huang Z, Molkenin JD, Shang W, and Sun Z. **Requirement of calcineurin a beta for the survival of naive T cells.** *J Immunol*, 2008, **180**(1): 106-12.
58. Crabtree GR and Olson EN. **NFAT signaling: choreographing the social lives of cells.** *Cell*, 2002, **109 Suppl**: S67-79.
59. Arendt CW, Albrecht B, Soos TJ, and Littman DR. **Protein kinase C-theta; signaling from the center of the T-cell synapse.** *Curr Opin Immunol*, 2002, **14**(3): 323-30.
60. Ebinu JO, Bottorff DA, Chan EY, Stang SL, Dunn RJ, and Stone JC. **RasGRP, a Ras guanyl nucleotide- releasing protein with calcium- and diacylglycerol-binding motifs.** *Science*, 1998, **280**(5366): 1082-6.
61. Bivona TG, Perez De Castro I, Ahearn IM, Grana TM, Chiu VK, Lockyer PJ, Cullen PJ, Pellicer A, Cox AD, and Philips MR. **Phospholipase Cgamma activates Ras on the Golgi apparatus by means of RasGRP1.** *Nature*, 2003, **424**(6949): 694-8.
62. Ebinu JO, Stang SL, Teixeira C, Bottorff DA, Hooton J, Blumberg PM, Barry M, Bleakley RC, Ostergaard HL, and Stone JC. **RasGRP links T-cell receptor signaling to Ras.** *Blood*, 2000, **95**(10): 3199-203.
63. Buday L, Egan SE, Rodriguez Viciano P, Cantrell DA, and Downward J. **A complex of Grb2 adaptor protein, Sos exchange factor, and a 36-kDa membrane-bound tyrosine phosphoprotein is implicated in ras activation in T cells.** *J Biol Chem*, 1994, **269**(12): 9019-23.
64. Leever SJ, Paterson HF, and Marshall CJ. **Requirement for Ras in Raf activation is overcome by targeting Raf to the plasma membrane.** *Nature*, 1994, **369**(6479): 411-4.
65. Chaudhary A, King WG, Mattaliano MD, Frost JA, Diaz B, Morrison DK, Cobb MH, Marshall MS, and Brugge JS. **Phosphatidylinositol 3-kinase regulates Raf1 through Pak phosphorylation of serine 338.** *Curr Biol*, 2000, **10**(9): 551-4.
66. Yang SH, Yates PR, Whitmarsh AJ, Davis RJ, and Sharrocks AD. **The Elk-1 ETS-domain transcription factor contains a mitogen-activated protein kinase targeting motif.** *Mol Cell Biol*, 1998, **18**(2): 710-20.
67. Smith ER, Smedberg JL, Rula ME, Hamilton TC, and Xu XX. **Disassociation of MAPK activation and c-Fos expression in F9 embryonic carcinoma cells following retinoic acid-induced endoderm differentiation.** *J Biol Chem*, 2001, **276**(34): 32094-100.
68. Isakov N and Altman A. **Protein kinase C(theta) in T cell activation.** *Annu Rev Immunol*, 2002, **20**: 761-94.
69. Loeser S and Penninger JM. **Regulation of peripheral T cell tolerance by the E3 ubiquitin ligase Cbl-b.** *Semin Immunol*, 2007, **19**(3): 206-14.
70. Oeckinghaus A, Wegener E, Welteke V, Ferch U, Arslan SC, Ruland J, Scheidereit C, and Krappmann D. **Malt1 ubiquitination triggers NF-kappaB signaling upon T-cell activation.** *Embo J*, 2007, **26**(22): 4634-45.
71. Sun L, Deng L, Ea CK, Xia ZP, and Chen ZJ. **The TRAF6 ubiquitin ligase and TAK1 kinase mediate IKK activation by BCL10 and MALT1 in T lymphocytes.** *Mol Cell*, 2004, **14**(3): 289-301.
72. Thome M. **Multifunctional roles for MALT1 in T-cell activation.** *Nat Rev Immunol*, 2008, **8**(7): 495-500.

73. Ghosh S, May MJ, and Kopp EB. **NF-kappa B and Rel proteins: evolutionarily conserved mediators of immune responses.** *Annu Rev Immunol*, 1998, **16**: 225-60.
74. Schmitz ML, Bacher S, and Dienz O. **NF-kappaB activation pathways induced by T cell costimulation.** *Faseb J*, 2003, **17**(15): 2187-93.
75. Fruman DA and Bismuth G. **Fine tuning the immune response with PI3K.** *Immunol Rev*, 2009, **228**(1): 253-72.
76. Park SG, Schulze-Luehrman J, Hayden MS, Hashimoto N, Ogawa W, Kasuga M, and Ghosh S. **The kinase PDK1 integrates T cell antigen receptor and CD28 coreceptor signaling to induce NF-kappaB and activate T cells.** *Nat Immunol*, 2009, **10**(2): 158-66.
77. Silva A, Yunes JA, Cardoso BA, Martins LR, Jotta PY, Abecasis M, Nowill AE, Leslie NR, Cardoso AA, and Barata JT. **PTEN posttranslational inactivation and hyperactivation of the PI3K/Akt pathway sustain primary T cell leukemia viability.** *J Clin Invest*, 2008.
78. Mora A, Komander D, van Aalten DM, and Alessi DR. **PDK1, the master regulator of AGC kinase signal transduction.** *Semin Cell Dev Biol*, 2004, **15**(2): 161-70.
79. Valensin S, Paccani SR, Ulivieri C, Mercati D, Pacini S, Patrussi L, Hirst T, Lupetti P, and Baldari CT. **F-actin dynamics control segregation of the TCR signaling cascade to clustered lipid rafts.** *Eur J Immunol*, 2002, **32**(2): 435-46.
80. David R, Ma L, Ivetic A, Takesono A, Ridley AJ, Chai JG, Tybulewicz VL, and Marelli-Berg FM. **T-cell receptor- and CD28-induced Vav1 activity is required for the accumulation of primed T cells into antigenic tissue.** *Blood*, 2009, **113**(16): 3696-705.
81. Ardouin L, Bracke M, Mathiot A, Pagakis SN, Norton T, Hogg N, and Tybulewicz VL. **Vav1 transduces TCR signals required for LFA-1 function and cell polarization at the immunological synapse.** *Eur J Immunol*, 2003, **33**(3): 790-7.
82. Zeng R, Cannon JL, Abraham RT, Way M, Billadeau DD, Bubeck-Wardenberg J, and Burkhardt JK. **SLP-76 coordinates Nck-dependent Wiskott-Aldrich syndrome protein recruitment with Vav-1/Cdc42-dependent Wiskott-Aldrich syndrome protein activation at the T cell-APC contact site.** *J Immunol*, 2003, **171**(3): 1360-8.
83. Mor A, Dustin ML, and Philips MR. **Small GTPases and LFA-1 reciprocally modulate adhesion and signaling.** *Immunol Rev*, 2007, **218**: 114-25.
84. Lin A, Minden A, Martinetto H, Claret FX, Lange-Carter C, Mercurio F, Johnson GL, and Karin M. **Identification of a dual specificity kinase that activates the Jun kinases and p38-Mpk2.** *Science*, 1995, **268**(5208): 286-90.
85. Angel P and Karin M. **The role of Jun, Fos and the AP-1 complex in cell-proliferation and transformation.** *Biochim Biophys Acta*, 1991, **1072**(2-3): 129-57.
86. van der Houven van Oordt W, Diaz-Meco MT, Lozano J, Krainer AR, Moscat J, and Caceres JF. **The MKK(3/6)-p38-signaling cascade alters the subcellular distribution of hnRNP A1 and modulates alternative splicing regulation.** *J Cell Biol*, 2000, **149**(2): 307-16.
87. Price MA, Cruzalegui FH, and Treisman R. **The p38 and ERK MAP kinase pathways cooperate to activate Ternary Complex Factors and c-fos transcription in response to UV light.** *Embo J*, 1996, **15**(23): 6552-63.
88. Riley JL and June CH. **The CD28 family: a T-cell rheostat for therapeutic control of T-cell activation.** *Blood*, 2005, **105**(1): 13-21.

89. Yong PF, Salzer U, and Grimbacher B. **The role of costimulation in antibody deficiencies: ICOS and common variable immunodeficiency.** *Immunol Rev*, 2009, **229**(1): 101-13.
90. Murphy TL and Murphy KM. **Slow down and survive: Enigmatic immunoregulation by BTLA and HVEM.** *Annu Rev Immunol*, 2010, **28**: 389-411.
91. Brunet JF, Denizot F, Luciani MF, Roux-Dosseto M, Suzan M, Mattei MG, and Golstein P. **A new member of the immunoglobulin superfamily--CTLA-4.** *Nature*, 1987, **328**(6127): 267-70.
92. Linsley PS, Brady W, Urnes M, Grosmaire LS, Damle NK, and Ledbetter JA. **CTLA-4 is a second receptor for the B cell activation antigen B7.** *J Exp Med*, 1991, **174**(3): 561-9.
93. Brunner-Weinzierl MC, Hoff H, and Burmester GR. **Multiple functions for CD28 and cytotoxic T lymphocyte antigen-4 during different phases of T cell responses: implications for arthritis and autoimmune diseases.** *Arthritis Res Ther*, 2004, **6**(2): 45-54.
94. Tivol EA, Borriello F, Schweitzer AN, Lynch WP, Bluestone JA, and Sharpe AH. **Loss of CTLA-4 leads to massive lymphoproliferation and fatal multiorgan tissue destruction, revealing a critical negative regulatory role of CTLA-4.** *Immunity*, 1995, **3**(5): 541-7.
95. Khattri R, Auger JA, Griffin MD, Sharpe AH, and Bluestone JA. **Lymphoproliferative disorder in CTLA-4 knockout mice is characterized by CD28-regulated activation of Th2 responses.** *J Immunol*, 1999, **162**(10): 5784-91.
96. Walunas TL, Bakker CY, and Bluestone JA. **CTLA-4 ligation blocks CD28-dependent T cell activation.** *J Exp Med*, 1996, **183**(6): 2541-50.
97. Brunner MC, Chambers CA, Chan FK, Hanke J, Winoto A, and Allison JP. **CTLA-4-Mediated inhibition of early events of T cell proliferation.** *J Immunol*, 1999, **162**(10): 5813-20.
98. Krummel MF and Allison JP. **CTLA-4 engagement inhibits IL-2 accumulation and cell cycle progression upon activation of resting T cells.** *J Exp Med*, 1996, **183**(6): 2533-40.
99. Olsson C, Riesbeck K, Dohlsten M, and Michaelsson E. **CTLA-4 ligation suppresses CD28-induced NF-kappaB and AP-1 activity in mouse T cell blasts.** *J Biol Chem*, 1999, **274**(20): 14400-5.
100. Li D, Gal I, Vermes C, Alegre ML, Chong AS, Chen L, Shao Q, Adarichev V, Xu X, Koreny T, Mikecz K, Finnegan A, Glant TT, and Zhang J. **Cutting edge: Cbl-b: one of the key molecules tuning CD28- and CTLA-4-mediated T cell costimulation.** *J Immunol*, 2004, **173**(12): 7135-9.
101. Dong H, Zhu G, Tamada K, and Chen L. **B7-H1, a third member of the B7 family, co-stimulates T-cell proliferation and interleukin-10 secretion.** *Nat Med*, 1999, **5**(12): 1365-9.
102. Augello A, Tasso R, Negrini SM, Amateis A, Indiveri F, Cancedda R, and Pennesi G. **Bone marrow mesenchymal progenitor cells inhibit lymphocyte proliferation by activation of the programmed death 1 pathway.** *Eur J Immunol*, 2005, **35**(5): 1482-90.
103. Nakae S, Suto H, Iikura M, Kakurai M, Sedgwick JD, Tsai M, and Galli SJ. **Mast cells enhance T cell activation: importance of mast cell costimulatory molecules and secreted TNF.** *J Immunol*, 2006, **176**(4): 2238-48.
104. Tsushima F, Yao S, Shin T, Flies A, Flies S, Xu H, Tamada K, Pardoll DM, and Chen L. **Interaction between B7-H1 and PD-1 determines initiation and reversal of T-cell anergy.** *Blood*, 2007, **110**(1): 180-5.

105. Kinter AL, Godbout EJ, McNally JP, Sereti I, Roby GA, O'Shea MA, and Fauci AS. **The common gamma-chain cytokines IL-2, IL-7, IL-15, and IL-21 induce the expression of programmed death-1 and its ligands.** *J Immunol*, 2008, **181**(10): 6738-46.
106. Nishimura H, Okazaki T, Tanaka Y, Nakatani K, Hara M, Matsumori A, Sasayama S, Mizoguchi A, Hiai H, Minato N, and Honjo T. **Autoimmune dilated cardiomyopathy in PD-1 receptor-deficient mice.** *Science*, 2001, **291**(5502): 319-22.
107. Reynoso ED, Elpek KG, Francisco L, Bronson R, Bellemare-Pelletier A, Sharpe AH, Freeman GJ, and Turley SJ. **Intestinal tolerance is converted to autoimmune enteritis upon PD-1 ligand blockade.** *J Immunol*, 2009, **182**(4): 2102-12.
108. Keir ME, Liang SC, Guleria I, Latchman YE, Qipo A, Albacker LA, Koulmanda M, Freeman GJ, Sayegh MH, and Sharpe AH. **Tissue expression of PD-L1 mediates peripheral T cell tolerance.** *J Exp Med*, 2006, **203**(4): 883-95.
109. Huang CT, Huso DL, Lu Z, Wang T, Zhou G, Kennedy EP, Drake CG, Morgan DJ, Sherman LA, Higgins AD, Pardoll DM, and Adler AJ. **CD4+ T cells pass through an effector phase during the process of in vivo tolerance induction.** *J Immunol*, 2003, **170**(8): 3945-53.
110. Smith JA, Tso JY, Clark MR, Cole MS, and Bluestone JA. **Nonmitogenic anti-CD3 monoclonal antibodies deliver a partial T cell receptor signal and induce clonal anergy.** *J Exp Med*, 1997, **185**(8): 1413-22.
111. Hundt M, Tabata H, Jeon MS, Hayashi K, Tanaka Y, Krishna R, De Giorgio L, Liu YC, Fukata M, and Altman A. **Impaired activation and localization of LAT in anergic T cells as a consequence of a selective palmitoylation defect.** *Immunity*, 2006, **24**(5): 513-22.
112. Wells AD. **New insights into the molecular basis of T cell anergy: anergy factors, avoidance sensors, and epigenetic imprinting.** *J Immunol*, 2009, **182**(12): 7331-41.
113. Saibil SD, Deenick EK, and Ohashi PS. **The sound of silence: modulating anergy in T lymphocytes.** *Curr Opin Immunol*, 2007, **19**(6): 658-64.
114. Feske S. **Calcium signalling in lymphocyte activation and disease.** *Nat Rev Immunol*, 2007, **7**(9): 690-702.
115. Li W, Whaley CD, Mondino A, and Mueller DL. **Blocked signal transduction to the ERK and JNK protein kinases in anergic CD4+ T cells.** *Science*, 1996, **271**(5253): 1272-6.
116. Macian F, Garcia-Cozar F, Im SH, Horton HF, Byrne MC, and Rao A. **Transcriptional mechanisms underlying lymphocyte tolerance.** *Cell*, 2002, **109**(6): 719-31.
117. Harris JE, Bishop KD, Phillips NE, Mordes JP, Greiner DL, Rossini AA, and Czech MP. **Early growth response gene-2, a zinc-finger transcription factor, is required for full induction of clonal anergy in CD4+ T cells.** *J Immunol*, 2004, **173**(12): 7331-8.
118. Safford M, Collins S, Lutz MA, Allen A, Huang CT, Kowalski J, Blackford A, Horton MR, Drake C, Schwartz RH, and Powell JD. **Egr-2 and Egr-3 are negative regulators of T cell activation.** *Nat Immunol*, 2005, **6**(5): 472-80.
119. Thomas RM, Chunder N, Chen C, Umetsu SE, Winandy S, and Wells AD. **Ikaros enforces the costimulatory requirement for IL2 gene expression and is required for anergy induction in CD4+ T lymphocytes.** *J Immunol*, 2007, **179**(11): 7305-15.

120. Bandyopadhyay S, Dure M, Paroder M, Soto-Nieves N, Puga I, and Macian F. **Interleukin 2 gene transcription is regulated by Ikaros-induced changes in histone acetylation in anergic T cells.** *Blood*, 2007, **109**(7): 2878-86.
121. Quirion MR, Gregory GD, Umetsu SE, Winandy S, and Brown MA. **Cutting edge: Ikaros is a regulator of Th2 cell differentiation.** *J Immunol*, 2009, **182**(2): 741-5.
122. Olenchock BA, Guo R, Carpenter JH, Jordan M, Topham MK, Koretzky GA, and Zhong XP. **Disruption of diacylglycerol metabolism impairs the induction of T cell anergy.** *Nat Immunol*, 2006, **7**(11): 1174-81.
123. Zha Y, Marks R, Ho AW, Peterson AC, Janardhan S, Brown I, Praveen K, Stang S, Stone JC, and Gajewski TF. **T cell anergy is reversed by active Ras and is regulated by diacylglycerol kinase-alpha.** *Nat Immunol*, 2006, **7**(11): 1166-73.
124. Davidson D, Schraven B, and Veillette A. **PAG-associated FynT regulates calcium signaling and promotes anergy in T lymphocytes.** *Mol Cell Biol*, 2007, **27**(5): 1960-73.
125. Smida M, Posevitz-Fejfar A, Horejsi V, Schraven B, and Lindquist JA. **A novel negative regulatory function of the phosphoprotein associated with glycosphingolipid-enriched microdomains: blocking Ras activation.** *Blood*, 2007, **110**(2): 596-615.
126. Gajewski TF, Qian D, Fields P, and Fitch FW. **Anergic T-lymphocyte clones have altered inositol phosphate, calcium, and tyrosine kinase signaling pathways.** *Proc Natl Acad Sci U S A*, 1994, **91**(1): 38-42.
127. Quill H, Riley MP, Cho EA, Casnellie JE, Reed JC, and Torigoe T. **Anergic Th1 cells express altered levels of the protein tyrosine kinases p56lck and p59fyn.** *J Immunol*, 1992, **149**(9): 2887-93.
128. Yu SC and Nag B. **Differential expression of protein tyrosine kinases and their phosphorylation in murine Th1 cells anergized with class II MHC-peptide complexes.** *Immunol Cell Biol*, 1997, **75**(3): 295-302.
129. Fields P, Fitch FW, and Gajewski TF. **Control of T lymphocyte signal transduction through clonal anergy.** *J Mol Med*, 1996, **74**(11): 673-83.
130. Adams CL, Grierson AM, Mowat AM, Harnett MM, and Garside P. **Differences in the kinetics, amplitude, and localization of ERK activation in anergy and priming revealed at the level of individual primary T cells by laser scanning cytometry.** *J Immunol*, 2004, **173**(3): 1579-86.
131. Morton AM, McManus B, Garside P, Mowat AM, and Harnett MM. **Inverse Rap1 and phospho-ERK expression discriminate the maintenance phase of tolerance and priming of antigen-specific CD4+ T cells in vitro and in vivo.** *J Immunol*, 2007, **179**(12): 8026-34.
132. Hattori S and Matsuda M. **[Activation of Rap1, antagonist to ras, by Crk-C3G].** *Gan To Kagaku Ryoho*, 1997, **24**(11): 1414-21.
133. Tanaka S, Morishita T, Hashimoto Y, Hattori S, Nakamura S, Shibuya M, Matuoka K, Takenawa T, Kurata T, Nagashima K, and et al. **C3G, a guanine nucleotide-releasing protein expressed ubiquitously, binds to the Src homology 3 domains of CRK and GRB2/ASH proteins.** *Proc Natl Acad Sci U S A*, 1994, **91**(8): 3443-7.
134. Swaminathan G and Tsygankov AY. **The Cbl family proteins: ring leaders in regulation of cell signaling.** *J Cell Physiol*, 2006, **209**(1): 21-43.
135. Besson A, Gurian-West M, Schmidt A, Hall A, and Roberts JM. **p27Kip1 modulates cell migration through the regulation of RhoA activation.** *Genes Dev*, 2004, **18**(8): 862-76.

136. Chopra S, Fernandez De Mattos S, Lam EW, and Mann DJ. **Jab1 co-activation of c-Jun is abrogated by the serine 10-phosphorylated form of p27Kip1.** *J Biol Chem*, 2002, **277**(36): 32413-6.
137. Simons K and Toomre D. **Lipid rafts and signal transduction.** *Nat Rev Mol Cell Biol*, 2000, **1**(1): 31-9.
138. Horejsi V. **The roles of membrane microdomains (rafts) in T cell activation.** *Immunol Rev*, 2003, **191**: 148-64.
139. Grakoui A, Bromley SK, Sumen C, Davis MM, Shaw AS, Allen PM, and Dustin ML. **The immunological synapse: a molecular machine controlling T cell activation.** *Science*, 1999, **285**(5425): 221-7.
140. Monks CR, Freiberg BA, Kupfer H, Sciaky N, and Kupfer A. **Three-dimensional segregation of supramolecular activation clusters in T cells.** *Nature*, 1998, **395**(6697): 82-6.
141. Carlin LM, Yanagi K, Verhoef A, Nolte-'t Hoen EN, Yates J, Gardner L, Lamb J, Lombardi G, Dallman MJ, and Davis DM. **Secretion of IFN-gamma and not IL-2 by anergic human T cells correlates with assembly of an immature immune synapse.** *Blood*, 2005, **106**(12): 3874-9.
142. Wyllie AH, Kerr JF, and Currie AR. **Cell death: the significance of apoptosis.** *Int Rev Cytol*, 1980, **68**: 251-306.
143. Thornberry NA and Lazebnik Y. **Caspases: enemies within.** *Science*, 1998, **281**(5381): 1312-6.
144. Strasser A, Jost PJ, and Nagata S. **The many roles of FAS receptor signaling in the immune system.** *Immunity*, 2009, **30**(2): 180-92.
145. Huang DC and Strasser A. **BH3-Only proteins-essential initiators of apoptotic cell death.** *Cell*, 2000, **103**(6): 839-42.
146. Hengartner MO. **The biochemistry of apoptosis.** *Nature*, 2000, **407**(6805): 770-6.
147. Song J, Lei FT, Xiong X, and Haque R. **Intracellular signals of T cell costimulation.** *Cell Mol Immunol*, 2008, **5**(4): 239-47.
148. Nasmyth K. **Viewpoint: putting the cell cycle in order.** *Science*, 1996, **274**(5293): 1643-5.
149. Zetterberg A, Larsson O, and Wiman KG. **What is the restriction point?** *Curr Opin Cell Biol*, 1995, **7**(6): 835-42.
150. Weinberg RA. **The retinoblastoma protein and cell cycle control.** *Cell*, 1995, **81**(3): 323-30.
151. Hengst L and Reed SI. **Translational control of p27Kip1 accumulation during the cell cycle.** *Science*, 1996, **271**(5257): 1861-4.
152. Albanese C, Johnson J, Watanabe G, Eklund N, Vu D, Arnold A, and Pestell RG. **Transforming p21ras mutants and c-Ets-2 activate the cyclin D1 promoter through distinguishable regions.** *J Biol Chem*, 1995, **270**(40): 23589-97.
153. Harbour JW, Luo RX, Dei Santi A, Postigo AA, and Dean DC. **Cdk phosphorylation triggers sequential intramolecular interactions that progressively block Rb functions as cells move through G1.** *Cell*, 1999, **98**(6): 859-69.
154. Muller D, Thieke K, Burgin A, Dickmanns A, and Eilers M. **Cyclin E-mediated elimination of p27 requires its interaction with the nuclear pore-associated protein mNPAP60.** *Embo J*, 2000, **19**(10): 2168-80.
155. Delmas C, Aragou N, Poussard S, Cottin P, Darbon JM, and Manenti S. **MAP kinase-dependent degradation of p27Kip1 by calpains in choroidal melanoma cells. Requirement of p27Kip1 nuclear export.** *J Biol Chem*, 2003, **278**(14): 12443-51.

156. Sutterluty H, Chatelain E, Marti A, Wirbelauer C, Senften M, Muller U, and Krek W. **p45SKP2 promotes p27Kip1 degradation and induces S phase in quiescent cells.** *Nat Cell Biol*, 1999, **1**(4): 207-14.
157. Liu YC, Penninger J, and Karin M. **Immunity by ubiquitylation: a reversible process of modification.** *Nat Rev Immunol*, 2005, **5**(12): 941-52.
158. Pickart CM. **Ubiquitin in chains.** *Trends Biochem Sci*, 2000, **25**(11): 544-8.
159. Mukhopadhyay D and Riezman H. **Proteasome-independent functions of ubiquitin in endocytosis and signaling.** *Science*, 2007, **315**(5809): 201-5.
160. Bonifacino JS and Traub LM. **Signals for sorting of transmembrane proteins to endosomes and lysosomes.** *Annu Rev Biochem*, 2003, **72**: 395-447.
161. Hicke L. **Protein regulation by monoubiquitin.** *Nat Rev Mol Cell Biol*, 2001, **2**(3): 195-201.
162. Sun L and Chen ZJ. **The novel functions of ubiquitination in signaling.** *Curr Opin Cell Biol*, 2004, **16**(2): 119-26.
163. Hershko A and Ciechanover A. **The ubiquitin system.** *Annu Rev Biochem*, 1998, **67**: 425-79.
164. Weissman AM. **Themes and variations on ubiquitylation.** *Nat Rev Mol Cell Biol*, 2001, **2**(3): 169-78.
165. Xu P, Duong DM, Seyfried NT, Cheng D, Xie Y, Robert J, Rush J, Hochstrasser M, Finley D, and Peng J. **Quantitative proteomics reveals the function of unconventional ubiquitin chains in proteasomal degradation.** *Cell*, 2009, **137**(1): 133-45.
166. Sun SC. **Deubiquitylation and regulation of the immune response.** *Nat Rev Immunol*, 2008, **8**(7): 501-11.
167. Bhoj VG and Chen ZJ. **Ubiquitylation in innate and adaptive immunity.** *Nature*, 2009, **458**(7237): 430-7.
168. Welchman RL, Gordon C, and Mayer RJ. **Ubiquitin and ubiquitin-like proteins as multifunctional signals.** *Nat Rev Mol Cell Biol*, 2005, **6**(8): 599-609.
169. Schartner JM, Fathman CG, and Seroogy CM. **Preservation of self: an overview of E3 ubiquitin ligases and T cell tolerance.** *Semin Immunol*, 2007, **19**(3): 188-96.
170. Mueller DL. **E3 ubiquitin ligases as T cell anergy factors.** *Nat Immunol*, 2004, **5**(9): 883-90.
171. VanDemark AP and Hill CP. **Structural basis of ubiquitylation.** *Curr Opin Struct Biol*, 2002, **12**(6): 822-30.
172. Kentsis A, Gordon RE, and Borden KL. **Control of biochemical reactions through supramolecular RING domain self-assembly.** *Proc Natl Acad Sci U S A*, 2002, **99**(24): 15404-9.
173. Thien CB and Langdon WY. **Cbl: many adaptations to regulate protein tyrosine kinases.** *Nat Rev Mol Cell Biol*, 2001, **2**(4): 294-307.
174. Gustin SE, Thien CB, and Langdon WY. **Cbl-b is a negative regulator of inflammatory cytokines produced by IgE-activated mast cells.** *J Immunol*, 2006, **177**(9): 5980-9.
175. Han C, Jin J, Xu S, Liu H, Li N, and Cao X. **Integrin CD11b negatively regulates TLR-triggered inflammatory responses by activating Syk and promoting degradation of MyD88 and TRIF via Cbl-b.** *Nat Immunol*, 2010, **11**(8): 734-42.
176. Choi EY, Orlova VV, Fagerholm SC, Nurmi SM, Zhang L, Ballantyne CM, Gahmberg CG, and Chavakis T. **Regulation of LFA-1-dependent inflammatory cell recruitment by Cbl-b and 14-3-3 proteins.** *Blood*, 2008, **111**(7): 3607-14.

177. Bachmaier K, Toya S, Gao X, Triantafillou T, Garrean S, Park GY, Frey RS, Vogel S, Minshall R, Christman JW, Tiruppathi C, and Malik AB. **E3 ubiquitin ligase Cblb regulates the acute inflammatory response underlying lung injury.** *Nat Med*, 2007, **13**(8): 920-6.
178. Lane HC, Anand AR, and Ganju RK. **Cbl and Akt regulate CXCL8-induced and CXCR1- and CXCR2-mediated chemotaxis.** *Int Immunol*, 2006, **18**(8): 1315-25.
179. Yasuda T, Tezuka T, Maeda A, Inazu T, Yamanashi Y, Gu H, Kurosaki T, and Yamamoto T. **Cbl-b positively regulates Btk-mediated activation of phospholipase C-gamma2 in B cells.** *J Exp Med*, 2002, **196**(1): 51-63.
180. Sohn HW, Gu H, and Pierce SK. **Cbl-b negatively regulates B cell antigen receptor signaling in mature B cells through ubiquitination of the tyrosine kinase Syk.** *J Exp Med*, 2003, **197**(11): 1511-24.
181. Kitaura Y, Jang IK, Wang Y, Han YC, Inazu T, Cadera EJ, Schlissel M, Hardy RR, and Gu H. **Control of the B cell-intrinsic tolerance programs by ubiquitin ligases Cbl and Cbl-b.** *Immunity*, 2007, **26**(5): 567-78.
182. Naramura M, Jang IK, Kole H, Huang F, Haines D, and Gu H. **c-Cbl and Cbl-b regulate T cell responsiveness by promoting ligand-induced TCR down-modulation.** *Nat Immunol*, 2002, **3**(12): 1192-9.
183. Heissmeyer V, Macian F, Im SH, Varma R, Feske S, Venuprasad K, Gu H, Liu YC, Dustin ML, and Rao A. **Calcineurin imposes T cell unresponsiveness through targeted proteolysis of signaling proteins.** *Nat Immunol*, 2004, **5**(3): 255-65.
184. Alcazar I, Cortes I, Zaballos A, Hernandez C, Fruman DA, Barber DF, and Carrera AC. **p85{beta} phosphoinositide 3-kinase regulates CD28 co-receptor function.** *Blood*, 2009.
185. Zhang J, Bardos T, Li D, Gal I, Vermes C, Xu J, Mikecz K, Finnegan A, Lipkowitz S, and Glant TT. **Cutting edge: regulation of T cell activation threshold by CD28 costimulation through targeting Cbl-b for ubiquitination.** *J Immunol*, 2002, **169**(5): 2236-40.
186. Shamim M, Nanjappa SG, Singh A, Plisch EH, LeBlanc SE, Walent J, Svaren J, Seroogy C, and Suresh M. **Cbl-b regulates antigen-induced TCR down-regulation and IFN-gamma production by effector CD8 T cells without affecting functional avidity.** *J Immunol*, 2007, **179**(11): 7233-43.
187. Thien CB and Langdon WY. **c-Cbl and Cbl-b ubiquitin ligases: substrate diversity and the negative regulation of signalling responses.** *Biochem J*, 2005, **391**(Pt 2): 153-66.
188. Zha Y and Gajewski TF. **An adenoviral vector encoding dominant negative Cbl lowers the threshold for T cell activation in post-thymic T cells.** *Cell Immunol*, 2007, **247**(2): 95-102.
189. Michel F, Mangino G, Attal-Bonnefoy G, Tuosto L, Alcover A, Roumier A, Olive D, and Acuto O. **CD28 utilizes Vav-1 to enhance TCR-proximal signaling and NF-AT activation.** *J Immunol*, 2000, **165**(7): 3820-9.
190. Qiao G, Li Z, Molinero L, Alegre ML, Ying H, Sun Z, Penninger JM, and Zhang J. **T-cell receptor-induced NF-kappaB activation is negatively regulated by E3 ubiquitin ligase Cbl-b.** *Mol Cell Biol*, 2008, **28**(7): 2470-80.
191. Fang D and Liu YC. **Proteolysis-independent regulation of PI3K by Cbl-b-mediated ubiquitination in T cells.** *Nat Immunol*, 2001, **2**(9): 870-5.
192. Teh CE, Daley SR, Enders A, and Goodnow CC. **T-cell regulation by casitas B-lineage lymphoma (Cblb) is a critical failsafe against autoimmune disease due to autoimmune regulator (Aire) deficiency.** *Proc Natl Acad Sci U S A*, 2010.

193. Jeon MS, Atfield A, Venuprasad K, Krawczyk C, Sarao R, Elly C, Yang C, Arya S, Bachmaier K, Su L, Bouchard D, Jones R, Gronski M, Ohashi P, Wada T, Bloom D, Fathman CG, Liu YC, and Penninger JM. **Essential role of the E3 ubiquitin ligase Cbl-b in T cell anergy induction.** *Immunity*, 2004, **21**(2): 167-77.
194. Bachmaier K, Krawczyk C, Kozieradzki I, Kong YY, Sasaki T, Oliveira-dos-Santos A, Mariathasan S, Bouchard D, Wakeham A, Itie A, Le J, Ohashi PS, Sarosi I, Nishina H, Lipkowitz S, and Penninger JM. **Negative regulation of lymphocyte activation and autoimmunity by the molecular adaptor Cbl-b.** *Nature*, 2000, **403**(6766): 211-6.
195. Chiang YJ, Kole HK, Brown K, Naramura M, Fukuhara S, Hu RJ, Jang IK, Gutkind JS, Shevach E, and Gu H. **Cbl-b regulates the CD28 dependence of T-cell activation.** *Nature*, 2000, **403**(6766): 216-20.
196. St Rose MC, Qui HZ, Bandyopadhyay S, Mihalyo MA, Hagymasi AT, Clark RB, and Adler AJ. **The E3 ubiquitin ligase Cbl-b regulates expansion but not functional activity of self-reactive CD4 T cells.** *J Immunol*, 2009, **183**(8): 4975-83.
197. Wohlfert EA, Callahan MK, and Clark RB. **Resistance to CD4+CD25+ regulatory T cells and TGF-beta in Cbl-b-/- mice.** *J Immunol*, 2004, **173**(2): 1059-65.
198. Wohlfert EA, Gorelik L, Mittler R, Flavell RA, and Clark RB. **Cutting edge: deficiency in the E3 ubiquitin ligase Cbl-b results in a multifunctional defect in T cell TGF-beta sensitivity in vitro and in vivo.** *J Immunol*, 2006, **176**(3): 1316-20.
199. Adams CO, Housley WJ, Bhowmick S, Cone RE, Rajan TV, Forouhar F, and Clark RB. **Cbl-b-/- T Cells Demonstrate In Vivo Resistance to Regulatory T Cells but a Context-Dependent Resistance to TGF- $\beta$ .** *J Immunol*, 2010, **185**(4): 2051-8.
200. Harada Y, Harada Y, Elly C, Ying G, Paik JH, DePinho RA, and Liu YC. **Transcription factors Foxo3a and Foxo1 couple the E3 ligase Cbl-b to the induction of Foxp3 expression in induced regulatory T cells.** *J Exp Med*, 2010, **207**(7): 1381-91.
201. Loeser S, Loser K, Bijker MS, Rangachari M, van der Burg SH, Wada T, Beissert S, Melief CJ, and Penninger JM. **Spontaneous tumor rejection by cbl-b-deficient CD8+ T cells.** *J Exp Med*, 2007, **204**(4): 879-91.
202. Kojo S, Elly C, Harada Y, Langdon WY, Kronenberg M, and Liu YC. **Mechanisms of NKT cell anergy induction involve Cbl-b-promoted monoubiquitination of CARMA1.** *Proc Natl Acad Sci U S A*, 2009.
203. Yang B, Gay DL, MacLeod MK, Cao X, Hala T, Sweezer EM, Kappler J, Marrack P, and Oliver PM. **Nedd4 augments the adaptive immune response by promoting ubiquitin-mediated degradation of Cbl-b in activated T cells.** *Nat Immunol*, 2008, **9**(12): 1356-63.
204. Gruber T, Hermann-Kleiter N, Hinterleitner R, Fresser F, Schneider R, Gastl G, Penninger JM, and Baier G. **PKC-theta modulates the strength of T cell responses by targeting Cbl-b for ubiquitination and degradation.** *Sci Signal*, 2009, **2**(76): ra30.
205. Magnifico A, Ettenberg S, Yang C, Mariano J, Tiwari S, Fang S, Lipkowitz S, and Weissman AM. **WW domain HECT E3s target Cbl RING finger E3s for proteasomal degradation.** *J Biol Chem*, 2003, **278**(44): 43169-77.
206. Varma R, Campi G, Yokosuka T, Saito T, and Dustin ML. **T cell receptor-proximal signals are sustained in peripheral microclusters and terminated**

- in the central supramolecular activation cluster. *Immunity*, 2006, **25**(1): 117-27.**
207. Cenciarelli C, Wilhelm KG, Jr., Guo A, and Weissman AM. **T cell antigen receptor ubiquitination is a consequence of receptor-mediated tyrosine kinase activation.** *J Biol Chem*, 1996, **271**(15): 8709-13.
  208. Doherty M, Osborne DG, Browning DL, Parker DC, and Wetzel SA. **Anergic CD4+ T cells form mature immunological synapses with enhanced accumulation of c-Cbl and Cbl-b.** *J Immunol*, 2010, **184**(7): 3598-608.
  209. Zhang W, Shao Y, Fang D, Huang J, Jeon MS, and Liu YC. **Negative regulation of T cell antigen receptor-mediated Crk-L-C3G signaling and cell adhesion by Cbl-b.** *J Biol Chem*, 2003, **278**(26): 23978-83.
  210. Hustad CM, Perry WL, Siracusa LD, Rasberry C, Cobb L, Cattanaach BM, Kovatch R, Copeland NG, and Jenkins NA. **Molecular genetic characterization of six recessive viable alleles of the mouse agouti locus.** *Genetics*, 1995, **140**(1): 255-65.
  211. Perry WL, Hustad CM, Swing DA, O'Sullivan TN, Jenkins NA, and Copeland NG. **The itchy locus encodes a novel ubiquitin protein ligase that is disrupted in a18H mice.** *Nat Genet*, 1998, **18**(2): 143-6.
  212. Matesic LE, Haines DC, Copeland NG, and Jenkins NA. **Itch genetically interacts with Notch1 in a mouse autoimmune disease model.** *Hum Mol Genet*, 2006, **15**(24): 3485-97.
  213. Shembade N, Harhaj NS, Parvatiyar K, Copeland NG, Jenkins NA, Matesic LE, and Harhaj EW. **The E3 ligase Itch negatively regulates inflammatory signaling pathways by controlling the function of the ubiquitin-editing enzyme A20.** *Nat Immunol*, 2008, **9**(3): 254-62.
  214. Tao M, Scacheri PC, Marinis JM, Harhaj EW, Matesic LE, and Abbott DW. **ITCH K63-ubiquitinates the NOD2 binding protein, RIP2, to influence inflammatory signaling pathways.** *Curr Biol*, 2009, **19**(15): 1255-63.
  215. Tachibana K, Hirota S, Iizasa H, Yoshida H, Kawabata K, Kataoka Y, Kitamura Y, Matsushima K, Yoshida N, Nishikawa S, Kishimoto T, and Nagasawa T. **The chemokine receptor CXCR4 is essential for vascularization of the gastrointestinal tract.** *Nature*, 1998, **393**(6685): 591-4.
  216. Bhandari D, Robia SL, and Marchese A. **The E3 ubiquitin ligase atrophin interacting protein 4 binds directly to the chemokine receptor CXCR4 via a novel WW domain-mediated interaction.** *Mol Biol Cell*, 2009, **20**(5): 1324-39.
  217. Bhandari D, Trejo J, Benovic JL, and Marchese A. **Arrestin-2 interacts with the ubiquitin-protein isopeptide ligase atrophin-interacting protein 4 and mediates endosomal sorting of the chemokine receptor CXCR4.** *J Biol Chem*, 2007, **282**(51): 36971-9.
  218. Venuprasad K, Huang H, Harada Y, Elly C, Subramaniam M, Spelsberg T, Su J, and Liu YC. **The E3 ubiquitin ligase Itch regulates expression of transcription factor Foxp3 and airway inflammation by enhancing the function of transcription factor TIEG1.** *Nat Immunol*, 2008, **9**(3): 245-53.
  219. Ahn YH and Kurie JM. **MKK4/SEK1 is negatively regulated through a feedback loop involving the E3 ubiquitin ligase itch.** *J Biol Chem*, 2009.
  220. Oberst A, Malatesta M, Aqeilan RI, Rossi M, Salomoni P, Murillas R, Sharma P, Kuehn MR, Oren M, Croce CM, Bernassola F, and Melino G. **The Nedd4-binding partner 1 (N4BP1) protein is an inhibitor of the E3 ligase Itch.** *Proc Natl Acad Sci U S A*, 2007, **104**(27): 11280-5.
  221. Huang H, Jeon MS, Liao L, Yang C, Elly C, Yates JR, 3rd, and Liu YC. **K33-linked polyubiquitination of T cell receptor-zeta regulates proteolysis-independent T cell signaling.** *Immunity*, 2010, **33**(1): 60-70.

222. Fang D, Elly C, Gao B, Fang N, Altman Y, Joazeiro C, Hunter T, Copeland N, Jenkins N, and Liu YC. **Dysregulation of T lymphocyte function in itchy mice: a role for Itch in TH2 differentiation.** *Nat Immunol*, 2002, **3**(3): 281-7.
223. Scharschmidt E, Wegener E, Heissmeyer V, Rao A, and Krappmann D. **Degradation of Bcl10 induced by T-cell activation negatively regulates NF-kappa B signaling.** *Mol Cell Biol*, 2004, **24**(9): 3860-73.
224. Parravicini V, Field AC, Tomlinson PD, Albert Basson M, and Zamoyska R. **Itch-/-{alpha}{beta} and {gamma}{delta} T cells independently contribute to autoimmunity in Itchy mice.** *Blood*, 2008, **111**(8): 4273-7282.
225. Berland R and Wortis HH. **Origins and functions of B-1 cells with notes on the role of CD5.** *Annu Rev Immunol*, 2002, **20**: 253-300.
226. Gao M, Labuda T, Xia Y, Gallagher E, Fang D, Liu YC, and Karin M. **Jun turnover is controlled through JNK-dependent phosphorylation of the E3 ligase Itch.** *Science*, 2004, **306**(5694): 271-5.
227. Li B, Tournier C, Davis RJ, and Flavell RA. **Regulation of IL-4 expression by the transcription factor JunB during T helper cell differentiation.** *Embo J*, 1999, **18**(2): 420-32.
228. Gallagher E, Gao M, Liu YC, and Karin M. **Activation of the E3 ubiquitin ligase Itch through a phosphorylation-induced conformational change.** *Proc Natl Acad Sci U S A*, 2006, **103**(6): 1717-22.
229. Gao B, Lee SM, and Fang D. **The tyrosine kinase c-Abl protects c-Jun from ubiquitination-mediated degradation in T cells.** *J Biol Chem*, 2006, **281**(40): 29711-8.
230. Yang C, Zhou W, Jeon MS, Demydenko D, Harada Y, Zhou H, and Liu YC. **Negative regulation of the E3 ubiquitin ligase itch via Fyn-mediated tyrosine phosphorylation.** *Mol Cell*, 2006, **21**(1): 135-41.
231. Hoff H, Kolar P, Ambach A, Radbruch A, and Brunner-Weinzierl MC. **CTLA-4 (CD152) inhibits T cell function by activating the ubiquitin ligase Itch.** *Mol Immunol*, 2010, **47**(10): 1875-81.
232. Oliver PM, Cao X, Worthen GS, Shi P, Briones N, MacLeod M, White J, Kirby P, Kappler J, Marrack P, and Yang B. **Ndfip1 protein promotes the function of itch ubiquitin ligase to prevent T cell activation and T helper 2 cell-mediated inflammation.** *Immunity*, 2006, **25**(6): 929-40.
233. Anandasabapathy N, Ford GS, Bloom D, Holness C, Paragas V, Seroogy C, Skrenta H, Hollenhorst M, Fathman CG, and Soares L. **GRAIL: an E3 ubiquitin ligase that inhibits cytokine gene transcription is expressed in anergic CD4+ T cells.** *Immunity*, 2003, **18**(4): 535-47.
234. Seroogy CM, Soares L, Ranheim EA, Su L, Holness C, Bloom D, and Fathman CG. **The gene related to anergy in lymphocytes, an E3 ubiquitin ligase, is necessary for anergy induction in CD4 T cells.** *J Immunol*, 2004, **173**(1): 79-85.
235. Kriegel MA, Rathinam C, and Flavell RA. **E3 ubiquitin ligase GRAIL controls primary T cell activation and oral tolerance.** *Proc Natl Acad Sci U S A*, 2009, **106**(39): 16770-5.
236. Nurieva RI, Zheng S, Jin W, Chung Y, Zhang Y, Martinez GJ, Reynolds JM, Wang SL, Lin X, Sun SC, Lozano G, and Dong C. **The E3 ubiquitin ligase GRAIL regulates T cell tolerance and regulatory T cell function by mediating T cell receptor-CD3 degradation.** *Immunity*, 2010, **32**(5): 670-80.
237. Taylor JJ, Krawczyk CM, Mohrs M, and Pearce EJ. **Th2 cell hyporesponsiveness during chronic murine schistosomiasis is cell intrinsic and linked to GRAIL expression.** *J Clin Invest*, 2009.

238. MacKenzie DA, Schartner J, Lin J, Timmel A, Jennens-Clough M, Fathman CG, and Seroogy CM. **GRAIL is up-regulated in CD4+ CD25+ T regulatory cells and is sufficient for conversion of T cells to a regulatory phenotype.** *J Biol Chem*, 2007, **282**(13): 9696-702.
239. Egawa S, Iijima H, Shinzaki S, Nakajima S, Wang J, Kondo J, Ishii S, Yoshio T, Irie T, Nishida T, Kakiuchi Y, Yasumaru M, Yoshihara H, Kanto T, Tsujii M, Tsuji S, and Hayashi N. **Upregulation of GRAIL is associated with remission of ulcerative colitis.** *Am J Physiol Gastrointest Liver Physiol*, 2008, **295**(1): G163-G169.
240. Kostianovsky AM, Maier LM, Baecher-Allan C, Anderson AC, and Anderson DE. **Up-regulation of gene related to anergy in lymphocytes is associated with Notch-mediated human T cell suppression.** *J Immunol*, 2007, **178**(10): 6158-63.
241. Schartner JM, Simonson WT, Wernimont SA, Nettenstrom LM, Huttenlocher A, and Seroogy CM. **Gene related to anergy in lymphocytes (GRAIL) expression in CD4+ T cells impairs actin cytoskeletal organization during T Cell: Antigen presenting cell interactions.** *J Biol Chem*, 2009.
242. Su L, Lineberry N, Huh Y, Soares L, and Fathman CG. **A novel E3 ubiquitin ligase substrate screen identifies Rho guanine dissociation inhibitor as a substrate of gene related to anergy in lymphocytes.** *J Immunol*, 2006, **177**(11): 7559-66.
243. Olofsson B. **Rho guanine dissociation inhibitors: pivotal molecules in cellular signalling.** *Cell Signal*, 1999, **11**(8): 545-54.
244. Grewal IS and Flavell RA. **CD40 and CD154 in cell-mediated immunity.** *Annu Rev Immunol*, 1998, **16**: 111-35.
245. Lineberry NB, Su LL, Lin JT, Coffey GP, Seroogy CM, and Fathman CG. **Cutting edge: The transmembrane E3 ligase GRAIL ubiquitinates the costimulatory molecule CD40 ligand during the induction of T cell anergy.** *J Immunol*, 2008, **181**(3): 1622-6.
246. Lineberry N, Su L, Soares L, and Fathman CG. **The single subunit transmembrane E3 ligase gene related to anergy in lymphocytes (GRAIL) captures and then ubiquitinates transmembrane proteins across the cell membrane.** *J Biol Chem*, 2008, **283**(42): 28497-505.
247. Soares L, Seroogy C, Skrenta H, Anandasabapathy N, Lovelace P, Chung CD, Engleman E, and Fathman CG. **Two isoforms of otubain 1 regulate T cell anergy via GRAIL.** *Nat Immunol*, 2004, **5**(1): 45-54.
248. Lin JT, Lineberry NB, Kattah MG, Su LL, Utz PJ, Fathman CG, and Wu L. **Naive CD4 t cell proliferation is controlled by mammalian target of rapamycin regulation of GRAIL expression.** *J Immunol*, 2009, **182**(10): 5919-28.
249. Schwamborn JC, Muller M, Becker AH, and Puschel AW. **Ubiquitination of the GTPase Rap1B by the ubiquitin ligase Smurf2 is required for the establishment of neuronal polarity.** *Embo J*, 2007, **26**(5): 1410-22.
250. Wang HR, Zhang Y, Ozdamar B, Ogunjimi AA, Alexandrova E, Thomsen GH, and Wrana JL. **Regulation of cell polarity and protrusion formation by targeting RhoA for degradation.** *Science*, 2003, **302**(5651): 1775-9.
251. Zhu H, Kavsak P, Abdollah S, Wrana JL, and Thomsen GH. **A SMAD ubiquitin ligase targets the BMP pathway and affects embryonic pattern formation.** *Nature*, 1999, **400**(6745): 687-93.
252. Kavsak P, Rasmussen RK, Causing CG, Bonni S, Zhu H, Thomsen GH, and Wrana JL. **Smad7 binds to Smurf2 to form an E3 ubiquitin ligase that**

- targets the TGF beta receptor for degradation.** *Mol Cell*, 2000, **6**(6): 1365-75.
253. Wiesner S, Ogunjimi AA, Wang HR, Rotin D, Sicheri F, Wrana JL, and Forman-Kay JD. **Autoinhibition of the HECT-type ubiquitin ligase Smurf2 through its C2 domain.** *Cell*, 2007, **130**(4): 651-62.
254. Fukunaga E, Inoue Y, Komiya S, Horiguchi K, Goto K, Saitoh M, Miyazawa K, Koinuma D, Hanyu A, and Imamura T. **Smurf2 Induces Ubiquitin-dependent Degradation of Smurf1 to Prevent Migration of Breast Cancer Cells.** *J Biol Chem*, 2008, **283**(51): 35660-7.
255. Murphy KM, Heimberger AB, and Loh DY. **Induction by antigen of intrathymic apoptosis of CD4+CD8+TCRlo thymocytes in vivo.** *Science*, 1990, **250**(4988): 1720-3.
256. Haskins K, Kubo R, White J, Pigeon M, Kappler J, and Marrack P. **The major histocompatibility complex-restricted antigen receptor on T cells. I. Isolation with a monoclonal antibody.** *J Exp Med*, 1983, **157**(4): 1149-69.
257. Harding FA, McArthur JG, Gross JA, Raulet DH, and Allison JP. **CD28-mediated signalling co-stimulates murine T cells and prevents induction of anergy in T-cell clones.** *Nature*, 1992, **356**(6370): 607-9.
258. Gonzalez LC, Loyet KM, Calemine-Fenaux J, Chauhan V, Wranik B, Ouyang W, and Eaton DL. **A coreceptor interaction between the CD28 and TNF receptor family members B and T lymphocyte attenuator and herpesvirus entry mediator.** *Proc Natl Acad Sci U S A*, 2005, **102**(4): 1116-21.
259. Macian F, Garcia-Rodriguez C, and Rao A. **Gene expression elicited by NFAT in the presence or absence of cooperative recruitment of Fos and Jun.** *Embo J*, 2000, **19**(17): 4783-95.
260. Chiodetti L, Choi S, Barber DL, and Schwartz RH. **Adaptive tolerance and clonal anergy are distinct biochemical states.** *J Immunol*, 2006, **176**(4): 2279-91.
261. Seyerl M, Bluml S, Kirchberger S, Bochkov VN, Oskolkova O, Majdic O, and Stockl J. **Oxidized phospholipids induce anergy in human peripheral blood T cells.** *Eur J Immunol*, 2008, **38**(3): 778-87.
262. Leontieva OV and Black JD. **Identification of two distinct pathways of protein kinase Calpha down-regulation in intestinal epithelial cells.** *J Biol Chem*, 2004, **279**(7): 5788-801.
263. Jonuleit T, van der Kuip H, Miething C, Michels H, Hallek M, Duyster J, and Aulitzky WE. **Bcr-Abl kinase down-regulates cyclin-dependent kinase inhibitor p27 in human and murine cell lines.** *Blood*, 2000, **96**(5): 1933-9.
264. Garside P, Ingulli E, Merica RR, Johnson JG, Noelle RJ, and Jenkins MK. **Visualization of specific B and T lymphocyte interactions in the lymph node.** *Science*, 1998, **281**(5373): 96-9.
265. Kearney ER, Pape KA, Loh DY, and Jenkins MK. **Visualization of peptide-specific T cell immunity and peripheral tolerance induction in vivo.** *Immunity*, 1994, **1**(4): 327-39.
266. Reinhardt RL, Khoruts A, Merica R, Zell T, and Jenkins MK. **Visualizing the generation of memory CD4 T cells in the whole body.** *Nature*, 2001, **410**(6824): 101-5.
267. Zell T, Khoruts A, Ingulli E, Bonnevier JL, Mueller DL, and Jenkins MK. **Single-cell analysis of signal transduction in CD4 T cells stimulated by antigen in vivo.** *Proc Natl Acad Sci U S A*, 2001, **98**(19): 10805-10.
268. Pape KA, Merica R, Mondino A, Khoruts A, and Jenkins MK. **Direct evidence that functionally impaired CD4+ T cells persist in vivo following induction of peripheral tolerance.** *J Immunol*, 1998, **160**(10): 4719-29.

269. Altin JG and Pagler EB. **A one-step procedure for biotinylation and chemical cross-linking of lymphocyte surface and intracellular membrane-associated molecules.** *Anal Biochem*, 1995, **224**(1): 382-9.
270. Harnett MM. **Laser scanning cytometry: understanding the immune system in situ.** *Nat Rev Immunol*, 2007, **7**(11): 897-904.
271. Grierson AM, Mitchell P, Adams CL, Mowat AM, Brewer JM, Harnett MM, and Garside P. **Direct quantitation of T cell signaling by laser scanning cytometry.** *J Immunol Methods*, 2005, **301**(1-2): 140-53.
272. Kametsky LA. **Laser scanning cytometry.** *Methods Cell Biol*, 2001, **63**: 51-87.
273. Darzynkiewicz Z, Juan G, and Bedner E. **Determining cell cycle stages by flow cytometry.** *Curr Protoc Cell Biol*, 2001, **Chapter 8**: Unit 8 4.
274. Kapuscinski J. **DAPI: a DNA-specific fluorescent probe.** *Biotech Histochem*, 1995, **70**(5): 220-33.
275. Frauwirth KA and Thompson CB. **Activation and inhibition of lymphocytes by costimulation.** *J Clin Invest*, 2002, **109**(3): 295-9.
276. Zheng Y, Zha Y, and Gajewski TF. **Molecular regulation of T-cell anergy.** *EMBO Rep*, 2008, **9**(1): 50-5.
277. Trickett A and Kwan YL. **T cell stimulation and expansion using anti-CD3/CD28 beads.** *J Immunol Methods*, 2003, **275**(1-2): 251-5.
278. Cenciarelli C, Hou D, Hsu KC, Rellahan BL, Wiest DL, Smith HT, Fried VA, and Weissman AM. **Activation-induced ubiquitination of the T cell antigen receptor.** *Science*, 1992, **257**(5071): 795-7.
279. Schwamborn JC, Khazaei MR, and Puschel AW. **The interaction of mPar3 with the ubiquitin ligase Smurf2 is required for the establishment of neuronal polarity.** *J Biol Chem*, 2007, **282**(48): 35259-68.
280. Li M, Brooks CL, Wu-Baer F, Chen D, Baer R, and Gu W. **Mono- versus polyubiquitination: differential control of p53 fate by Mdm2.** *Science*, 2003, **302**(5652): 1972-5.
281. Fenteany G, Standaert RF, Lane WS, Choi S, Corey EJ, and Schreiber SL. **Inhibition of proteasome activities and subunit-specific amino-terminal threonine modification by lactacystin.** *Science*, 1995, **268**(5211): 726-31.
282. Rao N, Miyake S, Reddi AL, Douillard P, Ghosh AK, Dodge IL, Zhou P, Fernandes ND, and Band H. **Negative regulation of Lck by Cbl ubiquitin ligase.** *Proc Natl Acad Sci U S A*, 2002, **99**(6): 3794-9.
283. Uhlin M, Masucci MG, and Levitsky V. **Regulation of lck degradation and refractory state in CD8+ cytotoxic T lymphocytes.** *Proc Natl Acad Sci U S A*, 2005, **102**(26): 9264-9.
284. Smith KM, McAskill F, and Garside P. **Orally tolerized T cells are only able to enter B cell follicles following challenge with antigen in adjuvant, but they remain unable to provide B cell help.** *J Immunol*, 2002, **168**(9): 4318-25.
285. Hirasaka K, Kohno S, Goto J, Furochi H, Mawatari K, Harada N, Hosaka T, Nakaya Y, Ishidoh K, Obata T, Ebina Y, Gu H, Takeda S, Kishi K, and Nikawa T. **Deficiency of Cbl-b gene enhances infiltration and activation of macrophages in adipose tissue and causes peripheral insulin resistance in mice.** *Diabetes*, 2007, **56**(10): 2511-22.
286. Arron JR, Vologodskaja M, Wong BR, Naramura M, Kim N, Gu H, and Choi Y. **A positive regulatory role for Cbl family proteins in tumor necrosis factor-related activation-induced cytokine (trance) and CD40L-mediated Akt activation.** *J Biol Chem*, 2001, **276**(32): 30011-7.

287. Minami Y, Kono T, Miyazaki T, and Taniguchi T. **The IL-2 receptor complex: its structure, function, and target genes.** *Annu Rev Immunol*, 1993, **11**: 245-68.
288. Tzachanis D, Appleman LJ, Van Puijenbroek AA, Berezovskaya A, Nadler LM, and Boussiotis VA. **Differential localization and function of ADP-ribosylation factor-6 in anergic human T cells: a potential marker for their identification.** *J Immunol*, 2003, **171**(4): 1691-6.
289. Takai Y, Sasaki T, and Matozaki T. **Small GTP-binding proteins.** *Physiol Rev*, 2001, **81**(1): 153-208.
290. D'Souza-Schorey C, Li G, Colombo MI, and Stahl PD. **A regulatory role for ARF6 in receptor-mediated endocytosis.** *Science*, 1995, **267**(5201): 1175-8.
291. Donaldson JG. **Arf6 and its role in cytoskeletal modulation.** *Methods Mol Biol*, 2002, **189**: 191-8.
292. Boshans RL, Szanto S, van Aelst L, and D'Souza-Schorey C. **ADP-ribosylation factor 6 regulates actin cytoskeleton remodeling in coordination with Rac1 and RhoA.** *Mol Cell Biol*, 2000, **20**(10): 3685-94.
293. Krawczyk C and Penninger JM. **Molecular controls of antigen receptor clustering and autoimmunity.** *Trends Cell Biol*, 2001, **11**(5): 212-20.
294. Gaschet J and Hsu VW. **Distribution of ARF6 between membrane and cytosol is regulated by its GTPase cycle.** *J Biol Chem*, 1999, **274**(28): 20040-5.
295. Kubsch S, Graulich E, Knop J, and Steinbrink K. **Suppressor activity of anergic T cells induced by IL-10-treated human dendritic cells: association with IL-2- and CTLA-4-dependent G1 arrest of the cell cycle regulated by p27Kip1.** *Eur J Immunol*, 2003, **33**(7): 1988-97.
296. Whitacre CC, Gienapp IE, Orosz CG, and Bitar DM. **Oral tolerance in experimental autoimmune encephalomyelitis. III. Evidence for clonal anergy.** *J Immunol*, 1991, **147**(7): 2155-63.
297. Zhang R, Zhang N, and Mueller DL. **Casitas B-lineage lymphoma b inhibits antigen recognition and slows cell cycle progression at late times during CD4+ T cell clonal expansion.** *J Immunol*, 2008, **181**(8): 5331-9.
298. Ruschmann J, Ho V, Antignano F, Kuroda E, Lam V, Ibaraki M, Snyder K, Kim C, Flavell RA, Kawakami T, Sly L, Turhan AG, and Krystal G. **Tyrosine phosphorylation of SHIP promotes its proteasomal degradation.** *Exp Hematol*, 2010, **38**(5): 392-402, 402 e1.
299. Chiang YJ, Jordan MS, Horai R, Schwartzberg PL, Koretzky GA, and Hodes RJ. **Cbl Enforces an SLP76-dependent Signaling Pathway for T Cell Differentiation.** *J Biol Chem*, 2009, **284**(7): 4429-38.
300. Mihalyo MA, Doody AD, McAleer JP, Nowak EC, Long M, Yang Y, and Adler AJ. **In vivo cyclophosphamide and IL-2 treatment impedes self-antigen-induced effector CD4 cell tolerization: implications for adoptive immunotherapy.** *J Immunol*, 2004, **172**(9): 5338-45.
301. Adler AJ, Huang CT, Yochum GS, Marsh DW, and Pardoll DM. **In vivo CD4+ T cell tolerance induction versus priming is independent of the rate and number of cell divisions.** *J Immunol*, 2000, **164**(2): 649-55.
302. Mouchantaf R, Azakir BA, McPherson PS, Millard SM, Wood SA, and Angers A. **The ubiquitin ligase itch is auto-ubiquitylated in vivo and in vitro but is protected from degradation by interacting with the deubiquitylating enzyme FAM/USP9X.** *J Biol Chem*, 2006, **281**(50): 38738-47.
303. Chastagner P, Israel A, and Brou C. **Itch/AIP4 mediates Deltex degradation through the formation of K29-linked polyubiquitin chains.** *EMBO Rep*, 2006, **7**(11): 1147-53.

304. Azakir BA, Desrochers G, and Angers A. **The ubiquitin ligase Itch mediates the antiapoptotic activity of epidermal growth factor by promoting the ubiquitylation and degradation of the truncated C-terminal portion of Bid.** *Febs J*, 2010, **277**(5): 1319-30.
305. Esposti MD. **The roles of Bid.** *Apoptosis*, 2002, **7**(5): 433-40.
306. Marchese A, Raiborg C, Santini F, Keen JH, Stenmark H, and Benovic JL. **The E3 ubiquitin ligase AIP4 mediates ubiquitination and sorting of the G protein-coupled receptor CXCR4.** *Dev Cell*, 2003, **5**(5): 709-22.
307. Hsiao HW, Liu WH, Wang CJ, Lo YH, Wu YH, Jiang ST, and Lai MZ. **Deltex1 is a target of the transcription factor NFAT that promotes T cell anergy.** *Immunity*, 2009, **31**(1): 72-83.
308. Lohr NJ, Molleston JP, Strauss KA, Torres-Martinez W, Sherman EA, Squires RH, Rider NL, Chikwava KR, Cummings OW, Morton DH, and Puffenberger EG. **Human ITCH E3 ubiquitin ligase deficiency causes syndromic multisystem autoimmune disease.** *Am J Hum Genet*, 2010, **86**(3): 447-53.
309. Soto-Nieves N, Puga I, Abe BT, Bandyopadhyay S, Baine I, Rao A, and Macian F. **Transcriptional complexes formed by NFAT dimers regulate the induction of T cell tolerance.** *J Exp Med*, 2009.
310. Su LL, Iwai H, Lin JT, and Fathman CG. **The transmembrane E3 ligase GRAIL ubiquitinates and degrades CD83 on CD4 T cells.** *J Immunol*, 2009, **183**(1): 438-44.
311. Pellegrini M, Calzascia T, Elford AR, Shahinian A, Lin AE, Dissanayake D, Dhanji S, Nguyen LT, Gronski MA, Morre M, Assouline B, Lahl K, Sparwasser T, Ohashi PS, and Mak TW. **Adjuvant IL-7 antagonizes multiple cellular and molecular inhibitory networks to enhance immunotherapies.** *Nat Med*, 2009, **15**(5): 528-36.
312. Chen TC, Cobbold SP, Fairchild PJ, and Waldmann H. **Generation of anergic and regulatory T cells following prolonged exposure to a harmless antigen.** *J Immunol*, 2004, **172**(10): 5900-7.
313. Jordan MS, Riley MP, von Boehmer H, and Caton AJ. **Anergy and suppression regulate CD4(+) T cell responses to a self peptide.** *Eur J Immunol*, 2000, **30**(1): 136-44.
314. King CG, Buckler JL, Kobayashi T, Hannah JR, Bassett G, Kim T, Pearce EL, Kim GG, Turka LA, and Choi Y. **Cutting edge: requirement for TRAF6 in the induction of T cell anergy.** *J Immunol*, 2008, **180**(1): 34-8.
315. Deng L, Wang C, Spencer E, Yang L, Braun A, You J, Slaughter C, Pickart C, and Chen ZJ. **Activation of the I $\kappa$ B kinase complex by TRAF6 requires a dimeric ubiquitin-conjugating enzyme complex and a unique polyubiquitin chain.** *Cell*, 2000, **103**(2): 351-61.
316. Kobayashi T, Walsh PT, Walsh MC, Speirs KM, Chiffoleau E, King CG, Hancock WW, Caamano JH, Hunter CA, Scott P, Turka LA, and Choi Y. **TRAF6 is a critical factor for dendritic cell maturation and development.** *Immunity*, 2003, **19**(3): 353-63.
317. Machado FS, Esper L, Dias A, Madan R, Gu Y, Hildeman D, Serhan CN, Karp CL, and Aliberti J. **Native and aspirin-triggered lipoxins control innate immunity by inducing proteasomal degradation of TRAF6.** *J Exp Med*, 2008, **205**(5): 1077-86.
318. Gomez-del Arco P, Koipally J, and Georgopoulos K. **Ikaros SUMOylation: switching out of repression.** *Mol Cell Biol*, 2005, **25**(7): 2688-97.
319. Gomez-del Arco P, Maki K, and Georgopoulos K. **Phosphorylation controls Ikaros's ability to negatively regulate the G(1)-S transition.** *Mol Cell Biol*, 2004, **24**(7): 2797-807.

320. Popescu M, Gurel Z, Ronni T, Song C, Hung KY, Payne KJ, and Dovat S. **Ikaros stability and pericentromeric localization are regulated by protein phosphatase 1.** *J Biol Chem*, 2009, **284**(20): 13869-80.
321. O'Neill DW, Schoetz SS, Lopez RA, Castle M, Rabinowitz L, Shor E, Krawchuk D, Goll MG, Renz M, Seelig HP, Han S, Seong RH, Park SD, Agalioti T, Munshi N, Thanos D, Erdjument-Bromage H, Tempst P, and Bank A. **An ikaros-containing chromatin-remodeling complex in adult-type erythroid cells.** *Mol Cell Biol*, 2000, **20**(20): 7572-82.
322. Kim J, Sif S, Jones B, Jackson A, Koipally J, Heller E, Winandy S, Viel A, Sawyer A, Ikeda T, Kingston R, and Georgopoulos K. **Ikaros DNA-binding proteins direct formation of chromatin remodeling complexes in lymphocytes.** *Immunity*, 1999, **10**(3): 345-55.
323. Koipally J, Renold A, Kim J, and Georgopoulos K. **Repression by Ikaros and Aiolos is mediated through histone deacetylase complexes.** *Embo J*, 1999, **18**(11): 3090-100.
324. Wiedemann A, Muller S, Favier B, Penna D, Guiraud M, Delmas C, Champagne E, and Valitutti S. **T-cell activation is accompanied by an ubiquitination process occurring at the immunological synapse.** *Immunol Lett*, 2005, **98**(1): 57-61.
325. Wang H, Matsuzawa A, Brown SA, Zhou J, Guy CS, Tseng PH, Forbes K, Nicholson TP, Sheppard PW, Hacker H, Karin M, and Vignali DA. **Analysis of nondegradative protein ubiquitylation with a monoclonal antibody specific for lysine-63-linked polyubiquitin.** *Proc Natl Acad Sci U S A*, 2008, **105**(51): 20197-202.
326. Hicke L and Dunn R. **Regulation of membrane protein transport by ubiquitin and ubiquitin-binding proteins.** *Annu Rev Cell Dev Biol*, 2003, **19**: 141-72.
327. Saeki Y, Kudo T, Sone T, Kikuchi Y, Yokosawa H, Toh-e A, and Tanaka K. **Lysine 63-linked polyubiquitin chain may serve as a targeting signal for the 26S proteasome.** *Embo J*, 2009, **28**(4): 359-71.
328. Kim HT, Kim KP, Lledias F, Kisselev AF, Scaglione KM, Skowyra D, Gygi SP, and Goldberg AL. **Certain pairs of ubiquitin-conjugating enzymes (E2s) and ubiquitin-protein ligases (E3s) synthesize nondegradable forked ubiquitin chains containing all possible isopeptide linkages.** *J Biol Chem*, 2007, **282**(24): 17375-86.
329. Berges C, Haberstock H, Fuchs D, Miltz M, Sadeghi M, Opelz G, Daniel V, and Naujokat C. **Proteasome inhibition suppresses essential immune functions of human CD4+ T cells.** *Immunology*, 2008, **124**(2): 234-46.
330. Asai K, Hachimura S, Kimura M, Toraya T, Yamashita M, Nakayama T, and Kaminogawa S. **T cell hyporesponsiveness induced by oral administration of ovalbumin is associated with impaired NFAT nuclear translocation and p27kip1 degradation.** *J Immunol*, 2002, **169**(9): 4723-31.
331. Utting O, Teh SJ, and Teh HS. **A population of in vivo anergized T cells with a lower activation threshold for the induction of CD25 exhibit differential requirements in mobilization of intracellular calcium and mitogen-activated protein kinase activation.** *J Immunol*, 2000, **164**(6): 2881-9.
332. Li L, Iwamoto Y, Berezovskaya A, and Boussiotis VA. **A pathway regulated by cell cycle inhibitor p27Kip1 and checkpoint inhibitor Smad3 is involved in the induction of T cell tolerance.** *Nat Immunol*, 2006, **7**(11): 1157-65.
333. Jacobs SR, Herman CE, Maciver NJ, Wofford JA, Wieman HL, Hammen JJ, and Rathmell JC. **Glucose Uptake Is Limiting in T Cell Activation and**

- Requires CD28-Mediated Akt-Dependent and Independent Pathways.** *J Immunol*, 2008, **180**(7): 4476-86.
334. Zheng Y, Collins SL, Lutz MA, Allen AN, Kole TP, Zarek PE, and Powell JD. **A role for mammalian target of rapamycin in regulating T cell activation versus anergy.** *J Immunol*, 2007, **178**(4): 2163-70.
335. Riley JL, Mao M, Kobayashi S, Biery M, Burchard J, Cavet G, Gregson BP, June CH, and Linsley PS. **Modulation of TCR-induced transcriptional profiles by ligation of CD28, ICOS, and CTLA-4 receptors.** *Proc Natl Acad Sci U S A*, 2002, **99**(18): 11790-5.
336. Diehn M, Alizadeh AA, Rando OJ, Liu CL, Stankunas K, Botstein D, Crabtree GR, and Brown PO. **Genomic expression programs and the integration of the CD28 costimulatory signal in T cell activation.** *Proc Natl Acad Sci U S A*, 2002, **99**(18): 11796-801.